UNIVERSIDAD DE GRANADA

Doctoral Thesis – Tesis Doctoral

Role of the extracellular protease ADAMTS1 as an immunomodulatory molecule: studies in syngeneic tumour mouse models

PROGRAMA DE DOCTORADO EN BIOMEDICINA (B11.56.1)

Doctoral candidate – Doctoranda

Silvia Redondo García

Thesis supervisor – Director de Tesis

Juan Carlos Rodríguez-Manzaneque Escribano

Granada, 2022

Genyo CENTRO PFIZER-UNIVERSIDAD DE GRANADA-JUNTA DE ANDALUCÍA DE **GENÓMICA** E **INVESTIGACIÓN ONCOLÓGICA**

Editor: Universidad de Granada. Tesis Doctorales
Autor: Silvia Redondo García
ISBN: 978-84-1195-505-8
URI: https://hdl.handle.net/10481/96723

CRITERIOS DE CALIDAD PARA OPTAR AL GRADO DE DOCTOR POR LA UNIVERSIDAD DE GRANADA

QUALITY CRITERIA TO APPLY FOR THE DEGREE OF PHD BY THE UNIVERSITY OF GRANADA

- Publicación en una revista de impacto en el ámbito de conocimiento de la tesis doctoral firmada por el doctorando, que incluya parte de los resultados de la tesis.
  Publication in a relevant journal in the field of knowledge of the Doctoral Thesis signed by the doctoral student, which includes part of the results of the Thesis.

  Rodríguez-Baena, FJ*., **Redondo-García, S*.,** Peris-Torres, C., Martino-Echarri, E., Fernández-Rodríguez, R., Plaza-Calonge, MC., Anderson, P. & Rodríguez-Manzaneque, JC. (2018). **ADAMTS1 protease is required for a balance immune cell repertoire and tumour inflammatory response**. *Scientific Reports*, 8:13103. DOI: 10.1038/s41598-018-31288-7. *Equal contribution.

  > Este artículo ha sido publicado en la revista *Scientific Reports* (ISSN: 2045-2322), con un factor de impacto en el año 2018 de 4.011 y en el 2020 de 4.379, ocupando la posición 15 de las 69 de la categoría MULTIDISCIPLINARY SCIENCES del Rank title del Journal Citation Reports Science Edition en el momento de la publicación del artículo (2018). Esta revista pertenece al cuartil Q1.
  This article has been publish in Scientific Reports journal (ISSN: 2045-2322), with an impact factor of 4.011 in 2018 and 4.379 in 2020, ocupping the 15thposition of a total of 69 in the Multidisciplinary Science category of Rank title of Journal Citation Reports Science Edition at the moment of the publication of the article (2018). This journal belongs to Q1 quartile.

CRITERIOS DE CALIDAD PARA OPTAR AL GRADO DE DOCTOR CON MENCIÓN INTERNACIONAL POR LA UNIVERSIDAD DE GRANADA

QUALITY CRITERIA TO APPLY FOR THE DEGREE OF INTERNATIONAL PHD BY THE UNIVERSITY OF GRANADA

- Estancia de al menos tres meses en un centro de investigación de prestigio de un país extranjero.
  Stay of at least three months in a prestigious research centre in a foreign country.

  Estancia de seis meses en el Tumor Stroma and Matrix Immunology Group, Center for Cancer Immune Therapy, Herlev Hospital, Herlev, (Dinamarca), desde el 31 de marzo de 2018 hasta el 3 de agosto de 2018, y desde el 26 de agosto de 2018 hasta el 23 de octubre de 2018. El nombre del proyecto es "Desarrollo de inmunoterapias anticancerígenas en modelos tumorales murinos: Valoración de la combinación con terapias antiangiogénicas y análisis de la contribución de la matriz extracelular", supervisado por el Dr. Daniel H. Madsen
  Six-month stay in the Tumor Stroma and Matrix Immunology Group, Center for Cancer Immune Therapy, Herlev Hospital, Herlev, (Denmark), from March 31st, 2018 to August 3rd, 2018 and from August 26th, 2018 to October 23rd, 2018. Project name was "Desarrollo de inmunoterapias anticancerígenas en modelos tumorales murinos: Valoración de la combinación con terapias anticancerígenas y análisis de la contribución de la matriz extracelular", supervised by Dr. Daniel H. Madsen.

- Informe de la tesis por dos expertas/os doctoras/es pertenecientes a alguna institución de educación superior o instituto de investigación no española.
  Thesis report by two PhD experts belonging to a non-Spanish higher education institution or research institute.

  Experta/*Expert* #1: Vanessa Morais Freitas, of the University of Sao Paulo.
  Experto/*Expert* #2: Marco Carretta, of the IO Biotech, Copenhagen, Denmark.

- Idioma de presentación de la tesis.
  Thesis presentation language.

  Esta tesis ha sido redactada y será defendida en inglés. Además, siguiendo los requerimientos de la Universidad de Granada, algunas partes están redactadas también en español (Resumen y Conclusiones). Dichas secciones serán defendidas en español.
  This Thesis has been written and will be defended in English. In addition, following the requirements of the University of Granada, some parts are also written in Spanish (Abstract and Conclusions). Such sections will be defended in Spanish.

TABLE OF CONTENTS

ABSTRACT

During the last decades, the way to study cancer has changed enormously. The former simplistic view defining tumours as a mass of cancer cells has evolved, consolidating now the co-participation of heterogeneous tumour and stromal cells, including fibroblasts, immune and endothelial cells, and also non-cellular components. Among the non-cellular constituents, the dynamism of the extracellular matrix is gaining great prominence, although more research is still needed. During tumour progression, remodelling of the extracellular matrix by proteases is essential for processes such as angiogenesis, invasion or immune regulation. In our group, we have been contributing to the knowledge of the extracellular protease ADAMTS1 (A Disintegrin and Metalloproteinase with Thrombospondin Motifs 1), the first member described of the ADAMTS family. To date, ADAMTS1 is known by its controversial role in cancer depending on the tumour type and context. It participates in angiogenesis and metastasis, and recent research has showed that this and other members of the ADAMTS family are regulating the immune system in cancer and other diseases.

Our earlier results showed that, whereas murine B16F1 melanoma tumours were reduced in deficient mice for ADAMTS1 (Ats1-KO), Lewis Lung Carcinoma (LLC) tumours were not affected in such background. Importantly, B16F1 and LLC tumours are highly immunogenic and sensitive to anti-angiogenic treatment, while LLC ones are poorly immunogenic and resistant. Knowing this different behaviour, we investigated how ADAMTS1 and its activities in the ECM could impact in those differences. Our studies using Ats1-KO mice to address stromal ADAMTS1 were complemented with Adamts1-inhibited tumour cell lines, focusing on its tumour origin.

Although the initial evaluation of tumour vasculature already revealed a common increase of vessel density in Ats1-KO conditions in both models, we still needed to expand our approaches to explain these differences in growth. For that, the increasing interest of the immune regulation by extracellular proteases motivated us to evaluate the immune environment of the Ats1-KO mouse, first in healthy animals and later in tumour-bearing mice.

Importantly, spleen and bone marrow of healthy animals displayed a pro-inflammatory phenotype, mostly represented by T cells, in Ats1-KO mice, although data on myeloid cells suggested a potential anti-inflammatory role. Then, we performed *in vitro* experiments with bone marrow-derived macrophages, revealing that their migratory and phagocytic abilities were compromised in the absence of the

protease, without affecting adhesion and polarisation. Definitively, all these results define ADAMTS1 as an immunomodulatory molecule.

Additional studies corroborated the distinct effect of these tumour cell lines on macrophage polarization, uncovering a main induction of a M2-protumorigenic phenotype by the conditioned media of LLC. Indeed, these assays allowed us to discover that the inhibition of ADAMTS1 in these cells provoked the polarisation of macrophages to an M1 pattern, suggesting the possible mediation of this effect by a variety of extracellular molecules such as Versican, osteopontin, IL33 and LDLR.

Our later studies were focused on the contribution of ADAMTS1 in the tumour immune compartment. Interestingly, B16F1-Ats1-KO tumours resemble the healthy mice immune landscape. However, the presence of LLC tumours provoked major alterations in the immune landscape challenging the supposed advantages of the Ats1-KO mouse to reduce tumour growth.

To confront this issue, we assessed RNA sequencing of tumours. These analyses of specific gene signatures related to inflammatory response and matrisome showed relevant differences. Interestingly, the comparison between B16F1-Ats1-KO and LLC-Ats1-KO tumours showed that the first ones had a reduced cell migration and motility and a higher T cell migration and chemotaxis, reflecting how the absence of ADAMTS1 modulates the differences that exist between the models.

Finally, we addressed the possible common mechanisms between the anti-angiogenic resistance of LLC tumours and the absence of effect of these tumours to the genetic deletion of ADAMTS1. Suggestively, these complex studies revealed that the absence of ADAMTS1 did not alter the final resistance of LLC model to our anti-angiogenic therapy, involving myeloid-derived suppressor cells but also pro-tumorigenic macrophages.

Concluding, this work reinforce and emphasize the newly described immunomodulatory functions of ADAMTS1, mainly reflected in the alteration of immune populations in spleen, bone marrow and tumours, but also according to our functional assessments of macrophages. Among future perspectives, main actions need to be pursued to unveil the implication of type I interferon pathway or collagen organisation, for example. Nevertheless, studying the putative contribution of the proteoglycan Versican and its proteolysis needs to be specially highlighted according its recognized activities in macrophage polarisation and immunosuppression, even to be considered as a therapeutic target.

RESUMEN

En las últimas décadas, la forma de estudiar el cáncer ha cambiado enormemente. La antigua visión simplista que consideraba un tumor como una masa de células tumorales similares entre sí ha evolucionado, consolidando la participación de otras células tumorales y células estromales como fibroblastos, células inmunes y endoteliales, y componentes no celulares. Dentro de esos componentes no celulares, el dinamismo de la matriz extracelular ha ganado interés, aunque se necesita un estudio más detallado. Durante la progresión tumoral, el remodelamiento de la matriz extracelular mediada por proteasas es esencial durante procesos como la angiogénesis, la metástasis o la regulación inmune. En nuestro grupo hemos contribuido al conocimiento acerca de la proteasa extracelular ADAMTS1 (A Disintegrin and Metalloproteinase with Thrombospondin Motifs 1), primer miembro descrito de la familia ADAMTS. ADAMTS1 es conocida por su papel dual en cáncer según el tipo tumoral y el contexto, participando en angiogénesis, metástasis, y como ha sido recientemente descrito, en la regulación del sistema inmune en cáncer y otras patologías, al igual que otros miembros de la misma familia.

Estudios preliminares de nuestro grupo muestran que el modelo murino de melanoma B16F1 se reduce al ser inyectado en ratones deficientes de la proteasa (Ats1-KO), mientras que el modelo *Lewis Lung Carcinoma* (LLC) no se ve afectado. Por otro lado, el modelo B16F1 se considera altamente inmunogénico y sensible a terapias anti-angiogénicas, al contrario que el modelo LLC, bajamente inmunogénico y resistente. Por todo ello, quisimos saber cómo ADAMTS1 y su actividad proteolítica regulaban esas diferencias. Para ello, usamos ratones Ats1-KO para evaluar la contribución de la proteasa estromal, e inhibimos la proteasa en las líneas celulares para evaluar su contribución tumoral.

Aunque la evaluación inicial de la vasculatura mostraba un aumento similar de la densidad en ambos modelos en ratones Ats1-KO, se necesitan otros análisis para explicar el cambio en el crecimiento del tumor. Para ello, el interés que se está generando entorno a la regulación del sistema inmune mediante proteasas extracelulares nos hizo evaluar el ambiente inmune del ratón Ats1-KO en condiciones fisiológicas y tumorales.

De manera relevante, la ausencia de ADAMTS1 generó un entorno pro-inflamatorio en bazo y médula ósea, principalmente debido a células T. Sin embargo, las poblaciones mieloides también sugieren un potencial ambiente anti-inflamatorio. Por otro lado, la caracterización *in vitro* de macrófagos derivados de médula ósea demostraron que la deficiencia de ADAMTS1 reducía su migración y fagocitosis, sin

afectar su adhesión y capacidad para polarizarse. Por todo ello, estos resultados definen a ADAMTS1 como una molécula inmunomoduladora.

Estudios adicionales demuestran la capacidad de las células tumorales en la polarización de macrófagos, mostrando una inducción de la polarización de macrófagos a M2 por parte del secretoma de las células LLC. Además, estos estudios nos permitieron describir que la inhibición tumoral de ADAMTS1 promovió la polarización de los macrófagos a M1, sugiriendo que moléculas como Versicano, osteopontina, IL33 y LDLR pueden mediar estos cambios

Estudios posteriores acerca de la contribución de ADAMTS1 en la regulación inmune en el tumor reflejan que los tumores B16F1 en ratones Ats1-KO tienen un fenotipo similar al ratón sano. En cambio, la presencia de tumores LLC atenúan las posibles ventajas inmunes generadas por la ausencia de ADAMTS1 para reducir el tumor.

Para confirmar estos cambios, llevamos a cabo una secuenciación del ARN de los tumores y analizamos firmas génicas concretas relacionadas con la respuesta inflamatoria y el matrisoma. De forma relevante, este estudio sugirió que los tumores B16F1-Ats1-KO mostraban una reducción de la migración celular y una mayor citotoxicidad mediada por células T que los tumores LLC-Ats1-KO, reflejando cómo la ausencia de ADAMTS1 modula las diferencias previamente mostradas entre los modelos tumorales.

Finalmente, en este trabajo evaluamos posibles mecanismos comunes entre la ausencia de respuesta en el ratón Ats1-KO y la resistencia a fármacos anti-angiogénicos del modelo LLC. Estos estudios demostraron que la reducción de ADAMTS1 no es capaz de modular dicha resistencia, la cual está mediada por células supresoras mieloides y macrófagos pro-tumorigénicos.

En resumen, este trabajo refuerza y enfatiza las nuevas propiedades inmunomoduladoras descritas para la proteasa ADAMTS1, reflejadas principalmente por la alteración de poblaciones inmunes en bazo, médula ósea y tumores, pero también gracias a los ensayos funcionales realizados con macrófagos. Entre las perspectivas futuras de este trabajo, las líneas más importantes se centran en el estudio de la implicación de las rutas del interferón I y la formación de estructuras de colágeno, entre otras. Sin embargo, el estudio del papel del Versicano y su proteólisis necesitan un estudio más detallado de acuerdo a sus propiedades inmunosupresoras y a su participación en la polarización de macrófagos, debiendo considerarlo como una posible diana terapéutica.

ABBREVIATIONS AND ACRONYMS

ABBREVIATION	DEFINITION
7AAD	7-amino-actinomycin D
AAD	Aortic aneurism and dissection
ADAM	A disintegrin and metalloprotease
ADAMTS	A disintegrin and metalloprotease with thrombospondin motif
ADAMTS1	A disintegrin and metalloprotease with thrombospondin motif 1
ANG-2	Angiopoietin 2
APC	Antigen-presenting cell
ARG1	Arginase 1
Ats1	ADAMTS1
Ats1-KO	Knockout mouse for ADAMTS1
BM	Bone marrow
BMDC	Bone marrow-derived cell
BMDM	Bone marrow-derived macrophages
Breg	Regulatory B cell
BSA	Bovine serum albumin
Bv8	Prokineticin 2
CAF	Cancer-assoaciated fibroblast
CAR	Chimeric antigen receptor
CCL	C-C motif chemokine ligand
CD	Cluster of differentiation
CD163	Macrophage scavenger receptor
CD206	Mannose receptor
cDC	Migratory dendritic cell
cDNA	Complementary cDNA
CFSE	Carboxyfluorescein diacetate succinimidyl ester
CL	Cell lysate
CM	Conditioned medium
COX-2	Cyclooxygenase-2
CRC	Colorectal cancer
CS	Chondroitin sulphates
CSC	Cancer stem cell
CSF	Colony stimulating factor
CTL	Cytotoxic T lymphocytes
CTLA-4	Cytotoxic T lymphocyte-associated antigen 4
CXCL	C-X-C chemokine ligand

ABBREVIATION	DEFINITION
DABCO	1,4-Diazabicyclo(2,2,2)octane
DAMP	Damage-associated molecular patterns
DAPI	4', 6-diamidine-2-fenilindol
DC	Dendritic cell
DMEM	Dulbecco's Modified Eagle's Medium
DMSO	Dimethyl sulfoxide
DNA	Deoxyribonucleic acid
EC	Endothelial cell
ECM	Extracellular matrix
EDTA	Ethylenediamine tetraacetic acid
EGF	Epithelial growth factor
EGF	Epithelial growth factor
EMT	Epithelial-to-mesenchymal transition
FBS	Fetal bovine serum
FC	Flow cytometry
FDA	Food and Drug Administration
FGF	Fibroblast growth factor
FN	Fibronectin
GAG	Glycosaminoglycan
GM-CSF	Granulocyte-macrophage colony-stimulating factor
GO	Gene Ontology
HEK293T	Human embryonic kidney 293T cells
HRP	Horseradish peroxidase
HUVEC	Human umbilical vein endothelial cells
i.p.	Intraperitoneal
ICI	Immune checkpoint inhibitors
IDO	Indole 2,3-dioxygenase
IF	Immunofluorescence
IFN	Interferon
IGF	Insulin growth factor
IGFBP2	Insulin-like growth factor binding protein 2
IgG	Immunoglobulin G
IHC	Immunohistochemistry
IIC	Infiltrating immune cell
IL	Interleukin

ABBREVIATION	DEFINITION
IRF9	IFN regulatory factor 9
ISG	IFN-stimulated gene
ITH	Intra-tumour heterogeneity
KO	Knockout
LDLR	Low-density lipoprotein receptor
LLC	Lewis Lung Carcinoma cell line
LPS	Lipopolysaccharide
MCP	Monocyte chemotactic protein
M-CSF	Macrophage colony-stimulating factor
MDSC	Myeloid-derived suppressor cell
MHC-I	Major histocompatibility class I
MMP	Matrix metalloproteinase
MPAEC	Mouse primary aortic endothelial cells
NID1	Nidogen 1
NID2	Nidogen 2
NK	Natural killer
NO	Nitric oxide
NOS2	Nitric oxide synthase 2
P/S	Penicillin/Streptomycin
PBS	Phosphate buffered saline
PCA	Principal Component Analysis
PD-1	Programmed cell death protein 1
PDGF	Platelet derived growth factor
PD-L1	Programmed cell death 1 ligand 1
PF4	Platelet factor 4
PFA	Paraformaldehyde
PG	Proteoglycan
PGE2	Prostaglandin E2
PHA-P	Phytohemagglutinin P
PlGF	Placental growth factor
PVDF	Polyvinylidene difluoride
qPCR	Quantitative polymerase chain reaction
RBC	Red blood cell lysis buffer
RGD	Arg-Gly-Asp domain
RIN	RNA integrity value

ABBREVIATION	DEFINITION
RIPA	Radioimmunoprecipitation assay
RNA	Ribonucleic acid
RNAseq	RNA sequencing
RT	Room temperature
s.c.	Subcutaneous
SDF1	Stromal cell-derived factor 1
SDS-PAGE	Sodium dodecyl sulphate polyacrylamide gel electrophoresis
SEM	Standard error of the mean
SMA	Smooth muscle actin
STAT	Signal transducer and activator of transcription
TAM	Tumour-associated macrophages
TAN	Tumour-associated neutrophils
TEM	TIE2-expressing TAM
TFPI-2	Tissue factor pathway inhibitor 2
TGFβ	Transforming growth factor β
Th1	$CD4^+$ T helper 1 cell
Th2	$CD4^+$ T helper 2 cell
TIMP	Tissue-inhibitors of metalloproteases
TKI	Tyrosine kinase inhibitor
TLR	Toll-like receptor
TME	Tumour microenvironment
TNFα	Tumour necrosis factor α
Treg	Regulatory T cells
TSP	Thrombospondin
TSR	Thrombospondin type 1 repeat
uPA	Urokinase-type plasminogen activator
vBM	Vascular basement membrane
VCAN	Versican
VEGF	Vascular endothelial growth factor
VEGFR	VEGF receptor
WB	Western blot
WT	Wild type
α2M	α2-macroglobulin

INTRODUCTION

1. The heterogeneity of cancer

Decades ago, cancer research was focused on the malignancy of cancer cells, trying to understand how the regulation of oncogenes and tumour suppressor genes transform normal cells into cancerous. However, after years of research, the development of new tools such as genome sequencing or transcriptional profiling and all the data they generate, a new tumour concept has appeared and cancer is currently studied as a complex and heterogeneous environment (Hanahan & Coussens, 2012).

1.1. New tumour concept and hallmarks of cancer

The existence of tumour heterogeneity was already identified in the 1800s due to morphological and histological variations, genetic and growth rates abnormalities and altered response to therapies among different tumours. Indeed, those observations postulated that genetically distinct tumour sublines were the result of natural selection following Darwinian evolutionary patterns. According to it, genetic changes that provide selective advantage to a tumour sub-clone may lead to its dominance in the cancer cell population (Caiado, Silva-Santos, & Norell, 2016)(Marusyk & Polyak, 2010). However, this simplistic view of cancer being an homogeneous mass of cancer cells has been deeply refuted (Hanahan & Weinberg, 2000)(Hanahan & Weinberg, 2011)(Hanahan & Coussens, 2012)(Hanahan, 2022).

In their first approach, Hanahan and Weinberg proposed that the simplistic view of the tumour concept should be replaced by a new one, introducing new players such as other type of cells (Hanahan & Weinberg, 2000). In this review, they included the relevance of fibroblasts, endothelial and immune cells which instruct their neighbour cells by paracrine and autocrine signals. This crosstalk between all the players evolved in the definition of six hallmarks that tumours acquire during tumorigenesis (Hanahan & Weinberg, 2000). In 2011, they formulated other two new hallmarks and two enabling characteristics, and reviewed the previous ones, including in this case the recruitment of cells such as pericytes, cancer stem cells, immune inflammatory cells or invasive cells, and the relevance of non-cellular components (Figure 1) (Hanahan & Weinberg, 2011). Finally, this year Hanahan has updated this cancer conceptualization with two new enable characteristics and two new hallmarks up to a total of 14 concepts, which are summarised in the following lines (Figure 2).

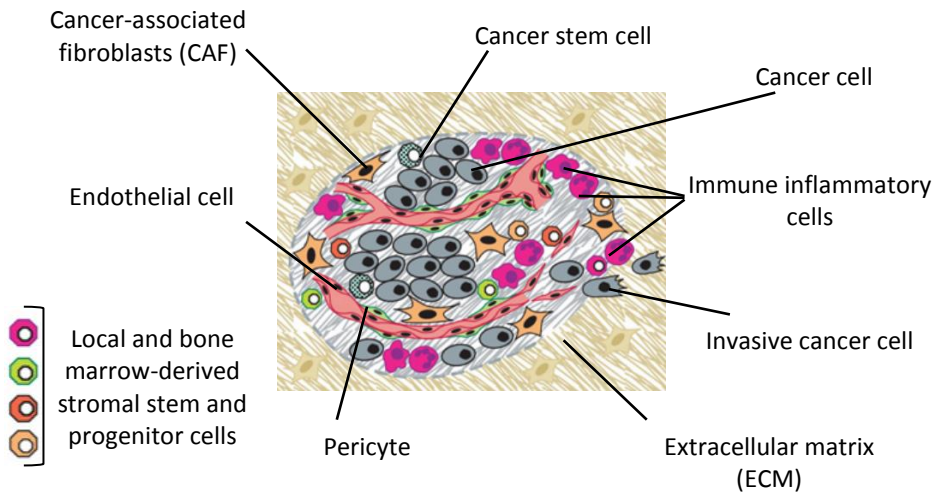

Figure 1. Core of primary tumour. Distinct cell types constituting most solid tumours and regulating their progression. Apart from the cancer cells, there are others which have both tumour-promoting and tumour-killing functions, such as cancer-associated fibroblasts, endothelial cells and pericytes, inflammatory cells, and cancer stem cells and invasive cells. The representation also includes the extracellular matrix. Adapted from (Hanahan and Weinberg, 2011).

Among the six firstly described hallmarks that enable tumour growth and metastatic dissemination, these authors talk about *sustaining proliferative signalling*, regarding the production and release of growth-promoting signals that make the cells self-sufficient in order to proliferate. Closely related is the second hallmark, *evading growth suppressors*. Once tumour cells are independent to the environment to grow, they have to avoid all the cell programs that negatively regulate cell proliferation and maintain cellular quiescence The third one, *resisting cell death*, refers to the ability of cancer cells to trigger the apoptosis mechanisms in response to physiologic stress, and the forth, *enabling replicative immortality*, remarks the capacity of avoiding senescence. *Inducing of accessing vasculature* was other defined concept, which is very relevant for this work, so it will be extendedly discussed later (Introduction, section 3). Finally, they described *activating invasion and metastasis* as the sixth hallmark, referring to the ability of tumour cells to disseminate to other tissues by altering their shape and their attachment to other cells and the extracellular matrix (ECM) (Hanahan & Weinberg, 2000) (Figure 2).

In their second work one decade later, Hanahan and Weinberg added *deregulating cellular metabolism* as a new hallmark, due to the necessity of tumour cells to reprogram their metabolism to achieve their effective proliferation (Hanahan & Weinberg, 2011). Moreover, they included the concept of “enabling characteristics”

in order to describe tumour features that are essential to acquire the described hallmarks. Among these characteristics, they defined *genome instability and mutation*, which refers to the ability of acquiring selective advantages and which was speculated since tumour heterogeneity discovery. Likewise, they also included *avoiding immune destruction* and *tumour-promoting inflammation* as hallmark and enabling characteristic, respectively. Again, due to the particular relevance of these processes for this work, they will be fully discussed in section 2 of this introduction (Hanahan & Weinberg, 2011) (Figure 2).

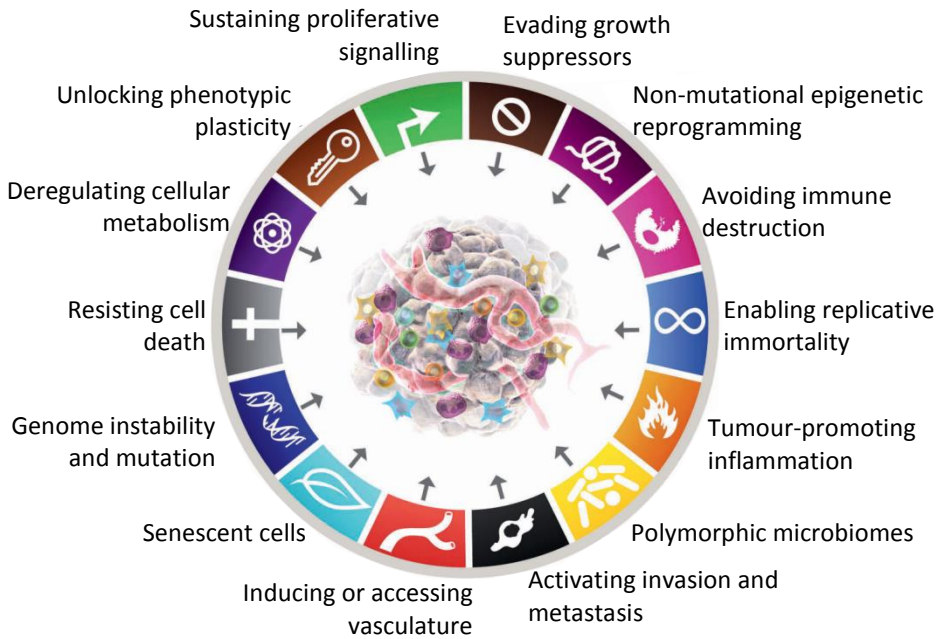

Figure 2. Hallmarks of cancer. State of the art regarding the canonical and already described hallmarks of cancer, which are mostly generic to multiple forms of human cancer. Adapted from (Hanahan, 2022).

Finally, in his later review, Hanahan incorporated four new terms (Hanahan, 2022). First, he included u*nlocking phenotypic plasticity*, known as the disruption of the differentiation process. Secondly, he also added *non-mutational epigenetic reprogramming*, referring to the gene-regulatory circuits that in tumour cells are governed by corrupted mechanisms which are independent to genome instability and gene mutation (other core hallmark). The third one was *polymorphic microbiome*, which intersects with other hallmarks but which can have its own identity due to its potential to modulate cancer development, progression and response to therapies. And finally, he introduced *senescence cells*, mechanism that is

activated to maintain homeostasis, and which is underwent by cancer cells. However, nowadays it is known that in certain contexts, senescence cells stimulate tumour progression (Figure 2) (Hanahan, 2022).

All these hallmarks describe different characteristics of tumour cells and environment, which are mostly common to all the tumour types. In fact, they are crucial in the generation and regulation of the complexity and heterogeneity of the tumour, which orchestrate tumour behaviour since its early development.

1.2. Intra-tumour heterogeneity (ITH)

All the cellular and non-cellular components that form the tumour microenvironment (TME), as well as the crosstalk between them, modulate the heterogeneity that is specifically found in every tumour. There are different levels of tumour heterogeneity according to their nature; between patients, within the same patient, and within the cells that are located in the same tumour (intra-tumour heterogeneity, ITH). All of them have been derived from genetic, epigenetic and transcriptional alterations between tumours (Hausser & Alon, 2020). This thesis is focused on the different components of the TME and their crosstalk. For that reason, we will only consider ITH for this and future sections.

As mentioned, ITH refers to the complex environment that is found in a tumour, in which coexists cells with different phenotypic and molecular features within the same tumour. This heterogeneity can be spatial (occurring at the same time in different locations of same patient) or temporal (with variations in the same lesion over time), as well as it can be the result of linear or branched tumour evolution (Figure 3). On the one hand, linear pattern refers to a tumour cell with selective growth advantages that form a clone that is able to outcompete the preceding one, surviving only dominant clones. On the second hand, in the branched evolution pattern there are different populations that emerge from a common ancestral clone at different moments, but co-existing between them (Dagogo-Jack & Shaw, 2018).

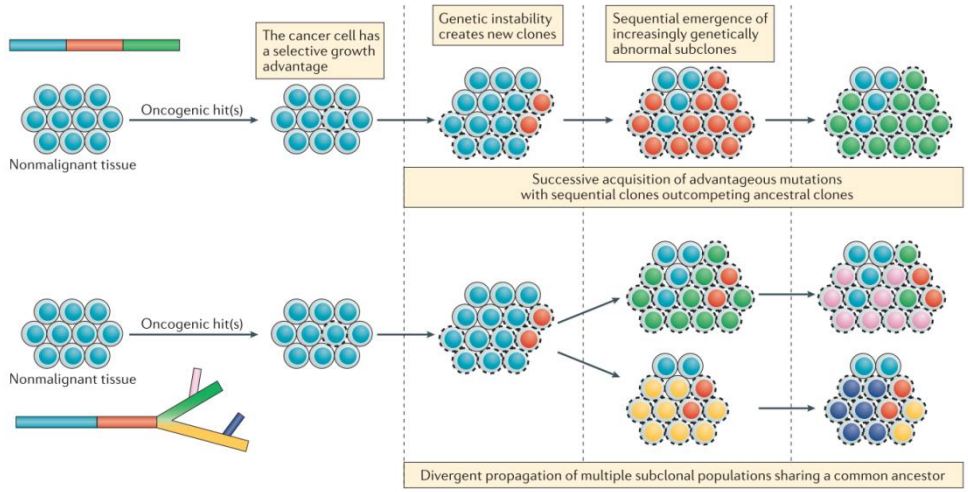

Figure 3. Linear and branched tumour evolution. Patters of evolution within the context of clonal selection. Adapted from (Dagogo-Jack and Shaw, 2018).

Moreover, it has been explained by different models, which are not exclusive. One model defends a Darwinian pattern, in which stochastic and unpredictable subsequent genetic alterations within neoplastic cells can create sub-clones with evolutionary advantages that would force their nature selection, evolving in a malignant tumour. This old model has been corroborated by next-generation sequencing and bioinformatics tools (Caiado et al., 2016)(Marusyk & Polyak, 2010)(Marusyk, et al., 2020). However, it is known that ITH does not manifest exclusively at genetic level, but also at epigenetic, transcriptional, phenotypic, metabolic and secretory ones (Vitale, et al., 2021). A second model, part of the non-genetic sources of ITH, is the epigenetic regulation one, which includes the biochemical modification of the deoxyribonucleic acid (DNA), histones and nucleosomes among other components, whose regulation is aberrant in cancer (Caiado et al., 2016). These alterations are critical for the establishment of the cell-type-specific gene expression pattern, and will be essential for the transcriptomic, proteomic and phenotypic variability (Hinohara & Polyak, 2019)(Vitale et al., 2021). Furthermore, the regulation of these processes in tumour cells can trigger the crosstalk with other cells (Dagogo-Jack & Shaw, 2018)(Marusyk et al., 2020). The third model refers to the hierarchical cellular differentiation, closely related to the concept of cancer stem cells (CSCs). This model suggest that a fraction of tumour cells (CSCs) possess the ability of both self-renew and differentiation, and are the responsible for the maintenance and progression of tumours. Moreover, this model is intimately related to the previous ones, since genetic and non-genetic alterations

can provide to the CSCs their plastic phenotype (Marusyk & Polyak, 2010)(Caiado et al., 2016).

As previously mentioned, these three models (genetic, epigenetic and hierarchical) explaining ITH are closely interconnected and all of them take part during tumour progression, revoking the idea of the most simplistic tumour concept. Indeed, all the genetic, epigenetic and cellular differentiations that provoke ITH are the responsible of the complex TME that regulates tumour behaviour (Junttila & Sauvage, 2013)(Vitale et al., 2021). Due to those models of evolution and the complexity that they generate, cellular and non-cellular components and their crosstalk is being increasingly studied. For that reason, and due to the relevance for this work, TME will be presented individually in the next section.

1.3. Tumour microenvironment (TME)

Knowing that tumour is not as simply as a mass of cancerous cells, years of research has demonstrated that TME and tumour-cell-interactions are essential during tumour progression. In addition, the co-existence and crosstalk between tumours cells and the cellular and non-cellular components of the stroma are topics of interest (Marusyk & Polyak, 2010). Studies following this new perspective have documented that while stromal cell constituents act as barrier against tumorigenesis, when they are found in aberrant TME, possess diverse contributions toward cancer phenotypes. These changes in the stroma involved the recruitment of cell types such as fibroblasts, endothelial cells (ECs), immune cells and the remodelling of the ECM, as it occurs during organ development (Junttila & Sauvage, 2013) (Figure 1). In fact, in 2012, Hanahan and Coussens detailed how each cell type is involved in the regulation of each specific hallmark that was already defined by that time, what is summarised in Figure 4 (Hanahan & Coussens, 2012). Next, most relevant types of cells in the TME and their roles are briefly presented. However, depending on the tumour type, other cell populations can be also found.

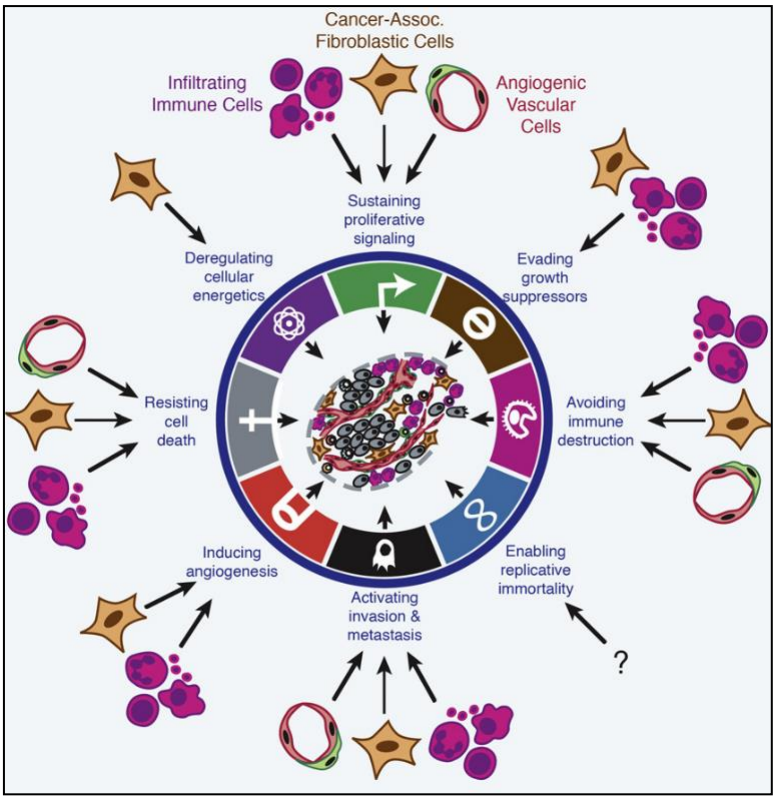

Figure 4. Contribution of recruited stromal cells to cancer hallmarks. Illustration showing the contribution of specific player of TME (infiltrating immune cells, cancer-associated fibroblasts and angiogenic vascular cells) to the eight hallmarks that were described by Hanahan and Weinberg in 2011. Adapted from (Hanahan & Coussens, 2012).

1.3.1. Cancer-associated fibroblasts (CAFs)

Normal fibroblasts are responsible of suppressing tumour formation. However, the education and differentiation of resident fibroblast into CAFs in response to injured tissue cause organ fibrosis and enhances the risk of cancer (Biffi & Tuveson, 2020). CAFs have pro-tumorigenic functions due to their extensive cytokine secretion. Among all the signalling molecules secreted by this type of cells, some of them are mitogenic such as epithelial growth factor member (EGF), fibroblast growth factor (FGF), insulin-like growth factor I (IGF1) or stromal cell-derived factor 1 (SDF1/CXCL12), which promote tumour malignancy. Moreover, CAFs also induced epithelial-to-mesenchymal transition (EMT) and favours metastasis through the secretion of transforming growth factor β (TGFβ), molecule that is also related to the

suppression of the immune system (named as immunosuppression) (Balkwill, et al., 2012). Apart from that, CAFs express pro-inflammatory molecules that support tumour growth by recruiting and educating infiltrating immune cells. Furthermore, CAFs are well-known by their main role in the synthesis and remodelling of a neoplastic ECM, different to the normal stroma, due to the high production of ECM components and remodelling proteases. Finally, CAFs are involved in the regulation of tumour angiogenesis. Firstly, because they produce pro-angiogenic factors such as vascular endothelial growth factor (VEGF), FGF2 and platelet derived growth factor (PDGF) (Siemann, 2010). Secondly, due to the fact that CAFs are the major producers of ECM, in which pro-angiogenic factors are sequestered. And finally, they contribute indirectly to tumour angiogenesis because CAFs secrete chemoattractants for pro-angiogenic macrophages and neutrophils that stimulate the recruitment of endothelial precursors (Junttila & Sauvage, 2013)(Biffi & Tuveson, 2020).

1.3.2. Infiltrating immune cells (IICs)

The second important group of cells are the infiltrating immune cells (IICs). In this group, there are lymphoid and myeloid lineage cells, which can have both pro- and anti-tumorigenic roles. Among these cells, TME includes T and B lymphocytes, tumour-associated macrophages (TAMs), natural killer cells (NKs), myeloid-derived suppressor cells (MDSCs), neutrophils and dendritic cells (DCs). The balance of all the cells is the responsible of promoting tumour progression (Balkwill et al., 2012). However, as in the case of angiogenic vascular cells and due to their relevance for this work, they will be presented in an independent section (Introduction, section 2).

1.3.3. Angiogenic vascular cells

Angiogenesis refers to the processes by which new capillaries are created from pre-existing ones (Yoo & Kwon, 2013). When a blood vessel is stimulated by angiogenic signals from malignant or immune cells, or in certain environments as hypoxic ones, endothelial cells (ECs) start sprouting to form new vessels. Moreover, tumour vasculature is chaotic and needs supporting cells. Pericytes cover those vessels in order to reduce vessel leakiness and to improve blood flow. However, these structures are not well-established in tumours, increasing metastasis and reducing the recruitment of immune cells that block tumour progression (Balkwill et al., 2012).

Nevertheless, due to the relevance of angiogenesis mechanisms during this project, this topic will be extensively discussed in the next section (Introduction, section 3).

1.3.4. Other TME cellular components

Despite the main and well-known roles of these three groups of cells, several works support the relevance of additional components to the TME that were not directly involved in the hallmarks reviewed in 2012. Among these components, CSCs have been identified as one of the most relevant, since their self-renew ability allows them to initiate new tumours (Hanahan & Coussens, 2012). Although less studied, there are other cellular types that are known to have relevant role in tumour growth. Some cancers display a relevant contribution of adipocytes, which can recruit malignant cells whose growth is potentiated by adipokines. Moreover, apart from endothelial vessels, lymphatic vasculature is also involved in tumour cell dissemination when lymphatic vessels are stimulated by VEGFc and VEGFd from tumour cells (Balkwill et al., 2012). Moreover, microbiome has been increasingly studied due to its described connection to TME. It has been reported that microbiome acts locally and at distant sites, secreting toxic metabolites or oncogenic products or inducing inflammation and immunosuppression. Moreover, it also affects to the response to therapies. Finally, it is known that even the nervous system participates in tumour development, since its interaction with cancer cells remodel the immune infiltrate and vascularization (Laplane, et al., 2019). Apart from the cellular components, ECM is one of the key contributors to tumour progression. It participates in processes such as immune cell infiltration, angiogenesis or tumour dissemination among others. However, since it is one of the main pillars of this research, it will be explained in a following section (Introduction, section 4).

ITH and the complexity that it produces in the TME are extremely dynamic and are continuously being remodelled. Indeed, there are two main principles leading their evolution along tumour progression. First, it is known that each cell type suffers continuous changes around a spectrum of phenotypic and behavioural states in response the alterations in their environment, differently to what was defended by classical models of tumour evolution. This is particularly represented by CAFs or IICs, which can have two opposite functions depending on the environment, but which move through different states with other characteristics (Figure 5A). And secondly, that these alterations must occur behind a threshold. There is an optimal fitness that tumour cells can tolerate in order to maintain their plasticity and adaptability to the

environment but without having cell survival or compartment architecture compromised (Vitale et al., 2021) (Figure 5B).

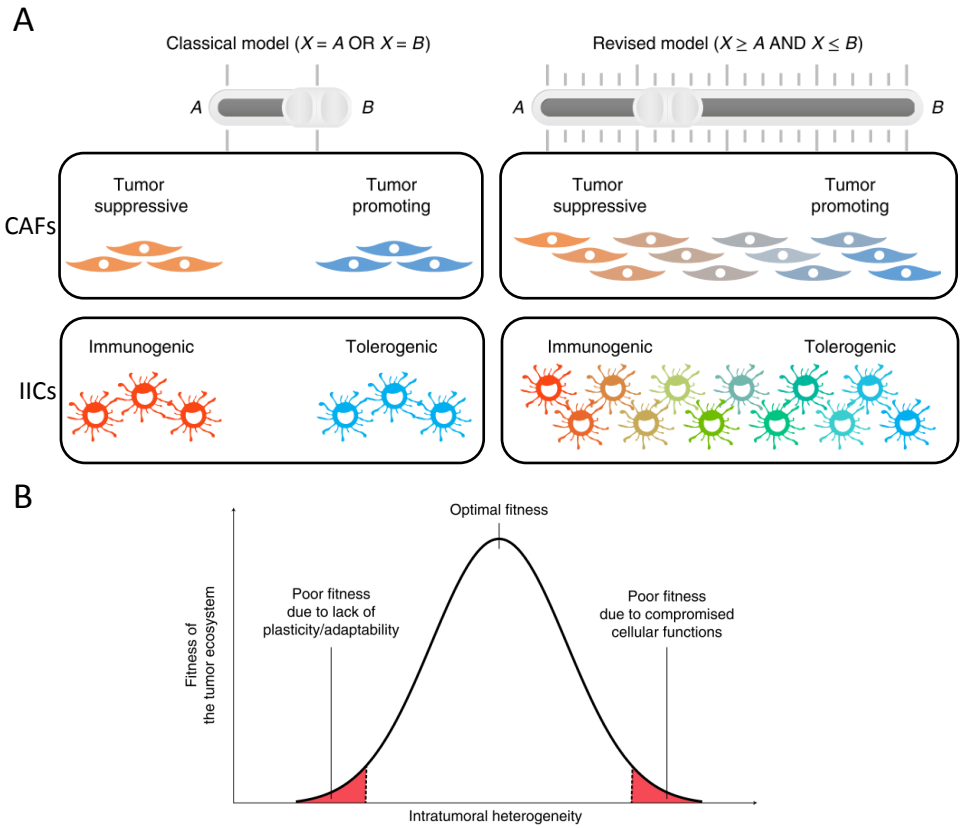

Figure 5. Principles governing ITH and TME. (A) Illustration of the plasticity of some TME players along tumour progression, moving from the classical model of two states (left) to the continuous one (right). (B) Graph simulating the threshold of ITH that is tolerated by TME to support tumour progression. Adapted from (Vitale et al., 2021).

2. Relevance of inflammation and immune system during tumour progression

In 1863, Rudolf Virchow proposed a likely connection between inflammation and cancer (Li et al., 2020). However, it was not until 2011 and after years of research that *avoiding immune destruction* and *tumour-promoting inflammation* were considered as an emerging hallmark and an enabling characteristic, respectively. For that reason, immune system and inflammation have become a very relevant topic for oncology research (Hanahan & Weinberg, 2011).

During normal wound healing or infection, immune inflammation is a transitory mechanism. This ancient well-known process involves activation, recruitment and effect of innate and adaptive immune cells to restore homeostasis and prevent loss of tissue function (Khandia & Munjal, 2020). In this context, inflammatory response can be executed by three interdependent mechanisms. Firstly, local immune cells proliferate when slight insults take place. Secondly, there can be a recruitment of cells from bone marrow (BM) or lymphoid tissues due to strong insults. And thirdly, the environment enhances the recruitment and local activation of inflammatory cells (Greten & Grivennikov, 2019). The first line of defence is represented by innate immune cells such as macrophages, NKs, DCs, granulocytes and innate lymphocytes. In response to damage-associated molecular patterns (DAMPs), these cells secrete cytokines and chemokines to recruit other cells, initiating the immune response. Consequently, macrophages and mast cells secrete matrix-remodelling enzymes and cytokines to activate surrounding stromal cells. Then, DCs are the responsible of linking innate cells and antigen-specific lymphocytes of adaptive immune response. This linking allows the clonal expansion of naïve T cells and their recognition of foreign antigens. As a result, these T lymphocyte populations eliminate the threat, inflammation is resolved and homeostasis is re-established (Pitt et al., 2016).

Nevertheless, in the case of cancer there is a persistent and chronic inflammation in which some cells produce factors that are consumed by others, as loop of inflammation-induced signalling and inflammatory cell recruitment. Moreover, inflammatory cells are recruited from the BM to the TME, where they are educated by different types of cells and secreted factors in order to sustain tumour cells (Greten & Grivennikov, 2019)(Garner & de Visser, 2020) (Figure 6).

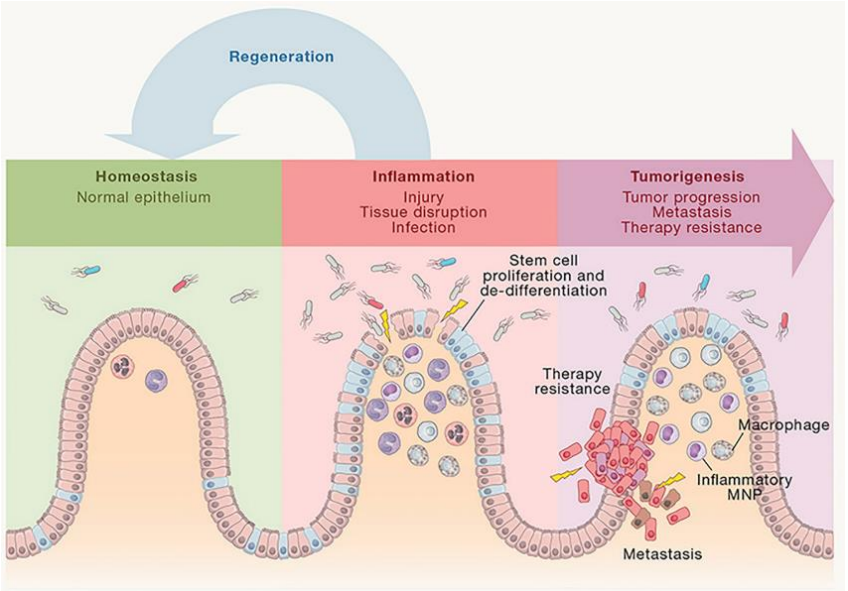

Figure 6. Inflammatory progression during tumour development. After tissue damage, inflammation starts and stem cells proliferate and expand to regenerate the tissue. However, if inflammation is not resolved and is transformed in chronic inflammation, tumours are generated as well as immunosuppressive immune cells are recruited, evolving in metastasis and therapy resistance. (Adapted from (Greten & Grivennikov, 2019).

It has been defended that inflammation at early stages of tumour progression can accelerate tumour genetic evolution towards more malignant states (Hanahan & Weinberg, 2011). Moreover, this immunosuppressive environment can be produced by an activation of the transcription factors that induce angiogenesis and immune evasion (Greten & Grivennikov, 2019). In tumours, these factors are continuously activated in myeloid and tumour cells. Finally, hypoxia or exhausted T cells also trigger the immunosuppressive environment (Li et al., 2020).

2.1. Relevant immune cell types

It was firstly thought that IICs in tumours were limited to DCs, cytotoxic T lymphocytes (CTLs) or NKs with anti-tumorigenic roles, exerting immunosurveillance functions and immunological sculpting of ITH. However, now it is known that there is a group of IICs such as regulatory T cells (Treg), alternatively activated macrophages (M2) or MDSCs, that contribute to evade immune destruction by shaping the TME towards a more tumour-permissive state, limiting immunological killing and tumour

cell eradication (Pitt et al., 2016)(Greten & Grivennikov, 2019)(Li et al., 2020). Following, all the immune cells involved in inflammation and immune response will be presented, trying to follow their consecutive appearance in inflammatory processes, when possible.

2.1.1. Dendritic cells (DCs)

As it was explained before, DCs are specialized antigen-presenting cells (APCs) that decide if adaptive immunity needs to be activated or not, and which are found in almost every tissue (Gonzalez et al., 2018). For that response, they activate naïve and memory T cells through co-stimulatory molecules and cytokines (Garner & de Visser, 2020). While high infiltration of mature DC has been associated with good prognosis, low number has been linked to a non-favourable clinical outcome. Moreover, infiltration of DCs is related with delayed tumour progression and metastasis, being less found in invasive tumours (Khandia & Munjal, 2020). These anti-tumoral DCs are recognised by the expression of CD11c, CD8 and CD103 markers on their surface, improving the engulfment and presentation of tumour antigens.

In spite of it, antigen presentation can result also in antigen tolerance, impairing NKs and T cell activity and favouring tumour progression. However, there is a need of better understanding how anti-tumour NK- and T-cell attack fails to contain tumour development (Gonzalez et al., 2018). Moreover, the same immunotolerance can be derived from dysfunctional and/or reduced numbers of migratory DCs (cDC1) that move antigens to lymph nodes. Furthermore, even when cDC1 infiltrate tumours, other factors can alter DC and T cell action (Garner & de Visser, 2020).

2.1.2. T and B lymphocytes

These cells belong to the adaptive immunity and, after TAMs, T cells are extensively found in tumours. Depending on the immunological context, they can acquire inflammatory or anti-inflammatory roles. At early stages of tumour development, naïve T cells are produced and recruited to the TME in order to eliminate cancer cells after antigen presentation by DCs. For that reason, high content of T cells evolves in high immunogenicity and correlates with good prognosis. In the beginning, T cells might not recognise tumour antigens as foreign since they are arisen from host cells. Nevertheless, rapid proliferation of tumour cells and necrosis are highly

immunogenic (Garner & de Visser, 2020). Then, $CD8^+$ T cells expand and differentiate into CTLs, what results in the destruction of tumour cells. Moreover, the $CD4^+$ T helper 1 (Th1) population provokes also anti-tumoral activity of macrophages and NKs by the secretion of pro-inflammatory cytokines such as tumour necrosis factor α (TNFα) and interferon ɣ (IFNɣ) (Pitt et al., 2016)(Figure 8). In spite of it, at advanced stages cancer cells are able to create an immunosuppressive environment that impairs T cell activity and infiltration, and increase the recruitment of Treg (Garner & de Visser, 2020). Moreover, Th1 cells can shift towards $CD4^+$ T helper 2 cells (Th2), which also have immunosuppressive roles due to the secretion of inflammatory cytokines (Goswami et al., 2017). According to it, T cell activity depends on the ability of DCs to present external antigens, on the inhibitory signals that impair T cell action and on the balance between Th1 and Th2 response (Gonzalez et al., 2018)(Figure 7).

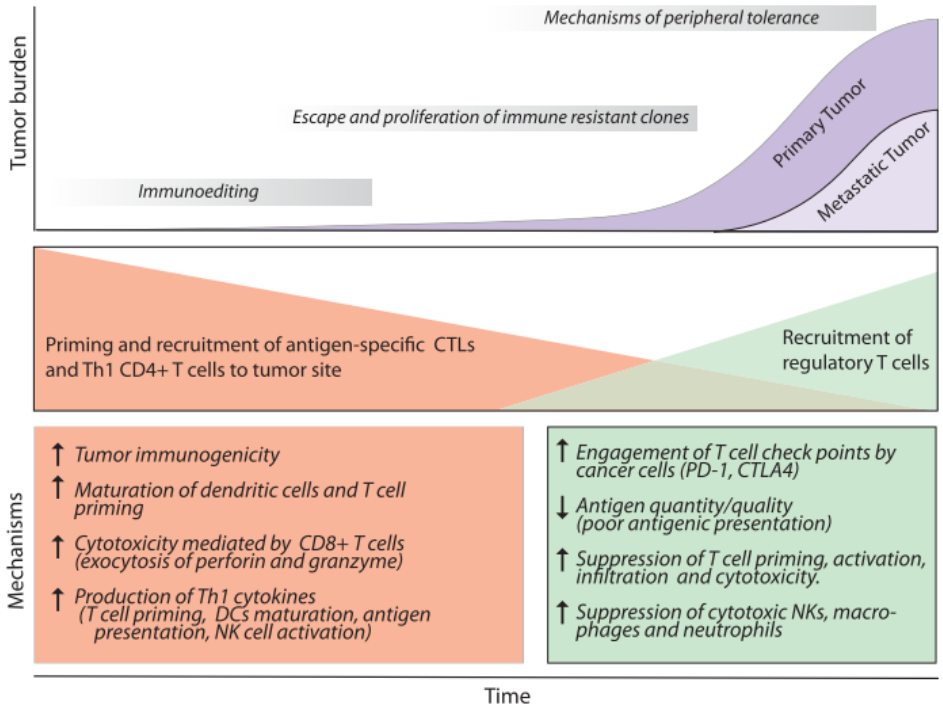

Figure 7. Dual T cell activity in tumour progression. Evolution of T cell roles at different tumour stages. While they have anti-tumorigenic properties at early stages, environmental pressure select tumour variants that evade immune recognition and increase Treg recruitment. Adapted from (Gonzalez et al., 2018).

The specific population of Treg is responsible for suppressing Th1 and CTLs cells as well as macrophages, NK cells or neutrophils, evolving in worse patient prognosis

(Figure 7). This population is mainly induced by the tryptophan catabolization by the indole 2,3-dioxygenase (IDO), an enzyme that is mainly expressed by cancer cells and myeloid cells (Pitt et al., 2016). Moreover, they promote tumour-progression due to the secretion of tumour-promoting cytokines (Greten & Grivennikov, 2019). These lymphocytes are well recognised by the expression of FoxP3 and CD25 markers on their surface, and their immunosuppression is mediated by contact-dependent mechanisms involving cytotoxic T lymphocyte-associated antigen 4 (CTLA-4), programmed cell death protein 1 (PD-1) and programmed cell death 1 ligand 1 (PD-L1), which are basic molecules for immunotherapy, a current leading treatment for primary tumours such as melanoma, which will be discussed later in this section (Shiao et al., 2011). Moreover, contact-independent mechanisms have been also described, including sequestration of pro-inflammatory cytokines or the production of anti-inflammatory ones such as IL10, TGFβ or prostaglandin E2 (PGE2) among others (Gonzalez et al., 2018).

Finally, although classically disregarded for analysis, B lymphocytes, which are the responsible of secreting memory cells against pathogens, are currently being explored. However, its role in cancer progression is not well understood. Indeed, some works support their tumour-promoting role by secreting immunosuppressive molecules (IL10 or TGFβ) or by the activation of angiogenesis and myeloid cells. This population has been defined as regulatory B cells (Breg) (Gonzalez et al., 2018).

2.1.3. Natural killer cells (NKs)

Natural killer cells (NK) are a type of innate immune system cells that provoke a rapid and powerful cytotoxic response. NKs are mainly recruited by IL15 and target cancer cells when they do not express major histocompatibility class I (MHC-I), inducing their programmed cell death. Otherwise, NKs function would be inhibited (Gonzalez et al., 2018). Moreover, these cells attack tumour cells by producing granzyme B and perforin or by death-receptor mediated pathways. Apart from that, a minor subset of circulating NKs secretes IFNɣ, TNFα, IL6 and C-C motif chemokine ligand 5 (CCL5), what enhances anti-tumour immunity (Bruno, Mortara, Baci, Noonan, & Albini, 2019). Although high infiltration of NKs relates to good prognosis, their deficiency does not correlate with increased tumours (Khandia & Munjal, 2020). In spite of it, it has been described that there is a population of NKs called tumour infiltrated NKs that are known by their pro-angiogenic and pro-metastatic functions (Bruno et al., 2019).

2.1.4. Tumour-associated macrophages (TAMs)

Macrophages are innate immune cells of myeloid lineage, differentiated from extravasated monocytes and defined as phagocytic cells (Garner & de Visser, 2020). They are found in different tissues in order to defend the organism from pathogens, as well as maintain tissue homeostasis and remodelling, and eliminate cellular debris (Khandia & Munjal, 2020). Indeed, during tumoral chronic inflammation, macrophages participate at different levels from neoplastic transformation to therapy resistance (Pitt et al., 2016)(Gonzalez et al., 2018).

Under the long-term influence of TME and chronic inflammation, macrophages can polarise towards two main stages with different functions (Vitale et al., 2021), although they are not stable and exclusive states as it is shown in Figure 8. Nevertheless, this thesis work focuses in these two main populations of polarised macrophages.

During carcinogenesis, monocytes are recruited after chronic inflammation by the secretion of monocyte chemotactic protein 1 (MCP-1/CCL2) and CCL5/RANTES. Moreover, other chemokines have been also described as monocyte-attractants (CCL3, CCL4, CCL8/MCP-2 and CCL22) as well as other TME factors such as hypoxia, necrosis, macrophage-colony stimulating factor (M-CSF/CSF1) and VEGFa (Goswami et al., 2017). On the one hand, at early tumour stages TAMs can be activated by lipopolysaccharide (LPS) and IFNɣ, resulting in macrophages polarised to M1/pro-inflammatory/classically activated (K. Wu et al., 2020). Those M1 macrophages have anti-tumorigenic properties and can be recognised by the detection of markers on their surface, although those markers are highly controversial (Mantovani et al., 2002)(K. Wu et al., 2020). The most extensively used ones are CD68, CD80, CD86 and also intracellular markers such as enzyme inducible nitric oxide synthase (iNOS/NOS2) (K. Wu et al., 2020)(Figure 8), Moreover, this anti-tumorigenic population secretes pro-inflammatory cytokines and chemokines (IL1β, IL6, IL12, IL23, TNFα, CXCL9 and CXCL10) and nitric oxide (NO) that block tumour growth both directly and indirectly and increase the recruitment of CTLs and NKs (K. Wu et al., 2020).

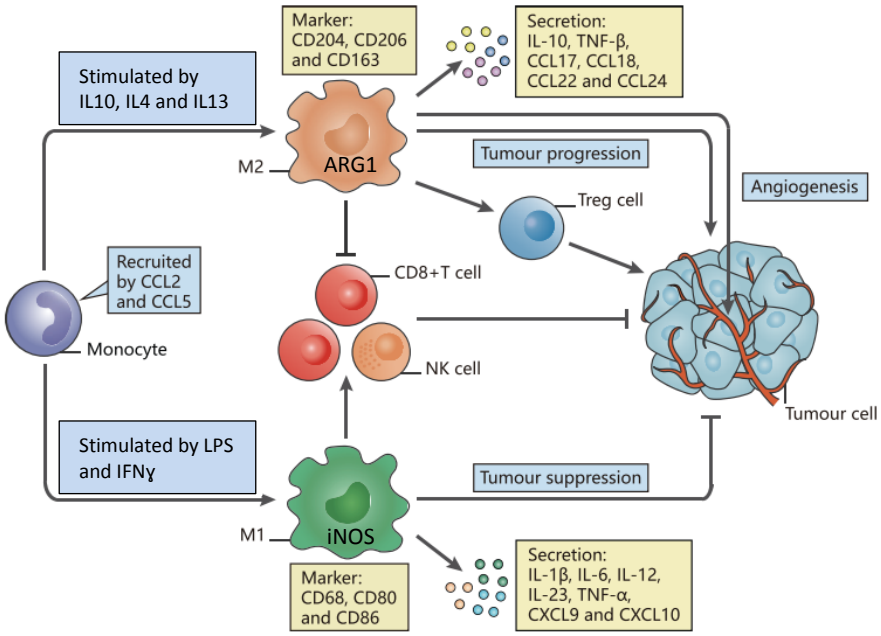

Figure 8. Two main macrophage polarisation states and functions. Monocytes are recruited to TME by CCL2 and CCL5. There, they polarise to M1 or M2 depending on the secreted cytokines and the immune environment. These polarised macrophages release different cytokines that affect to the recruitment and action of other immune cells, as well as to tumour progression and angiogenesis (Wu et al., 2020).

On the other hand, recruited macrophages can be activated by IL4, IL10 and IL13, cytokines that are secreted in the TME mainly by Treg and Th2 cells (Khandia & Munjal, 2020). These molecules polarise macrophages to M2/anti-inflammatory/alternatively activated state. Despite the controversy in the field, the most used markers are CD204, macrophage scavenger receptor (CD163) and mannose receptor (MR/CD206) on their surface and the enzyme arginase 1 (ARG1) (Shiao et al., 2011)(Khandia & Munjal, 2020). In this case, M2 macrophages secrete immunosuppressive cytokines including IL10, CCL18, CCL22 and CCL24, which block the action of CTLs and NKs, increase the recruitment of Treg to the tumour and promote tumour growth, EMT and angiogenesis (Figure 8). Similar to the balance between Th1 and Th2 T lymphocytes, the ratio between M1 *versus* M2 macrophage can lead the different immune response(K. Wu et al., 2020). Indeed, M1 TAMs are involved in Th1 response since they are able to present antigens, although less efficiently than DCs (Garner & de Visser, 2020). On the contrary, M2 TAMs are activated by the same cells and anti-inflammatory cytokines that activate Th2 T cells.

Due to their essential role in tumour development and dissemination, M2 macrophages require special attention in tumour progression and in this project. Apart from the recently explained role in suppressing the immune response, as it was mentioned before, this population promotes tumour angiogenesis via secretion of VEGF, PDGF, TGFβ, pro-angiogenic chemokines (C-X-C motif chemokine ligand 1 (CXCL1), CXCL8, CXCL12/SDF1, CXCL13, CCL2 and CCL5) and remodelling enzymes (matrix metalloproteinases MMPs and cyclooxygenase-2 COX-2) (Stockmann et al., 2014)(Goswami et al., 2017). Moreover, these enzymes not only affect angiogenesis, but also ECM remodelling and tumour invasiveness. In fact, proteolytic enzymes such as MMPs, plasmin, urokinase-type plasminogen activator (uPA) and its receptor are continuously remodelling ECM composition (Goswami et al., 2017)(Gonzalez et al., 2018). Figure 9 summarises the different roles of M2 macrophages in cancer (Sica et al., 2006).

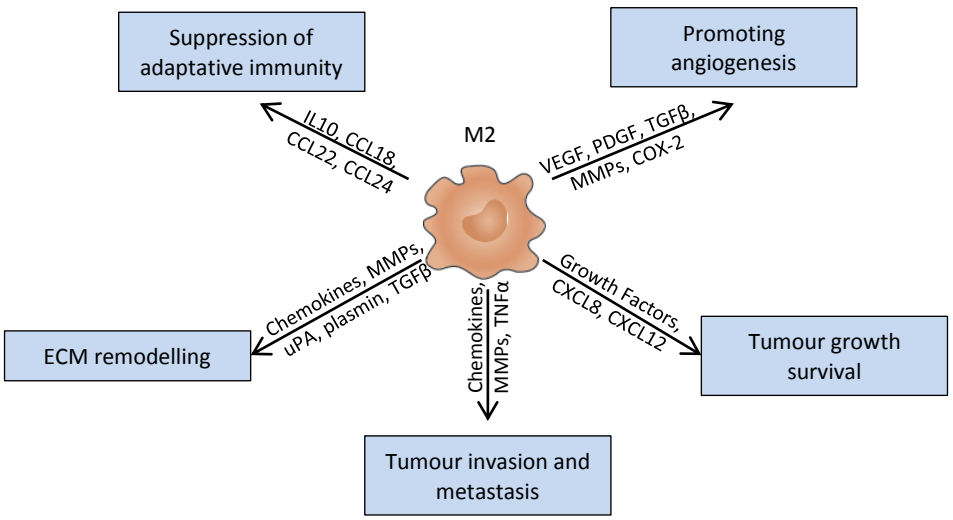

Figure 9. Roles of M2 macrophages in cancer. Scheme including the different cancer-related pathways in which M2 pro-tumorigenic macrophages are involved due to the secretion of different molecules. Adapted from (Sica et al., 2006).

2.1.5. Tumour-associated neutrophils (TANs) and myeloid-derived suppressor cells (MDSCs)

In addition to the differentiated macrophages, there are partially differentiated myeloid progenitors in tumours, which are intermediaries between circulating cells of BM origin and differentiated immune cells (Shiao et al., 2011). In this group of cells, it is particularly interesting the tumour-associated neutrophils (TANs) and MDSCs. There is a clear controversy in the scientific community regarding the identity of both populations, since some works define them as the same population, whereas others differentiate them. Both populations have been attributed with immunosuppressive functions. However, the problem arises from the markers on the surface of the murine populations (Gonzalez et al., 2018)(Garner & de Visser, 2020). For this study, as it will be detailed in the material and methods section, both CD11b and Gr1 markers were used for MDSCs detection, always considering that it comprises a heterogeneous population but which has been defined as immunosuppressive. Nevertheless, in this introduction, they will be presented individually.

Neutrophils are the main effector cells in inflammation. As in the case of monocytes or DCs, they do not have their local precursors in the tissue. For that reason, their action in tumour progression takes place after precursor recruitment (Greten & Grivennikov, 2019). At early stages of tumour development, neutrophils are found only in the periphery of the tumour. However, when inflammation starts, they are recruited to modulate it by mechanisms such as phagocytosis, so their infiltration has been associated with adverse prognosis (Garner & de Visser, 2020). Similar to M1/M2 TAMs or Th1/Th2 T cells, TANs can be mainly divided in N1 (activated by type I IFN) and N2 (activated by TGFβ), with similar anti- and pro-tumorigenic properties that other dual populations (Khandia & Munjal, 2020)(Li et al., 2020). N2 TANs create an immunosuppressive environment that recruit Treg and TAMs and block the action of CTL and NKs (Garner & de Visser, 2020)(Li et al., 2020). Moreover, N2 TANs regulate tumour angiogenesis by secreting MMP9 for the release of VEGF and CXCL1/KC as well as promote metastasis by the secretion of other remodelling enzymes (Gonzalez et al., 2018)(Khandia & Munjal, 2020).

In the case of the immunosuppressive population of MDSCs, their infiltration has been linked to a reduced infiltration of cytotoxic T cells in tumours. Moreover, they are closely related to tumour cells and the TME can differentiate them into TAMs. They are recruited by cytokines and chemokines such as IL17, CCL2, CCL5, CXCL8/IL8 and CXCL12/SDF1 and secrete immunosuppressive cytokines such as PGE2, ARG1, NO, TGFβ, COX-2, IDO or IL10 (Bruno et al., 2019). Moreover, MDSCs can block IFNɣ

production, what inhibits CTL and NKs activity and transforms $CD4^+$ T cells into Treg, enhancing immune evasion (Bruno et al., 2019)(Garner & de Visser, 2020)(Mabuchi, Sasano, & Komura, 2021). As all the pro-tumorigenic immune cells, MDSCs also promote angiogenesis, invasion and EMT (Li et al., 2020)(Mabuchi et al., 2021)(Figure 10). Most works study these populations not only in the tumours but also in blood, spleen and BM. This illustrates the immunomodulatory capacity of these cells, which educate the environment and produce a systematic regulation of immune populations (Garner & de Visser, 2020). Indeed, these $CD11b^+/Gr1^+$ have been found to mediate the resistance to different therapies, such as anti-angiogenic one (Shojaei et al., 2007)(Shiao et al., 2011). For all the described aspects, high infiltration of this population correlates with bad prognosis (Bruno et al., 2019).

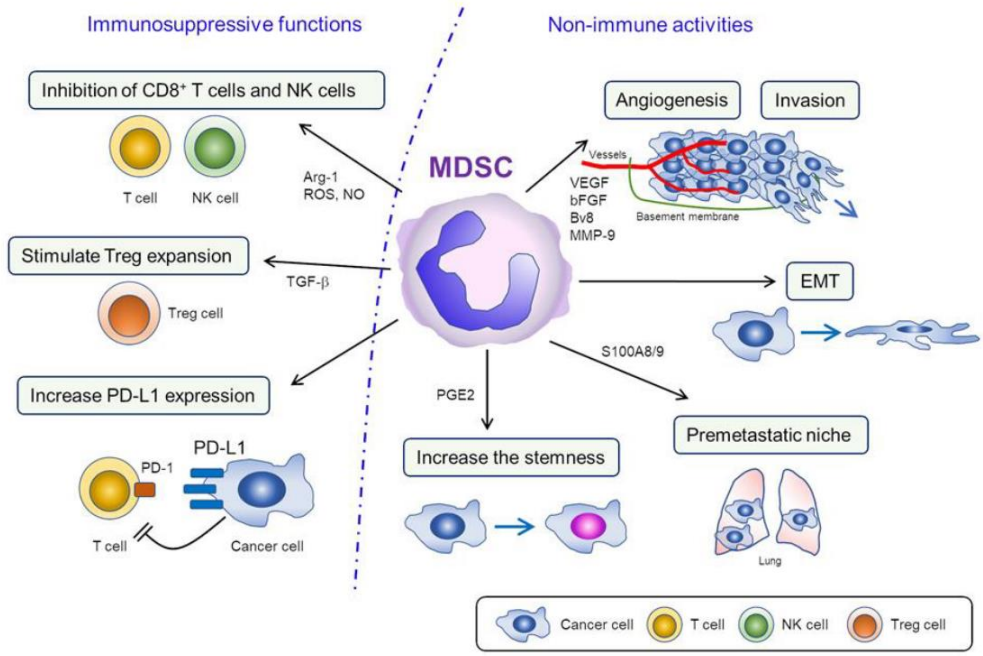

Figure 10. Myeloid-derived suppressor cells (MDSCs) functions in cancer. Roles of MDSC during cancer development both regarding immunosuppression (left) and other pro-tumorigenic mechanisms (right). Adapted from (Mabuchi et al., 2021).

As it has been described before, all the infiltrated immune cells are plastic and have different roles depending on the environment (Figure 11). Indeed, large tumours create a more immunosuppressive environment, both locally and systemically. For that reason, oncological research is focusing its attention in the modulation of this

pro-tumorigenic environment towards anti-tumorigenic, mimicking the one that is found at early stages (S. I. Kim, Cassella, & Byrne, 2021).

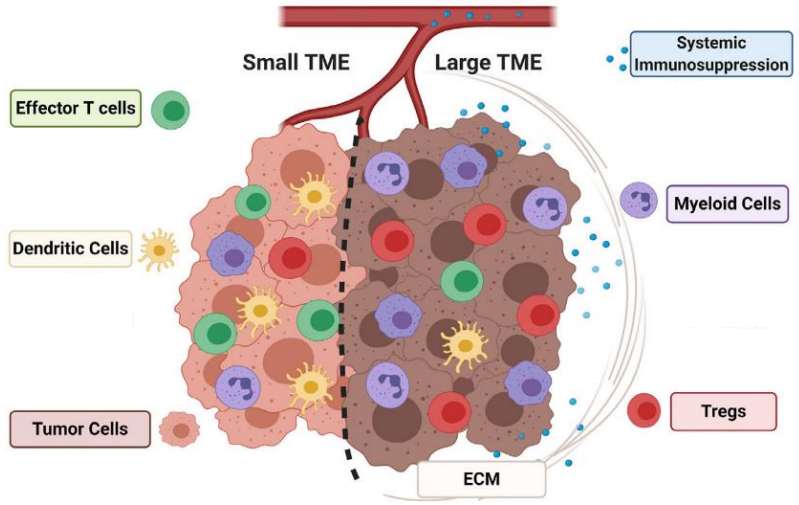

Figure 11. Different infiltrated immune cells at different tumour stages. At early stages of tumour progression (left), tumours are mainly infiltrated by effector T cells and DCs. However, at later stages TME shift to a more immunosuppressive landscape, including the infiltration of myeloid cells (TAMs, TANs and MDSCs) and Treg. Moreover, this advance stage is also known by the increased ECM deposition. Adapted from (Kim et al., 2021).

The crosstalk between the different components of the TME affects several processes and cancer hallmarks (Figure 4). They participate in cancer hallmarks such as *sustaining of the proliferative signalling* and *evading growth suppressors* by the secretion or liberation from the ECM of mitogenic agents. Moreover, they enhanced the *resistance to cell death* by altering tissue integrity and participate in *activating invasion and metastasis* by the secretion of remodelling enzymes and pro-invasiveness cytokines. Finally they *induce angiogenesis, metabolism reprogramming* and *immune destruction evasion* due to the infiltration of pro-angiogenic and immunosuppressive subpopulations (Hanahan & Coussens, 2012).

2.2. Use of immunotherapy

As it has been previously detailed, immune system and inflammatory response are crucial in tumour development. In fact, the crosstalk between immune cells and the proportions of the different populations orchestrate opposite immune responses. For

that reason, great efforts have been put in order to modulate the immune landscape, appearing immunotherapy as new anti-tumoral strategy. The efficacy of immunotherapy on different patients shows a lot of variability depending on their immune profile before therapy. For that reason, it is important to define it prior to start the treatment (Junttila & Sauvage, 2013)(Binnewies et al., 2018). There are three immune profiles (Figure 12).

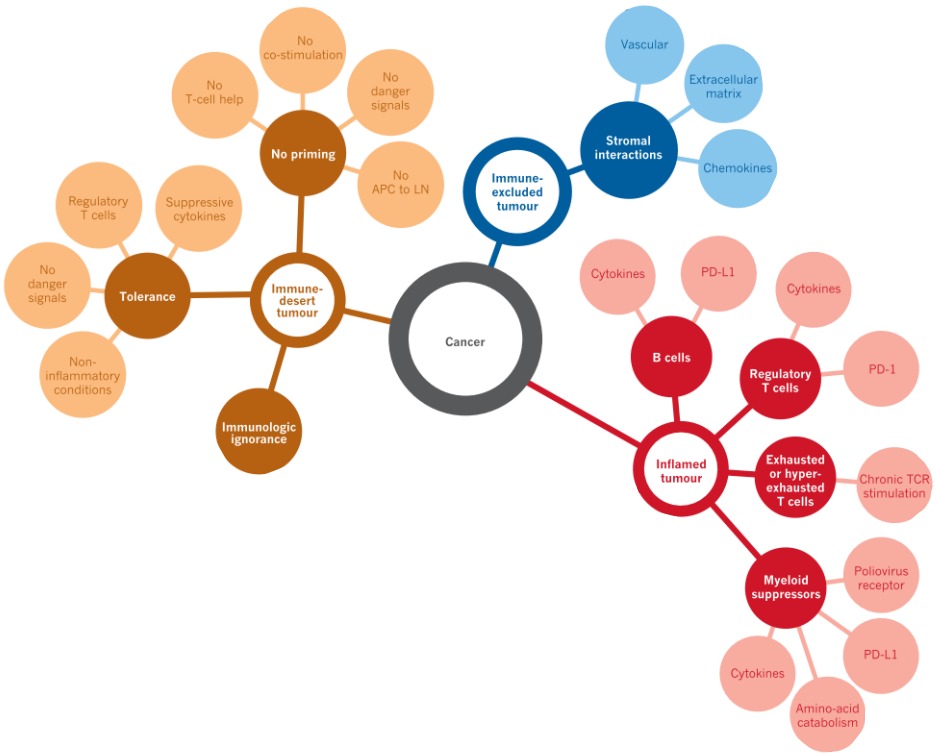

Figure 12. Immune profiles in cancer attending to the immune infiltration. According to the mechanisms that defend the host from cancer, tumours can be classified as immune-dessert (brown) when immune system is almost absence, immune excluded (blue) when they have barriers that block the infiltration and action of the immune system in the tumour nests and inflamed (red) when they have infiltration of immunosuppressive immune cells. Adapted from (Chen & Mellman, 2017).

The first profile is called immune-inflamed (Figure 12, red branches), which has a high infiltration of PD-1-expressing T cells, apart from myeloid cells and pro-inflammatory cytokines. Moreover, in this case immune cells are located close to tumour cells. They are also known as highly immunogenic or “hot” tumours due to their immune infiltration (Binnewies et al., 2018) (Figure 13B). This prolife indicates an arrest of a

pre-existing anti-tumour immunity, probably due to the immunosuppressive environment generated by Treg, exhausted T cells or myeloid cells. Patients with this type of tumours are the ones with more probability to respond to immunotherapy, but might be insufficient (Gajewski, Schreiber, & Fu, 2013)(Chen & Mellman, 2017). Secondly, immune-desert tumours (Figure 12, brown branches) are characterised by the poor infiltration of CTLs both in the parenchyma and the stroma, but with presence of myeloid cells. This environment forces the immunologic ignorance of the tumour, which reflects an absence of pre-existing anti-tumour immunity. The third profile is represented by immune-excluded tumours (Figure 12, blue branches). In this group, abundant immune cells are retained in the stroma and do not penetrate into the tumour parenchyma. These tumours suggest that there was an inefficient pre-existing immunity (Chen & Mellman, 2017). Both immune-desert and immune-excluded tumours are considered as non-inflamed tumours, also known as poorly immunogenic or "cold" (Figure 13A). Indeed, response to immunotherapy is almost inexistent in both cases, due to the absence of tumour-specific T cells in immune-desert tumours or due to the deficient T cell migration in immune-excluded ones (Binnewies et al., 2018). For that reason, therapeutic strategy in these cases is focused on enhancing inflammation (Gajewski et al., 2013).

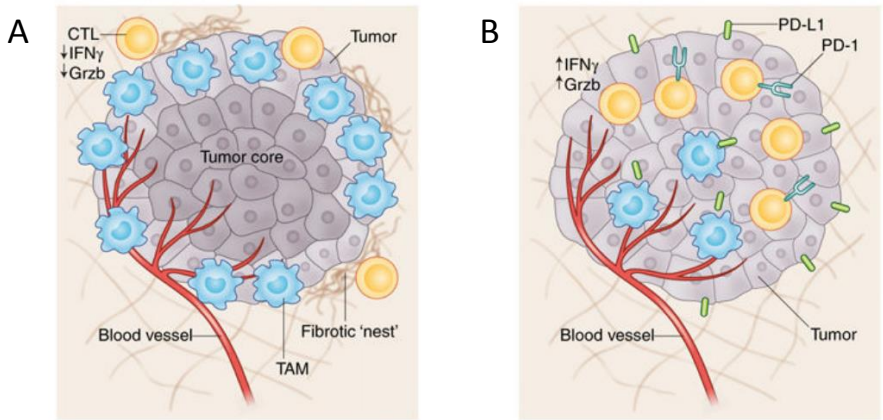

Figure 13. Immune profile of cold and hot tumours. Representation of the immune landscape of (A) cold tumours, with poor infiltration in the tumour parenchyma and higher representation of myeloid cells than T cells, and (B) hot tumours, where T cells are highly represented inside de tumour mass. Adapted from (Binnewies et al., 2018).

Taking into consideration the existence of these profiles, but also the complexity of tumour heterogeneity, current immunomodulatory therapies are focused on the

reactivation of cytotoxic cells (increasing the infiltration or the functionality of T cells) or on the inhibition of immunosuppressive cells (mainly Treg, TAMs and MDSCs) (Shiao et al., 2011)(Junttila & Sauvage, 2013).

When talking about immunosuppression, MDSCs are ones of the major players in this phenomenon. There are four main strategies against this population. The first one consists on the depletion of MDSCs by inducing their apoptosis or by inhibiting their production. For this purpose, it is extensively described the use of antagonists of Gr1 and granulocyte-macrophage colony-stimulating factor (GM-CSF), but also of CXCR2, CXCR4, PGE2 or COX-2. Another strategy resides in preventing their recruitment using chemokine receptor antagonists, while the third strategy tries to inhibit their immunosuppressive role using inhibitors of pathways related to COX-2 or IDO among others. Finally, MDSCs can be reduced by differentiating these immature cells into mature non-immunosuppressive ones by vitamins D3, E, or all-trans-retinoic acid (Shiao et al., 2011)(Goswami et al., 2017) (Bruno et al., 2019)(De Cicco et al., 2020)(Kim et al., 2021)(Mabuchi et al., 2021).

Similar to MDSCs, pro-tumorigenic roles of TAMs are blocked by different strategies. First, macrophages can be depleted by DNA-binding agents that are selective toxic to monocytes or by anti-VEGF therapies due to their high production of VEGF. Moreover, this depletion can be also carried using clodronate liposomes, which will be used in this project. Thanks to their phagocytic activity, TAMs engulf liposomes containing clodronate, which is toxic for the cells. As a result, TAMs go into apoptosis. The second strategy is focused on the limitation of TAM recruitment using chemokines antagonists or inhibitors of CD11b, CCL2 and CSF1R. Since TAMs are mature cells, in contrast to MDSCs, the third strategy is based on their reprogramming to suppress M2 state (blocking COX-2 pathways, for instance) or reprogramming to M1 state (treating with IFNα) (Shiao et al., 2011)(Goswami et al., 2017)(Poh & Ernst, 2018). Furthermore, macrophages are important cells not only in tumours but also during infections and to maintain the homeostasis. For that reason, reprogramming strategies are more effective than the previous ones, taking into consideration the necessity of a balance between M1 and M2 macrophages for other processes. Other strategy against TAMs resides in their phagocytic capacity. Tumour cells express CD47 on their membrane as a “don’t-eat-me” signal. Antibodies targeting CD47 can improve tumour cell clearance by macrophages. Finally, since TAMs express PD-L1, the use of immune checkpoint inhibitors (ICIs) is also indicated to inhibit this population (Shiao et al., 2011)(Goswami et al., 2017)(Li et al., 2021)(S. I. Kim et al., 2021).

As part of the immunosuppressive populations, Treg have been also aim of therapies. In this case, treatment is focused mainly on the use of anti-CD25 antibodies. This marker is highly expressed in Treg. However, it is also expressed by activated anti-tumorigenic T cells, so blocking this molecule can have non-desired effect (Shiao et al., 2011)(Gajewski et al., 2013). Other strategies consist on targeting glucocorticoid-induced TNF receptor family related protein via agonistic antibody or the use of agonistic CD40 administration (Goswami et al., 2017)(S. I. Kim et al., 2021).

The reduction of these MDSCs, TAMs and Treg immunosuppressive cells make tumours sensitive to immunotherapy, allowing the activation of cytotoxic T cells and therapeutic response. Nevertheless, it is necessary to study whether their combination with other therapies such as chemotherapy, radiotherapy or anti-angiogenic treatments can even enhance the therapeutic potential (Shiao et al., 2011)(Zhao & Subramanian, 2017).

In addition to the reduction of immunosuppressive landscape, increasing T cell cytotoxicity is also necessary. Intra-tumour T cell activity is blocked by different mechanisms. On the one hand, tumours cells, as well as some immunosuppressive cells or exhausted T cells expressed on their surface PD-L1 (and PD-L2). This molecule is the ligand of PD-1 which is expressed by T cells. When ligand and receptor interact, T cell inhibitory signalling is induced (Zhao & Subramanian, 2017). On the other hand, when CTLA-4 (expressed by T cells) interacts with CD80/86 (expressed by DCs) T cell expansion and migration is blocked (Pitt et al., 2016)(He & Xu, 2020). For that reason, the use of ICIs that block the interaction of T cells with the cells that block their action have gained ground and have been approved for clinical use. In fact, when monoclonal antibodies against these molecules disrupt those interactions, there is an increase of CTLs infiltration and survival in the tumour (Chen & Mellman, 2017). Moreover, these and others ICI have drastically improved the clinical outcome of patients. Nevertheless, the higher efficacy has been observed only at early stages, and sometimes when more than one ICIs were used (S. I. Kim et al., 2021). For that reason, it is essential to define the immune phenotype of each patient before the treatment, and sometimes ICIs are only indicated when there is a high expression of PD-L1 together with a infiltration of CTLs (Gajewski et al., 2013).

Finally, to avoid resistance and the negative impact of ICIs, there are alternative treatments that have gained interest in oncology. Other known therapies are the co-stimulation of molecules to increase anti-tumour activity, the use of cancer vaccines and oncolytic viruses to induce a tumour-specific adaptive immune response, the

activation of antigen-presenting cells such as DCs, or the use of adoptive and chimeric antigen receptor (CAR) T cell therapies (S. I. Kim et al., 2021).

Immune profiling is essential to understand tumour behaviour and prognosis. Although several therapies have been designed to benefit from the anti-tumorigenic role of immune cells, it is not the only factor that must be considered during tumour progression. Tumour vasculature and angiogenesis are key parameters give the fact that immune cells are recruited into tumours after their mobilization through the blood stream.

3. Angiogenesis as a key factor in tumour development

The growth of new capillaries from pre-existing blood vessels is called angiogenesis. This phenomenon, in which different and complex cellular events take place, is essential in a variety of physiological processes since fetal development to tissue repair (Yoo & Kwon, 2013). The main aim of angiogenesis is supplying of oxygen and nutrients to all the tissues and disposing of waste, although it is also necessary for the extravasation of immune cells to inflammatory sites. For that reason, every alteration of normal vascularisation contributes to several diseases such as inflammatory disorders, neurodegeneration, blinding eye diseases or cancer. Indeed, in adults, angiogenesis only occurs during female reproductive cycle and under pathological circumstances (Carmeliet & Jain, 2011a)(Jászai & Schmidt, 2019).

3.1. Angiogenesis in physiological conditions

Blood vessels are formed by ECs that are structured in a monolayer and interconnected by junctional molecules such as VE-cadherin or claudins that maintain the structure of the tube (Viallard & Larrivée, 2017). Moreover, those quiescent ECs are covered by pericytes, supporting and stabilising cells that suppress EC proliferation and which secrete cell-survival signals. Both ECs and pericytes generate a matrix known as vascular basement membrane (vBM). During angiogenesis, there is a secretion of pro-angiogenic factors by hypoxic, tumoral or inflammatory cells that forces quiescent vessels activation. In this moment, pericytes detach from the vessel wall in response to angiopoietin 2 (ANG-2) and from the vBM due to its proteolysis by different metalloproteinases. Then, ECs change their shape and behaviour and loss their junctions and permeability, so vasodilation and extravasation is enhanced. Because of that, a provisional ECM containing pro-angiogenic molecules is created, where ECs migrate. After that, one endothelial cell is selected as the *tip cell* following a still unveiled mechanism in order to avoid the moving of a mass of ECs toward the angiogenic signal (Carmeliet & Jain, 2011a)(Viallard & Larrivée, 2017)(Figure 14A).

Once the tip cell is selected, it navigates in response to guidance signals thanks to filopodia and is adhered and migrated to the ECM through integrins. Then, neighbour cells act as stalk cells and divide in order to elongate the stalk (Carmeliet & Jain, 2011a). Then, lumen is established and myeloid cells are recruited to produce or liberate different angiogenic factors from the ECM (Figure 14B). Moreover, these myeloid cells act as a bridge to aim the fusion of both vessel branches, allowing the

blood flow (Carmeliet & Jain, 2011a). To become functional and to stabilise the basement membrane, vessels are covered by pericytes and vBM and cell junctions are generated again (Potente, Gerhardt, & Carmeliet, 2011)(Viallard & Larrivée, 2017)(Figure 14C).

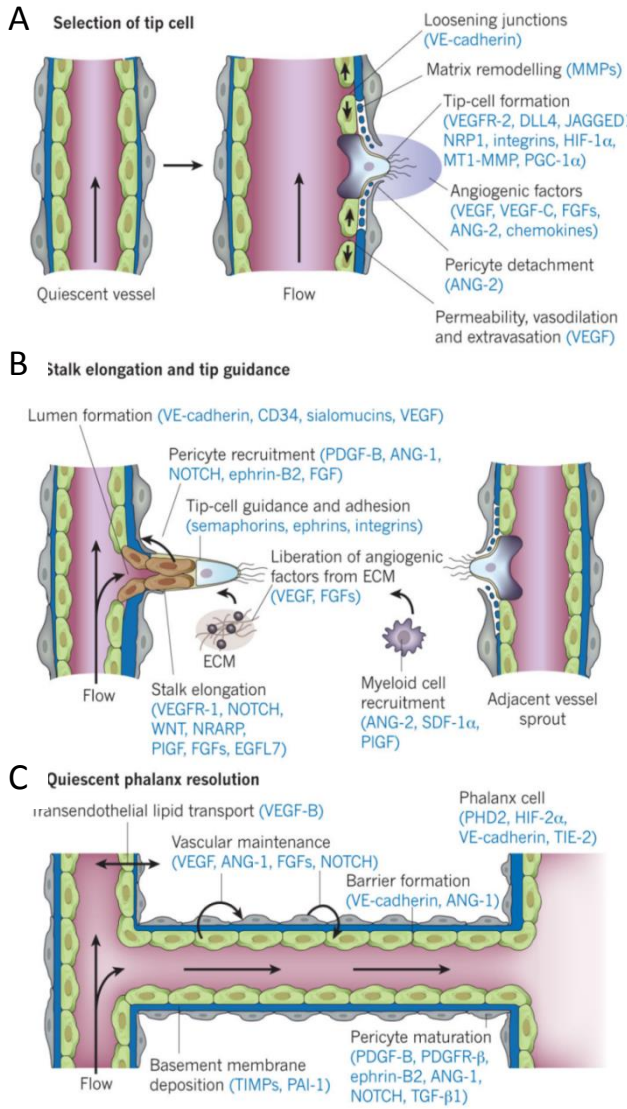

Figure 14. Molecular and physiological steps during angiogenesis. Representation of the angiogenesis process. (A) Endothelium activation and tip cell selection. (B) Tip cell elongation, migration and sprouting. (C) Branch fusion and vessel quiescence. Adapted from (Carmeliet & Jain, 2011).

3.2. Tumour vascularisation

During tumour development, tumour vascularisation is so essential that it has been included as one of the most relevant hallmarks of cancer (Hanahan & Weinberg, 2011). Although cellular and molecular mechanisms under angiogenesis are common between physiological and tumour environments, pro-angiogenic signals derived from TME generate chaotic and unstable vessels. Historically, tumour angiogenesis was thought to be regulated just by cancer cells, which express pro-angiogenic factors. However, now it is known that stromal cells in the TME such as fibroblast or immune cells are also essential for this activation (Hanahan & Coussens, 2012).

In premalignant stages of tumours, there is a basal lamina that surrounds the tumour and impedes the infiltration of quiescent blood vessels to the tumour mass, which receives oxygen and nutrients by diffusion when its size is lower than 1-2mm^3. However, invasive malignant tumours need blood flow in order to thrive, so stromal response is induced to activate angiogenesis. This triggering and development of an actively growing and infiltrative vascular network is called *angiogenic switch*, and it is associated with tumour progression from a benign to a malignant stage (De Palma, et al., 2017)(Lugano et al., 2020). Angiogenic switch can be activated by different processes (hypoxia, low pH), mechanical stress produced by proliferating tumour cells or inflammation, being hypoxia the most relevant one (Jászai & Schmidt, 2019). During this process, stressed tumour cells continuously secrete pro-angiogenic factors such as VEGF, FGF2, TGFβ, PDGFβ, EGF, ANG-1 and ANG-2, which stimulate ECs. In contrast, those stressed cells also secrete anti-angiogenic factors such as thrombospondin 1 and 2 (TSP1/2), angiostatin and endostatin, IFNα, platelet factor 4 (PF4), IL4 and IL12 or tissue-inhibitors of metalloproteases (TIMPs) (Teleanu, et al., 2020). Although normal vessels are well-organised structures and their ECs are supported by the vBM and pericytes to generate stable cell-cell junctions, this imbalance in angiogenic stimulation makes tumour vessels being chaotic and tortuous (Figure 15). These aberrant vessels are characterised by the disruption of EC junctions and poor pericyte coverage, what increases vessel leakiness (Viallard & Larrivée, 2017). Moreover, they are strikingly heterogeneous such a mosaic and exhibit a spectrum of different vessel subtypes, with different vessel diameters and maturation states. Moreover, vBM is also abnormal, including variable thickness and loss of association with ECs. This environment reduces blood flow, so hypoxia and tumour cell intravasation are enhanced. Furthermore, this aberrant vasculature reduces immune cell migration and drug delivery (Carmeliet & Jain, 2011b).

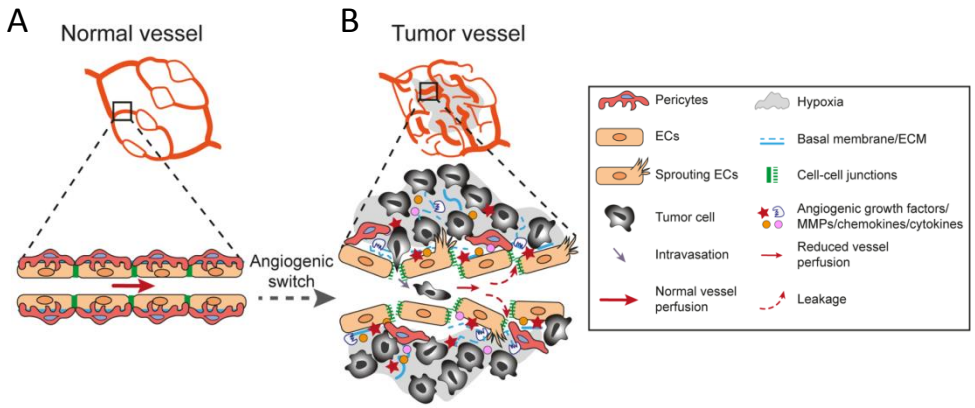

Figure 15. Morphological and functional differences between normal and tumour vasculature. Cell and molecular changes in chaotic tumour vessels (B) compared to normal ones (A). Adapted from (Lugano et al., 2020).

Angiogenesis is the most typical mechanism to form vessels to enhance tumour progression (Figure 16A). Nevertheless, blood vessel formation can be induced by other processes. One of those alternative mechanisms is *intussusceptive angiogenesis*, referring to the formation of transluminal tissue pillars within an existing vessel, and which fuse later with it. However, the exact molecular mechanism of this alternative vascularisation is not well understood (Figure 16B). However, this model shows a clear advantage over sprouting angiogenesis, since it leads to a faster generation of new blood vessels with fewer metabolic needs, allowing a rapid adaptation to changing environments (Viallard & Larrivée, 2017). *Vasculogenesis* was previously described as *de novo* blood vessel formation mechanisms during organ development by progenitor EC, and it is found also during tumour progression (Figure 16C). However, those progenitors can, instead of forming a complete new vessel, be recruited to already existing vessels, being differentiated there to mature ECs (Figure 16D). Another mechanism that has been well-defined in tumours is *vasculogenic mimicry*. It has been found in particularly aggressive tumours, and consists on the formation of vessel-like structures without EC contribution. In these structures, tumour cells acquire endothelial-like phenotype and markers, aiding in mosaic tubular structure formation and stabilization to source sufficient blood supply and nutrients (Figure 16E). Finally, the last alternative mechanism described is *transdifferentiation of cancer cells*. It can be confused with the previous one. However, in this case tumour cells do differentiate to actual ECs due to stemness properties of CSCs populations (Lugano et al., 2020)(Figure 16F).

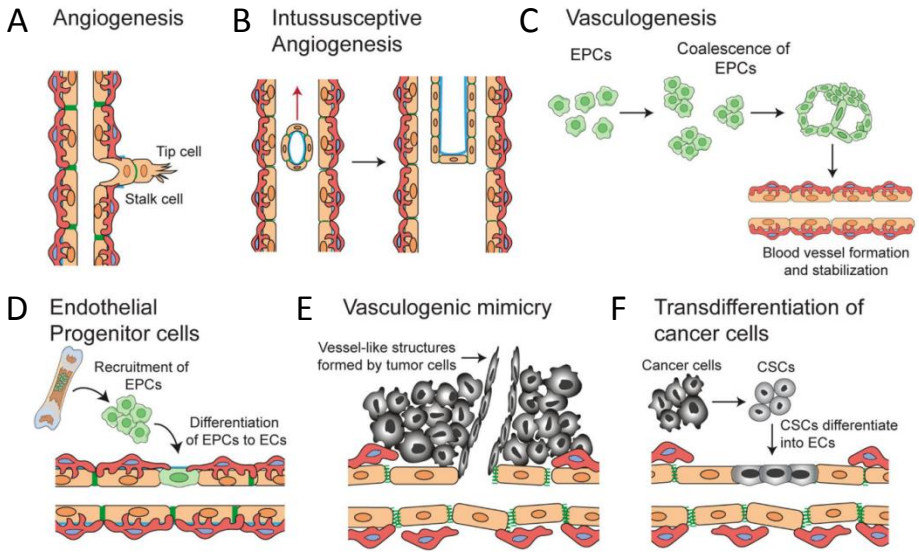

Figure 16. Different mechanisms of blood vessel formation. Schematic illustration of the different models of vascularisation including angiogenesis (a) and the alternative ones. Adapted from (Lugano et al., 2020).

Apart from those alternative models, there is a non-angiogenic process that has been also described: *vessel co-option*. In this model, tumour cells use the pre-existing vessels of non-tumoral tissue as oxygen and nutrient suppliers, growing along them and integrating them during tumour expansion (Viallard & Larrivée, 2017)(Lugano et al., 2020).

As shown in Figure 4, angiogenic vascular cells are involved in several hallmarks of cancer. For example, they participate in *resisting cell death* due to the attenuation of hypoxia or nutrients deprivation. Moreover, tumour angiogenesis is one of the main drivers of *activating invasion and metastasis*, since increased vessel density and poor pericyte coverage enhance the tumour cell dissemination. Apart from that, the leakiness of tumour vessels reduces immune cell recruitment and inflammation, hampering immune anti-tumoral response and *evading immune destruction* (Hanahan & Coussens, 2012).

3.3. Role of immune cells on tumour vascularisation

Although cancer cells are one of the main sources of VEGFa and pro-angiogenic molecules, infiltrated leukocytes also increase VEGFa availability and signalling during angiogenic switch. In fact, tumour-associated stromal cells affecting angiogenesis can be derived from two origins. First, they can be haematopoietic cells recruited from the BM via the systemic circulation, including different subtypes such as monocytes, macrophages, neutrophils, lymphocytes or immature precursors. And second, they can be non-haematopoietic BM-derived endothelial or mesenchymal progenitors (De Palma et al., 2017). These cells interact with ECs, impacting on their remodelling and angiogenesis. In fact, macrophages and MDSCs are essential during anti-angiogenic therapy and they are particularly interesting for this work. For this thesis, the most relevant group of cells is the one of haematopoietic origin, so each subtype is described next (Figure 17).

3.3.1. Macrophages

One of the most important cell types are macrophages, a very plastic population. Furthermore, M2 phenotype has been associated to immune suppression, tissue remodelling and angiogenesis. In hypoxic conditions and in response to DAMPs, monocytes are recruited to tumour sites and differentiate into M2 TAMs. Those pro-tumorigenic macrophages promote angiogenesis by producing pro-angiogenic factors that stimulate ECs proliferation and sprouting, as well as promote vessel maturation. These factors include VEGFa, VEGFc, VEGFd, EGF, FGF2, and chemokines such as IL1β, IL6, CXCL8/IL8, CXCL12/SDF1, tumour necrosis factor α (TNFα) or CCL2/MCP-1) (Potente et al., 2011). Moreover, they also release angiogenesis-modulating enzymes (COX-2 or iNOS/NOS2), and matrix metalloproteases that degrade basement membrane and ECM during angiogenesis (Figure 17). They also promote indirectly angiogenesis by inhibiting the expression of angiogenesis inhibitors. Moreover, they are able to support vessel stability by blocking the effect of vascular disrupting agents (Lugano et al., 2020) and enhance vascular permeability and cell intravasation (De Palma et al., 2017). Finally, there is a specific TAM population with expresses the angiopoietin receptor TIE2 and stimulates angiogenesis called perivascular TIE2-expressing TAMs (TEMs), which is recruited to the tumour by high levels of CXCL12/SDF1 (Ramadan, et al., 2020). However, it role has been controversially discussed in the last months (Jakab, et al., 2022)(Y. Zhang & Brekken, 2022).

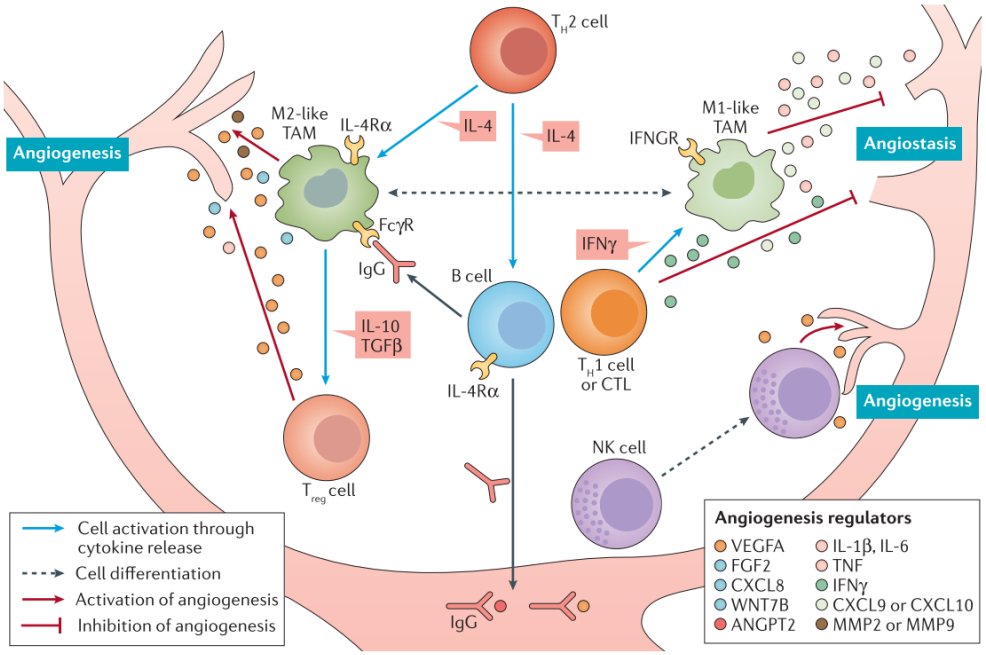

Figure 17. Crosstalk between myeloid cells and lymphocytes during tumour angiogenesis. Regulation of tumour vascularisation by the direct effect of lymphocytes and myeloid cells on ECs and indirectly by the interaction between both lineages (De Palma et al., 2017).

3.3.2. Lymphocytes

The role of lymphocytes on tumour angiogenesis includes the modulation of myeloid cell activation, although lymphocyte-derived cytokines do directly influence ECs as well. On the one hand, B cells regulate angiogenesis by the expression of pro-angiogenic cytokines such as VEGFa, FGF2 or MMP9 in a signal transducer and activator of transcription 3 (STAT3)-dependent manner. Moreover, they also stimulate vascularisation indirectly through immunoglobulin G (IgG) and by polarising macrophages. On the other hand, T cells also affect angiogenesis directly by $CD4^+$ Th1 cells, which express IFNɣ that acts as an anti-angiogenic cytokine. In spite of it, IFNɣ secretion by $CD4^+$ Th1 or by $CD8^+$ CTLs cells might stimulate TAMs to produce pro-angiogenic factors in a STAT1-dependent manner (pro-angiogenic) or can polarise the macrophages to M1, with angiostatic functions. Moreover, $CD4^+$ Th2 cells secrete IL4 and stimulate M2 macrophage polarisation, affecting indirectly to angiogenesis. In the case of Treg, they express VEGFa and suppress IFNɣ-expressing cells in order to

enhance angiogenesis (De Palma et al., 2017). These cells are in continuous interaction with myeloid cells to regulate tumour angiogenesis (Figure 17).

3.3.3. Natural killer cells (NKs)

Although NKs have a well-known pro-angiogenic role in uterine vasculature, their function in tumour vasculature is not well-studied. Among these cells, there is a specific subtype that is characterised by its poor cytotoxicity and high pro-angiogenic capacity (Figure 17). Moreover, in presence of TGFβ, these cells polarise and induce VEGF secretion by other NKs (Lugano et al., 2020).

3.3.4. Deactivated dendritic cells (DCs) and myeloid-derived suppressor cells (MDSCs)

The ability of these immature myeloid cells to affect tumour angiogenesis is similar to the one produced by M2 TAMs. They secrete MMPs that enhances angiogenesis by increasing VEGF bioavailability, starting a loop due to the potentiated recruitment by that VEGF. In presence of this growth factor, these cells release chemokines that enhance MDSCs recruitment and maintain the vicious circle. Furthermore, MDSCs also express prokineticin 2 (Bv8), which participate in angiogenesis. Moreover, the accumulation of MDSCs are the responsible to anti-angiogenic therapies, but it will be detailed in the following lines (Lugano et al., 2020).

3.3.5. Neutrophils

Neutrophils are one of the main sources of VEGF. As in the case of macrophages, neutrophils can be found in two main states, being N2 TANs the ones that have pro-angiogenic functions. In tumours, neutrophil stimulation triggers the angiogenic switch, what is crucial during early stages of tumour progression (Lugano et al., 2020). Moreover, when neutrophils are stimulated they secrete Bv8 that induce MDSCs mobilization and EC proliferation (De Palma et al., 2017).

3.4. Anti-angiogenic therapies against endothelial cells and vessel normalization

Traditional therapeutics approaches against tumour cells shifted towards tumour angiogenesis as a potential therapeutic target, establishing a new field in oncology (Jászai & Schmidt, 2019). Indeed, it is also relevant its combination with other therapies such as immunotherapy, chemotherapy or radiotherapy.

The concept of tumour starvation was introduced in 1971 by Judah Folkman (Folkman, 1971). However, the inhibition of EC proliferation by anti-angiogenic therapy damages the viability of tumour cells not only by their starvation and deprivation (Li et al., 2018). During vessel depletion, EC junctions are disrupted, which provokes a starvation of the tumour and an increase of hypoxia. To compensate this challenge, the recruitment of pro-angiogenic myeloid cells such as MDSCs and TAMs is enhanced. Moreover, this situation impedes drug delivery (Lugano et al., 2020)(Figure 18A). Regarding immune populations, hypoxia after anti-angiogenic therapy upregulates immune checkpoint molecules, reprograms TAMS to an M2 phenotype and affects the efficacy of DCs and T cells (Benavente, et al., 2020).

Pharmacological suppression of VEGF induces vessel normalization, producing less chaotic vessels and better pericyte coverage (Hanahan & Coussens, 2012)(De Palma et al., 2017). This vessel normalization window occurs transiently during the first days of treatment and is characterised by a balance of pro- and anti-angiogenic factors that benefit drug delivery and efficacy, explaining the increased progression-free survival in patients treated with anti-angiogenic and chemotherapy compared to only chemotherapy. This normalization reveals a restoration of EC junctions, a decrease in vessel diameter and permeability and a reduced edema. Moreover, it promotes the expression of endothelial adhesion molecules that enhanced immune cell infiltration and reduced cell invasiveness (Ribatti, et al., 2019)(Lugano et al., 2020)(Figure 18B).

In addition, the continuous exposition to pro-angiogenic factors in tumours reduces the secretion of pro-inflammatory molecules, impeding the infiltration of CTLs and increasing their exhaustion. For that reason, the normalization of blood vessels after anti-angiogenic therapy improves their recruitment and activation (Ribatti et al., 2019). Among all the changes in the tumour immune landscape, it is important to highlight the increased infiltration and activation of CTLs, the decrease in the recruitment of Treg and MDSCs, the increased maturation of DCs and the polarisation of macrophages towards M1 or anti-tumorigenic phenotype (Lugano et al., 2020)(Figure 18C).

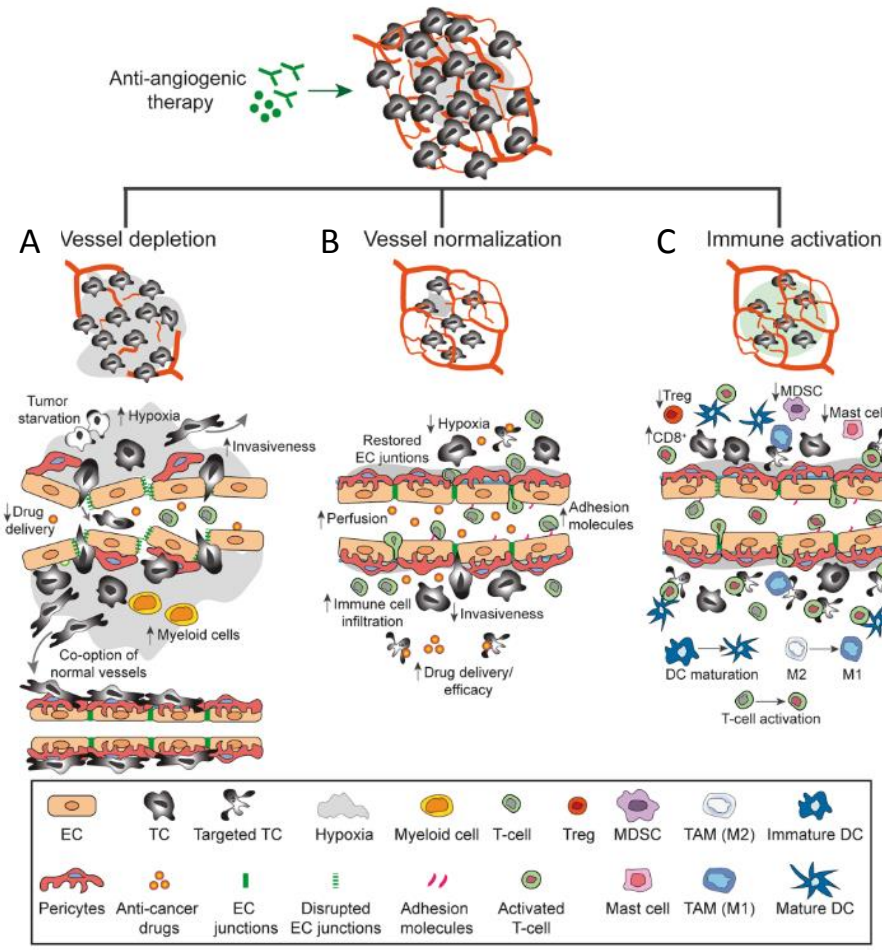

Figure 18. Effect of anti-angiogenic therapies on vessel depletion and normalization. (A) Tumour cell starvation and hypoxia due to vessel depletion. (B) Vessel normalization by restored Ecs junctions and pericyte coverage. (C) Immune activation and polarisation towards and anti-tumorigenic phenotype. Adapted from (Lugano et al., 2020).

Despite the different pro-angiogenic factors that have been identified, anti-angiogenic therapies are focused on the VEGF signalling pathway. The interaction of the ligands with the receptors leads to the dimerization of them, which triggers a down-stream intracellular phosphorylation cascade. For that reason, many efforts have been put to withdraw the pro-angiogenic ligands (Aflibercept or Bevacizumab, the first VEGF-targeted agent approved by the Food and Drug Administration (FDA) in 2004 for the treatment of metastatic colorectal cancer (CRC)), to block the receptors (Ramucirumab) or to interfere with the kinase activity of the VEGF receptors (VEGFR)

(tyrosine kinase inhibitors, TKIs) (Ciombor, et al., 2013)(Jászai & Schmidt, 2019)(Tian, et al., 2020) (Figure 19). This type of therapies has been used in several types of cancers as monotherapy. Nevertheless, once it was understood how vessel pruning could benefit the use of other therapies, its modest benefit was increased in combination with other drugs (De Bock, et al., 2011).

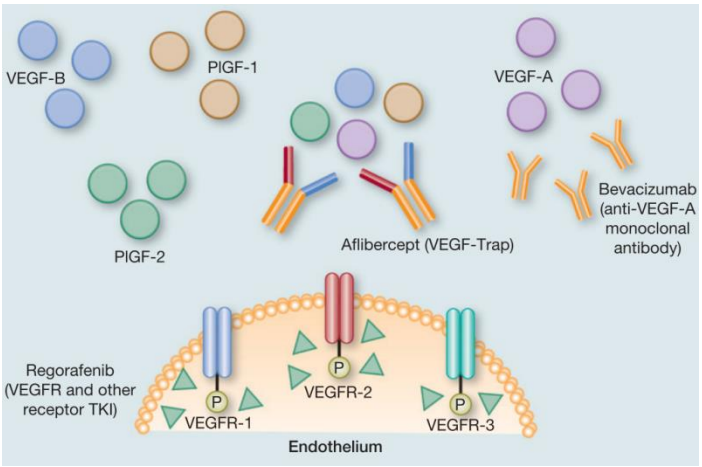

Figure 19. Mechanisms of action of anti-angiogenic agents. Structure and target molecules of the anti-angiogenic agents Aflibercept, Bevacizumab and Regorafenib. Adapted from (Ciombor, et al., 2013).

As it has been previously mentioned, there are several types of therapies with different approaches. One relevant part of this thesis is focused on the use of anti-angiogenic therapies and its connection with immune cells. Specifically, as it is detailed in the materials and methodology section, we will use Aflibercept, a VEGF-Trap (Figure 19).

3.4.1. VEGF-Trap (Aflibercept)

Aflibercept is a decoy receptor for VEGFa, VEGFb and placental growth factor (PlGF), which was developed to avoid anti-VEGFa resistance. It is a soluble recombinant fusion protein containing the extracellular domains of VEGFR1 and VEGFR2, which are fused to the Fc portion of human IgG1 (Ciombor et al., 2013)(Figure 20). It was approved by the FDA in 2012 for metastatic CRC treatment in combination with chemotherapy (Itatani et al., 2018). Compared to other anti-VEGFa agents, it binds it with higher affinity and offers a longer inhibitory effect. Moreover, it is more specific

blocking the amino acids that are necessary for VEGFR1/2 binding, reducing undesirable effects. Due to its action over the spectrum of ligands and not only over VEGFa, it can affect also to macrophage polarisation (Jászai & Schmidt, 2019). Its effect on tumour angiogenesis is clear. However, there is still associated toxicity and the financial costs of the treatment are high, as well as its optimal sequence or treatment or combination is not well-defined (Ciombor et al., 2013). Nevertheless, due to its known effect, it will be used in this project.

3.5. Resistance to anti-angiogenic therapy and its combination with other therapies

The efficacy of pharmaceutical proteins such as monoclonal antibodies is limited due to its short half-life, the high costs of production and treatment and the interference with endogenous molecules (Li et al., 2018). In the case of the inhibition of tumour angiogenesis, certain therapies can lead to the selection of cancer cells that are able to survive in hypoxia and generate pro-tumorigenic scenarios (De Palma et al., 2017) (Lugano et al., 2020). Apart from that, these therapies can produce compensatory mechanisms that evolve in therapy resistance and refractoriness. Among these mechanisms, involving tumour, endothelial and stromal cells, there have been defined 1) activation and secretion of alternative angiogenic factors; 2) metabolic adaptation and reprogramming; 3) increased tumour invasiveness and metastasis; 4) increase of alternative mechanisms of vascularisation; 5) increased pericyte-covered tumour vessels; and/or 6) enhanced recruitment of pro-angiogenic cells (De Palma et al., 2017)(Haibe et al., 2020)(Lopes-Coelho, et al., 2021). Among all the pro-angiogenic cells that can be recruited after anti-angiogenic treatment (6), $CD11b^{+}/Gr1^{+}$ MDSCs has been clearly linked to this resistance. In fact, they secrete other pro-tumorigenic and pro-angiogenic molecules that enhance tumour progression (Shojaei et al., 2007)(Carmeliet & Jain, 2011a)(Zhang et al., 2013). That is one of the main reasons why they are relevant for this work. Moreover, therapy resistance is forcing the use of combined therapies of anti-angiogenic drugs with other type of therapies, which are mainly benefited from the normalisation window during vessel normalisation. In spite of it, there is an hypothesis that defends the existence of a physical niche that protects tumour cells during drug treatment, with a protective role in certain locations (Junttila & Sauvage, 2013). Among the therapy combination, the ones that have been historically used with anti-angiogenic drugs are radiotherapy and chemotherapy. Both benefit from the normalisation window after anti-angiogenic therapy, especially to avoid the resistance due to reduction of

hypoxia by anti-angiogenic treatment. Nevertheless, in both cases the combination has shown poor survival improvement and unfavourable safety (Crawford & Ferrara, 2009)(Tian et al., 2020). In addition, in the last decades the combination of anti-angiogenic therapies with immunotherapy is extensively used to reduce the contribution of pro-tumorigenic and pro-angiogenic immune cells.

3.5.1. Combination with immunotherapy

During tumour development and anti-angiogenic therapy, several immune populations are key players in the crosstalk with ECs. Moreover, the role of endothelium in regulating immune cell trafficking suggests the value of exploring combination of both therapies (Junttila & Sauvage, 2013). The emerging study of immunotherapy has opened a new horizon in cancer therapy. It is mainly based on the use of ICIs, which decrease T cell exhaustion and are efficient in reprogramming the immunosuppressive TME and immune evasion (Jászai & Schmidt, 2019). The most relevant ICIs are CTLA-4 PD-1 and PD-L1 inhibitors (Ribatti et al., 2019). For their efficacy, TME must be immunosupportive. However, as it has been previously detailed, aberrant vessels create immunosuppressive environments with a reduced recruitment of cytotoxic cells and an inhibition of anti-tumour immune response (Lopes-Coelho et al., 2021). Anti-angiogenic therapy shifts this environment, which can be used for improving immunotherapy efficacy and increasing CTL infiltration. Combined therapy has been proved to continuously removing Treg and MDSCs, at the same time that reduced PD-1 and PD-L1 levels (Teleanu et al., 2020). Interestingly, the combination of angiogenesis inhibitors and ICIs has been proved to be safety and efficient, with several on-going clinical trials. Nevertheless, the understanding of the combination is still limited (Tian et al., 2020). More recently, anti-angiogenic therapy has been combined with TAM-based therapeutic strategies, since these cells have a powerful pro-tumorigenic and pro-angiogenic role (De Palma et al., 2017)(Ishikawa, et al., 2021).

4. The extracellular milieu during tumour development

Although a majority of this introduction has been devoted to all cellular types forming the TME, still there are other non-cellular components that also regulate tumour behaviour by the crosstalk between them and with other members of the TME (Hanahan & Weinberg, 2011). Among those non-cellular components, the most relevant one for this project are the ECM and the extracellular proteases, which will be introduced next.

4.1. The extracellular matrix (ECM)

The ECM is a three-dimensional structure with biochemical and biomechanical properties that acts as scaffold in all tissues and organs and regulates development, homeostasis and processes such as cell growth, survival, morphology, motility and differentiation (Pickup et al., 2014)(Eble & Niland, 2019)(Rowley et al., 2019) (Najafi et al., 2019)(Cox, 2021). Fibroblasts are one of the main producers of ECM, which is formed by molecules encoded by around 300 core-matrisome genes and 800 matrisome-associated genes (Cox, 2021)(Figure 20A-B). Among all these molecules, the most relevant ones are collagens, proteoglycans (PGs), glycosaminoglycans (GAGs), elastin, hyaluronic acid and adhesive glycoproteins such as laminin or fibronectin. Moreover, ECM also acts as a reservoir of growth factors, cytokines and chemokines that are bioactive mediators of local signalling (Eble & Niland, 2019)(Bejarano et al., 2021). Cells are anchored to the ECM where they receive information about the environment. This adhesion is mediated by adhesion receptors, among which integrins and PGs play an essential role (Eble & Niland, 2019). These properties are modulated by post-translational modifications of the ECM components, including cross-linking, glycosylation, sulfation, oxidation or degradation among others, reflecting the dynamism of this structure (Cox, 2021)(Figure 20C).

ECM can be divided in interstitial matrix and highly specialized matrix, which are strongly compartmentalized (Cox, 2021). On the one hand, the interstitial matrix forms a porous membrane that connects cells in the stroma between themselves and with the basement membrane (Winkler et al., 2020). This specific matrix is formed by collagens, fibronectin, PGs, GAGs, tenascin C and elastin (Bonnans et al., 2014). On the other hand, basement membrane is a highly specialized and stable ECM that is produced by ECs and mural cells, and which connects cells to their interstitial matrix,

being a prerequisite for normal tissue development and function (De Palma et al., 2017)(Figure 20D).

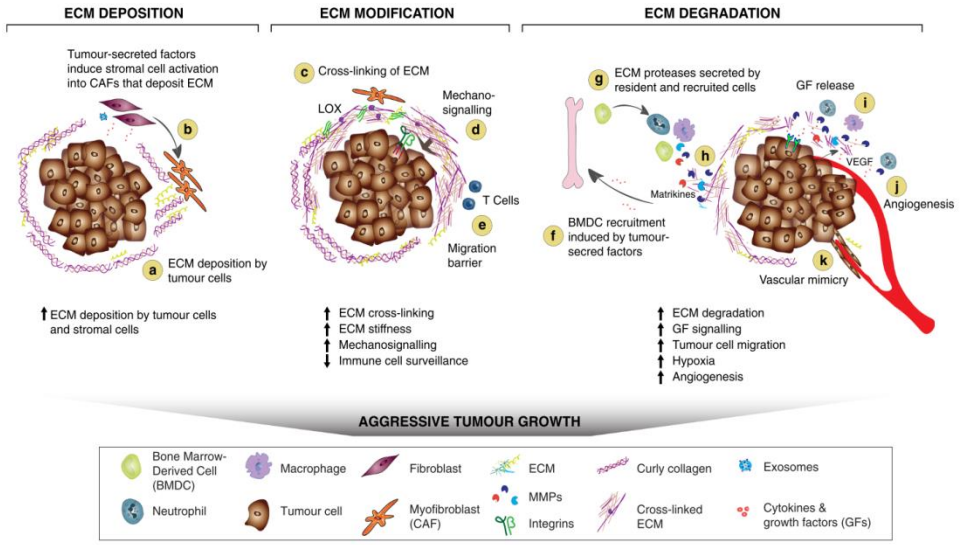

Figure 20. ECM remodelling in the primary tumour. Representation of the different processes during ECM remodelling in cancer. (A-B) Activation of CAFs to produce ECM, (C) cross-linking of ECM components to increase matrix stiffness, (D) signalling by ECM-cell interaction, (E) formation of the physical barrier to evade immune surveillance by T cells, (F) recruitment of bone marrow-derived cells (BMDC) by cytokine, chemokine and growth factor release, that (G) secrete ECM proteases and (H) produce the degradation of ECM components in matrikines and (I) the release of matrix-bounded growth factors such as VEGF that (J) enhance angiogenesis. Adapted from (Winkler et al., 2020).

Its composition is different depending on the organ of origin and it can change according to cell requirements. However, the most relevant components are laminin, perlecan, collagen IV and nidogens (Kruegel & Miosge, 2010)(Sorokin, 2010)(Bonnans et al., 2014)(Figure 21). Laminin and collagen form two independent well-organised networks that are stabilised by nidogens and perlecans. In addition, perlecans are PGs that control growth factors signalling and activation while nidogen 1 (NID1) and nidogen 2 (NID2) are glycoproteins known as linking proteins of the basement membrane (Kruegel & Miosge, 2010).

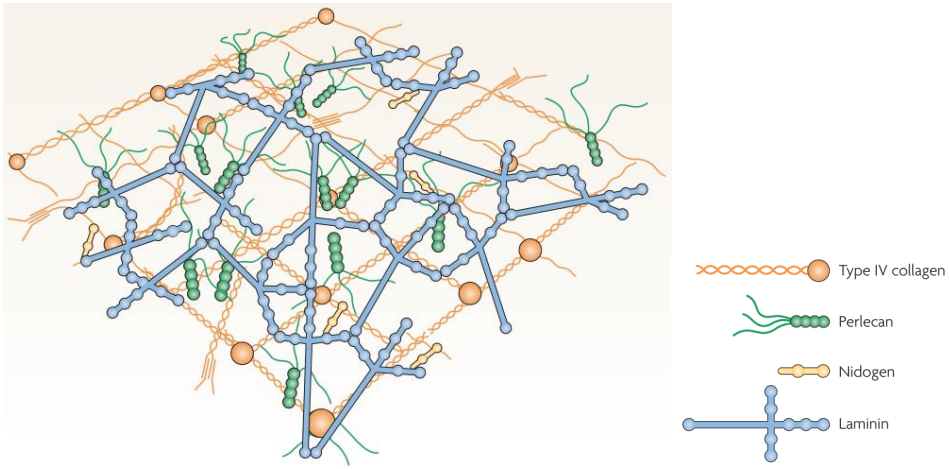

Figure 21. Molecular composition of the basement membrane. Representation of the three-dimensional structure of the specialized ECM known as basement membrane. Adapted from (Sorokin 2010).

In cancer, this environment and the ECM are highly deregulated, supporting processes such as cell proliferation, angiogenesis, therapy resistance, immune evasion and cell invasion and metastasis (Lu et al., 2012)(Karamanos et al., 2021). Indeed, the participation of ECM has been suggested in several hallmarks of cancer. Relevantly, ECM stiffness has been linked to tumour growth, increased metastasis and poor clinical outcome (Pickup et al., 2014). Moreover, collagen and fibronectin usually accumulate in the periphery of the tumours, increasing compressive stress, T cell inaccessibility and impeding drug delivery (Najafi et al., 2019)(Boyle et al.l, 2021)(Figure 20E). For all this, ECM has emerged as a predictive, diagnostic and prognostic biomarker (Cox, 2021).

4.2. The extracellular proteases

During cancer development and growth, there is an extensive remodelling of the ECM, causing alterations in both density and composition. Moreover, these variations have been related to tumour evolution and cancer cell drug resistance (Najafi et al., 2019). Increased deposition and crosslinking of ECM components are considered as tumour-promoting and cell-spreading (Pickup et al., 2014). For that reason, the proteolysis of the ECM mediated by the proteases plays an important

role in the reduction of the well-characterized pro-tumorigenic density. In addition, its proteolysis also provokes the release of different growth factors that are anchored to that ECM, triggering intracellular signalling responses. Indeed, the liberation of those molecule mediate relevant processes such as angiogenesis or the recruitment of bone marrow-derived cells (BMDCs) that will develop tumour immunity (Cox, 2021)(Figure 20F). This remodelling is possible by different proteolytic enzymes secreted by cancer cells and other TME cell types such as CAFs or TAMs (Rowley et al., 2019)(Karamanos et al., 2021)(Figure 20G). In addition, degradation of ECM components generates the formation of matrikines, molecules which have alternative biological functions to the proteins they come from (Winkler et al., 2020)(Figure 20H). Moreover, the degradation of the ECM by remodelling enzymes contributes to cell invasion and metastasis (Najafi et al., 2019). For all that reasons, the enzymatic activity of proteolytic enzymes has a strong interest in oncology.

Among the different remodelling proteases, the most known are matrix metalloproteinases (MMPs), which can be secreted in the TME or anchored to the cell membrane (Karamanos et al., 2021). The MMP family has 24 members in humans. This family has been widely reported to be involved in matrix integrity, cell behaviour and tissue turnover due to the degradation of ECM components and the release of cytokines, growth factors and their receptors (Cox, 2021). The activity of this family is usually low in physiological conditions but, in cancer, its regulation is lost or altered, provoking their contribution to anti-tumorigenic and pro-tumorigenic processes (Bonnans et al., 2014). Another relevant family of proteases for ECM remodelling is the well-known ADAM (a disintegrin and metalloprotease) family of proteases. This group includes 21 members of membrane-associated molecules that have been linked to tumour growth and angiogenesis (Campbell et al., 2010). Similar to ADAM family, a disintegrin and metalloprotease with thrombospondin motifs (ADAMTS) family is also relevant in tumour development. There are 19 ADAMTSs which, opposite to ADAMs, are all secreted. However, both families cleave transmembrane protein ectodomains and are deregulated in cancer, contributing to its progression (Bonnans et al., 2014)(Winkler et al., 2020)(Cox, 2021). For this project, the first member of the ADAMTS family (ADAMTS1) is a pillar molecule and accordingly, the whole family will be specifically described later in this introduction (Introduction, section 5 and 6). Other group of proteases are the cathepsins, which degrade both intracellular and extracellular matrix proteins. Moreover, there are also heparanases and sulphatases, which contribute to ECM disassembly. In fact, this last group modulates pathological processes that go from gene transcription to signal transduction, autophagy, anti-inflammatory mechanisms and DNA damage (Bonnans

et al., 2014)(Karamanos et al., 2021)(Cox, 2021). Although less known, other remodelling enzymes are the bone morphogenetic protein 1, the tolloid-like proteinases and the hyaluronidase family (Cox, 2021).

These extracellular proteases can suffer post-translational modifications such as glycosylation or mannosylation among other, which can alter protease's secretion, localization, activation or catalytic functions (Kelwick et al., 2015). In addition, their activity can be blocked by tissue inhibitors (Bonnans et al., 2014)(Cox, 2021).

4.3. Role in tumour progression, inflammation and angiogenesis

As already mentioned, both intact and proteolysed ECM can act as pro- and anti-tumorigenic molecules (Winkler et al., 2020). In fact, ECM remodelling by chronic inflammation is known to suppress adaptive immunity at the same time that increases angiogenesis and the release of immunomodulatory factors (Garner & de Visser, 2020). Additionally, abnormal ECM alters other processes such as immune cell behaviour, infiltration, differentiation and activation, and its composition and remodelling can be modulated according to the necessity of the tissue (Sorokin, 2010).

As it has been previously detailed, tumour development is accompanied by inflammation at early stages, in which ECM remodelling is also necessary. When leukocytes extravasate, they found two physical barriers: vBM and the interstitial matrix, which have to be degraded. This structure offers them a scaffold and a place for their adhesion and activation, being necessary for tumour blockade (Sorokin, 2010)(Wight et al., 2017). Apart from the structural role, ECM components are highly interactive and bind inflammatory chemoattractants such as TNFα, TGFβ and several interleukins, CC and CXC chemokines, whose release mediated by proteases is essential for inflammatory processes (Vaday & Lider, 2000). For that reason, extracellular proteases and their crosstalk to othe TME components is essential. It is extensively demonstrated that dense ECM acts as a physical barrier for anti-tumorigenic immune cells and supports immune tolerance, while soft or proteolysed ECM is related to a more immunogenic environments (Figure 22). Indeed, dense ECM reduces T cell infiltration and activation and increases pro-tumorigenic immune cell recruitment. In contrast, ECM clevage and the release of matrikines is associated to the recruitment of anti-tumorigenic immune cells. These findings support the

necessity of using ECM as a therapeutic target to control tumour immune inflammation (Pengfei Lu et al., 2012)(Mushtaq et al., 2018).

During tumour growth, another process in which ECM remodelling is crucial is angiogenesis. Sprouting angiogenesis requires the degradation of the vBM by remodelling enzymes. Moreover, this process is enhanced by hypoxia and pro-angiogenic factors such as VEGFA or FGFs that are released in their bioactive forms through ECM proteolysis (Eble & Niland, 2019)(Winkler et al., 2020). In addition, the release of those factors attract pro-angiogenic inflammatory cells such as TAMs (Lu et al., 2012)(De Palma et al., 2017)(Figure 20I-J). Apart from allowing sprouting angiogenesis, ECM remodelling enhances EC survival. In spite of it, the release of both pro-angiogenic and anti-angiogenic factors from the ECM is what produce a disrupted tumour vasculature (Winkler et al., 2020).

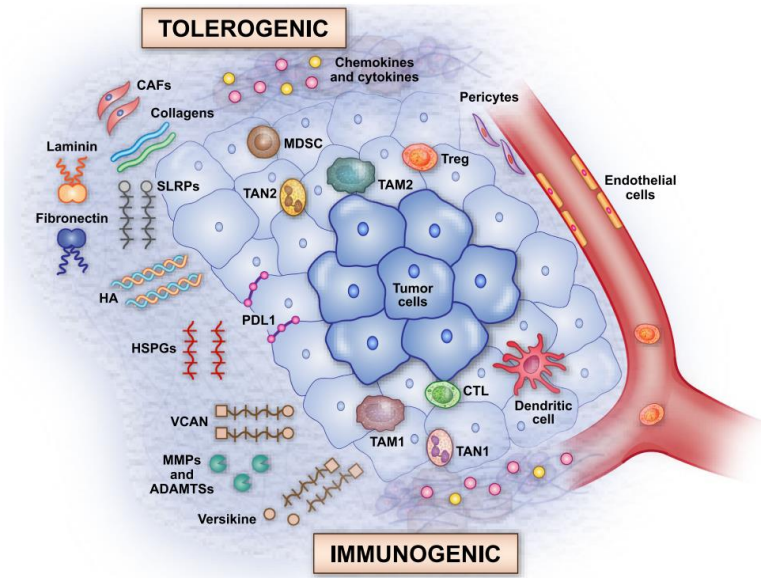

Figure 22. ECM in the inflamed TME. Schematic representation of the how different ECM compositions of degradation states regulate tumour immune infiltration, dividing tumours in tolerogenic (up, dense and unaltered ECM) or immunogenic (down, proteolysed ECM). Adapted from (Mushtaq et al., 2018).

Finally, parallel to the extravasation of leukocytes to inflamed tissues, ECM regulates cancer cell spreading and metastasis development, including intravasation to the primary site to blood flow, cancer cell survival in circulation, generation of pre-metastatic and metastatic niches and colonisation (Lu et al., 2012)(Pengfei Lu et al., 2012)(Eble & Niland, 2019)(Winkler et al., 2020).

4.4. Therapies targeting the extracellular compartment

Regarding the previously defined roles of ECM in tumour progression, angiogenesis and inflammation, different therapies has been developed using this environment as a target to reduce pro-tumorigenic scenarios. Essentially, it is important to obtain a balance between matrix accumulating and degrading factors, which is also relevant for the efficiency of other therapies (Najafi et al., 2019).

Knowing that aberrant ECM that is produced by CAFs after their activation in TME, some therapies are focused on the renormalisation or deactivation of this population. Indeed, as in the case of TAMs-targeted therapies, these approaches are more efficient than the complete depletion since they have other roles far from cancer progression (Cox, 2021). Similarly, other strategies have put their attention on the inhibition of *de novo* synthesis of ECM components blocking signalling pathways related to TGFβ or hypoxia, or on the use of antifibrotic drugs (Winkler et al., 2020)(Bejarano et al., 2021)(Cox, 2021).

Another strategy is based on the use of inhibitors of transcription, activation or activity of MMPs, heparanases and other remodelling proteases. Although it appeared as a promising approach, the secretion of proteases by different type of cells and their effect on others made broad-spectrum MMPs inhibitors a strategy with several adverse effects. Nevertheless, the therapeutic approaches working on specific spatio-temporal modulation of their activity are showing promising results (Eble & Niland, 2019)(Karamanos et al., 2021)(Cox, 2021). Contrary, the treatment with degrading enzymes such as collagenases or hyaluronidases has been also studied, but they are toxic and have detrimental effects in many cases (Bejarano et al., 2021).

Apart from targeting the extracellular proteases, there are other therapies that block the function of ECM components. In the case of collagen, PGs and GAGs, their synthesis crosslinking can be blocked. In contrast, other molecules such as heparan sulphates or fibronectin are inhibited by neutralizing antibodies, inhibitory peptides or small molecules (Vaday & Lider, 2000)(Winkler et al., 2020)(Karamanos et al., 2021). Finally, other strategies are related with the targeting of interactions between tumour cells and their environment, usually affecting integrin-dependent crosstalk (Winkler et al., 2020)(Boyle et al., 2021)(Karamanos et al., 2021)(Bejarano et al., 2021)(Cox, 2021).

5. The ADAMTS family

A disintegrin and metalloproteinase with thrombospondin motif (ADAMTS) family belongs to the zinc metalloendopeptidases family, as well as MMPs and ADAMs. This family of secreted proteases play key roles in the formation, maintenance and remodelling of the ECM. Nevertheless, aberrant processes evolve in different pathologies (Mead & Apte, 2018)(Rose et al., 2021).

ADAMTS family comprises a total of 19 members both in human and mouse, encoded by genes dispersed by the whole genome. They can be classified in subgroups attending to their substrates: hyalectanases or proteoglycanases (ADAMTS1, 4, 5, 8, 9, 15 and 20), procollagen peptidases (ADAMTS2, 3 and 14), von Willebrand factor protease (ADAMTS13), mucin-proteoglycanases (ADAMTS7 and 12) and other fibrillin or fibronectin-associated proteases (ADAMTS6, 10, 16, 17, 18 and 19) (Dubail & Apte, 2015)(Mead & Apte, 2018). Importantly, this classification has a clear reflection reflected in the phylogenetic tree of all the members (Rose et al., 2021)(Figure 23).

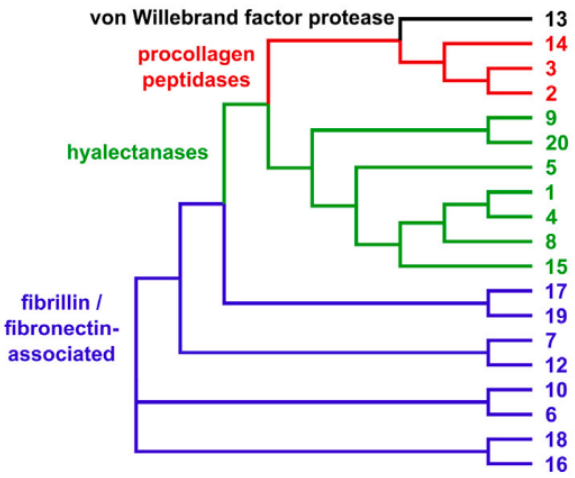

Figure 23. ADAMTS family. Phylogenetic tree of the human ADAMTS proteases and the four subfamilies. Numbers represent each ADAMTS and colour each subfamily. Adapted from (Rose et al., 2021).

All ADAMTSs share a similar structure. First, there is a protease domain in the amino-terminal region that is maintained in all the members. This domain contains a signal peptide and a pro-domain followed by a metalloproteinase motif (zinc-binding active-site) and a disintegrin-like domain. Such protease domain is attached to an ancillary domain that differs between ADAMTSs (Rodríguez-Manzaneque et al., 2000)(Zhong & Khalil, 2019). At the beginning of this domain, there is a central thrombospondin type 1 repeat (TSR), a cysteine-rich domain and a cysteine-free spacer region that appears in all the members of the family. Nevertheless, the spacer region is followed by one or more TSR (although ADAMTS4 has no extra TSR at carboxy-terminal variable region) and other motifs (protease and lacunin module,

gon-1-like or mucin-like domains among others) that differentiate between ADAMTSs (Apte, 2004)(Porter et al., 2005)(Cal & López-Otín, 2015)(Figure 24).

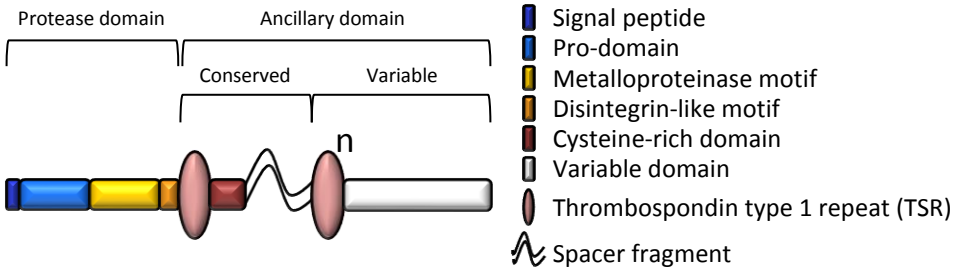

Figure 24. ADAMTS structure. Domain organization of the ADAMTS family of the protease domain (signal peptide, pro-domain, metalloproteinase motif and disintegrin-like motif) and the ancillary domain (thrombospondin type 1 repeat TSR, cysteine-rich domain, spacer fragment and variable domain). Adapted from (Apte, 2004).

ADAMTSs are synthesised as zymogens whose pro-domain is removed intracellularly in the trans-Golgi or at the cell surface by protein convertases as furin or by other proteases (including MMPs) to activate the protease (Rodríguez-Manzaneque et al., 2000)(Apte & Parks, 2015)(Dubail & Apte, 2015) (Figure 25). Likewise, the ancillary domain can be also proteolysed. To date, this ancillary domain has been reported as the responsible of connecting the protease with the cellular surface or the pericellular matrix, mainly by interactions with glycosaminoglycans and other ECM components. For that reason, the proteolysis of this domain can affect the motility of the protease (Apte, 2004)(Apte & Parks, 2015)(Zhong & Khalil, 2019).

5.1. Role in tumour development, angiogenesis and inflammation

Since the first member was described in 1997 in a model of cachexia (K Kuno et al., 1997), ADAMTS family has been related to physiological and pathological processes such as cell proliferation and invasion, angiogenesis or inflammation in tumoral and non-tumoral conditions (Redondo-García et al., 2021). Nevertheless, there is a high controversy regarding their pro-tumorigenic and anti-tumorigenic properties (Cal & López-Otín, 2015)(Mead & Apte, 2018). This variability would depend on many cases on the tissue or tumour type (Redondo-García et al., 2021). In addition, the same proteases have been defined with opposite roles in other tumour types (Cal & López-Otín, 2015). Moreover, ADAMTS role can change according to the substrate that is

being proteolysed. Due to the still not well described dependency to their substrates, ADAMTS functions must be deeper studied.

Similarly to ADAMTS1, described as angioinhibitory since its discovery, anti-angiogenic properties have been associated with ADAMTS2, 4, 5, 8, 9, 12, 13 and 15 while pro-angiogenic ones were attributed to ADAMTS1,3, 4 and 9 and 15 (Porter et al., 2005)(Cal & López-Otín, 2015)(Rodríguez-Manzaneque et al., 2015)(Sun, Huang, & Yang, 2015)(Zhong & Khalil, 2019). In addition, there are enzymatic-dependent functions affecting the vasculature as the ones described for proteoglycanases, ADAMTS12 and ADAMTS13 (Rodríguez-Manzaneque et al., 2015).

As in the case of its link to angiogenesis, ADAMTS1 was defined as an inflammation related genes since its discovery (K Kuno et al., 1997), and similar roles has been attributed to other partners. ADAMTS2, 4, 5, 8 and 16 are regulated by inflammatory cytokines (Rose et al., 2021). Moreover, the role of ADAMTSs in inflammatory processes and diseases can be proteolytic-dependent or proteolytic-independent. For instance ADAMTS2 is anti-inflammatory ADAMTS7, 8 and 9 are pro-inflammatory, independently on their substrates. In contrast, ADAMTS1, 4 and 12 have been associated with both anti- and pro-inflammatory properties (Redondo-García et al., 2021).

Considering the high homology in the catalytic site of all the ADAMTSs, it is a challenge to develop specific inhibitors for each protease without affecting the beneficial roles of other members of the family (Rose et al., 2021). For that reason, strategies are focused on decreasing their expression, preventing their activation and blocking their proteolytic activity (Rose et al., 2021).

6. ADAMTS1

ADAMTS1, as previously mentioned, was the first member of the ADAMTS family, described in 1997 (K Kuno et al., 1997), encoded by human *ADAMTS1* gene located in the chromosome 21. Due to the presence of thrombospondin motifs, originally it was also named as METH-1 (metalloprotease with thrombospondin motifs 1), and it was thought to be a chimera of the ADAM family (Vázquez et al., 1999).

Throughout all these years, ADAMTS1 has been associated with different pathological processes. This protease is involved in cardiovascular disorders such as the formation of atherosclerotic plaques, in aortic aneurysm and dissection (AAD) and in Marfan syndrome (characterized by thoracic AAD) (Reynolds et al., 2010)(S. Wang et al., 2018)(Zhong & Khalil, 2019)(Redondo-García et al., 2021). Moreover, it has been also related with different pathologies of the central nervous system, including Alzheimer's disease (Mohamedi, Fontanil, Cobo, Cal, & Obaya, 2020). Indeed, the knockout mouse for *Adamts1* (Ats1-KO) exhibits reduced body weight and epididymal fat mass, kidney and ureter malformations, aberrant ovaries and reduced fertility, polyuria (high amount of urine) and lower amounts of sodium and potassium in urine and increased lethality at neonatal stage (Shindo et al., 2000)(Mittaz et al., 2004). Furthermore, our group has demonstrated that two main immune organs, spleen and bone marrow, are also altered, affecting the regulation of immune populations (Rodríguez-Baena, Redondo-García, Peris-Torres, et al., 2018).

6.1. Structure, location and regulation of ADAMTS1

Remarking the general structure of ADAMTS proteases (Introduction, section 5), the variable structure of ADAMTS1 is composed by two TSR after the spacer region (K Kuno et al., 1997)(Vázquez et al., 1999)(Figure 25). After its discovery, different isoforms were reported, which are named attending to their molecular weight (Figure 25). ADAMTS1 is synthetized as an inactive zymogen in the pro-active form (p110, 110kDa) containing the pro-domain. This form is activated by the cleavage of a furin-peptidase in the trans-Golgi network before its secretion. This cleavage generates the first active form (p87, 87kDa), which is found mainly anchored to the ECM or cell surface. Finally, p87 can be cleaved by MMPs in the spacer region after the cysteine-rich region, removing the two amino-terminal TSR repeats and generating the soluble, also active, p65 isoform (65kDa) (Rodríguez-Manzaneque et

al., 2000)(Figure 25). Interestingly, ADAMTS1 has been also located in the nucleus of normal and tumoral breast cancer cell lines associated with aggrecan, suggesting its possible proteolytic activity in that cell compartment (Silva et al., 2016). Lately, it was described the ability of ADAMTS1 to be cleaved by itself in tumoral conditions, proteolysis that can be prevented by the addition of heparin/heparan sulphate (Liu et al, 2006). Moreover, its proteolytic activity can be also endogenously blocked by TIMP2 and TIMP3 and by α2-macroglobulin (α2M) (Rodríguez-Manzaneque et al., 2002)(Zhong & Khalil, 2019)(Rose et al., 2021), and mediated by TGFβ (Rocks et al., 2008).

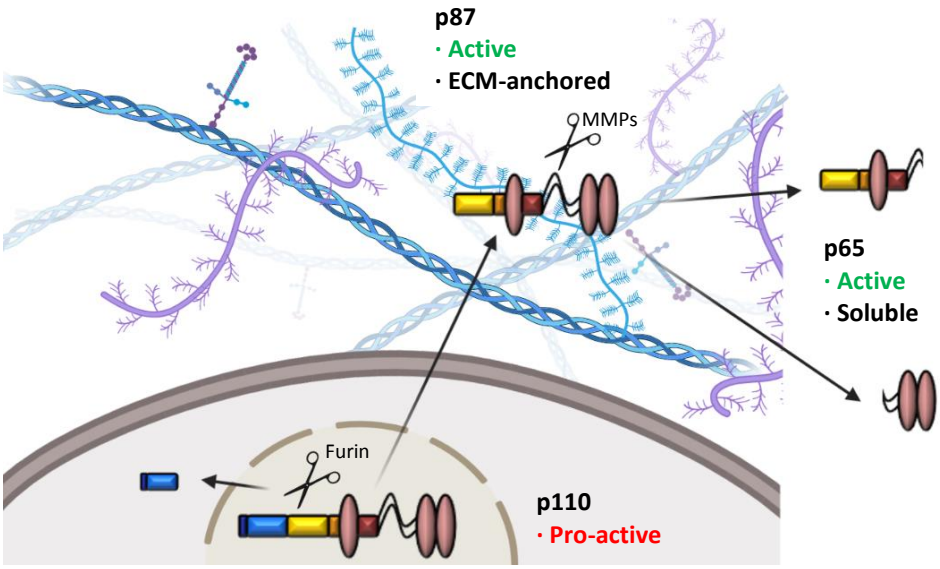

Figure 25. Different ADAMTS1 isoforms during the maturation process. Structure of the different ADAMTS1 isoforms (pro-active p100 and active p87 and p65) and location during the maturation process. Adapted from (Rodríguez-Manzaneque et al., 2000). [Created in BioRender].

Gene expression of *ADAMTS1* is regulated by different molecules. Indeed, *Adamts1* was first described as an IL1-inducible gene (K Kuno et al., 1997). Later, its regulation by progesterone and luteinizing hormones has been reported during ovulation, and by parathyroid hormone in bone and osteoblasts (Porter et al., 2005). Moreover, *ADAMTS1* was repressed by BRG1-mediated chromatin remodelling during cardiac development (Rose et al., 2021). Finally, it has been described that its expression is induced under hypoxia (Zhong & Khalil, 2019).

6.2. ADAMTS1 substrates

To date, some ADAMTS1 functions have been described to be independent to its proteolytic activity. Nevertheless, its implication in some physiological and pathological processes has also been related with its catalytic activity over its substrates. The first identified group of substrates for this protease are several proteoglycans, which includes aggrecan, mainly related with cartilage alterations (Rodríguez-Manzaneque et al., 2002), syndecan-4 that controls cell interactions with ECM and other cells (Rodríguez-Manzaneque et al., 2009) (Table 1). Moreover, among proteoglycans, versican is also included (Sandy et al., 2001). Due to its relevant implication in tumour development, immunity and inflammation, Versican is a molecule of interest in this work. As it happened with ADAMTS1, its proteolytic state is essential for its function, being intact versican associated with pro-tumorigenic scenarios and the proteolysed isoforms with anti-tumorigenic ones. Indeed, there are different versican gene splicing variants, which also have different functions, but the most studied one and in which will be focused is the V0/V1 isoforms, the ones containing GAGβ-containing domains (Papadas et al., 2020)(Islam & Watanabe, 2020)(Wight et al., 2020).

Table 1. **List of ADAMTS1 substrates.** Table including updated information of the known substrates of the protease ADAMTS1, including the group of protein and the most relevant reference for each one.

Group of proteins	Substrate	Reference
Glycoproteins	Aggrecan	(Rodríguez-Manzaneque et al., 2002)
	Syndecan-4	(Rodríguez-Manzaneque et al., 2009)
	Versican	(Sandy et al., 2001)
Basement membrane	Nidogen 1/2	(Canals, Colome, Ferrer, Plaza-Calonge Mdel, & Rodriguez-Manzaneque, 2006)
Soluble and ECM-anchored proteins	Semaphorin 3C	(Esselens et al., 2010)
	TSP1/2	(Lee et al., 2006)
	IGFBP2	(Martino-Echarri et al., 2014)
	TFPI-2	(Torres-Collado et al., 2006)
	Gelatins	(Lind et al., 2006)
EGF family	EGF-like ligands	(Liu et al., 2006)

Apart from these proteoglycans, other substrates of ADAMTS1 have been identified, such as the basement membrane glycoproteins nidogen 1 and 2 (Canals et al., 2006). Due to the relevance for this work, both nidogen and versican implication in cancer will be briefly reviewed in a following section. Furthermore, there are soluble or ECM-anchored proteins that are also ADAMTS1 substrates, including semaphorin 3C involved in neural development (Esselens et al., 2010), TSP1 and TSP2 that are anti-angiogenic molecules (Lee et al., 2006), insulin-like growth factor binding protein 2 (IGFBP2) (Martino-Echarri et al., 2014), tissue factor pathway inhibitor 2 (TFPI-2) (Torres-Collado et al., 2006) and gelatins, which are products of collagen I degradation (Lind et al., 2006). Finally, some members of EGF family are also cleaved by ADAMTS1 (Liu et al., 2006) (Table 1).

6.3. Role in tumour progression and angiogenesis

ADAMTS1 is involved in different processes that take place during tumour development such as cell proliferation, survival and migration or angiogenesis (De Arao Tan, Ricciardelli, & Russell, 2013). Still, there are controversies regarding the role of ADAMTS1 both in cancer and angiogenesis. Indeed, it is known that ADAMTS1 functions depend on its proteolytic activity and its cleavage status. While full-length ADAMTS1 shows pro-metastatic and pro-angiogenic functions by the release of angiogenesis stimulant molecules, the fragments exhibit inhibitory roles (Liu et al., 2006)(Sun et al., 2015). Moreover, it has been also reported that the functions of ADAMTS1 in tumour progression can be due to its cellular origin, differentiating between stromal and tumoral contribution of the protease in a B16F1 melanoma model (Fernández-Rodríguez et al., 2016).

It has been described that ADAMTS1 acts as a pro-tumorigenic molecule in breast, ovarian, prostate, hepatocellular, pancreatic and renal cancers as well as in melanoma and uveal melanoma and glioblastoma. In addition, it has been reported that ADAMTS1-dependent accumulation of cleaved versican affects breast cancer progression and metastasis (Gustavsson et al., 2009)(Ricciardelli et al., 2011)(De Arao Tan et al., 2013)(Martino-Echarri et al., 2014)(Fernández-Rodríguez et al., 2016)(Peris-Torres et al., 2020)(Redondo-García et al., 2021)(Serrano-Garrido et al., 2021). Furthermore, ADAMTS1 has been also related with tumour growth increase by an enhanced endothelial-like phenotype in several tumour cells (Casal et al., 2010). Moreover, given its proteolytic activity, it also promotes metastasis of murine Lewis lung carcinoma (LLC), and in breast and cancer patients (Cal & López-Otín, 2015).

Furthermore, full-length and proteolysed fragments display opposite effects (Liu et al., 2006). In contrast, it has been also demonstrated that ADAMTS1 has tumour-protective roles in human breast, gastric and colon cancer, fibrosarcoma and prostate cancer. In the case of pancreatic, CRC and lung cancer, it appears as hypermethylated (De Arao Tan et al., 2013)(Cal & López-Otín, 2015), while in the case of human breast cancer, it was mediated by the inhibition of angiogenesis and by the ADAMTS1-mediated proteolysis of NID1 and NID2 (Martino-Echarri et al., 2013a)

Regarding vascular biology and angiogenesis, ADAMTS1 has been identified as a "tip-cell" specific protease (Su et al., 2008). Following its discovery, ADAMTS1 was defined as an anti-angiogenic molecule due to its capacity to block endothelial cell proliferation by the release of TSP1 and, and to inactivate VEGFR2 (Vázquez et al., 1999)(Iruela-Arispe et al., 2003)(Sun et al., 2015)(Rodríguez-Manzaneque et al., 2015). Moreover, these angioinhibitory effects can occur by the sequestration of $VEGF_{165}$ isoform by the carboxy-terminal TSR motifs. In addition, the proteolysis of TSP1 and TSP2 by ADAMTS1 provoked the release of TSR fragments, inhibiting angiogenesis (Luque et al., 2003)(Rodríguez-Manzaneque et al., 2015). When proteolysing NID1 and NID2 in a mouse model of breast cancer, it also showed an anti-angiogenic effect, as in the proteolysis of syndecan-4, what reduced EC adhesion and angiogenesis (Porter et al., 2005)(Cal & López-Otín, 2015)(Rodríguez-Manzaneque et al., 2015). In addition, decreased expression of ADAMTS1 in mammary and prostate tumours was involved in increased levels of TSP1, turning large vessels into small vessels. Nevertheless, overexpression of the protease has the opposite effect. Moreover, it was probed that ADAMTS1 inhibits angiogenesis by inducing EC apoptosis in human prostate cancer DU145, human fibrosarcoma HT1080 and Chinese hamster ovarian cells independently to the proteolytic activity. However, this protease reduced EC proliferation and angiogenesis in human breast carcinoma T47D cells depending on the catalytic activity (Sun et al., 2015).

6.4. Recent findings regarding the immune system

Adamts1 was described as an inflammatory related gene since it was induced by IL1 (K Kuno et al., 1997). Lately, it was reported an induction of the protease in the spleen of rats stimulated with LPS (Oveland et al., 2012) and a downregulation by TGFβ and IL33 (Ng et al., 2006)(Ashlin et al., 2014). In spite of all these works linking ADAMTS1 with inflammation, little is known about the regulation of specific immune populations or its contribution during putative inflammatory processes. It has been

reported the pro- and anti-inflammatory contribution of ADAMTS1 during the atherosclerosis, as well as in AAD due to the regulation of macrophage migration. Moreover, in a model of Marfan syndrome the deficiency of ADAMTS1 was accompanied by an overexpression of NOS2, a marker of pro-inflammatory macrophages (Ashlin et al., 2013)(Oller et al., 2017)(Redondo-García et al., 2021). In addition, using a mouse deficient for CXC3CR1 that showed a downregulation of *Adamts1* and *Tsp1*, it was observed a colocalization between ADAMTS1 and the macrophage marker F4/80 (Peirong Lu et al., 2017)

In cancer, Ricciardelli et all probed that ADAMTS1 correlated with a reduced infiltration of $CD45^+$ cells, observing a switch to a Th1 immunity in breast cancer in absence of the protease (Ricciardelli et al., 2011). Similarly, using the Ats1-KO mouse, it was reported that two immune organs (spleen and bone marrow) were altered in absence of the protease. Moreover, healthy Ats1-KO mice suffered splenomegaly accompanied by an increase of T cells both in spleen and BM. In fact, same mouse model was challenged with B16F1 tumours and the reduction in tumour growth in absence of the stromal protease correlated with the regulation of the immune populations, specifically the increased infiltration of T cells, myeloid cells and the reduction of the M2 macrophage marker *Cd163* (Rodríguez-Baena, Redondo-García, Peris-Torres, et al., 2018). Interestingly, apart from the differences in the alteration of the immune populations between both tumour models, they also showed a different cleavage of Versican, suggesting its contribution in the immune system, which will be detailed later in this section of the introduction.

6.5. ADAMTS1 substrates in the tumour immune landscape: Nidogen 1 and Versican

As it has been previously reported, ADAMTS1 can affect tumour progression both dependently and independently to its proteolytic activity. For that reason, the role of two of its main substrates (nidogen 1 and versican) is included in this section in more detail. Moreover, due to the relevance for this work, we will address their connection with the immune system.

6.5.1 Nidogen 1

Both Nidogens 1 and 2 are globular multi-domain glycoprotein found in the basement membrane where they act as cross-linkers with other ECM components. Accordingly, it appears to participate in tumour-related processes (Martino-Echarri et al., 2013a). However, little is known about the possible contribution of this molecule in tumour progression. It has been defined as a good prognosis factor in ovarian serous cancer patients and its inhibition reduced the migration and invasion of endometrial cancer cells (Zhou et al., 2017). Moreover, its proteolysis in a human breast cancer model regulates vessel maturity (Martino-Echarri et al., 2013a).

Although there are other works showing the role of this ECM component to tumour development, there is still a necessity of elucidate its function in the immune system. As far as it is known, nidogen 1 has been only related with neutrophils and pro-B cells regulation. In the first case, nidogen 1 increases neutrophil adhesion and chemotaxis by the interaction with the Arg-Gly-Asp (RGD) domain (Senior et al., 1992) and reduced their cytotoxicity activity by NKp44 receptors (Gaggero et al., 2018). In fact, it has been recently described the necessity of nidogen 1 to be expressed in tumour cells for being recognised and sensitive to neutrophils cytotoxicity (Sionov et al., 2022). In the case of the of pro-B cells, nidogen 1 is in charge of the maintenance of this cells in a dedifferentiated condition, mainly in IL7-enriched BM niches (Balzano et al., 2019).

6.5.2. Versican

Versican is a large chondroitin sulphate proteoglycan with GAGs that is proteolysed by ADAMTS1 but also ADAMTS4, 5, 9, 15 and 20, and which has crucial roles in organ development and disease (Islam & Watanabe, 2020). Different to nidogen 1, versican has been associated with different pathologies but in most of the cases due to its impact on inflammation (Wight et al., 2020). Versican regulates leukocyte trafficking, which promote the inflammatory response by the release of inflammatory cytokines (Papadas et al., 2020). For that reason, it is an ECM component that must be considered in this work. Versican is involved in wound repair, lung inflammation or systemic sclerosis by higher recruitment of macrophages, which are a major source of this molecule together with fibroblasts and ECs, and $CD4^+$ Treg cells (Islam & Watanabe, 2020)(Redondo-García et al., 2021). Moreover, the negatively charged chondroitin sulphates (CS) chains that are found in its structure promote the release

of pro-inflammatory cytokines that modify antigen presentation and T cell activation. In contrast, binding to toll-like receptor 2 (TLR2) on dendritic cells and macrophages increases the release of TNFα, IL6 and IL10, deregulating T cell cytotoxicity (Wight et al., 2020)(Papadas et al., 2020)(Redondo-García et al., 2021). Furthermore, TLR and type I IFN signalling upregulates versican, inducing the production of the anti-inflammatory molecules IFNβ and IL10 (Islam & Watanabe, 2020)(Wight et al., 2020).

Increased expression of *Versican* has been associated with a variety of malignancies such as leukemia, melanoma, glioblastoma, osteosarcoma and breast, lung and prostate cancers among others. Indeed, it is central for apoptosis, migration, immune surveillance evasion, immunomodulation and tumour-promoting inflammation (Keire et al., 2017). However, as it happened with ADAMTS1, there is a huge controversy regarding the pro- and anti-tumorigenic functions of Versican. Indeed, the origin of this substrate (stromal or tumoral) and its proteolytic state (intact/full length or proteolysed) affect its role during tumorigenesis. Regarding stromal versican, it has been described that can be induced by TGFβ and promotes CCL2/MCP-1 levels, enhancing the recruitment of monocytes that are activated in breast cancer and LLC tumours via TLR2 (Kim et al., 2009)(Keire et al., 2017)(Pappas et al., 2019)(Hatano & Watanabe, 2020). In addition, it is also accumulated in myeloma, CRC, leiomyosarcoma and metastatic urine cancer, and it is associated with a tolerogenic scenario represented by less CD8 cells, more tolerogenic DCs, anti-inflammatory macrophages and MDSCs (Gorter et al., 2010)(Wang et al., 2015)(Hope et al., 2016)(Keire et al., 2017)(Hope et al., 2017)(Asano et al., 2017)(Wight et al., 2020)(Figure 26). In spite of it, other groups have defined the anti-tumorigenic roles of Versican (Ricciardelli et al., 2011)(Fanhchaksai et al., 2016)(Gao et al., 2020). In the case of tumour-derived versican, there is less controversy and it is related with pro-tumorigenic scenarios in mesothelioma, in which promotes M2 macrophage polarisation and inhibits their phagocytic activity (Pappas et al., 2019), glioblastoma (Hu et al., 2015) and in hepatocellular tumours (Zhangyuan et al., 2020).

Due to this complexity and variation in versican roles, its proteolytic state appeared as a main regulator of these functions. When versican is cleaved by ADAMTSs, including ADAMTS1, it is released as a matrikine called versikine (Wight et al., 2020). This amino terminal fragment has lost the CS chains, also interacts with TLR2 and is known to have anti-tumorigenic functions, opposite to the most extended role of the full-length protein (Hatano & Watanabe, 2020). It has been described that versikine stimulates the secretion of pro-inflammatory cytokines such as IL1β and IL6 by macrophages (Hope et al., 2016)(Schmitt, 2016)(Gupta et al., 2016)(Dhakal et al.,

2019). Moreover, in CRC, versikine enhanced the infiltration and activation of DCs, promoting T cell anti-tumorigenic activation (Hope et al., 2017)(Keire et al., 2017)(Papadas et al., 2020)(Wight et al., 2020)(Islam & Watanabe, 2020)(Figure 26).

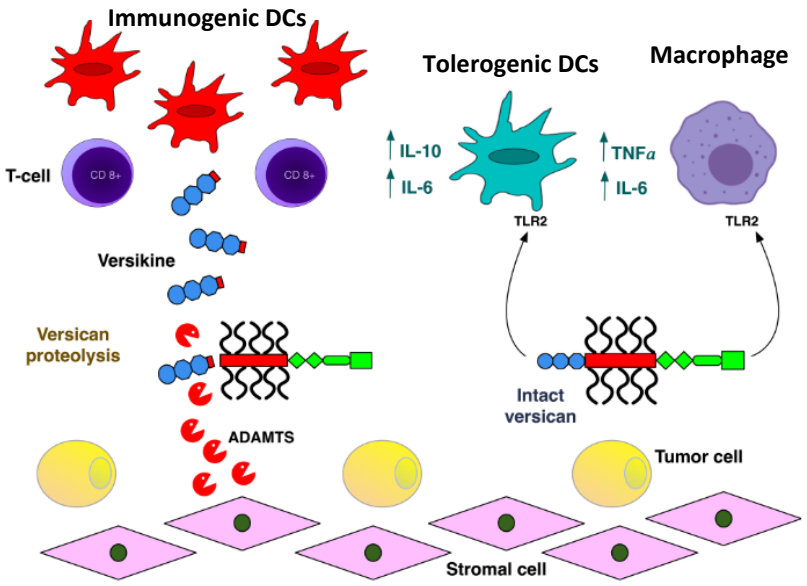

Figure 26. Known actions of versican and versikine in tumour immune infiltration. Intact versican interacts with DCs and macrophages through TLR2, polarising them to pro-tumorigenic states. In contrast, versikine promotes anti-tumorigenic DCs that enhance T cell cytotoxicity. Adapted from (Papadas et al., 2020).

For all the discussed data, versican is an ECM molecule that acts as prognosis factor as well as can modify the response the cancer therapies, especially immunotherapy. Indeed, some works relate versican expression with increase PD-L1 expression (Wight et al., 2020).

HYPOTHESIS

The microenvironment that regulates tumour behaviour is highly complex. Apart from the heterogeneity and crosstalk implicating all the cellular components, from both tumoral and non-tumoral origins, it is also essential to consider the interaction with the non-cellular elements. In this scenario, extracellular matrix composition and its regulation appeared to play a crucial role, claiming the necessity to receive more attention in oncology research.

Extracellular matrix nature and its remodelling by proteases are essential in both physiological and pathological conditions. Importantly, extracellular matrix can act as a physical barrier limiting the efficacy of therapeutic strategies, and its implication in angiogenesis, infiltration and maturation of immune populations has also been described. Moreover, the contribution of tumour-associated macrophages or myeloid-derived suppressor cells limiting the response to anti-angiogenic therapies has been highlighted. Among the constituents of this extracellular environment, the protease ADAMTS1, whose anti-angiogenic activities have been previously reported, appeared as a candidate participating in the regulation of all these intricate processes.

Preliminary results in our lab using wild type and knockout mice for ADAMTS1 have reported different behaviour of the syngeneic murine tumour models B16F1 melanoma and Lewis Lung Carcinoma (LLC). While B16F1 tumours size was clearly reduced in absence of stromal ADAMTS1, LLC tumours were not affected. Indeed, their immune infiltrate was different, and they are classified as sensitive and refractory to anti-angiogenic therapy, respectively, as summarised in Figure 27.

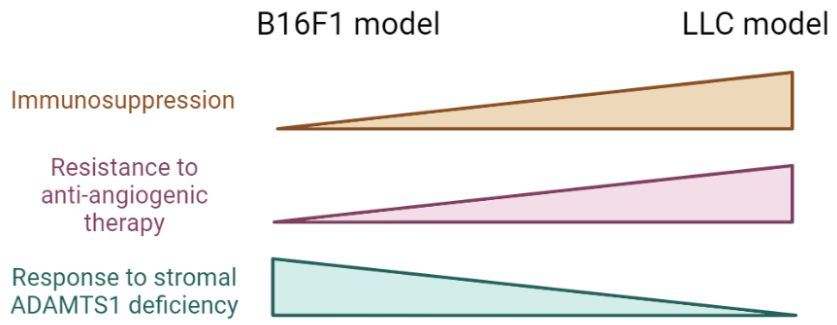

Figure 27. Differences between B16F1 and LLC models. Characterisation of both tumour models regarding immunogenicity, response to anti-angiogenic therapy and to stromal ADAMTS1 deficiency.

The hypothesis of this work is based on the awareness that ADAMTS1 regulates, at some extent, angiogenesis and the immune system. Knowing that B16F1 and LLC tumours produced different extracellular environments (Figure 27), we wanted to unveil how the activity of ADAMTS1 was behind these alterations. Importantly, a closer knowledge of the presence and nature of its substrates, and the ECM in general, is still required. To date, detailed studies of ADAMTS1, angiogenesis, extracellular matrix and immune system are still necessary to understand their connections. The possibility of using in vitro and in vivo models in which ADAMTS1 has been silenced represented an excellent scenario to investigate the immune landscape and the response to anti-angiogenic treatments.

OBJECTIVES

1. **To evaluate the contribution of stromal ADAMTS1 in the immune system regulation of Lewis Lung Carcinoma syngeneic tumours.**
   1.1. Study of LLC progression and vascularisation in absence of stromal ADAMTS1 (Ats1-KO mouse).
   1.2. To study the alteration of different immune organs in absence of stromal ADAMTS1.
   1.3. To assess the regulation of immune system in LLC-tumour bearing mice in absence of stromal ADAMTS1.

2. **To evaluate the contribution of tumour-derived ADAMTS1 in Lewis Lung Carcinoma progression and the immune landscape.**
   2.1. Generation and characterisation of ADAMTS1-knockdown LLC cells.
   2.2. Study of the effect of tumoral inhibition of ADAMTS1 in LLC progression and vascularisation.
   2.3. To assess the regulation of immune system in LLC-tumour bearing mice in absence of stromal ADAMTS1.
   2.4. Evaluation of tumour-derived ADAMTS1 role in macrophage polarisation.

3. **To evaluate ADAMTS1 contribution during anti-angiogenic therapy.**
   3.1. Comparison between sensitive (B16F1) and resistant (LLC) models to anti-angiogenic treatments.
   3.2. To analyse ADAMTS1 role in LLC tumour progression and immune infiltration after Aflibercept treatment.

RESULTS

1. Addressing the relevance of stromal ADAMTS1 in LLC progression: a comparative study with B16F1 melanoma model.

As mentioned in the hypothesis, differences in immunogenicity (Yoshimura et al., 2015), response to anti-angiogenic therapy (Shojaei et al., 2007) and different behaviour in absence stromal ADAMTS1 (Figure 27) encouraged us to study in more detail the contribution of the protease from stromal origin during LLC tumour progression. For that, we benefited using Ats1-KO mice, as we previously performed using the B16F1 melanoma tumour. Importantly, those tumours displayed a reduced growth in absence of the stromal protease (Fernández-Rodríguez et al., 2016).

Following a similar approach, LLC cells were subcutaneously injected in both WT and Ats1-KO mice. Different to the previously observed findings on B16F1 model (Fernández-Rodríguez et al., 2016), final LLC tumour growth was not affected by the absence of stromal ADAMTS1 despite there is a slight difference at early stages (Figure 28A-B). In order to unveil the mechanisms provoking that difference with B16F1, a deeper study of LLC-derived tumours was pursued.

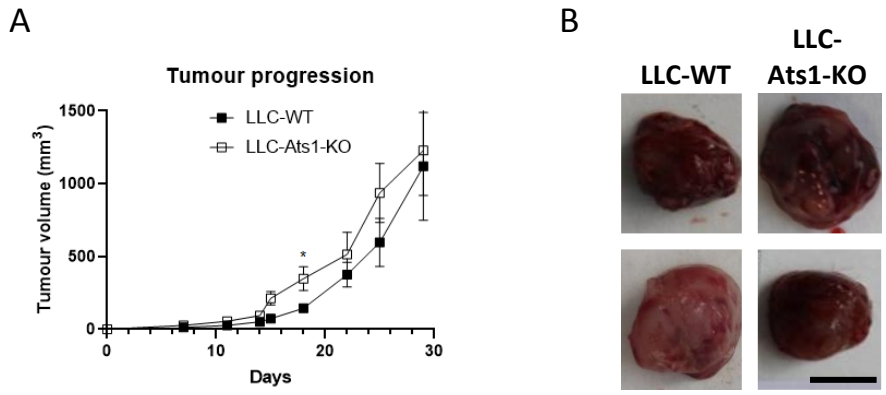

Figure 28. Contribution of stromal ADAMTS1 in Lewis Lung Carcinoma model. (A) Progression of tumour volume during the experiment represented as tumour volume ± s.e.m. (B) Representative LLC tumours in WT and Ats1-KO mice. Scale = 1 cm. (* *P*<0.05 two-tailed *t* Student, n=9 samples in each group).

1.1. Characterisation of tumour vasculature.

According to the described function of ADAMTS1 as an angiogenesis-related molecule, also in B16F1 tumours (Fernández-Rodríguez et al., 2016), vasculature was

evaluated by Endomucin staining (Rodríguez-Baena et al., 2018). As indicated in materials and methodology section, the analysed parameters included vessel density, percentage of vessel area related to total tumour area, and perimeter of vessels (Figure 29A-B). In LLC tumours, vessel density was significantly increased in absence of stromal ADAMTS1, similarly to what was observed in B16F1 tumours (Fernández-Rodríguez et al., 2016). However, B16F1 model suffered a reduction in vessel perimeter that was not observed in LLC model (Figure 29A-B).

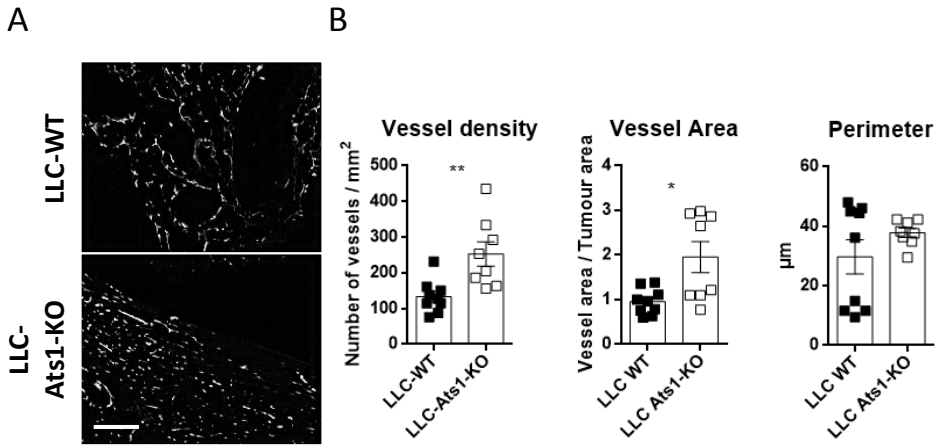

Figure 29. Effect of stromal ADAMTS1 in LLC tumour vasculature. (A) Representative images of Endomucin staining for morphometric vasculature quantification of each group. White scale = 200µm. (B) Graphs representing mean ± s.e.m of vessel density, perimeter of vessels and vessel area of each group of tumours after 29 days. (* *P*<0.05 , ** *P*<0.01 two-tailed *t* Student, n=9 samples in each group).

In parallel, measuring the expression of the endothelial-related genes *Endoglin*, *Cdh5* and *Cd31* did not show significant differences between both tumour groups (Figure 30A). Finally, to approach the maturation of tumour vasculature, the immunofluorescence evaluation of smooth muscle actin (SMA) deposition around tumour vessels did not show differences in LLC-Ats1-KO tumours compared to WT littermates (Figure 30B). Altogether, and despite vessel functionality or alternative angiogenesis mechanisms that could be involved, these results indicate that, at least at some extent, ADAMTS1 also has an inhibitory role in the vasculature in LLC tumours, but not as strong as in B16F1 tumours (Fernández-Rodríguez et al., 2016). Indeed, these studies imply that stromal ADAMTS1-dependent changes in vasculature are not enough to compromise the progression of LLC tumours in WT and Ats1-KO mice.

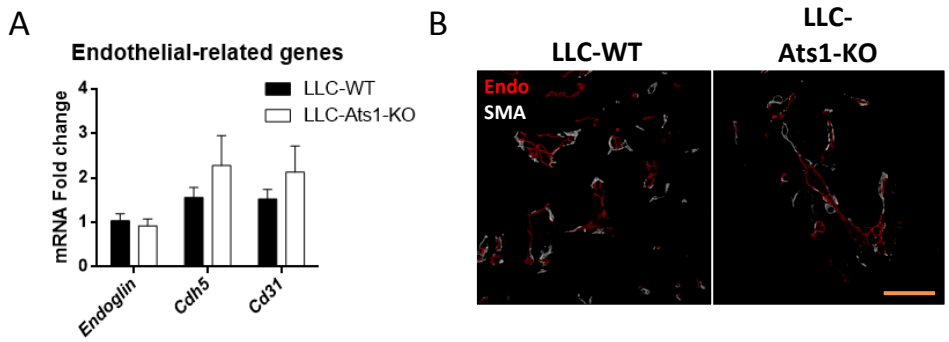

Figure 30. Regulation of endothelial molecules by stromal ADAMTS1 in LLC tumours. (A) Graphs representing relative mRNA fold change expression of genes related to vasculature (*Endoglin*, *Cdh5* and *Cd31*). (B) Representative confocal images of SMA deposition (white) together with the endothelial marker Endomucin (red) in tumours 29 days after cells inoculation. Yellow scale = 50µm. (N=9 samples in each group).

1.2. Study of ADAMTS1 and ADAMTS-related molecules.

Due to the proteolytic activity of ADAMTS1, molecules of the extracellular matrix were also evaluated as putative targets. From the known substrates of ADAMTS1, we analysed Nidogen 1 and Versican due to their functions in the organisation of the vBM and in immunity regulation, respectively. Apart from the expected reduction of *Adamts1* expression in LLC-Ats1-KO tumours (Figure 31A), the versicanases *Adamts4* and *Adamts9*, the ones with higher expression levels in LLC model, stayed unaltered. Moreover, levels of Nidogen 1 and Versican were also analysed. While their gene expression was not affected (Figure 31B), the protein accumulation of both molecules in tumours was highly increased in absence of stromal ADAMTS1 (Figure 31C), displaying a positive signal all around the tissue and not limited to the vascular network. These findings supported the reduced proteolysis of both substrates in the LLC-Ats1-KO tumours due to the reduced expression of the protease. Contrary to these current observations, B16F1 tumours in Ats1-KO mice showed lower expression of *Adamts4* and *Adamts9* but a decreased accumulation of intact Versican than WT group, differing from the LLC tumours and suggesting alternative mechanisms involved in Versican regulation (Rodríguez-Baena et al., 2018). In addition, it is important to highlight that the overall levels of *Adamts1* are higher in B16F1 tumours compared to LLC ones, whereas both Nidogen 1 and Versican are less represented in such melanoma model (data not shown).

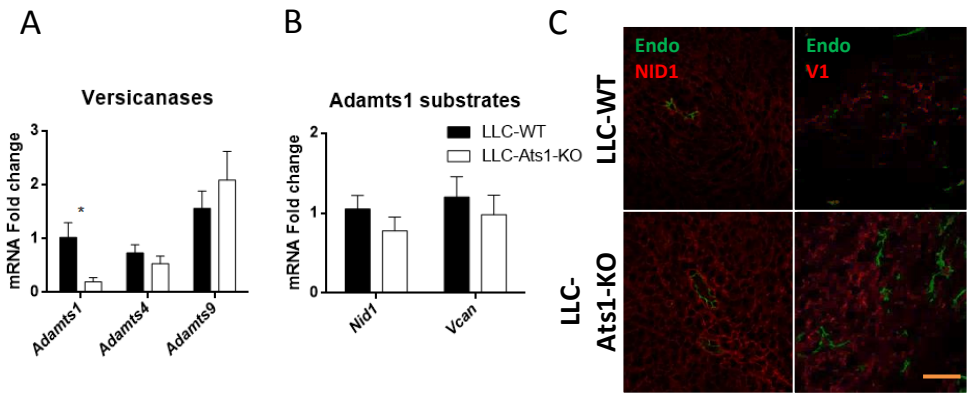

Figure 31. Effect of stromal ADAMTS1 in ECM gene expression and deposition. (A) Graph representing relative mRNA fold change expression of ADAMTS proteases with versicanase activity. (B) Graph representing relative mRNA fold change expression of relevant ADAMTS1 substrates (*Nidogen 1* and *Versican*). (C) Representative confocal images of NID1 and full-length VCAN deposition (red) together with the endothelial marker Endomucin (green) in tumours 29 days after cells inoculation. Yellow scale = 50µm. (* *P*<0.05 two-tailed *t* Student, n=9 samples in each group).

To sum up this section, we concluded that ADAMTS1 is affecting tumour vasculature, and also the accumulation of Nidogen 1 and Versican. Moreover, we have found a correlation between such increased levels of substrates and increased vascular density. However, these results do not explain the lack of effects on LLC growth in the absence of stromal ADAMTS1 whereas other model does. For that reason, a deeper analysis of other microenvironment constituents is still needed. Next, studies of the immune system are presented.

2. Alteration of immune compartment in the absence of ADAMTS1 protease in healthy and tumour conditions.

ADAMTS1, as well as other members of the extracellular milieu, has been recently studied due to its contribution on immune system regulation in both healthy conditions and tumoral environments. Indeed, our group has recently reviewed how members of the ADAMTS family and its substrates may participate in this regulation in diseases with a relevant inflammatory component, including cancer (Redondo-García, et al., 2021). Apart from the widely accepted analysis of the vasculature, we considered the evaluation of immune-related parameters, as another relevant contributor within the TME. In fact, previous results of our lab already showed changes in immune-related parameters induced by ADAMTS1 (Fernández-Rodríguez et al., 2016)(Rodríguez-Baena, et al., 2018). This encouraged us to study the immune system of LLC tumours in an ADAMTS1-dependent manner, in order to understand why the lack of the protease does not affect tumour growth, contrary to what was observed in other tumour models. Likewise, we first studied two relevant immune organs: spleen and BM, of healthy Ats1-KO mice.

2.1. Relevance of stromal ADAMTS1 in healthy tissues.

2.1.1. Spleen and its immune populations.

First, this thesis revealed a significant splenomegaly in Ats1-KO mice compared to WT littermates, whose weight was corrected according to body weight (detailed in the materials and methods section) (Figure 32A). Next, we identified and evaluated specific immune populations by flow cytometry (FC) (Figure 32B). Among these populations, the most significant value was the increase of $CD3^+$ T cells in Ats1-KO versus WT spleens. Finally, we completed this characterisation looking at the gene expression of T cells (*Cd3*, *Cd4* and *Cd8*) and macrophage-related (*Nos2*, *Cd163*, *Cd206*) markers (Figure 32C). These studies revealed an upregulation of *Cd3* and *Cd4*, corroborating the increase in CD3 cells in Ats1-KO mouse observed by FC. Despite the increase in the number of T cells, functionality of this population should be also evaluated.

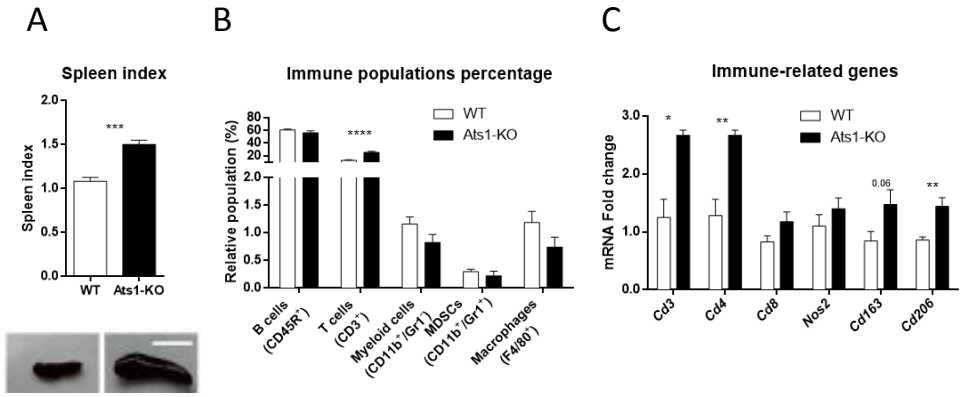

Figure 32. Spleen immunocharacterisation of healthy WT and Ats1-KO mice. (A) Representative images of spleens from WT and Ats1-KO mice (scale = 1cm) and graph representing the spleen index. (B) Flow cytometry data showing the percentage of immune populations represented as mean ± s.e.m of live cells in WT and Ats1-KO spleens. (C) Graphs representing relative mRNA fold change expression of genes related to immune system (*Cd3*, *Cd4*, *Cd8, Nos2, Cd163, Cd206*). (* *P<0.05*, ** *P<0.01*, *** *P<0.001*, **** *P<0.0001* two-tailed t Student, n=7 and n=5 samples in WT and Ats1-KO groups, respectively).

In the case of myeloid cells, although FC assays showed not altered proportions in the absence of ADAMTS1 (Figure 32B), a closer study of gene expression using specific polarization markers revealed some interesting differences. While *Nos2*, a M1 marker, did not show differences, both M2 markers, *Cd163* and *Cd206*, showed an upregulation, reflecting an increase in pro-tumorigenic macrophages in Ats1-KO spleens (Figure 32C) that should be considered.

2.1.2. Bone marrow and its immune populations.

In parallel to the spleen, we examined BM immune populations. Importantly, we observed a similar increase of T cells in Ats1-KO BM (Figure 33A), although this population is the least representative in this organ. Indeed, gene expression analyses confirmed the increase of T cells by an upregulation of *Cd3* and *Cd8* genes, suggesting again an induced cytotoxic environment. However, there was an unexpected downregulation of *Cd4* expression in Ats1-KO BM, opposite to the result observed in the spleen (Figure 33B). However, its contribution can be limited due to its low frequency.

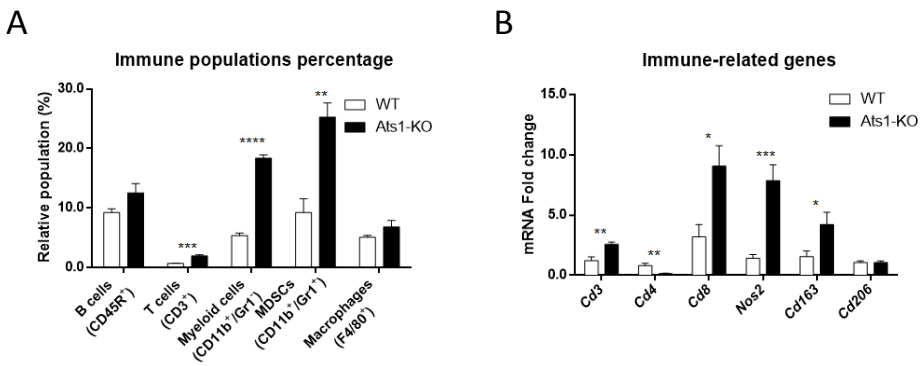

Figure 33. Bone marrow immune-characterisation of healthy WT and Ats1-KO mice. (A) Flow cytometry data showing the percentage of immune populations represented as mean ± s.e.m of live cells in WT and Ats1-KO bone marrow. (B) Graphs representing relative mRNA fold change expression of genes related to immune system (*Cd3*, *Cd4*, *Cd8, Nos2, Cd163, Cd206*). (* *P<0.05*, ** *P<0.01*, *** *P<0.001*, **** *P<0.0001* two-tailed t Student, n=6 samples in each group).

In contrast with the absence of changes in spleen, FC data on myeloid cells revealed a clear increase in $CD11b^{+}/Gr1^{-}$ and $CD11b^{+}/Gr1^{+}$ myeloid-derived suppressor cells (MDSCs) in Ats1-KO BM, probably accentuated by the higher abundance of these populations in BM (Figure 33A). Both of these myeloid populations are relevant inducing an immunosuppressive environment and are the responsible of resistance to some cancer therapies (Shiao et al., 2011)(Garner & de Visser, 2020). In agreement with this increase of myeloid cells in Ats1-KO BM, gene expression of both *Nos2* and *Cd163* macrophage markers were upregulated in absence of ADAMTS1 (Figure 33B).

As an overall perspective, this early characterisation of the immune organs spleen and BM revealed a consistent increase of T cells in Ats1-KO mice. In contrast, myeloid populations were enhanced just in the BM of Ats1-KO. Accordingly, these results encouraged us to perform deeper analyses of specific macrophage-related immune populations, as follows in next section.

2.1.3. Bone marrow-derived macrophages.

Myeloid populations appeared to be very important in LLC tumours. Moreover, taking into consideration the pro-tumorigenic properties of some of these cells and their responsibility for the resistance to some cancer therapies, we decided to study them in more detail, evaluating the contribution of ADAMTS1 to their functions and

activity. We obtained bone marrow-derived macrophages (BMDMs) from WT and Ats1-KO mice and we achieved several *ex vivo* experiments, including adhesion, migration, polarisation and phagocytosis assays.

Using an enriched population of $CD11b^+$ cells from both WT and Ats1-KO BMs (Figure 34A-B), we firstly approached their *in vitro* adhesive properties, observing that the absence of the protease did not affect this capacity (Figure 34C).

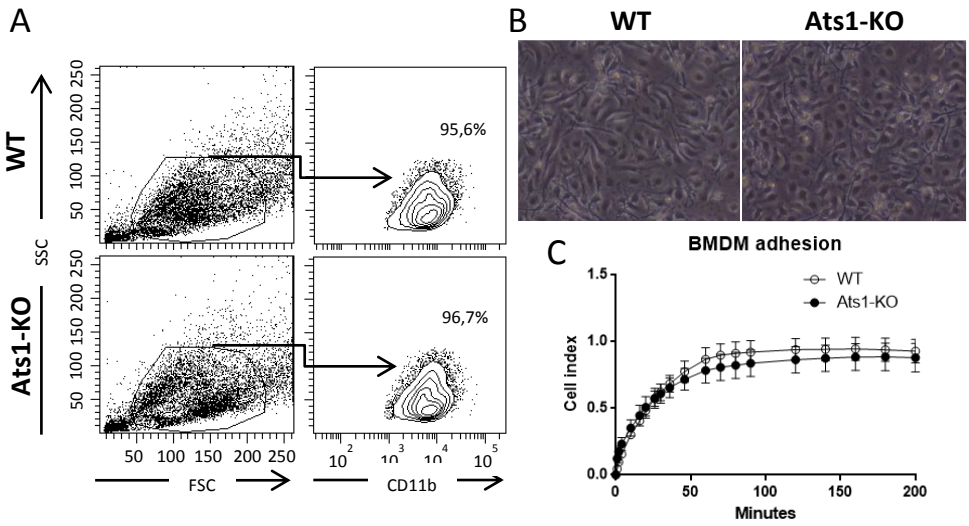

Figure 34. BMDM selection from WT and Ats1-KO and adhesion properties. (A) Representative gating strategy showing $CD11b^+$ population selection (mean percentage included) from bone marrow culture. (B) Representative bright field pictures of WT and Ats1-KO macrophages after selection. (C) Cell index representing the cell adhesion along the time performed in xCELLigence platform.

Apart from the ability to adhere, macrophages migrate to specific scenarios to accomplish their functions, including tumours. To evaluate this capacity, WT and Ats1-KO BMDMs were cultured on 8-µm pore transwell and let them to migrate in absence (negative control) or presence of FBS (positive control) (Figure 35A). After 24 hours, we observed a decreased in the migratory efficiency of Ats1-KO BMDM, although without statistically significant differences (Figure 35B).

As introduced in previous sections, it is important to determine the polarisation state of macrophages, since M1 and M2 macrophages have opposite functions regarding inflammation and tumour progression. Considering the differential regulation of genes between polarised macrophages in the BM, we performed 24-hour *in vitro* polarisation experiments to unveil a putative contribution of stromal ADAMTS1.

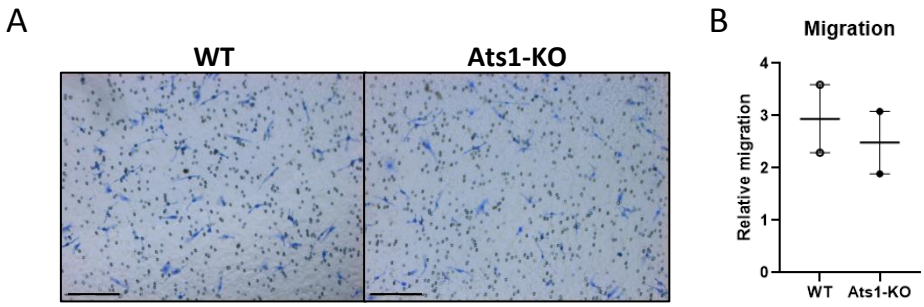

Figure 35. BMDM migration in transwell assays depending on stromal ADAMTS1. (A) Representative pictures after 24-hour migration experiment in presence of FBS. (B) Quantification of two independent experiments showing the relative induction of positive control (with FBS) compared to negative control (without FBS). Scale = 150µm. N=2 samples in each group.

In terms of morphology, the already described changes between M0, M1 and M2 states were detected without significant differences between different WT and Ats1-KO genotypes (Figure 36).

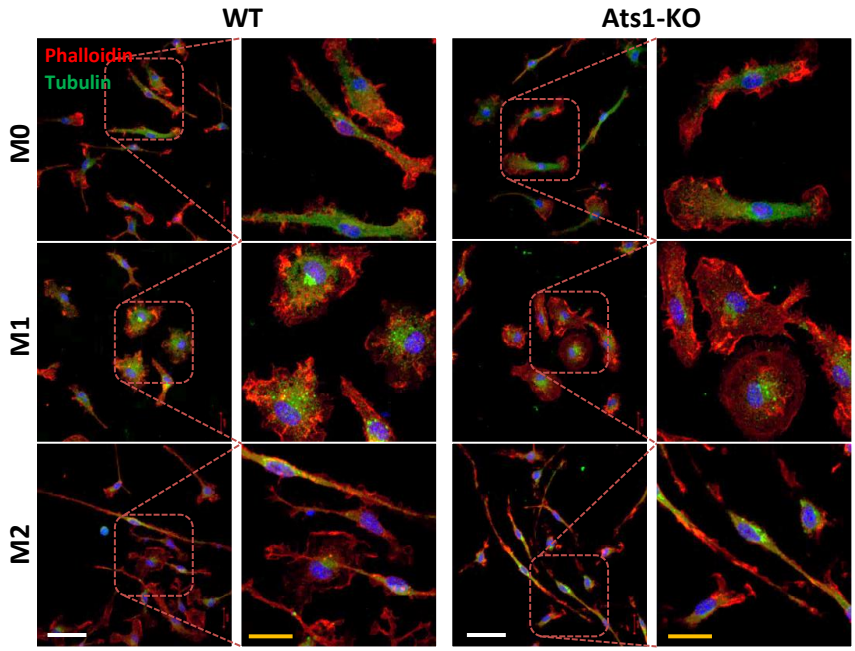

Figure 36. WT and Ats1-KO BMDM polarisation morphology. Representative immunofluorescence pictures of WT and Ats1-KO macrophages after 24 hours of polarisation to M1, M2 and non-polarised M0 BMDM. Cells were seeded and polarised on fibronectin-coated coverslips and stained with phalloidin-TRITC (red) and α-tubulin-FITC (green). White scale = 40µm, yellow scale = 20µm.

Furthermore, polarisation of both WT and Ats1-KO BMDMs was confirmed by analysing gene expression of canonical markers of each state. On the one hand, *Tnfa*, *Il6* and *Nos2* were examined for the M1 polarisation, observing a clear upregulation of these three genes (Figure 37A). On the other hand, M2 polarisation was confirmed by the induction of *Cd163*, *Cd206* and *Arg1* in M2 group compared to the others (Figure 37B).

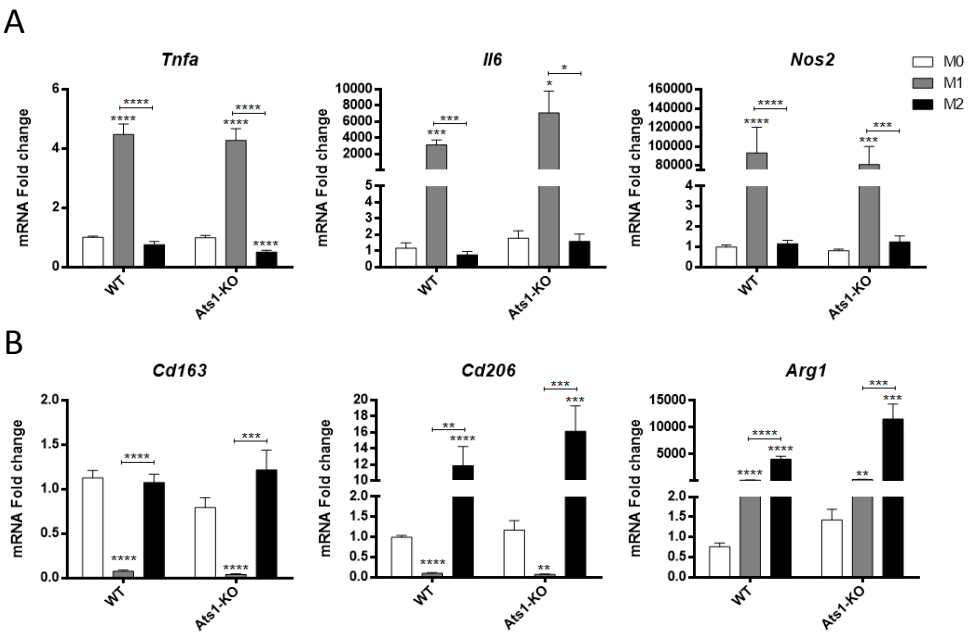

Figure 37. Gene expression analysis of WT and Ats1-KO BMDM polarisation state. Graphs representing relative mRNA fold change expression of genes related to (A) M1 polarisation (*Tnfα*, *Il6* and *Nos2*) and (B) M2 polarisation (*Cd163*, *Cd206* and *Arg1*). M0 group was used as control for statistics tests. (* *P<0.05*, ** *P<0.01*, *** *P<0.001*, **** *P<0.0001* two-tailed t Student, n=11 and n=7 samples in WT and Ats1-KO groups, respectively).

After confirming that both WT and Ats1-KO BMDM were polarizing to M1 and M2 states, next step was to assess whether the differential polarisation capacity could be impaired regarding ADAMTS1 deficiency. For that, gene expression of the analysed genes was contrasted between WT and Ats1-KO counterparts, without differences between them (data not shown). In parallel, polarisation was also checked by FC using NOS2 as M1 (Figure 38A), and CD206 as M2 markers (Figure 38B). Likewise, we confirmed an increase for each marker in their respective polarised groups, compared to M0 samples, but without showing differences between WT and Ats1-KO BMDMs.

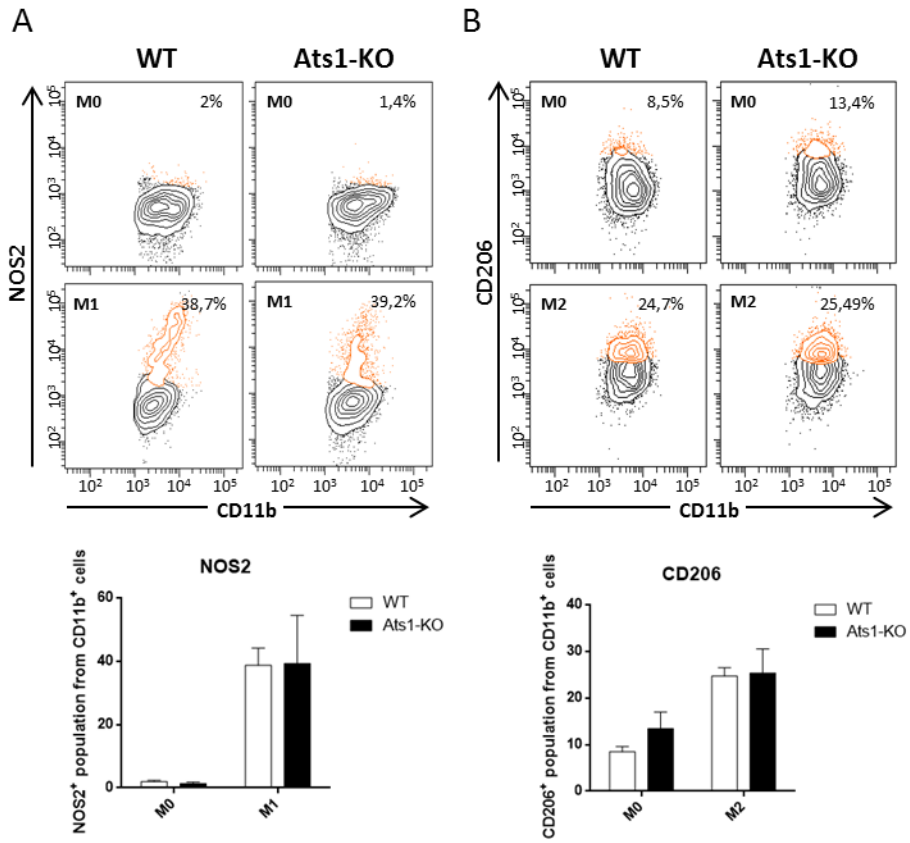

Figure 38. Effect of stromal ADAMTS1 in NOS2 and CD206 protein levels during BMDM polarisation. Representative flow cytometry plots including the mean percentage of (A) NOS2 and (C) CD206 in M1 and M2 24h-polarised $CD11b^+$ populations respectively and their quantification (orange population). N=9 and n=4 samples in WT and Ats1-KO groups, respectively.

Although these polarization assays (Figures 36-38) did not reveal significant alterations in the absence of the protease ADAMTS1, our studies also included the determination of the gene expression levels of the protease during the polarisation process in WT cells. In parallel, we studied Versican, as one of the ADAMTS1 substrates whose immunomodulatory properties have been more relevantly described (Wight et al., 2020). Interestingly, we found that *Adamts1* was overexpressed in M2 macrophages compared to M0 (Figure 39A). In the case of *Versican*, it was clearly overexpressed in M1 BMDMs independently of the presence or absence of stromal ADAMTS1. Significantly, we observed a slight induction of *Versican* expression in M2 macrophages derived from Ats1-KO BMs (Figure 39A). Moreover, the alteration induced by the absence of ADAMTS1 appears to have a

major impact on M2 macrophages, also patent when the comparison is between WT and Ats1-KO BMDMs (Figure 39B, black bar), whose consequences will need to be considered.

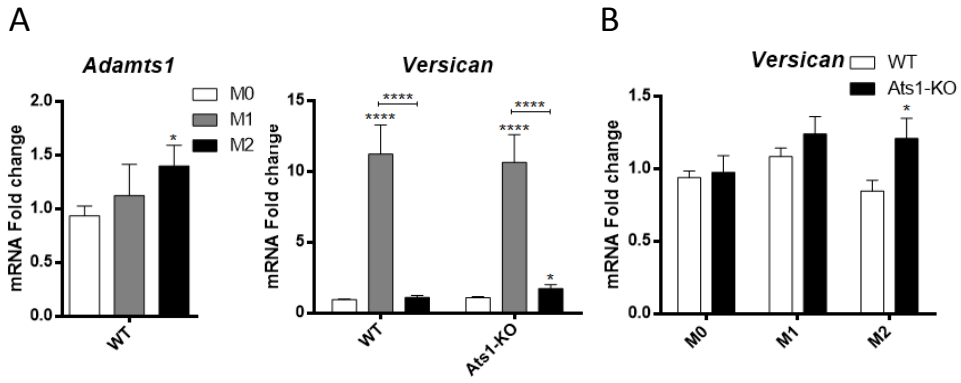

Figure 39. Regulation of *Adamts1* and *Vcan* during BMDM polarisation. Graphs representing relative mRNA fold change expression of *Adamts1* and *Vcan* depending on polarisation state (A) and depending on stromal ADAMTS1 levels for each polarisation state (B). (* *P<0.05*, **** *P<0.0001* two-tailed t Student, n=14 samples in each group).

Phagocytosis-mediated tumour clearance has been shown as another relevant function of these myeloid cells during tumour development (C. Li et al., 2021). Therefore, we assessed the phagocytic activity of macrophages *in vitro* considering the presence or absence of stromal ADAMTS1. As in previous assays, we used BMDM from WT and Ats1-KO mice. For these new experiments, phagocytosis was evaluated for three different tumour cells (murine LLC and B16F1, and human fibrosarcoma HT1080), properly labelled with carboxifluorescein diacetate succinimidyl ester (CFSE) and added to the BMDM monolayer (see materials and methodology section). This co-culture approach allowed us to measure the engulfment/phagocytosis of tumour cells by the macrophages, using FC. Since tumour cells were labelled with CFSE, and macrophages are positive for CD11b marker, we were able to detect four different populations: total macrophage population ($CD11b^+$), non-engulfed tumour cell population ($CD11b^-/CFSE^+$), macrophages not phagocytizing tumour cells ($CD11b^+/CFSE^-$), and macrophages engulfing tumour cells and have incorporated CFSE signal ($CD11b^+/CFSE^+$) (Figure 40A). Interestingly, after 2.5 hours we observed that the number of $CD11b^+/CFSE^+$ cells (Figure 40A, orange population) was lower in Ats1-KO samples in comparison with WT ones (Figure 40B). These results indicate that Ats1-KO BMDM were less efficient in phagocytising tumour cells, which can have important consequences during tumour progression.

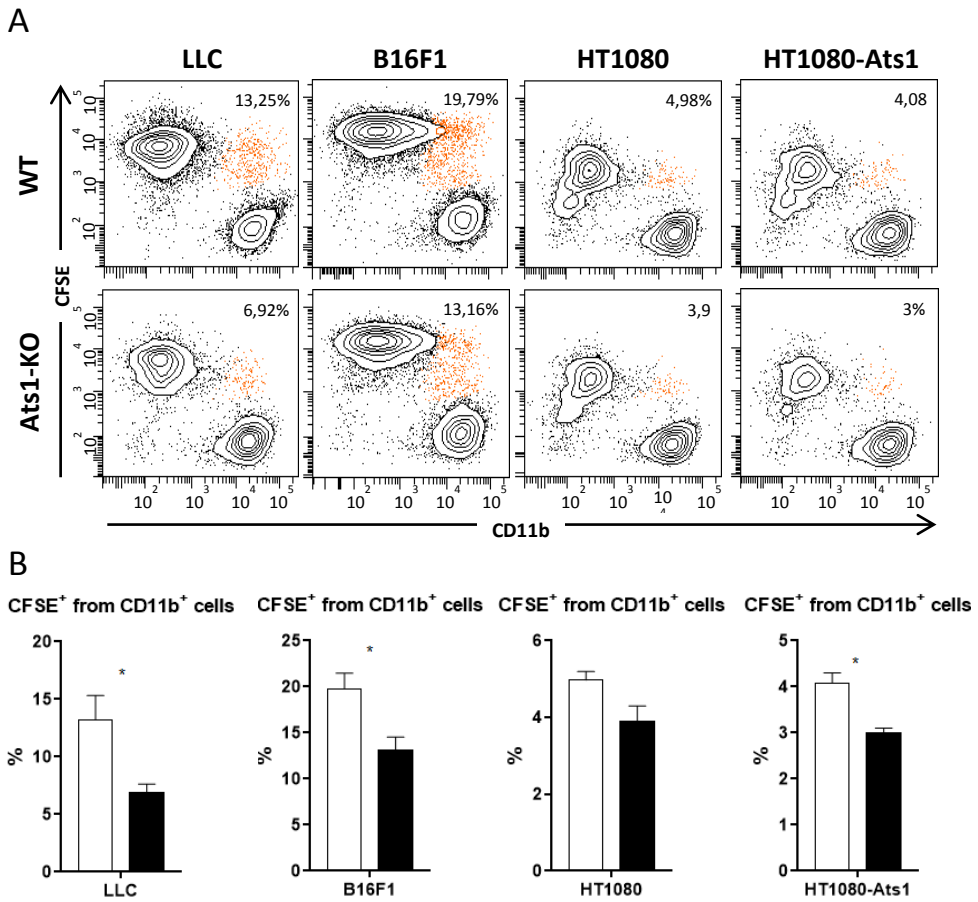

Figure 40. Effect of stromal and tumoral ADAMTS1 in macrophage-mediated tumour cell engulfment. (A) Representative flow cytometry plots showing the co-culture of tumour cells ($CFSE^+$) and macrophages ($CD11b^+$). (B) Quantification of $CFSE^+$ cells from total $CD11b^+$ populations (orange population). (* *P<0.05* two-tailed t Student, n=7, n=4, n=2 and n=2 samples in LLC, B16F1, HT1080 and HT1080-Ats1 groups, respectively).

According to the extracellular nature of ADAMTS1, we wondered if higher levels of the protease in the media could reverse the engulfment deficiency observed in Ats1-KO cells. With such purpose, we approached this assay using a tumour cell line overexpressing ADAMTS1 (HT1080-Ats1) (Figure 40A) (Casal et al., 2010). Though, the production of tumour-derived ADAMTS1 did not improve the phagocytic activity of Ats1-KO macrophages (Figure 40B). Moreover, when comparing the percentage of macrophages that have engulfed tumour cells ($CD11b^+/CFSE^+$, orange population) between HT1080 (4.97% in WT and 3.9% in Ats1-KO) and HT1080-Ats1 (4.075% in WT and 3% in Ats1-KO), it was observed that the overexpression of ADAMTS1 in the

tumour cells reduced the phagocytic capacity, indicating that tumour-derived ADAMTS1 can also affect this ability. However, deeper analyses are still needed.

As a different way to characterise the contribution of ADAMTS1 in macrophage phagocytosis, we also performed *in vitro* experiments using clodronate liposomes. These particles are extensively used *in vivo* for depleting macrophages due to the concurrence of macrophage-phagocytic capacity and the toxicity of clodronate (Rooijen & Sanders, 1994). According to our previous results, we expected a decrease in cell death of Ats1-KO BMDM since they are less efficient in phagocytising the clodronate liposomes. As expected, 24 hours after adding these liposomes, cell viability was reduced compared to PBS liposomes (Figure 41A), with a higher effect when macrophages were incubated with the highest clodronate concentration. Moreover, we observed an apoptosis-mediated cell death due to the clodronate since there is an increase in the percentage of Annexin V^+ cells comparing with the effect of PBS liposomes (Figure 41B). Although it is not statistically significant, Annexin V^+ population was smaller in Ats1-KO BMDM comparing with WT mates. Again, this result indicates that macrophages not expressing ADAMTS1 were less efficient phagocytising the liposomes, and in consequence, these cells suffered less apoptosis. In the case of $7AAD^+$ population, a similar reduction was observed in Ats1-KO BMDM compared to WT, corroborating the deficiency in phagocytosis.

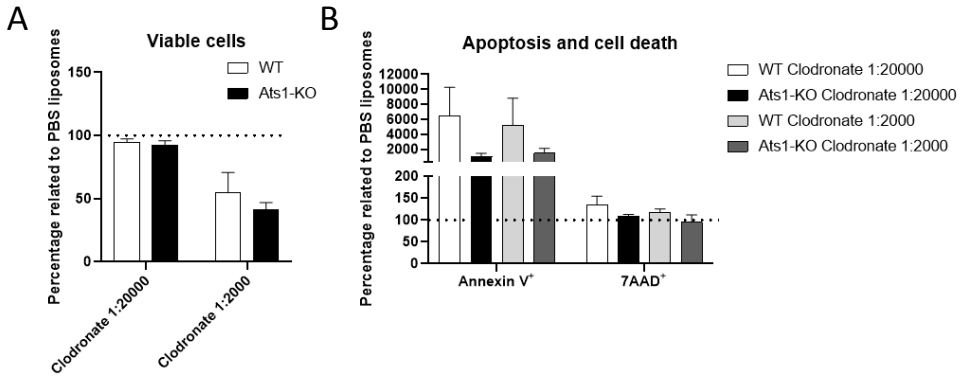

Figure 41. Effect of stromal ADAMTS1 in macrophage-mediated tumour cell engulftment. (A) Representative flow cytometry plots showing the co-culture of tumour cells ($CFSE^+$) and macrophages ($CD11b^+$). (B) Quantification of $CFSE^+$ cells from total $CD11b^+$ populations . Dot line is the reference, representing the treatment with PBS liposomes. N=3 samples in each group.

In an attempt to show a global perspective of this later section, the deep characterisation of BMDM to elucidate the role of the stromal ADAMTS1 protease demonstrated that Ats1-KO BMDM were less efficient in migrating, and also to

phagocytise external agents, functions in which ECM remodelling play a role and which can have essential effects on tumour progression. In contrast, the absence of stromal ADAMTS1 did not alter adhesion, neither the efficiency of macrophage polarisation. Knowing these alterations in macrophage behaviour, and considering the key contribution of this immune cell population during tumour progression (especially in the LLC model), next step comprised characterising the immune environment in tumour-bearing mice.

2.2. Relevance of stromal ADAMTS1 during tumour progression.

In line with the showed characterization of BMDM and knowing how that absence of stromal ADAMTS1 affects important properties such as migration and phagocytosis, we sought to study these and other immune cellular populations during tumour progression.

2.2.1. Alteration of tumour immune infiltration and immune organs by stromal ADAMTS1 in LLC and B16F1 tumour-bearing mice.

In the attempt to understand the differences between models and the contribution of ADAMTS1 in the regulation of tumour immune infiltrate, we compared both LLC and B16F1 tumours, which different behaviour has been already summarised (Figure 27).

In line with previous sections, both FC and gene expression analyses were also used for these new studies. First, considering the lymphoid lineage, FC data revealed no alteration of the minor percentage of B cells, while $CD3^+$ T cells were clearly increased in Ats1-KO tumours comparing with WT ones, independently of the tumour model (Figure 42A and C). This finding agreed with our previous results comparing healthy spleen and BM of WT and Ats1-KO mice (Results, section 2.1, Figures 32-33), and also showed a similar outcome to our different tumour cells.

Nevertheless, myeloid cells were differently regulated depending on the model. While the absence of stromal ADAMTS1 in the B16F1 model was accompanied by a significant increase of both myeloid CD11b$^+$/Gr1$^-$ and CD11b$^+$/Gr1$^+$ populations, LLC-Ats1-KO tumours did not display these alterations, and even were in the opposite direction for CD11b$^+$/Gr1$^+$ cells. Mature F4/80$^+$ macrophages were constant between the models with and without stromal ADAMTS1 (Figure 42A and C).

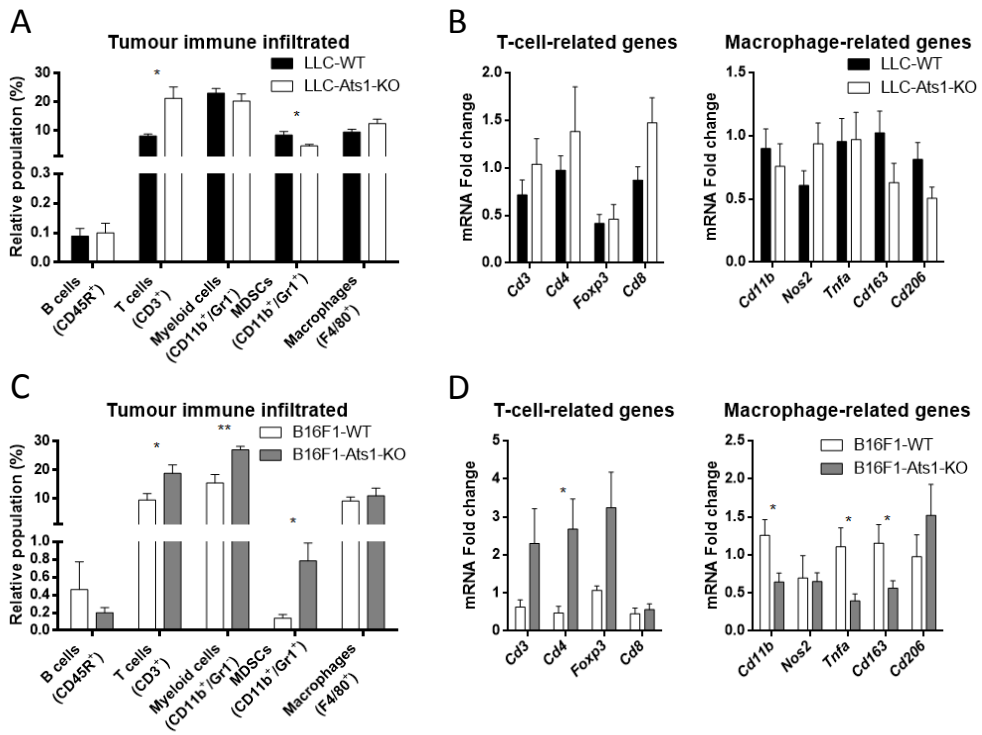

Figure 42. Immunocharacterisation of LLC and B16F1 tumours in WT and Ats1-KO mice. Flow cytometry data showing the percentage of immune populations represented as mean ± s.e.m of live cells in WT and Ats1-KO tumours (A and C, LLC and B16F1 tumours respectively). Graphs representing relative mRNA fold change expression of genes related to T cells (*Cd3*, *Cd4*, *FoxP3* and *Cd8*) and macrophages *(Cd11b*, *Nos2, Tnfa*, *Cd163* and *Cd206*) (B and D, LLC and B16F1 tumours respectively). (* *P<0.05*, ** *P<0.01*, two-tailed t Student, n=9 and n=8 samples in LLC model and n=5 and n=6 samples in B16F1 model in WT and Ats1-KO groups, respectively).

To complete the analysis, gene expression of specific markers related to T cells (*Cd3*, *Cd4*, *Foxp3* and *Cd8*) and macrophages (*Cd11b* as a general marker, *Nos2* and *Tnfa* for M1 macrophages, and *Cd163* and *Cd206* for M2) were evaluated (Figure 42B and D). In the case of the LLC model, none of the genes showed differences regarding the absence of stromal ADAMTS1 (Figure 42B). In contrast, B16F1 model did reveal

changes depending on ADAMTS1, including the overexpression in Ats1-KO tumours of T cell-related markers, *Cd3*, *Cd4* and *Foxp3*. This result reinforced the observed increment of $CD3^+$ cells observed by FC, which explains the reduction in tumour growth (Figure 42D). Regarding macrophage-related genes, we found a downregulation of *Tnfa* and *Cd163,* M1 and M2 marker respectively, following the *Cd11b* gene expression tendency but not the FC result (Figure 42B and D). Altogether, these results suggested that the differences between both models can be produced by changes in the myeloid lineage instead of T or B cells.

Furthermore, and according to the different immune landscape reported in healthy Ats1-KO mice (Results, section 2.1), we also studied how the different tumours would educate spleen and BM organs.

Splenomegaly observed in healthy mice was also confirmed in both models (Figure 43A and D). However, FC showed that no population was altered in LLC-tumour bearing mice (Figure 43B). Additionally, gene expression analyses were also performed including T cell-related genes (*Cd3*, *Cd4* and *Cd8*) and myeloid-related genes (*Cd11b* and *Gr1*). For this model, almost all the genes were upregulated, with statistically significant difference for *Cd8*, *Cd11b* and *Gr1*, although this data did not support FC results (Figure 43C).

Next, FC analysis of spleens from B16F1-bearing showed results that were similar to the healthy mice regarding T and B cells, different to LLC tumours. However, there was an increase of $F4/80^+$ macrophages in Ats1-KO mice in presence of B16F1 tumours (Figure 43E). Finally, gene expression data corroborated the increase of T cells by the overexpression of *Cd3*, *Cd4* and *Cd8*, as it was observed in absence of tumours. Nevertheless, the downregulation of *Cd11*b did not support FC data (Figure 43F).

Although mice bearing both tumour types showed similar splenomegaly than in healthy conditions, the education of this organ was different according to the tumour. In the case of T cells, B16F1 model was similar to healthy conditions while LLC tumours attenuated Ats1-KO differences in the spleen. Moreover, in the case of myeloid lineage, the only difference between models was that B16F1-bering mice had higher representation of $F4/80^+$ in Ats1-KO mice compare to WT, which was not observed in the LLC model. Nevertheless, myeloid-related markers were in opposite direction, suggesting the major contribution of this lineage for the differences between models.

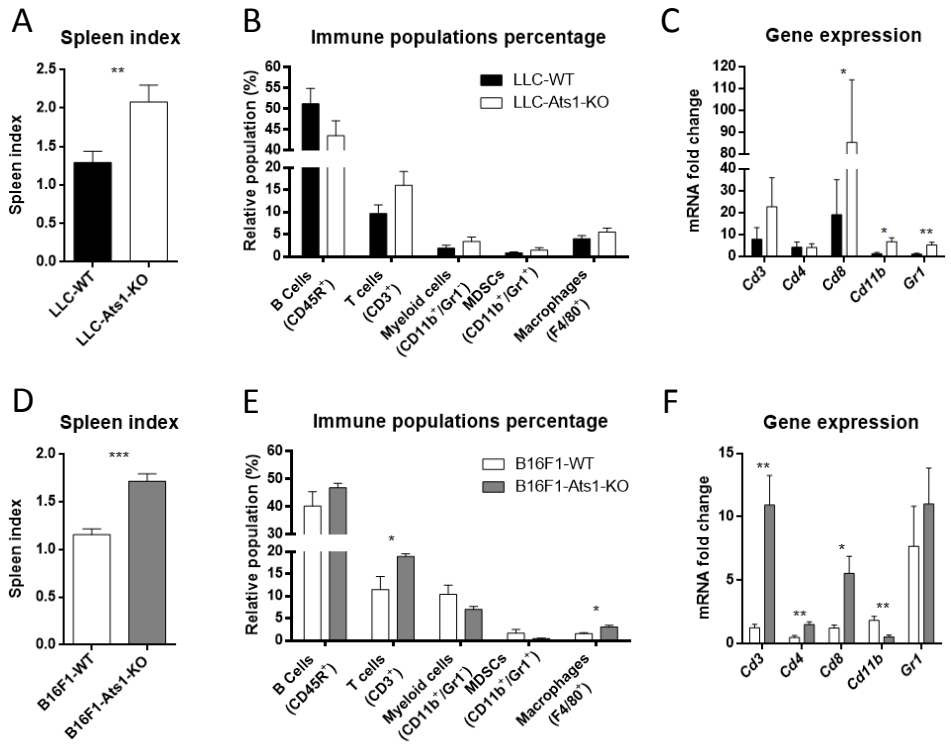

Figure 43. Regulation of spleen education by LLC and B16F1 tumours in WT and Ats1-KO mice. Graph representing the spleen index. (A and D, LLC and B16F1 respectively). Flow cytometry data showing the percentage of immune populations represented as mean ± s.e.m of live cells in WT and Ats1-KO spleens in LLC (B) and B16F1 (E) tumour-bearing mice. Expression leveles of genes of interest in spleens of LLC (C) and B16F1 (F) tumour-bearing mice. (* *P<0.05*, ** *P<0.01*, *** *P<0.001* two-tailed t Student, n=7 and n=9 samples in LLC model and n=5 and n=5 samples in B16F1 model in WT and Ats1-KO groups, respectively).

Similar studies were performed in the BM of tumour-bearing mice. As observed in the spleen, the differences in immune populations in Ats1-KO healthy BM compared to WT (Section 2.1, Figure 33), were attenuated in the presence of LLC tumours (Figure 44A). Moreover, gene expression corroborated the maintenance of *Cd3* and *Cd11b* with FC data (Figure 44B). However, *Gr1* was downregulated and *Cd163* was upregulated in Ats1-KO mice compare to WT mates (Figure 44B). These results suggest that LLC model induces an extreme alteration of the systemic immune landscape in mice, attenuating the possible benefits of the absence of ADAMTS1.

On the contrary, BM immune-characterisation of B16F1-tumour bearing revealed a similar pattern to what it was found in healthy mice (Results, Section 2.1, Figure 33), with the exception of the reduction of F4/80$^+$ macrophages (Figure 44C).

Additionally, gene expression analysis only showed a confirmation of higher levels of $CD3^+$ cells, and a contradictory downregulation of *Cd11b* expression, opposite to FC data (Figure 44D).

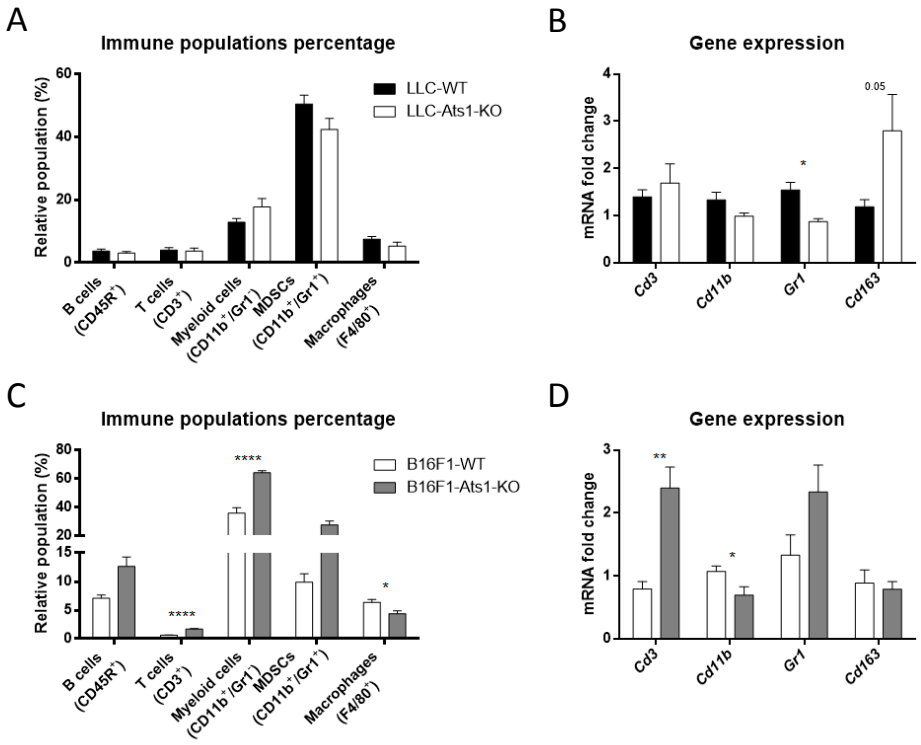

Figure 44. Regulation of bone marrow education by LLC and B16F1 tumours in WT and Ats1-KO mice. Flow cytometry data showing the percentage of immune populations represented as mean ± s.e.m of live cells in WT and Ats1-KO bone marrows in LLC (A) and B16F1 (C) tumour-bearing mice. Expression leveles of genes of interest in bone marrows of LLC (B) and B16F1 (D) tumour-bearing mice. (* *P<0.05*, ** *P<0.01*, *** *P<0.001*, **** *P<0.0001* two-tailed t Student, n=7 and n=9 samples in LLC model and n=5 and n=6 samples in B16F1 model in WT and Ats1-KO groups, respectively).

Results showed in this section demonstrate the different education that the immune landscape suffered depending of the nature of the tumour. Moreover, although T cell populations were more constant and following a similar tendency as in healthy state, the main differences observed between our three conditions (healthy and LLC- and B16F1-bearing mice) resides in the myeloid lineage. For that reason, we further pursued studying their relevance in the tumour scenario.

2.2.2. Contribution of stromal ADAMTS1 in LLC tumour-bearing mice after macrophage depletion.

The contribution of macrophages during tumour progression has been already described in different tumour contexts (K. Wu et al., 2020).According to our previous results, the myeloid lineage appeared as key candidates of the different responses to the lack of stromal ADAMTS1 between B16F1 and LLC tumours. In addition, our *in vitro* study of Ats1-KO macrophages showing a deficiency in their migratory and phagocytic capacity enhances this concept (Section 2.1, Figures 35, 40 and 41).

To demonstrate the role of these cells during tumour growth in presence and/or absence of stromal ADAMTS1, we next performed a macrophage depletion with clodronate liposomes in LLC-bearing mice (Materials and methodology, section 3.4) (Rooijen & Sanders, 1994). With that purpose, LLC cells were subcutaneouly injected in WT and Ats1-KO mice and they were treated every three days with liposomes as described.

Significantly, we already observed differences regarding the tumour engraftment in WT or Ats1-KO mice. While in clodronate-treated WT animals, 2 out of 6 injected mice did not engrafted, all the Ats1-KO injected mice developed tumour (Figure 45A). Tracking tumour progression (Figure 45B) also revealed a delay in the development of LLC-WT tumours in mice treated with clodronate that was not observed in Ats1-KO mice. However, at ending-point, tumours in WT mice did not display relevant differences with or without clodronate treatment, suggesting a stronger effect of clodronate liposomes at early stages.

In order to confirm the depletion of the macrophages, we evaluated myeloid populations in spleens and tumours by FC. First, spleen analyses (Figure 46A) confirmed a decrease of $CD11b^{+}/Gr1^{-}$ and $F4/80^{+}$ populations in WT mice under clodronate treatment, while these populations remained unaltered in Ats1-KO mice. Second, our analyses of tumours (Figure 46B) showed similar results than in spleen for the $CD11b^{+}/Gr1^{-}$ population. However, the depletion of $F4/80^{+}$ macrophages was not reproduced in the tumours. Surprisingly, $CD11b^{+}/Gr1^{+}$ cells were enhanced in the LLC-Ats1-KO tumours after the treatment, probably as a compensatory mechanism.

A

	Injected mice (PBS/Clod.)	Engrafted mice (PBS/Clod.)
LLC-WT	(5/6)	(5/4)
LLC-Ats1-KO	(5/5)	(5/5)

B

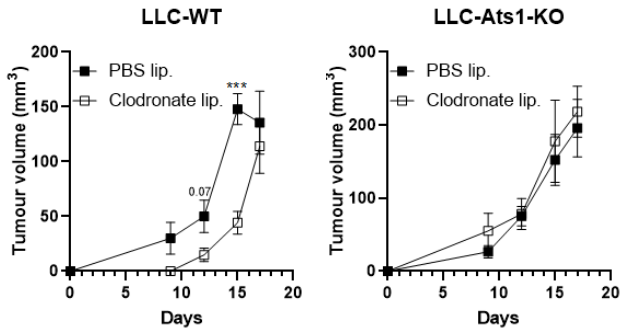

Figure 45. Contribution of stromal ADAMTS1 in Lewis Lung Carcinoma model during macrophage depletion by clodronate liposomes. (A) Table including the number of injected and engrafted mice for both WT and Ats1-KO groups treated with PBS or clodronate liposomes. (B) Progression of tumour volume during the experiment represented as tumour volume ± s.e.m. (*** *P*<0.001 two-tailed *t* Student).

These observations correlated with our *in vitro* results in which we demonstrated the deficient phagocytosis ability of Ats1-KO macrophages. Moreover, we observed an increase of MDSCs after clodronate treatment just in Ats1-KO mice, suggesting a possible compensation mechanism that might enhance a pro-tumorigenic environment.

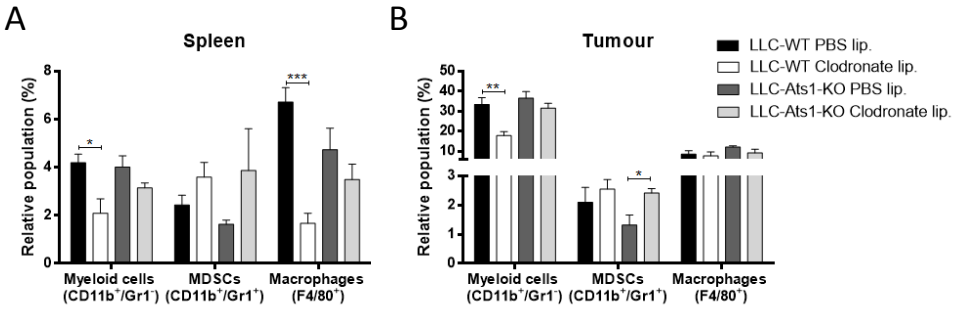

Figure 46. Effect of clodronate liposomes in immune populations of LLC-WT and LLC-Ats1-KO-bearing mice. Flow cytometry data showing the percentage of myeloid populations represented as mean ± s.e.m of live cells in spleens (A) and tumours (B) of WT and Ats1-KO LLC-tumour bearing mice after clodronate liposomes treatment. (* *P<0.05*, ** *P<0.01*, *** *P<0.001*, two-tailed t Student, n=5, 4, 5 and 5 from left to right).

Once more, the compilation of these later results remarked the strong differences between our tumour models, now in terms of regulation and education of the

immune system. Moreover, they corroborate the relevant role of macrophages in tumour development. In addition, we have demonstrated that their phagocytic capacity depends on ADAMTS1. In spite of it, this data is not enough to explain the differences in the behaviour of both models in absence of stromal ADAMTS1, so other analyses are still required.

2.3. Effect of stromal ADAMTS1 on specific gene signatures in both tumour models.

To elucidate the implicated mechanisms that differentiate the response of LLC and B16F1 tumours, not just between them but also addressing the absence of stromal ADAMTS1, we assessed RNA sequencing of tumours. Indeed, the characteristics of our research headed us to approach a deeper analysis of very specific signatures.

2.3.1. Comparison between B16F1 and LLC tumours in WT conditions.

We initiated this approach comparing both tumour models in WT mice. Considering the whole transcriptome, this comparison revealed 999 upregulated and 7869 downregulated genes in B16F1 *versus* LLC model. Using those genes, Gene Ontology (GO) enrichment was performed (Figure 47).

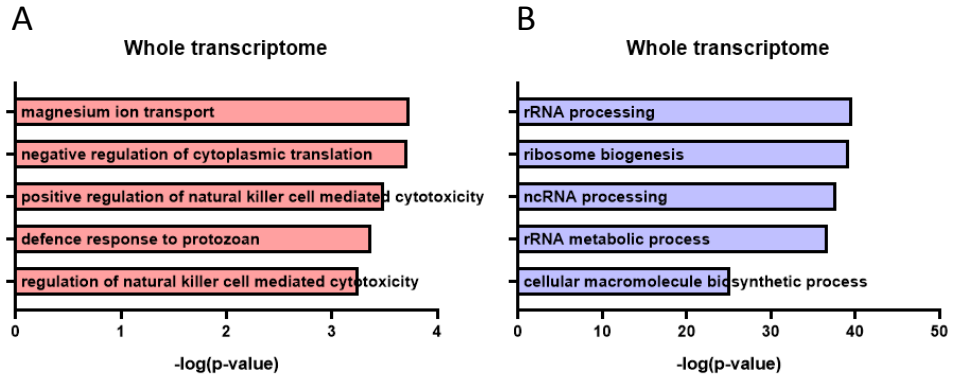

Figure 47. Gene ontology enrichment in the comparison of B16F1-WT tumours *versus* LLC-WT. Representation of top five Gene Ontology (GO) Biological Processes from the upregulated (A, red) and downregulated (B, blue) genes in B16F1-WT tumours compare to LLC-WT ones for the whole transcriptome.

From the top five terms, two of them indicated that overexpressed genes in B16F1-WT tumours activate NK cytotoxicity in comparison to LLC-WT ones (Figure 47A). In contrast, the biosynthesis of cellular macromolecules was more activated in LLC-WT tumours (Figure 47B).

Accordingly, we evaluated specific inflammatory response and matrisome signatures in more detail (Table 4). Heatmaps including the differentially expressed genes between both tumours showed a relevant group of genes identifying each tumour type (Figure 48A-C, Table 5). For example, the inflammatory response signature exhibited 18 upregulated and 107 downregulated genes in B16F1-WT compared to LLC-WT tumours (Figure 48A, Table 5), reinforcing their different inflammation environment.

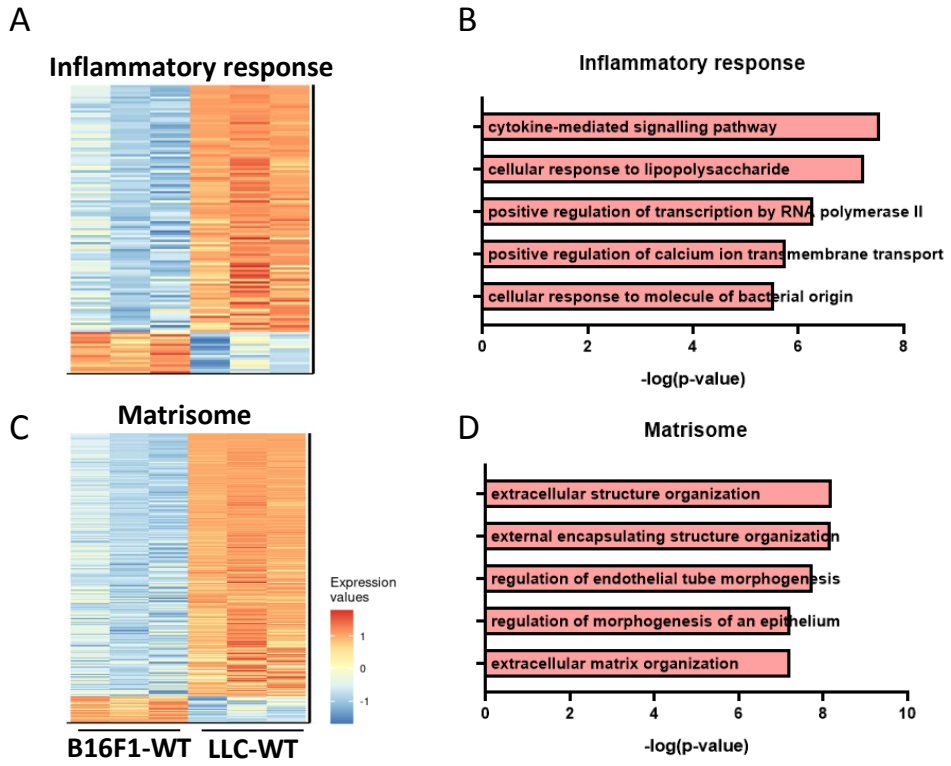

Figure 48. Heatmap and GO enrichment of inflammatory response for both models. Heatmaps representing gene expression comparison between B16F1-WT and LLC-Ats1-WT tumours for signature related to inflammatory response (A) and matrisome (C). (Colour code is based on relative expression values from upregulated (red) to downregulated (blue)). Representation of top five Gene Ontology (GO) Biological Processes from the upregulated genes of inflammatory response (B) and matrisome (D) signature-related genes.

Moreover, GO enrichment of upregulated genes in B16F1-WT tumours from the inflammatory response signature revealed an activation of cytokine-mediated signalling and cellular response to LPS (Figure 48B, Table 9). In contrast, GO enrichment using the 25 upregulated matrisome genes did not reveal any particularity (Figure 48D, Table 9), although heatmap showed a clear overexpression of most of the genes in LLC-WT tumours, suggesting a richer matrix of this model (Figure 48C) In addition, *Nidogen 1* and *Versican* appeared more expressed in LLC-WT tumours than in B16F1-WT ones.

Having characterised these specific signatures between models in WT backgrounds, their regulation by the absence of stromal ADAMTS1 absence was addressed next.

2.3.2. Gene regulation by ADAMTS1 in the LLC tumour model.

We initiated a whole transcriptome comparison between LLC tumours in a WT and Ats1-KO backgrounds. Significantly, the GO enrichment analysis, including the upregulated genes in WT tumours (248 genes), revealed main GO biological processes related to ECM and angiogenesis regulation within the top five (Figure 49A). In contrast, the downregulated genes (735 genes) reflected an alteration of immune pathways (Figure 49B). Indeed, cytokine-mediated signalling and two major processes related with type I interferon activity supported the possible contribution of this pathways in LLC-Ats1-KO tumours.

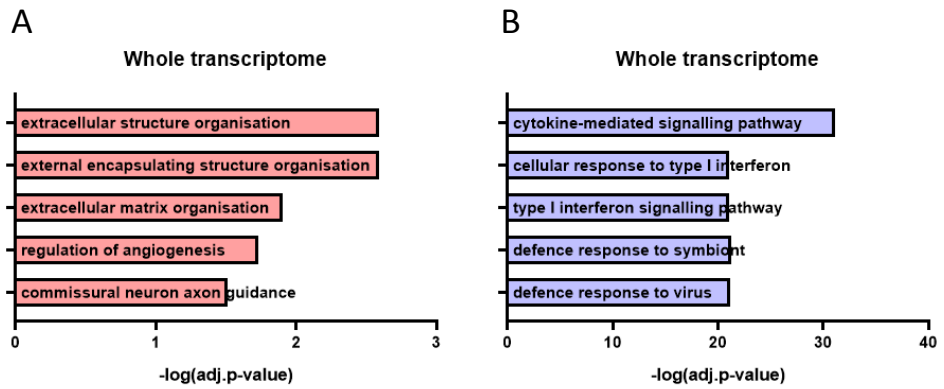

Figure 49. Gene ontology enrichment in LLC model. Representation of top five Gene Ontology (GO) Biological Processes from the upregulated (A, red) and downregulated (B, blue) genes in LLC-WT tumours compare to LLC-Ats1-KO ones for the whole transcriptome.

Due to the expertise of our group and according to the results obtained from the whole transcriptome, we analysed the consequences of the absence of stromal ADAMTS1 looking at specific gene signatures. Given the connection of ADAMTS1 with angiogenesis and is regulation in the previous GO enrichment, we also included an angiogenesis signature. However, only 8 genes were differently regulated in LLC-WT *versus* LLC-Ats1-KO (Figure 50, Table 6). In the case of inflammatory response, we found just 1 upregulated gene and 52 downregulated in LLC-WT group comparing with Ats1-KO mates (Figure 50, Table 6). In fact, such strong difference in the number of regulated genes at Ats1-KO mice might indicate the induction of a robust inflammatory landscape. Finally, evaluation of the matrisome signature showed 28 genes overexpressed and 44 underexpressed in WT group compared to Ats1-KO one (Figure 50, Table 6).

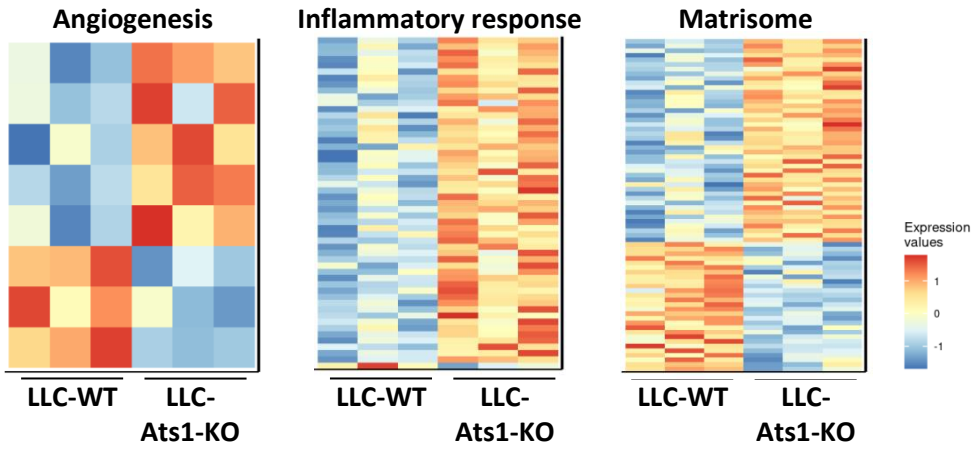

Figure 50. Heatmaps of specific signatures gene expression in LLC-WT and LLC-Ats1-KO tumours. Heatmaps representing gene expression comparison between LLC-WT and LLC-Ats1-KO tumours for signatures related to angiogenesis (left), inflammatory response (middle) and matrisome (right). (Colour code is based on relative expression values from upregulated (red) to downregulated (blue)).

Due to the relevance for this project and our group, and considering that it is the signature with the largest number of genes, we performed GO enrichment analysis just with matrisome signature. Indeed, our previous *in vivo* results revealed that matrisome molecules such as Nidogen 1 and Versican are differently regulated in LLC tumours (Figure 31). Quite significantly, the upregulated genes in LLC-WT tumours revealed GO terms related to collagen and supramolecular organisation (Figure 51A,

Table 10). Contrary, the downregulated ones were involved in cell proliferation, inflammation and cytokine signalling (Figure 51B, Table 10).

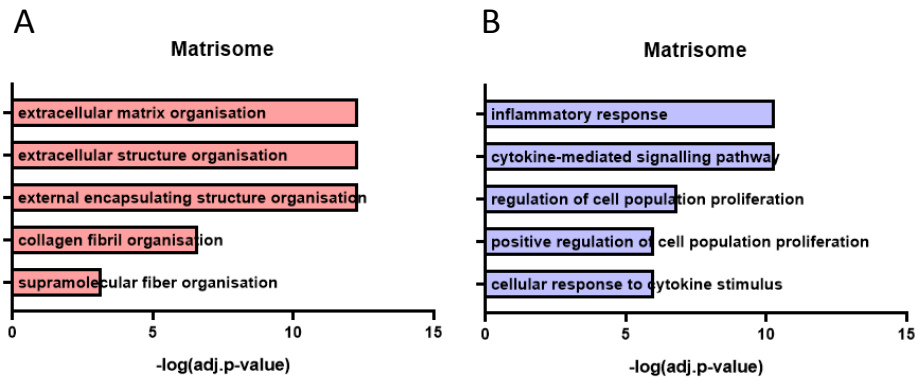

Figure 51. Gene ontology enrichment in LLC model. Representation of top five Gene Ontology (GO) Biological Processes from the upregulated (A, red) and downregulated (B, blue) genes in LLC-WT tumours compare to LLC-Ats1-KO ones for matrisome signature-related genes.

Altogether, these results reflect the important inflammatory response that takes place in LLC-Ats1-KO tumours compared to LLC-WT, not only represented by the difference in the inflammatory response signature, but it was also defined by the GO enrichment using matrisome genes, indicating that matrix-related genes regulate inflammation. Moreover, that matrisome signature revealed a difference in the type of structures (collagen and supramolecular fiber organisation) that are found in both groups.

2.3.3. Gene regulation by ADAMTS1 in the B16F1 model.

Similar analyses were approached for the B16F1 model, including a first whole transcriptome evaluation. Interestingly, upregulated genes (872 genes) in B16F1 WT tumours showed an upregulation of processes related to the type I IFN family (Figure 52A). Surprisingly, similar processes were downregulated in LLC-WT tumours compare to the Ats1-KO ones (Figure 49), suggesting type I IFN as a possible explanation for the different behaviour of both models. In contrast, downregulated genes (564 genes) in B16F1-WT tumours versus Ats1-KO revealed that processes related to ECM organization were downregulated (Figure 52B), opposite to LLC model. As in the case of type I IFN, the opposite regulation of those pathways in B16F1 and LLC tumours (parallel to the different response to the absence of ADAMTS1) suggest their relevance in the regulation of the different behaviour.

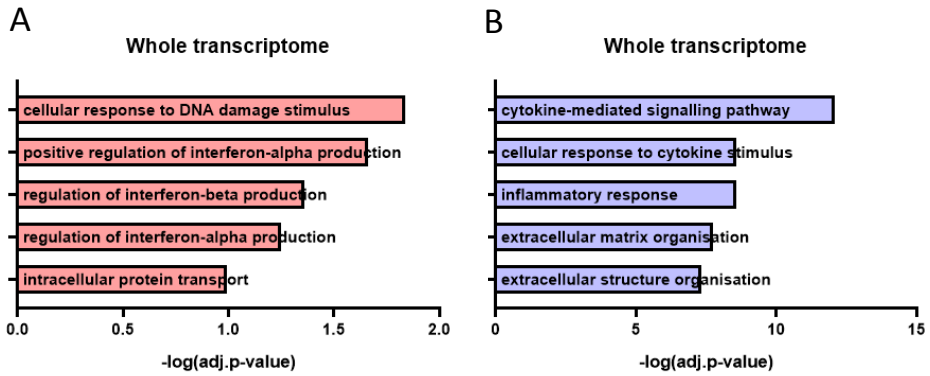

Figure 52. Gene ontology enrichment in B16F1 model. Representation of top five Gene Ontology (GO) Biological Processes from the upregulated (A, red) and downregulated (B, blue) genes in B16F1-WT tumours compare to B16F1-Ats1-KO ones for the whole transcriptome.

Following a similar rationale that for LLC tumours, specific gene signatures were evaluated. As in LLC tumours, few angiogenesis-related genes were differently regulated and most of the ones included in the inflammatory response signature were overexpressed in Ats1-KO conditions (Figure 53, Table 7). However, matrisome signature showed 7 and 65 over- and downexpressed genes in B16F1-WT tumours, respectively (Figure 53, Table 7).

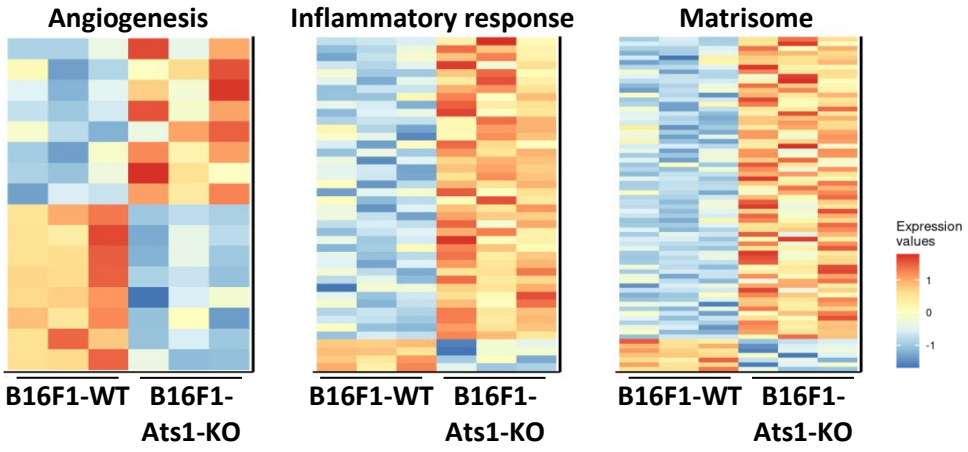

Figure 53. Heatmaps of specific signatures gene expression in B16F1-WT and B16F1-Ats1-KO tumours. Heatmaps representing gene expression comparison between B16F1-WT and B16F1-Ats1-KO tumours for signatures related to angiogenesis (left), inflammatory response (middle) and matrisome (right). (Colour code is based on relative expression values from upregulated (red) to downregulated (blue)).

Parallel to the LLC model and in order to compare with it, GO enrichment was performed using the differentially expressed genes from the matrisome signature (Figure 54, Table 7). The most interesting result was found using the downregulated genes in B16F1-WT tumours. Opposite to LLC model, B16F1-WT tumours had an inhibition of ECM, collagen and supramolecular fiber organisation processes (Figure 54B), which were activated in LLC-WT ones compare to LLC-Ats1-KO ones (Figure 51, Table 11). All these analyses confirm our hypothesis indicating that the different behaviour of both tumour models in absence of stromal ADAMTS1 can be mediated by the extracellular compartment and its organization.

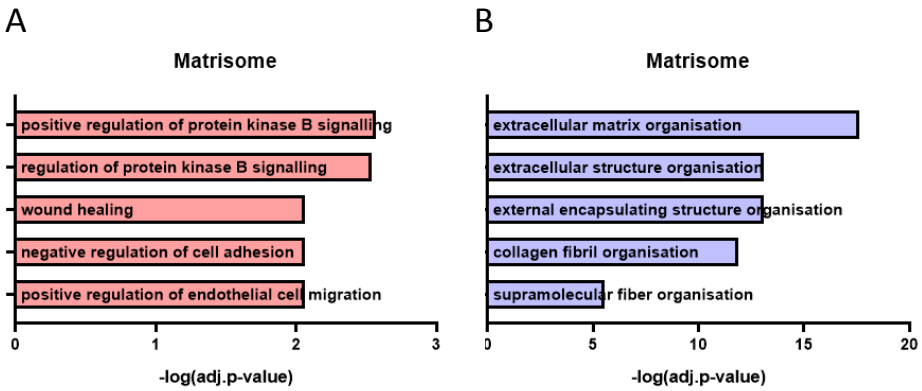

Figure 54. Gene ontology enrichment in B16F1 model. Representation of top five Gene Ontology (GO) Biological Processes from the upregulated (A, red) and downregulated (B, blue) genes in B16F1-WT tumours compare to B16F1-Ats1-KO ones for matrisome signature-related genes.

2.3.4. Comparison between B16F1 and LLC tumours in absence of stromal ADAMTS1.

Attending to the differences between WT and Ats1-KO conditions for each tumour type, opposite in some cases, we compared the whole transcriptome of B16F1-Ats1-KO and LLC-Ats1-KO tumours. GO enrichment showed similar terms that in WT comparison regarding NK cytotoxicity (Figure 55). However, B16F1-Ats1-KO tumours had a negative regulation of cell migration and motility compare to LLC-Ats1-KO, suggesting a higher aggressiveness in LLC tumours in absence of stromal ADAMTS1.

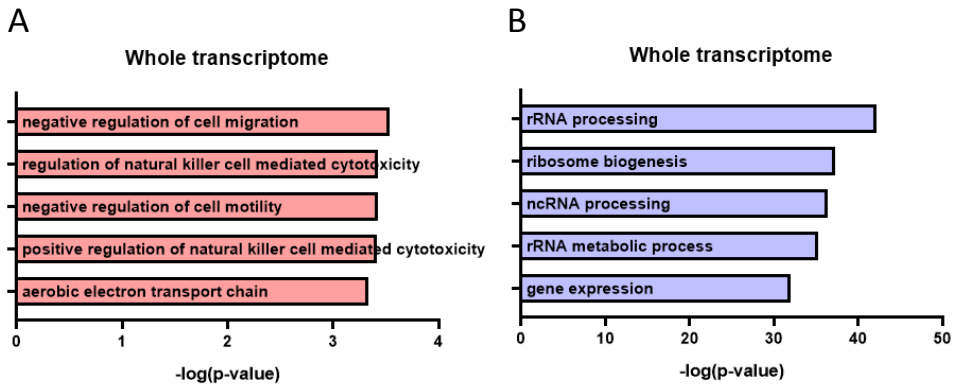

Figure 55. Gene ontology enrichment in the comparison of B16F1-Ats1-KO tumours *versus* LLC-Ats1-KO. Representation of top five Gene Ontology (GO) Biological Processes from the upregulated (A, red) and downregulated (B, blue) genes in B16F1-Ats1-KO tumours compare to LLC-Ats1-KO ones for the whole transcriptome.

Interestingly, inflammatory response signature revealed and activation of T cells migration and chemotaxis in B16F1-Ats1-KO tumours compared to LLC-Ats1-KO ones (Figure 56A-B, Table 8), different to what was observed in WT conditions (Figure 48). It indicates that the differences derived from the nature of each tumour regarding inflammatory response (B16F1-WT *versus* LLC-WT comparison) are modified by the absence of ADAMTS1, corroborating the immunomodulatory role of the protease.

Finally, GO enrichment with matrisome genes also showed different terms that in the comparison in WT conditions (Figure 56C-D, Table 12), losing GO biological processes related to ECM organisation that were found in the first comparison (Figure 48). This, as in the case of the inflammatory response signature, does demonstrate that ADAMTS1 also modulate matrisome signature. Controversially, this signature indicated that B16F1-Ats1-KO tumours had a positive regulation of cell migration, opposite to the GO terms obtained with the whole transcriptome.

Altogether, these *in silico* analyses demonstrated the different response to stromal ADAMTS1 absence depending on the tumour model. While LLC tumours had an activation GO terms involved in ECM organisation and an inhibition of IFN response when ADAMTS1 was not expressed by stromal cells, the B16F1 model had the opposite effect. Moreover, we have demonstrated that ADAMTS1 is able to modulate the differences that each model generates in inflammatory response and matrisome signatures. This modulation was reflected with the activation of T cell

pathways in B16F1-Ats1-KO tumours compare to LLC-Ats1-KO ones, what was not observed in WT conditions.

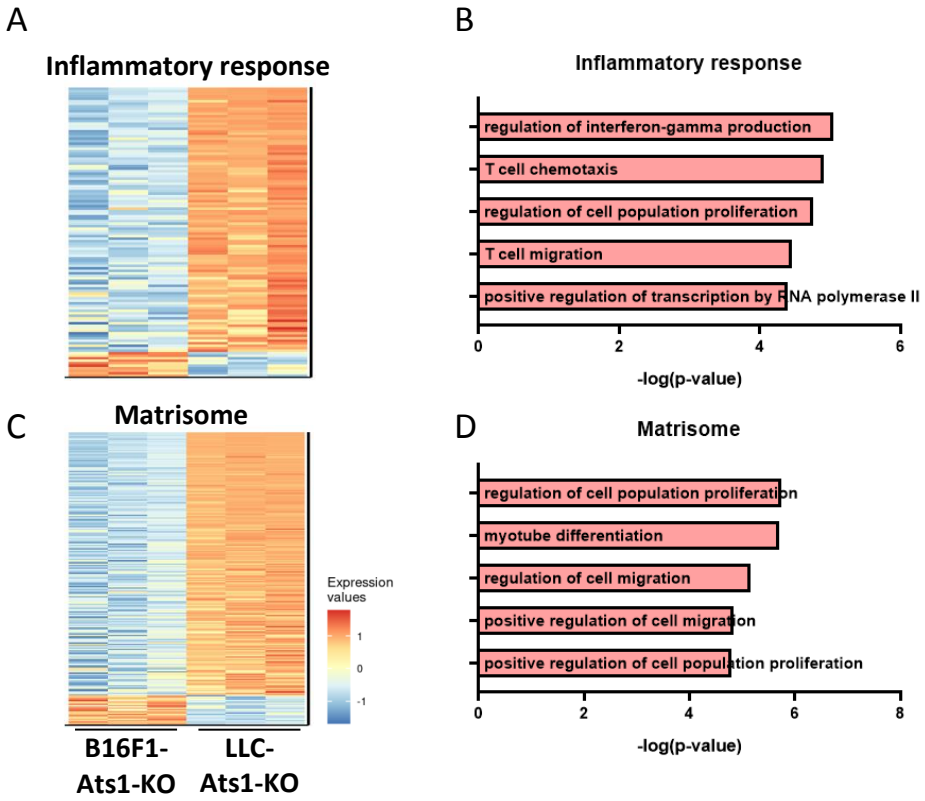

Figure 56. Heatmap and GO enrichment of inflammatory response for both models. Heatmaps representing gene expression comparison between B16F1-Ats1-KO and LLC-Ats1-Ats1-KO tumours for signature related to inflammatory response (A) and matrisome (C). (Colour code is based on relative expression values from upregulated (red) to downregulated (blue)). Representation of top five Gene Ontology (GO) Biological Processes from the upregulated genes of inflammatory response (B) and matrisome (D) signature-related genes.

3. Addressing the relevance of tumoral ADAMTS1 in LLC tumour model.

To date, the impact of tumour-derived ADAMTS1 in tumour development has been widely reported, although maintaining the controversy between its pro- and anti-tumorigenic activity (Ricciardelli et al., 2011)(Martino-Echarri et al., 2013a)(Peris-Torres et al., 2020). As showed in previous sections, our work included the characterisation of the immune system of the Ats1-KO mouse, fully focused on the alterations that the loss of stromal ADAMTS1 induced. Importantly, LLC cells prompt a strong modulation of the immune landscape but without major consequences in tumour halt in Ats1-KO mice. Accordingly, we wanted to evaluate if reducing the levels of ADAMTS1 in the tumour cells had any outcome on tumour progression, vasculature and immune regulation. We generated an ADAMTS1-inhibited cell line by short-hairpin technology (LLC-shAts1), whose *in vitro* characterization and *in vivo* performance is shown next. Importantly, we kept comparing these analyses with the partnership B16F1-WT and shAts1 model (Fernández-Rodríguez et al., 2016).

3.1. *In vitro* characterisation of ADAMTS1-inhibited LLC cells (LLC-shAts1).

First, we confirmed ADAMTS1 inhibition by gene expression (Figure 57A) and protein secretion to the conditioned medium (CM) (Figure 57B), displaying in both cases a more relevant inhibition in LLC cells than in B16F1.

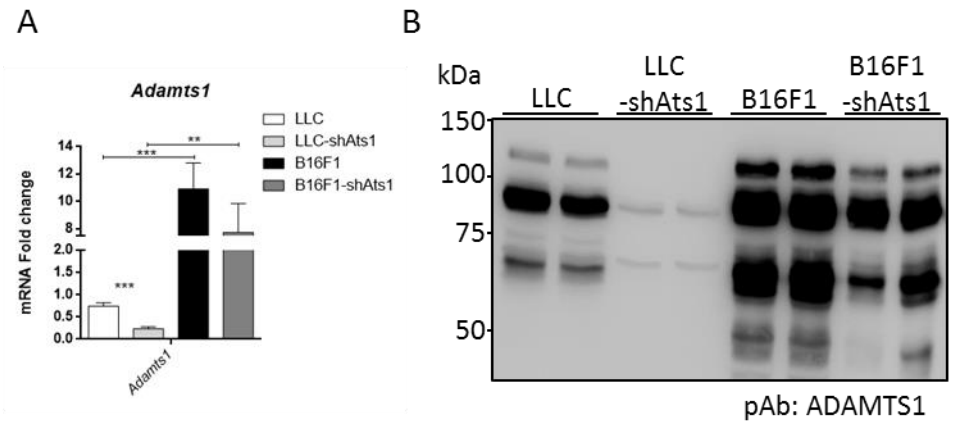

Figure 57. ADAMTS1 expression in both B16F1 and LLC cell lines after *Adamts1* inhibition. (A) Graph representing relative mRNA fold change expression of *Adamts1.* (B) Protein levels of ADAMTS1 detected by Western Blot in CM. (** *P*<0.01, *** *P*<0.001, **** *P*<0.0001 two-tailed *t* Student, n=8 and n=5 samples in WT and –shAts1 cells respectively, in both models).

In parallel, we evaluated two of the more relevant substrates of ADAMTS1: Nidogen 1 and Versican. Significantly, both molecules were almost absent in B16F1 cells compared to LLC (Figure 58). With a major focus in LLC cells, while *Nidogen 1* expression was not altered in inhibited cell lines (Figure 58A), its protein levels showed a slight decrease in shAts1 cells, although it can be due to posttranslational regulation (Figure 58B). More relevant, VCAN was clearly reduced. This reduction was found in the gene expression analysis in both cell line models (Figure 58A) but more interestingly by western blot (WB) (Figure 58B). In this case, LLC cell line had high expression of intact VCAN (450kDa), which is known by its pro-tumorigenic properties, and this isoform is extremely reduced in the LLC-shAts1 cell line.

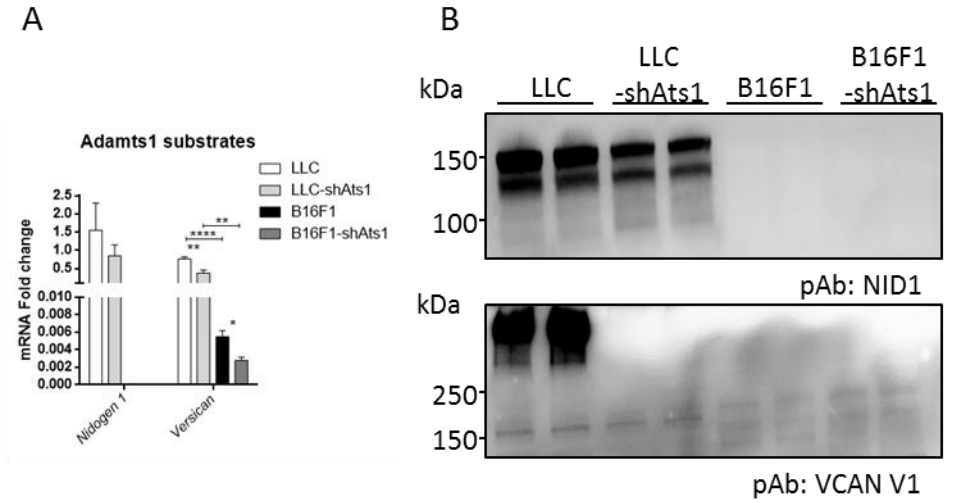

Figure 58. Gene expression and protein analysis of ADAMTS1 substrates in both B16F1 and LLC cell lines after *Adamts1* inhibition. (A) Graph representing relative mRNA fold change expression of relevant ADAMTS1 substrates (*Nidogen 1* and *Versican*). (B) Protein levels of NID1 and full-length VCAN detected by Western Blot in CM. (* $P<0.05$, ** $P<0.01$, **** $P<0.0001$ two-tailed *t* Student, n=8 and n=5 samples in WT and –shAts1 cells respectively, in both models).

Then, functional characterisation was assessed to know if the blockade of ADAMTS1 changed tumour cell properties. Indeed, adhesion to different matrices (Figure 59A) and proliferation (Figure 59B) were not altered when ADAMTS1 was inhibited.

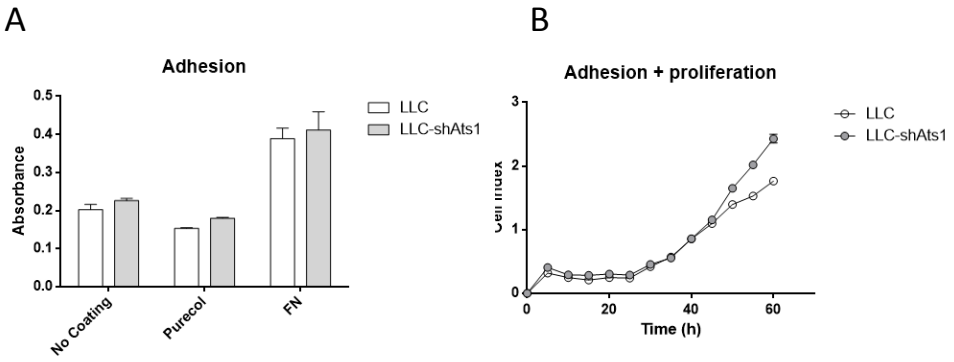

Figure 59. Adhesion and proliferation properties of LLC and LLC-shAts1 cell lines. (A) Graph representing the absorbance measure related to adhesion to different coatings after 1h and Toluidin blue staining. (B) Cell index representing the cell proliferation along the time performed in xCELLigence platform. N=4 and n=3 in adhesion and xCELLigence experiments, respectively.

Although this molecular and functional *in vitro* characterization indicated that ADAMTS1 does not affect basic cell properties, the changes of the substrates Nidogen 1 and Versican (reduced in LLC cells with down-regulated ADAMTS1), must be considered in successive studies.

3.2. Consequences of down-regulating tumoral ADAMTS1 in LLC tumour progression.

Both LLC-WT and LLC-shAts1 cells were injected in both WT and Ats1-KO mice. These new approaches added complexity and allowed us to generate different environments where the origin of ADAMTS1 is differently affected (Figure 60A).

Regarding tumour progression, some slight differences observed at early stages (Figure 60C) did not resulted in significant changes at the ending point (Figure 60B and D). These first results indicated that tumour-derived ADAMTS1 is not relevant for this model, similar to B16F1 model (Fernández-Rodríguez et al., 2016). However, additional tumour models such as breast cancer and uveal melanoma did show a clear contribution of the tumour-derived protease in tumour growth (Martino-Echarri et al., 2013a)(Peris-Torres et al., 2020).

Although tumour progression was not affected, vasculature was also evaluated and compared with the previous tumour groups.

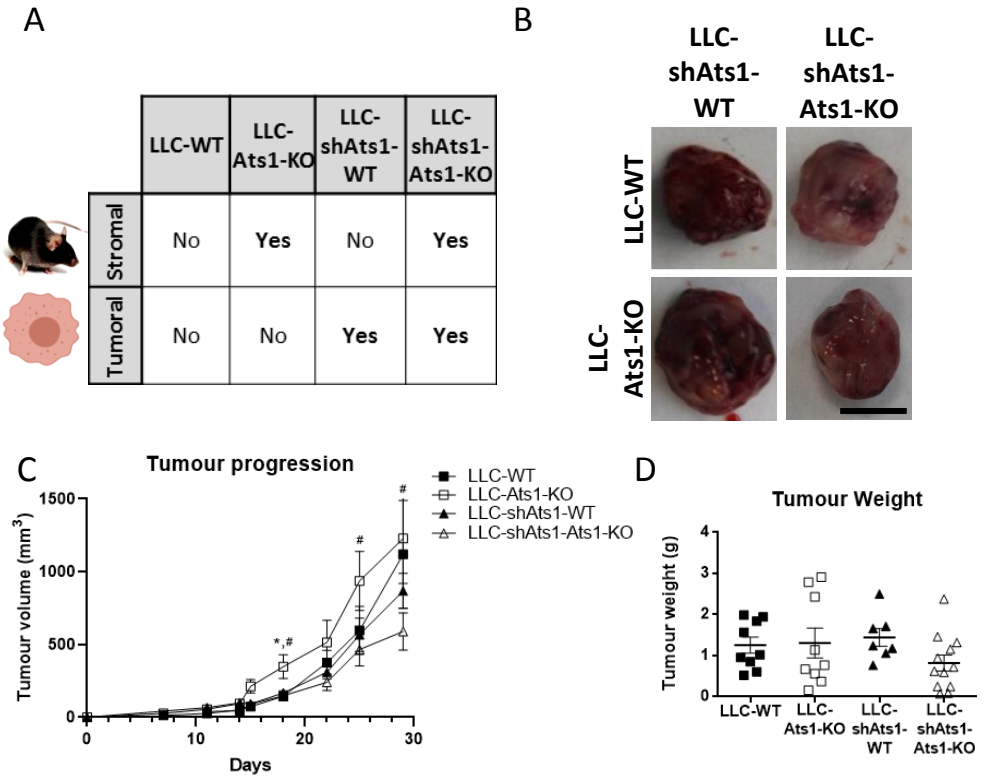

Figure 60. Contribution of stromal and tumoral ADAMTS1 in Lewis Lung Carcinoma model. (A) Table including the type of ADAMTS1 inhibition in each experimental group. (B) Representative LLC and LLC-shAts1 tumours in WT and Ats1-KO mice. Scale = 1 cm. (C) Progression of tumour volume during the experiment represented as tumour volume ± s.e.m. (D) Graph representing mean tumour weight ± s.e.m 29 days after cells inoculation (end point)). (* and # show statistically significant differences between LLC-WT *versus* LLC-Ats1-KO and LLC-Ats1-KO *versus* LLC-shAts1-Ats1-KO, respectively, two-tailed *t* Student, n=9, n=9, n=7 and n=12 samples in each group, respectively).

3.3. Characterisation of tumour vasculature.

The inhibition of tumour-derived ADAMTS1 provoked a similar increase in vessel density to the observed in Ats1-KO studies (Figure 61A-B). Furthermore, when combining the reduction of ADAMTS1 in the stroma and the tumour cells (LLC-shAts1-Ats1-KO), the number of vessels was even higher, reinforcing the angio-inhibitory role of ADAMTS1, corroborated by the upregulation of *Cd31* (Figure 61C). However, the evaluation of vessel perimeter revealed different actions depending of

the absence of stromal or tumoral ADAMTS1. When comparing LLC-Ats1-KO and LLC-shAts1 tumours, we found that inhibition of the protease in tumour cells provoked smaller vessels (Figure 61A-B). Furthermore, the maturity of the vessels, analysed by SMA deposition, did not show apparent differences (Figure 61D).

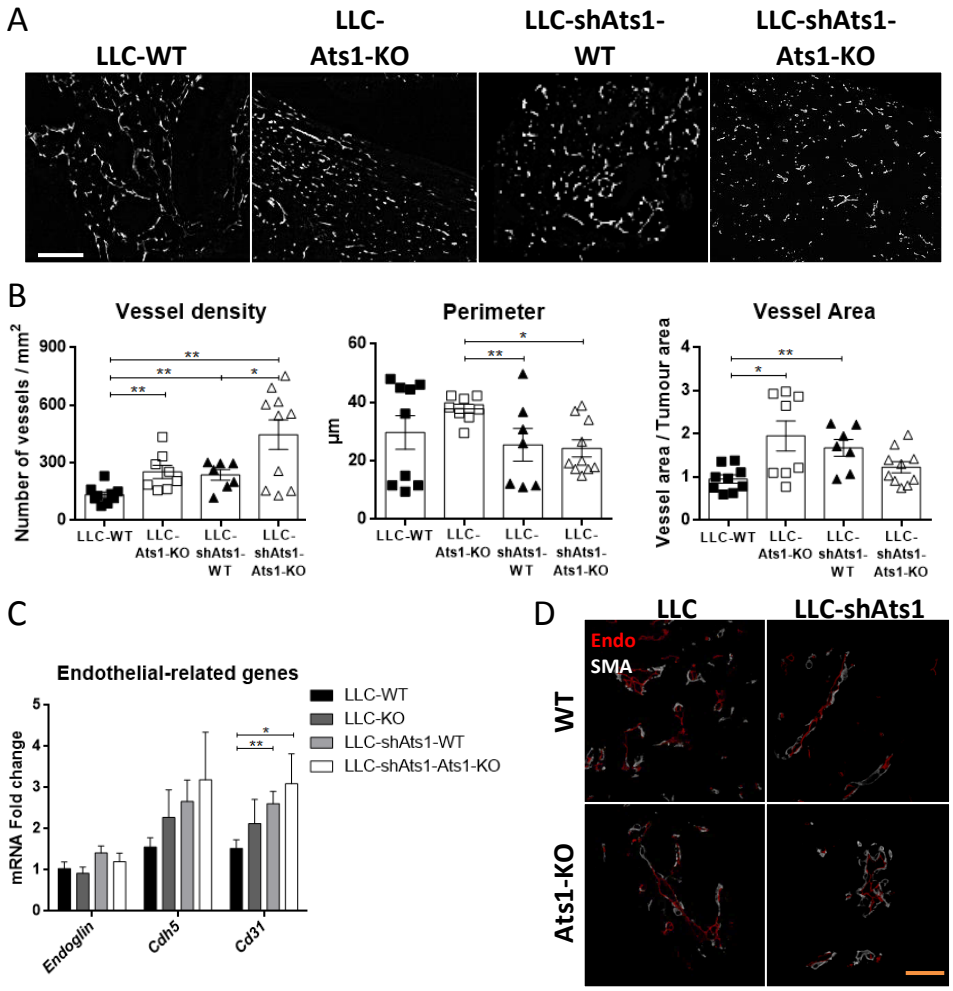

Figure 61. Effect of stromal and tumoral ADAMTS1 in LLC tumour vasculature. (A) Representative images of Endomucin staining for morphometric vasculature quantification of each group. White scale = 200µm. (B) Graphs representing mean ± s.e.m of vessel density, perimeter of vessels and vessel area of each group of tumours after 29 days. (C) Graphs representing relative mRNA fold change expression of genes related to vasculature (*Endoglin*, *Cdh5* and *Cd31*). (D) Representative confocal images of SMA deposition (white) together with the endothelial marker Endomucin (red) in tumours 29 days after cells inoculation. Yellow scale = 50µm. (* $P<0.05$, ** $P<0.01$ two-tailed *t* Student, n=9, n=8, n=7 and n=10 samples in each group, respectively).

Altogether, these results highlighted the role of ADAMTS1 in angiogenesis. In spite of the similar effect that lacking stromal or tumoral ADAMTS1 displays in tumour vessel density, and assuming that their combination did not induce a synergistic effect in tumour progression, further studies were still needed. Moreover, the actions on vasculature encouraged us to investigate the possible involvement of ADAMTS1 during anti-angiogenic therapies, which will be presented later (Results, section 5).

3.4. Study of ADAMTS1 and related molecules.

Following our studies to unveil the actions of tumoral ADAMTS1, we evaluated its closer ADAMTS-family members (versicanases) and relevant substrates (Figure 62).

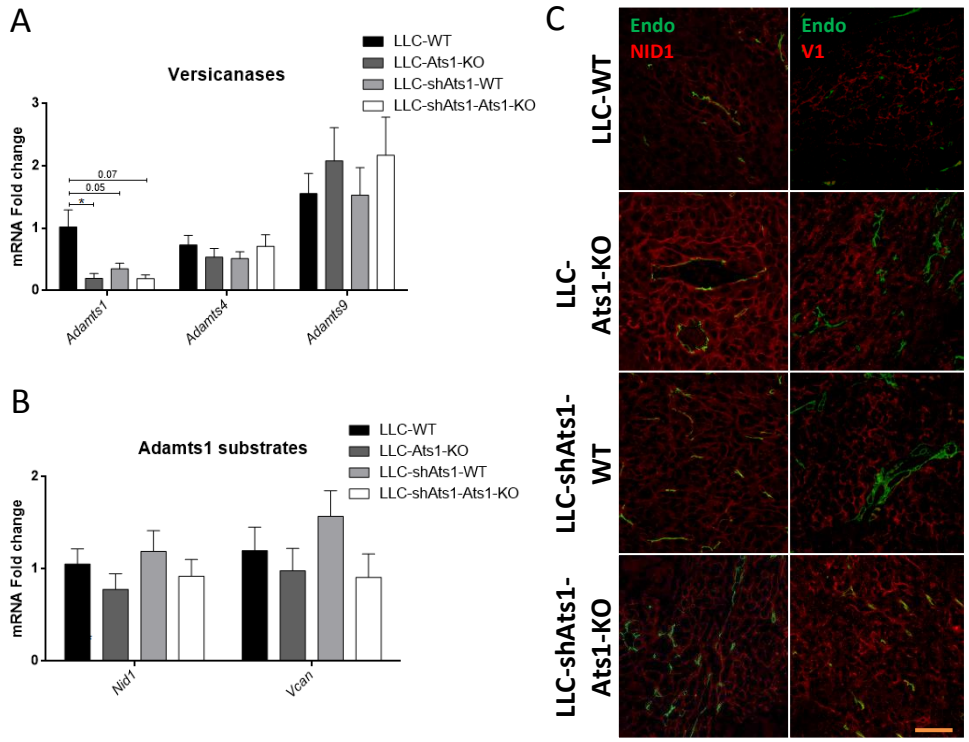

Figure 62. Effect of stromal and tumoral ADAMTS1 in ECM gene expression and deposition. (A) Graph representing relative mRNA fold change expression of ADAMTS proteases with versicanase activity. (B) Graph representing relative mRNA fold change expression of relevant ADAMTS1 substrates (*Nidogen 1* and *Versican*). (C) Representative confocal images of NID1 and full-length VCAN deposition (red) together with the endothelial marker Endomucin (green) in tumours 29 days after cells inoculation. Yellow scale = 50µm. (* *P*<0.05 two-tailed *t* Student, n=9, n=9, n=7 and n=4 samples in each group, respectively).

Neither the analysed versicanases (*Adamts4* and *Adamts9*) nor the substrates (*Nidogen 1* and *Versican*) were affected by the inhibition of tumoral ADAMTS1, apart from *Adamts1* itself (Figure 62A-B). In spite of it, protein accumulation of both substrates was enhanced after inhibition of the protease in tumour cells (Figure 62C), suggesting their posttranslational alteration that could also involve their proteolysis. Likewise, when ADAMTS1 was absent in stromal cells or inhibited in tumour cells, the proteolysis of its substrates may be affected.

At this level, our results indicate that both stromal and tumoral ADAMTS1 has a similar effect regarding Nidogen 1 and Versican regulation. However, understanding the behaviour of LLC tumours under these distinct scenarios would benefit from the analysis of their immune compartments, as we showed next.

3.5. Regulation of tumour immune infiltration and immune organs education by tumour-derived ADAMTS1.

As in the case of stromal absence of ADAMTS1 (sections 1.1 and 1.2), vasculature changes and the regulation of ADAMTS1 substrates induced by the inhibition of tumour-derived ADAMTS1 do not explain why LLC tumour progression is not affected. Moreover, our RNAseq data (section 2.3) corroborated that tumour cells can educate inflammatory response. For that reason, we wanted to evaluate whether the inhibition of ADAMTS1 in tumour cells also altered the immune landscape. These studies included FC analyses of tumour immune infiltrates. Interestingly, $CD3^+$ T cells were not affected by the inhibition of tumour-derived ADAMTS1, although they were increased in Ats1-KO conditions (Figure 63A). Looking at genes related with T cells, they do not support FC data. Interestingly, LLC-shAts1-Ats1-KO tumours showed an overexpression of *Foxp3* and a downregulation of *Cd8*, which could reflect a more immunosuppressive scenario (Figure 63B).

Next, evaluation of myeloid cell infiltration also showed that stromal and tumour-derived ADAMTS1 affected these populations in different ways, with high variability between groups. Among all the FC and gene expression data, the most relevant result was found in myeloid population $CD11b^+/Gr1^-$ (Figure 63C). It was increased only in the LLC-shAts1-Ats1-KO group. Moreover, this increase was accompanied by a downregulation of *Nos2* and an upregulation of *Cd163*, indicating a shift of macrophages to a more M2 or pro-tumorigenic state after the inhibition of ADAMTS1 in the tumour cells (Figure 63D).

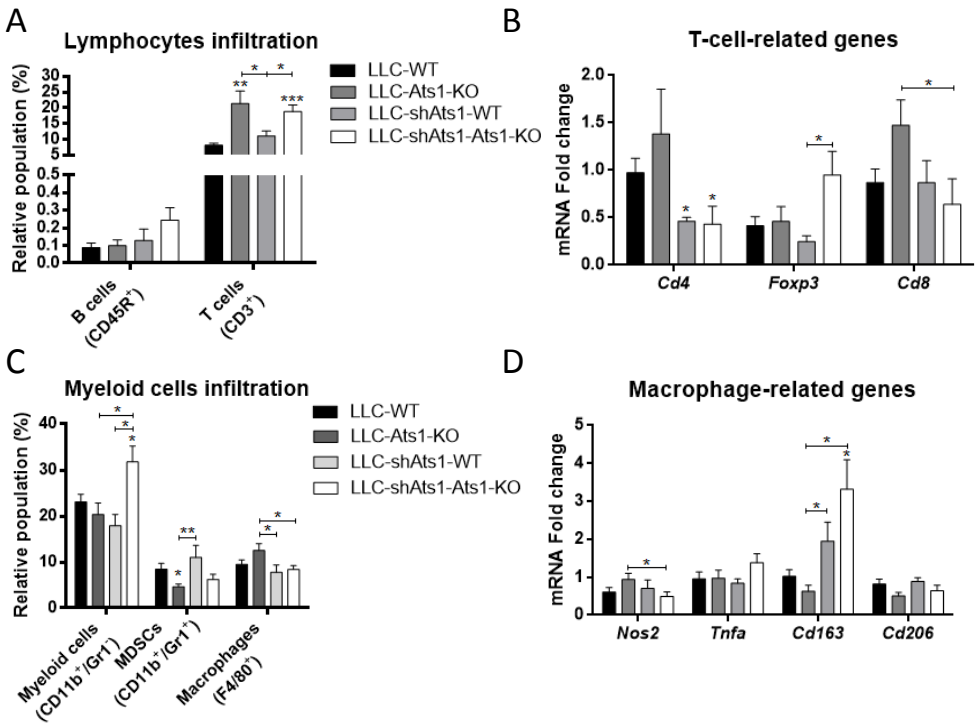

Figure 63. Immunocharacterisation of LLC tumour in WT and Ats1-KO mice. Flow cytometry data showing the percentage of lymphocytes (A) and myeloid cells (C) represented as mean ± s.e.m of live cells in WT and Ats1-KO tumours. Graphs representing relative mRNA fold change expression of genes related to T cells (B, *Cd4*, *FoxP3* and *Cd8*) and macrophages (D, *Nos2, Tnfa*, *Cd163* and *Cd206*). (* *P<0.05*, ** *P<0.01*, *** *P<0.001* two-tailed t Student, n=9, n=8, n=7 and n=11 samples in each group, respectively).

Although deeper analyses should be performed, our current immune-characterisation already suggests that, in LLC tumours, stromal ADAMTS1 mainly affects T cell populations while tumoral ADAMTS1 modulate myeloid populations and macrophage polarisation genes expression. Interestingly, the combination of stromal and tumoral ADAMTS1 reduction revealed a pro-tumorigenic environment reflected in a downregulation of *Cd8* and *Nos2* and upregulation of *Foxp3* and *Cd163*. These results suggest that the lower global expression of ADAMTS1 is, the higher the immunosuppression is.

Finally, we evaluated and compared distant organs such as spleen and BM, in line with our previous assessments. Regarding the spleen (Figure 64A), the most significant finding was that splenomegaly in Ats1-KO conditions was reverted in LLC-shAts1-Ats1-KO group. Moreover, analysis of immune populations in spleen showed

not changes for the most representative B and T cells (Figure 64B). However, $CD11b^{+}Gr1^{-}$ and $CD11b^{+}Gr1^{+}$ cells were increased in the spleen of LLC-shAts1 tumour-bearing mice. In contrast, $F4/80^{+}$ macrophages were reduced. These results on myeloid populations were pretty similar to the ones observed in the tumours. They might suggest that tumour-derived ADAMTS1 can impact distant immune organs and its cell composition such as spleen and BM which later, will have an effect in the tumour-immune infiltration.

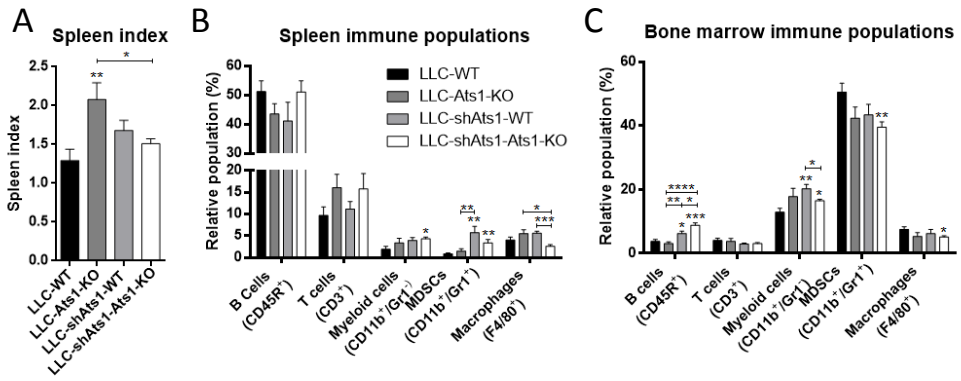

Figure 64. Regulation of spleen and bone marrow education by LLC and LLC-shAts1 tumours in WT and Ats1-KO mice. (A) Graph representing the spleen index. Flow cytometry data showing the percentage of immune populations represented as mean ± s.e.m of live cells in WT and Ats1-KO (B) spleens and (C) bone marrow. (* *P<0.05*, ** *P<0.01*, *** *P<0.001*, **** *P<0.0001* two-tailed t Student, n=7, n=9, n=5 and n=7 samples in each group, respectively).

For BM, its analysis also showed that LLC-shAts1 tumours provoked changes that there were not found in Ats1-KO conditions, as occurred in the spleen and the tumour. Although low represented, B cells were surprisingly increased (Figure 64C). This is the only condition in which our models showed an alteration in this population, including the analysis of healthy and B16F1 model. Nevertheless, it contribution in tumour immunity is not clear and these changes still did not explain LLC behaviour. In contrast, T cells were not affected (Figure 64C). When looking at myeloid cells, $CD11b^{+}Gr1^{-}$ cells and $F4/80^{+}$ macrophages followed a similar tendency to the spleen. However, $CD11b^{+}Gr1^{+}$ MDSCs were in the opposite direction that spleen, with a decrease just in the LLC-shAts1-Ats1-KO group.

These results indicate that tumour-derived ADAMTS1 had higher impact than the protease from stromal origin (Results, section 2.2), both in the tumour immune infiltrate and in the immune organ education. The alterations occurring in myeloid cells in tumours and distant organs are similar. Although those changes did not

provoke alterations in tumour growth, the regulation of immune populations suggests that stromal and tumoral ADAMTS1 regulate tumour behaviour in a different way.

4. Effect of tumour secretome in macrophage polarisation.

We have demonstrated that B16F1 and LLC tumour models modulate myeloid cells *in vivo* in different ways (Results, section 2.2.1, Figure 43). As showed throughout this work, the absence of stromal ADAMTS1 did not alter myeloid lineage infiltration or polarisation within LLC tumours (Results, section 2.2.1, Figure 42). Moreover, the *in vitro* characterisation of WT and Ats1-KO BMDM revealed that the absence of protease in macrophages did not affect their polarisation capacity (Results, section 2.1.3, Figure 38). On the contrary, tumoral inhibition of ADAMTS1 exerted a relevant impact in the immune regulation in the LLC model, although without effect in tumour progression (Results, section 3.5, Figures 63-64). For that reason, myeloid cells seem to be key players to explain the absence of effect in LLC tumours. Accordingly, we sought to evaluate the effect of secreted molecules (secretome) by tumour cells (both LLC and B16F1) on macrophages *in vitro*, also considering the genetic manipulation of ADAMTS1, represented by the use of WT and shAts1 cells.

4.1. Macrophage polarisation depending on different tumour cells conditioned medium.

As showed in the previous section 2.3, we benefited from bioinformatics-driven analysis of RNA sequencing data comparing specific signatures between LLC and B16F1 tumours. Moreover, the characterisation of both cell lines (Results, section 3.1, Figures 57-58) showed that they are different, including a higher expression of ADAMTS1 (and other versicanases, data not shown) in B16F1 cells, while the expression of its substrates was more relevant in the LLC ones.

At this point, we carried out *in vitro* polarisation experiments using CM from LLC and B16F1 cells (details in Materials and Methodology, section 3.1). To achieve this goal, we incubated WT BMDM with 24-hour CM of both cell lines and then, polarisation was evaluated both by gene expression and FC. After 24-hour polarisation, we observed that LLC CM induced the gene expression of both *Nos2* (M1 marker) and *Cd206* (M2 marker) in comparison with B16F1 CM (Figure 65A- B). Moreover, this increase was confirmed by FC (Figure 65C-D), supporting our hypothesis that LLC cells are more liable to educate macrophages.

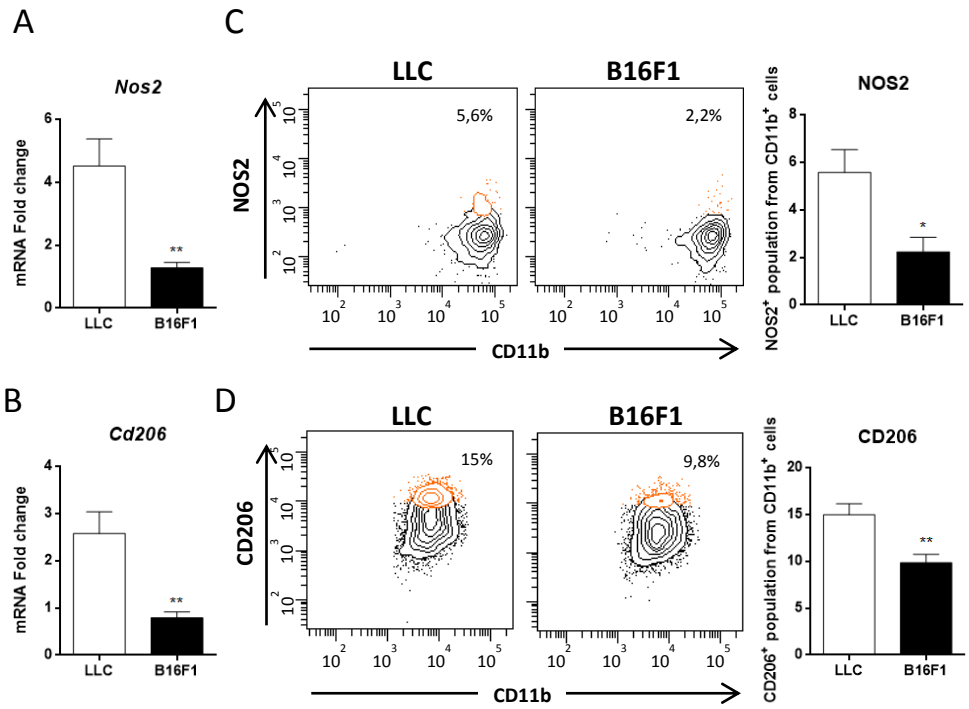

Figure 65. Effect of LLC and B16F1 CM in NOS2 and CD206 during BMDM polarisation. Graphs representing relative mRNA fold change expression of genes related to (A) M1 polarisation (*Nos2*) and (B) M2 polarisation (*Cd206*) in LLC and B16F1 (normalized to M0 control) 24h-polarised CD11b^{+} populations. Representative flow cytometry plots including the mean percentage of (C) NOS2 and (D) CD206 and their quantification. (* *P<0.05*, ** *P<0.01* two-tailed t Student, n=17 and n=13 samples in LLC and B16F1 respectively for gene expression, and n=7 for each group in FC).

Although we confirmed that CM of both cell lines is able to induce polarisation macrophages, we assessed a deeper analysis by RNA sequencing of macrophages treated with CM of both LLC and B16F1 cells, and also M0 and M2 controls of polarisation, this latest one due to its pro-tumorigenic properties. First, principal component analysis showed a clear aggrupation of samples by group (Figure 66A). Interestingly, while macrophages treated with B16F1 CM appeared close to M0 controls, we found a distinct location of M2 and LLC-CM-treated groups. Next, the analysis of differently expressed genes of the whole transcriptome between LLC and B16F1-CM-treated macrophages, represented in a MA-plot (Figure 66B), showed that macrophages polarised with LLC CM displayed higher expression of *Mrc1* (*Cd206*) (a M2 marker) than B16F1 group. Finally, a selection of genes of specific signatures (M1 and M2 polarisation and angiogenesis) was also represented in heat-maps (Figure 66C). In the case of M1 markers, some of them were more expressed in LLC group

compared to B16F1. However, there is not a clear pattern. In the case of M2 markers, some of them were overexpressed in M2 positive control and others in LLC group. This result suggests that although both are pro-tumorigenic macrophages, they induced mostly distinct gene expression patterns. Finally, some of the angiogenesis genes were upregulated in M2 control and some in LLC group. This result followed the same tendency that M2 genes, reinforcing the idea of LLC CM polarising macrophages to M2 in a different way than the IL4, which is used for the M2 control.

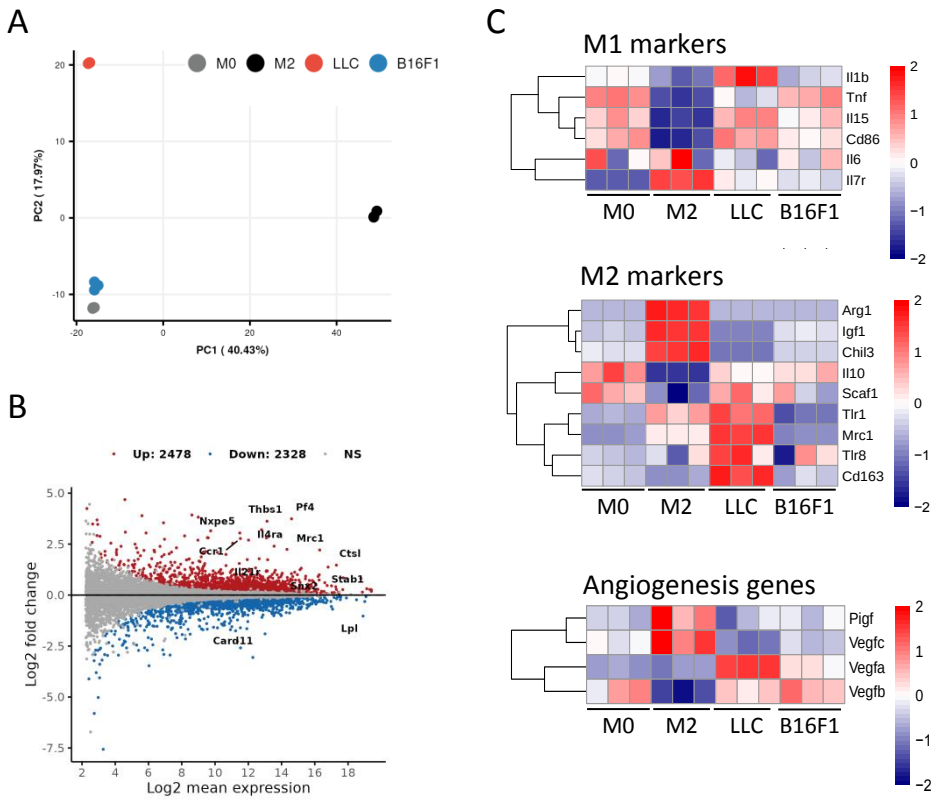

Figure 66. Bone marrow-derived macrophages polarization by tumour cell conditioned media *in vitro*. (A) Principal component analysis of each RNAseq replicate of each group of polarization. (B) MA-plot ilustrating the most differentially regulated genes (Adj. p-value < 0.05, Log2FoldChange +/- 1) between BMDM polarized in presence of LLC or B16F1 conditioned media. (C) Heatmaps of normalized (z-score) RNAseq read counts of genes related to M1 and M2 macrophages and angiogenesis. N=3 samples in each group.

These experiments clearly showed the different modulatory properties of each cell line during macrophage polarisation. In order to know which molecules in the CM induced such differences, secretome of both cell lines was evaluated. As described in the material and methodology section, we used a protein array including 111 molecules.

From all the analysed proteins, we found higher levels of 15 proteins in LLC *versus* B16F1 cells (Figure 67A-B). Among all of them, the ones with a well-defined implication on inflammatory processes are VEGF and several cytokines and chemokines (CX3CL1, CXCL1, CCL20, LIX/CXCL5, CCL2/MCP-1 and M-CSF/CSF-1) (Shiao et al., 2011)(Poh & Ernst, 2018)(Kohli et al, 2021).

A

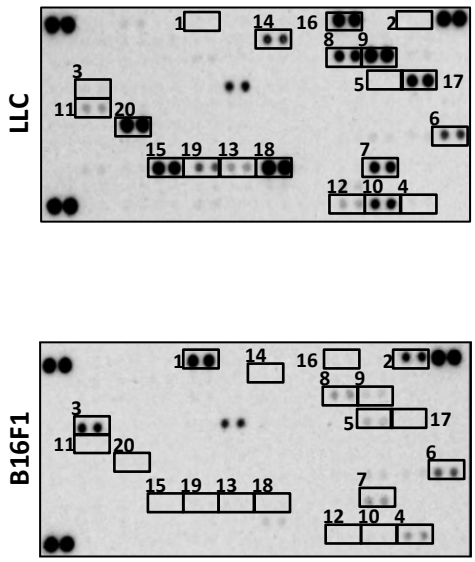

B

Number	Protein	LLC/B16F1 ratio
1	LDL R	1.35E+00
2	Osteopontin (OPN)	5.60E+00
3	CX3CL1/Fractalkine	5.73E+00
4	CXCL1/KC	1.84E+01
5	VEGF	7.24E+01
6	FGF-21	3.70E+05
7	VCAM-1/CD106	3.79E+05
8	MMP-2	5.14E+05
9	CCL20/MIP-3alpha	1.39E+06
10	LIX	1.68E+06
11	CCL2/JE/MCP-1	2.36E+06
12	Endostatin	2.39E+06
13	MMP-3	4.51E+06
14	M-CSF	1.10E+07
15	IGFBP-6	3.94E+07
16	Angiopoietin-2	2.10E-02
17	CCL5/RANTES	2.33E-02
18	CXCL10/IP-10	7.55E-02
19	WISP-1/CCN4	1.32E-01
20	Endoglin/CD105	1.38E-01

Figure 67. Cytokine array of CM of LLC and B16F1 cell lines. (A) Nitrocellulose membranes each containing the protein level of 111 molecules found in the CM of LLC (top) and B16F1 (bottom). Boxes show the most relevant differently expressed molecules between them. (B) Table including the upregulated (1-15, grey) and downregulated (16-20, blue) molecules in LLC *versus* B16F1 conditioned medium.

In contrast, 5 were more secreted by B16F1 cells than LLC ones, CCL5 and CXCL10, which are well recognised by their immunomodulatory functions and its connection to macrophages (Poh & Ernst, 2018) (Figure 67A-B). However, the real action of these candidates would require additional assays to confirm their implication in the effects of both LLC and B16F1 cells and, by extension, their derived tumours.

As detailed in the introduction, molecules such as VEGF, CCL2 or M-CSF (all of them more secreted by LLC cells) are chemoattractants for monocytes. In contrast, CXCL10, more secreted by B16F1 cells, is more related to anti-tumorigenic macrophages. In spite of it, our main interest is focused on the study of the contribution of ADAMTS1 to immune regulation in general, and macrophage specifically. In fact, our tumour experiments revealed that the biggest changes in macrophage polarisation genes where found when –shAts1 cells were injected. For that reason, it is important to evaluate the contribution of tumour-derived ADAMTS1 on macrophage polarisation *in vitro*.

4.2. Relevance of tumour ADAMTS1 for macrophage polarisation.

We have previously demonstrated that stromal ADAMTS1 regulate macrophage migration and phagocytosis ability (Results, section 2.1). However, it is not relevant in terms of macrophage polarisation. Nevertheless, when we injected LLC and LLC-shAts1 cells in mice we observed that tumour cells are more powerful modulating macrophages than the stroma. Accordingly, we evaluated whether the absence of ADAMTS1 in the tumour cells can regulate the *in vitro* polarisation of macrophages, as it happened *in vivo* (Figure 63).

For this purpose, we approached the polarization of macrophages using CM of WT and –shAts1 LLC and B16F1 cell lines. Polarisation was tested by measuring gene and protein levels of both Nos2 and Cd206. Interestingly, we observed that the inhibition of ADAMTS1 in both LLC and B16F1 tumour cell lines induced the expression of *Nos2* and reduced the levels of *Cd206* in the macrophages (Figure 68A and D), corroborated by FC in a tumour model-independent manner (Figure 68B-C and E-F). Surprisingly, this result could be indicating that the secretion of ADAMTS1 by the tumour cells impedes the polarisation of macrophages to M1. It was demonstrated because the inhibition of the protease in both tumour cell lines reduced its secretion and promoted the increase of M1 marker Nos2, probing that tumoral ADAMTS1 is involved in this phenomenon, in contrast to stromal contribution.

Our previous experiments showed that tumours generated with LLC-shAts1 cell line had an enhanced expression of the M2 marker *Cd163* (Figure 63). In contrast to it, the same cell line (and also B16F1-shAts1) reduced M2 BMDM polarisation *in vitro* (Figure 68). This opposite result highlights the relevance of the stroma and the tumour microenvironment.

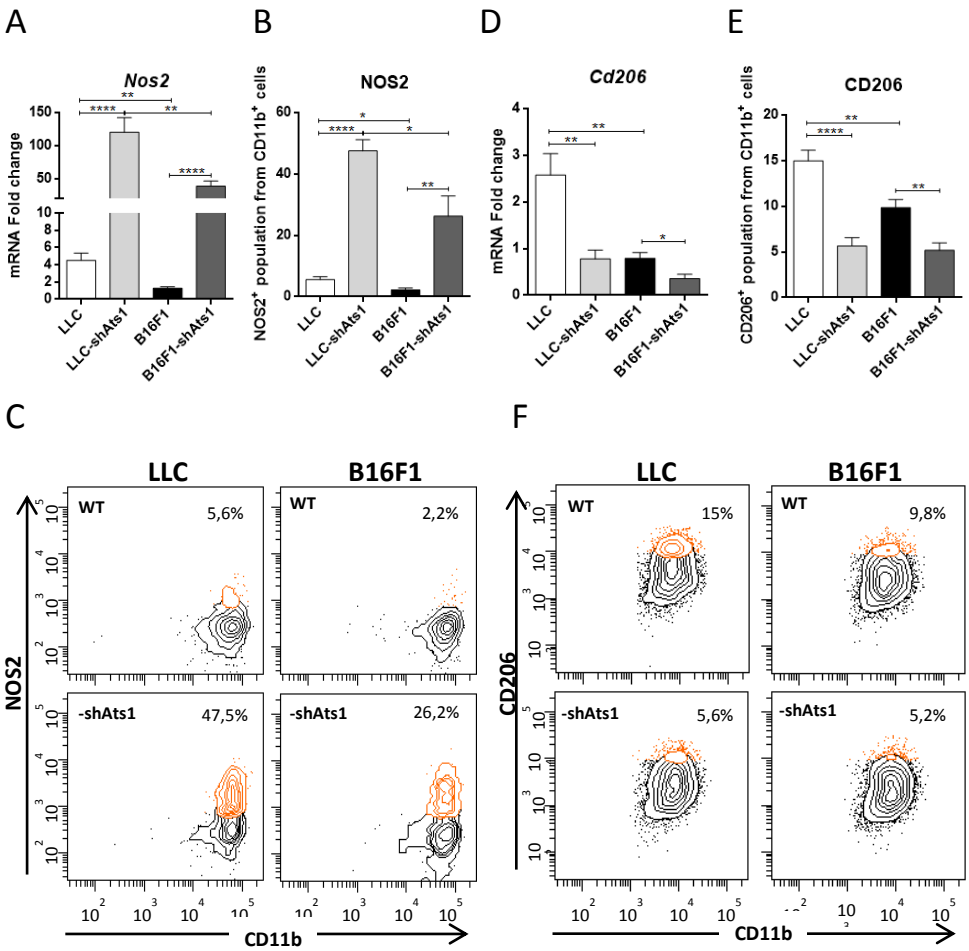

Figure 68. Effect of tumoral ADAMTS1 in NOS2 and CD206 during BMDM polarisation in presence of tumour CM. Graphs representing relative mRNA fold change expression of M1-related *Nos2* (A) and M2-related *Cd206* (D) genes in LLC, B16F1, LLC-shAts1 and B16F1-shAts1 24h-polarised CD11b$^+$ populations (normalized to M0 control). Flow cytometry quantification of NOS2 (B) and CD206 (E) in all the groups and their representative flow cytometry plots including the mean percentage (C and F, respectively). (* *P<0.05*, ** *P<0.01*, **** *P<0.0001* two-tailed t Student, n=17 and n=11 samples in WT and –shAts1 respectively for gene expression, and n=7 and n=5 samples in WT and –shAts1 for each group in FC).

Despite this controversy, we tried to elucidate the molecules that could induce this shift in the polarisation. With such purpose, we followed same guidelines to analyse the secretome of the inhibited cell lines (-shAts1), as reported above for WT cells (Figure 69A). The close study of each inhibited cell line with its WT counterpart revealed just four proteins that were similarly regulated in both LLC and B16F1 model (Figure 69B). Among these proteins, IL33 has been described to induce M2 polarisation) (Faas et al., 2021), while CXCL10 promotes M1 polarisation (K. Wu et al., 2020).

A

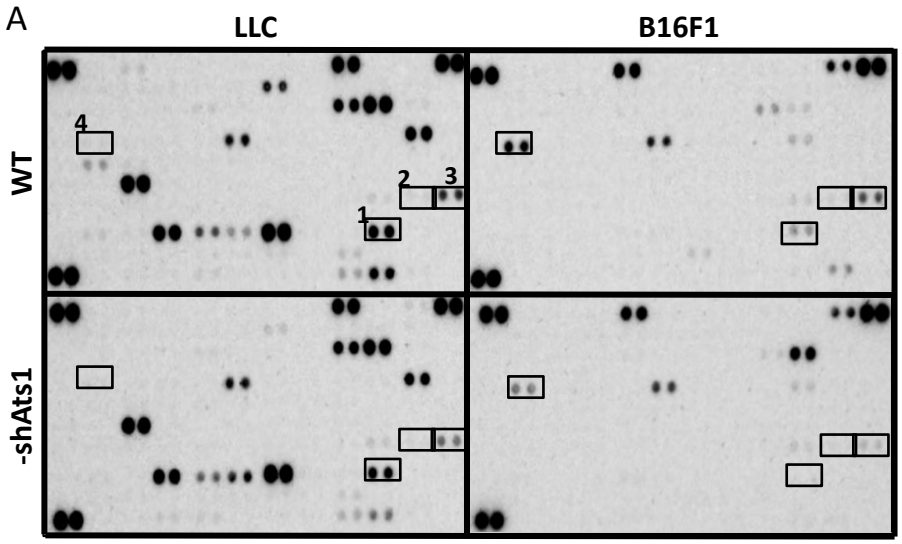

B

Number	Protein	LLC/LLC-shAts1 ratio	B16F1/B16F1-shAts1 ratio	LLC/B16F1 ratio
1	Osteopontin (OPN)	1.21E+00	4.41E+05	5.60E+00
2	IL-33	1.93E+00	2.52E+00	1.16E+00
3	LDL R	1.69E+00	4.72E+00	1.35E+00
4	CXCL10/IP-10	1.19E+00	2.65E+00	7.55E-02

Figure 69. Cytokine array of CM of every cell line. (A) Nitrocellulose membranes each containing the protein level of 111 molecules found in the CM of the different cell lines of the study. Boxes represent the most relevant differently expressed molecules similarly affected in WT and –shAts1 cells for both cell lines (1: Osteopontin, 2: IL33, 3: LDLR, 4: CXCL10/IP-10). (B) Table including the ratio between WT and –shAts1 cells for each molecule and cell line.

The four proteins were less secreted in absence of tumoral ADAMTS1. Considering that LLC enhanced M2 polarisation and that WT cells had a lower M1 polarisation, we only studied the molecules that were more secreted by both LLC *versus* B16F1 and

WT *versus* –shAts1. For that reason, we discarded CXCL10 (more secreted by B16F1) for further analysis. Moreover, due to the bibliography we continued our next experiments just with IL33 and LDLR. These experiments included polarisation experiments *in vitro* with neutralising antibodies for both molecules. However, we did not success in obtaining a result and it is still an open door for future approaches.

5. ADAMTS1 role during resistance and response to anti-angiogenic therapy.

Since its discovery, ADAMTS1 has been described as an anti-angiogenic molecule (Lee et al., 2006)(Rodríguez-Manzaneque, et al., 2015). However, this action has provoked a constant controversy, since this function depends on the tumour type and the protease's origin. In our LLC model, we observed that inhibition of both stromal and tumoral ADAMTS1 increased vessel density, corroborating the anti-angiogenic effect of the protease, but without consequences for final tumour growth. Following this rational, we headed the use of anti-angiogenic drugs in order to elucidate if there are common or different mechanisms in the way that these drugs and ADAMTS1 block angiogenesis. For this analysis, we continued using both tumour models, LLC and B16F1, which has been defined as refractory and sensitive to this type of therapies, respectively (Shojaei et al., 2007).

5.1. Comparison between sensitive and resistant tumours to anti-angiogenic therapy.

After evaluating the specificity of the anti-angiogenic VEGF-Trap Aflibercept *in vitro* for endothelial cells (data not shown), we injected both tumour cell lines in WT mice and treated them with the drug. Both cell lines have been previously treated with VEGF-Trap molecules such as Aflibercept. In the case B16F1 tumours, they have been defined as sensitive (Rudge et al., 2007)(Shojaei et al., 2007). In contrast, LLC tumours have been declared as resistant to anti-VEGF monoclonal antibodies G6.23 and G6-31 due to the increase of MDSCs (Shojaei et al., 2007)(Shojaei et al., 2009) but it did respond to subcutaneous administration of a recombinant VEGF-Trap (S. Zhou et al., 2013). For our experiments, tumour cells were subcutaneously injected and treated with Aflibercept twice per week as detailed in materials and methodology section.

As expected according to most of the literature, B16F1 tumour volume was reduced, while LLC was not affected (Figure 70A). Indeed, in the case of B16F1 tumours, differences were observed since the first dose. In spite of the different response, at the end of the experiment, vessel area was reduced in both models (Figure 70B), reflecting the role of other players in the resistance of LLC model. Knowing the relevance of the $CD11b^{+}/Gr1^{+}$ population to this resistance, infiltration of this population was evaluated by FC at end point, observing an increase in LLC tumours

after the treatment but no effect on B16F1 model (Figure 70C), in accordance to literature (Shojaei et al., 2007)(Shojaei et al., 2009).

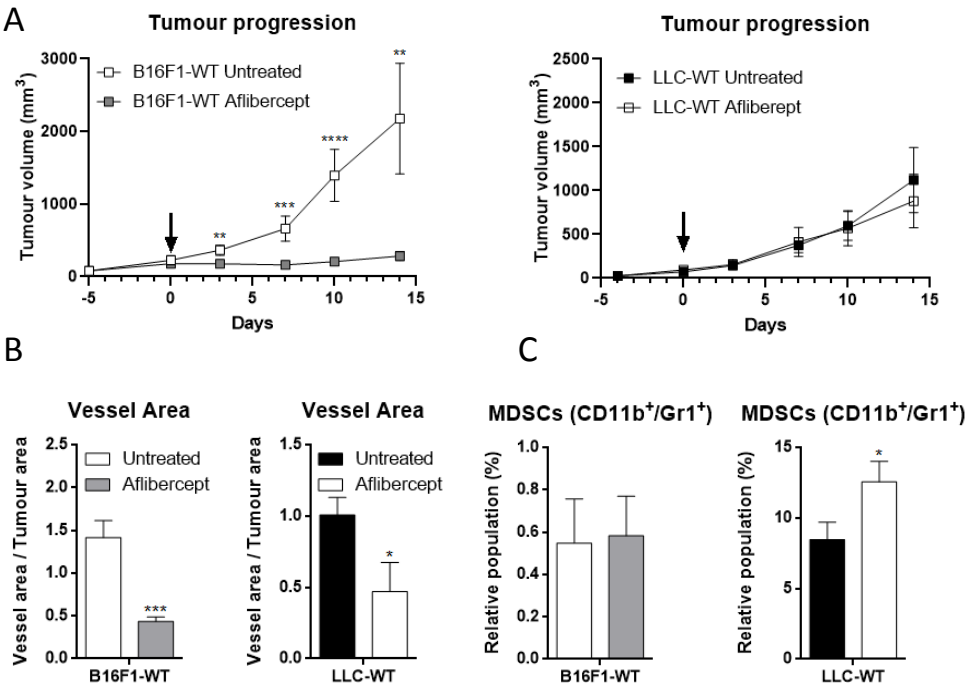

Figure 70. Effect of Aflibercept treatment on B16f1 and LLC tumours. Progression of tumour volume before and during Aflibercept treatment represented as tumour volume ± s.e.m for B16F1-WT (left) and LLC-WT tumours (right). Black arrow indicates the beginning of the treatment. (B) Graphs representing mean ± s.e.m of vessel density of untreated and treated mice for all the conditions. (C) Flow cytometry data showing the percentage of myeloid-derived suppressor cells (MDSCs) represented as mean ± s.e.m of live cells in untreated and treated tumours. (**P<0.05*, ** *P<0.01*, *** *P<0.001,* **** *P<0.0001* two-tailed t Student, n= 14, 18, 9 and 7 samples in each group from left to right).

These results bring out the relevance of looking for alternatives to refractory tumours such as LLC model. For that reason, we used Ats1-KO mice to see if tumour growth is affected by anti-angiogenic drugs, due to the link of ADAMTS1 and angiogenesis.

5.2. Contribution of stromal and tumoral ADAMTS1 in tumour progression and immune infiltration during anti-angiogenic therapy.

Since we have observed that both stromal and tumoral ADAMTS1 are able to modulate tumour angiogenesis, although without effect on LLC progression (sections

1.1 and 3.3), we approached the Aflibercept-treatment of all experimental groups reported in such sections. As described above, LLC-WT tumours did not respond to Aflibercept (Figure 70). Moreover, we found that the absence of ADAMTS1 in the stroma or its inhibition in tumour cells did not alter the results (Figure 71B-E), suggesting that ADAMTS1 is not as relevant contributing to the resistance to anti-angiogenic therapies, at least in this LLC model.

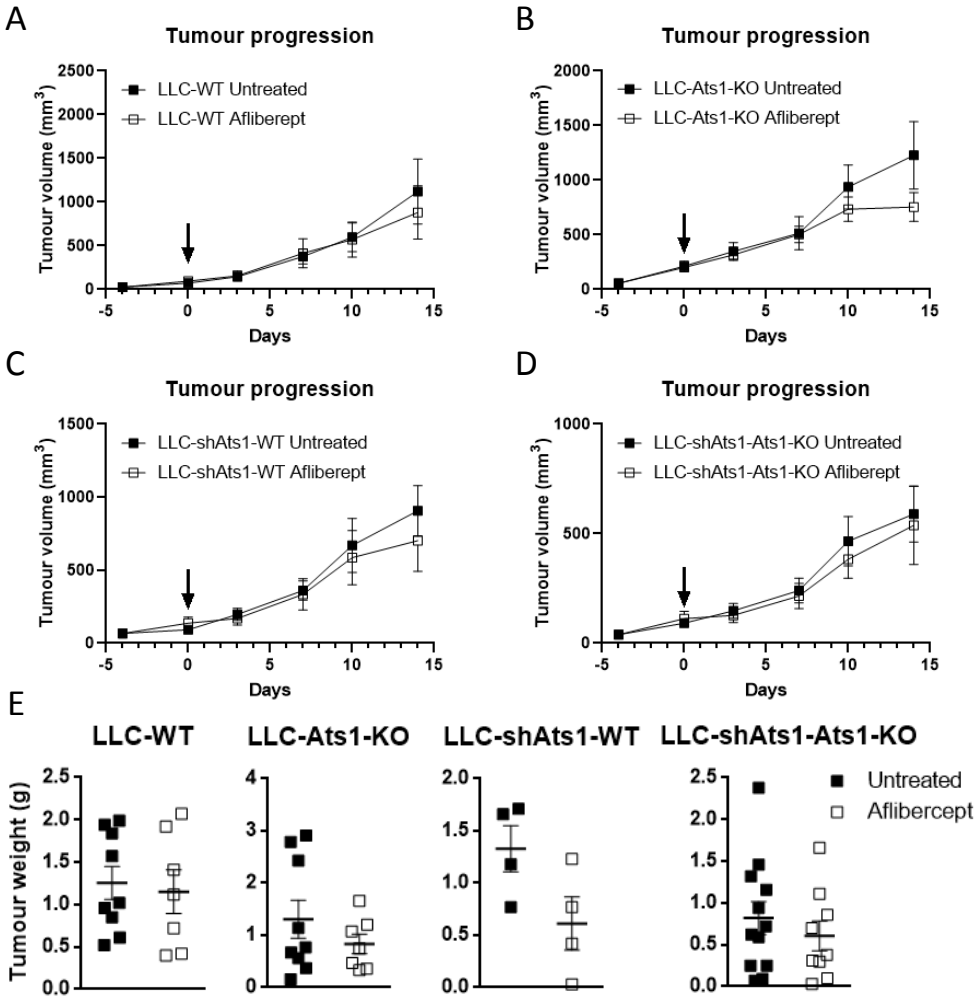

Figure 71. Contribution of stromal and tumoral ADAMTS1 in Lewis Lung Carcinoma model during antiangiogenic therapy. Progression of tumour volume before and during Aflibercept treatment represented as tumour volume ± s.e.m for LLC-WT (A), LLC-Ats1KO (B), LLC-shAts1-WT (C) and LLC-shAts1-Ats1-KO (D) groups. Black arrow indicates the beginning of the treatment. (E) Graphs representing mean tumour weight ± s.e.m after 2-week treatment for all the groups. N= 9, 7, 9, 7, 4, 4, 12 and 9 samples in each group from left to right in panel E.

Despite this lack of differences in tumour growth, we evaluated tumour vasculature to know whether the therapy exerted an anti-angiogenic action. Indeed, vessel density and vessel area were reduced in all the groups (Figure 72A). Parallel, gene expression analyses of vasculature-related genes revealed differences depending on the group. While the treatment of tumour originated with WT cells provoked a downregulation of *Endoglin*, *Cdh5* and *Cd31*, in tumours generated with –shAts1 cells (LLC-shAts1-WT and LLC-shAts1-Ats1-KO) those genes were not affected (Figure 72B). This result suggests the different behaviour according to ADAMTS1 origin, and although vasculature is reduced in all the groups, it is well known the participation of immune populations in anti-angiogenic therapy resistance, which must be analysed.

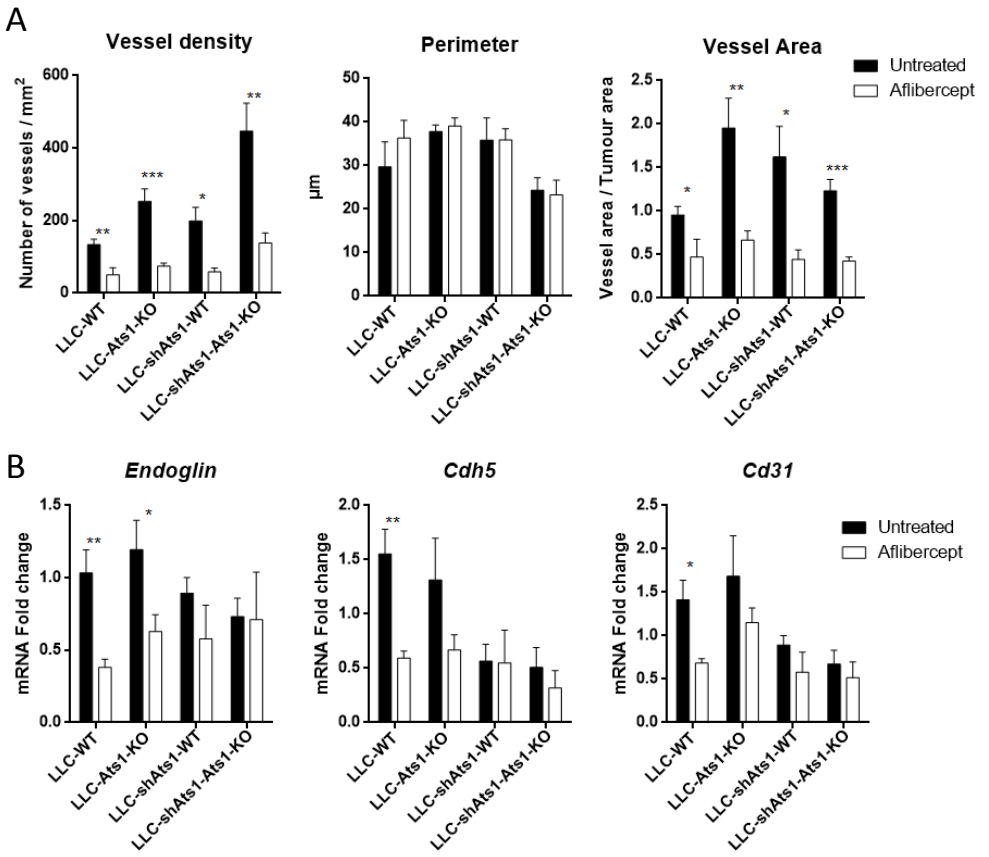

Figure 72. Effect of Aflibercept treatment on tumour vasculature. (A) Graphs representing mean ± s.e.m of vessel density, perimeter of vessels and vessel area of untreated and treated mice for all the conditions. (B) Graphs representing relative mRNA fold change expression of genes related to vasculature (*Endoglin*, *Cdh5* and *Cd31*). (**P<0.05*, ** *P<0.01*, *** *P<0.001* two-tailed t Student, n= 9, 7, 8, 7, 4, 3, 10 and 7 samples in each group from left to right).

It has been published that LLC resistance to anti-angiogenic therapy is due to the increase of MDSCs in treated tumours (Shojaei et al., 2007). For that reason, we tested the resistance looking at different immune populations within the tumours. We analysed T cells, but its infiltration and the expression of related genes were not affected by the treatment in any experimental group (Figure 73A-B), showing the poor contribution of T cells during anti-angiogenic therapy.

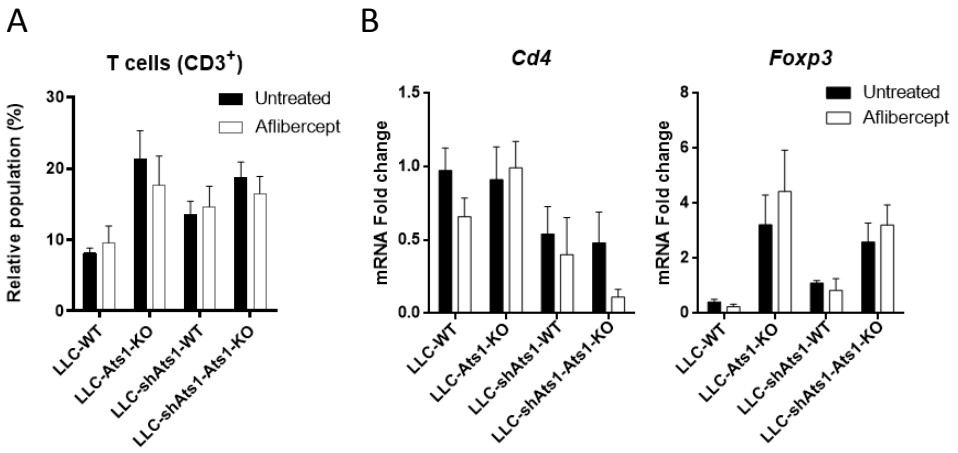

Figure 73. Contribution of stromal and tumoral ADAMTS1 in T cell infiltration during antiangiogenic therapy. (A) Flow cytometry data showing the percentage of T cells represented as mean ± s.e.m of live cells in untreated and treated tumours. (B) Graphs representing relative mRNA fold change expression of genes related to T cells (*Cd4* and *FoxP3*). N= 9, 7, 8, 7, 4, 4, 11 and 8 samples in each group from left to right.

Next, myeloid cells were studied, which are more relevant in this scenario. As it was observed for the LLC-WT group (Figure 70) and in the literature (Shojaei et al., 2007)(Shojaei et al., 2009), there was an increase in the infiltration of MDSCs after the therapy in LLC-Ats1-KO and LLC-shAts1-Ats1-KO groups, which was compensated with a reduction in F4/80^{+} macrophages (Figure 74A), suggesting the poor contribution of stromal ADAMTS1 to this resistance. In contrast, LLC-shAts1-WT tumours did not show changes in any of the populations, indicating its different behaviour according to tumour-derived ADAMTS1. Finally, we analysed macrophage polarisation markers by qPCR. We found an upregulation of *Nos2* in all groups, although it was not significant in the LLC-shAts1-WT group (Figure 74B). Moreover, *Cd163* was overexpressed just in the LLC-Ats1-KO group, with the same tendency in the group of the inhibited cell line in WT mice.

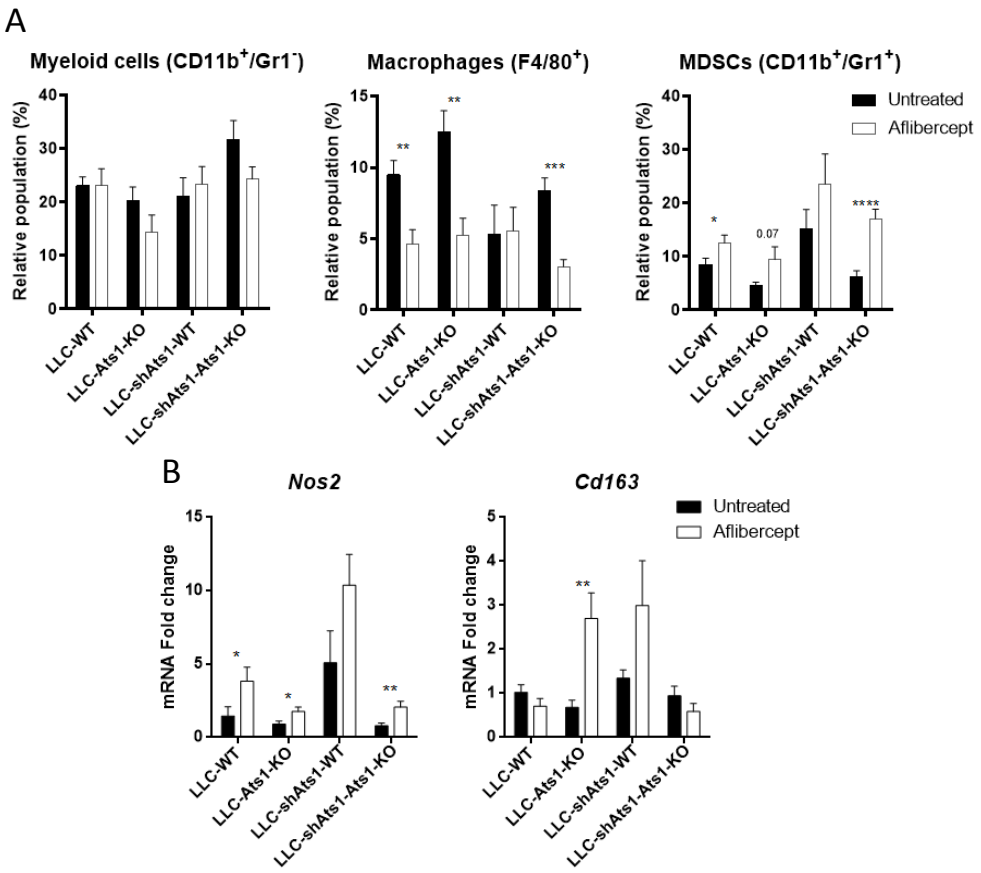

Figure 74. Contribution of stromal and tumoral ADAMTS1 in myeloid cell infiltration during antiangiogenic therapy. (A) Flow cytometry data showing the percentage of myeloid cells, macrophages and myeloid-derived suppressor cells represented as mean ± s.e.m of live cells in untreated and treated tumours. (B) Graphs representing relative mRNA fold change expression of genes related to macrophages *(Nos2* and *Cd163*). (* *P<0.05*, ** *P<0.01*, **** *P<0.0001* two-tailed t Student, n= 9, 7, 8, 7, 4, 4, 11 and 8 samples in each group from left to right).

Altogether, our results corroborated the resistance of LLC model to anti-angiogenic therapy, contrary to the B16F1, independently to the levels of stromal and tumoral ADAMTS1. However, the analysis of the tumour showed that this resistance can be modulated by different mechanisms. The study of the vasculature showed a reduction of the density in all the groups. However, endothelial-related genes were differently regulated between LLC and LLC-shAts1 tumours after the therapy, so other alternative mechanisms of neovascularisation can be involved. Regarding infiltrated immune cells, LLC-shAts1-WT group followed a different tendency to the other groups, suggesting a resistance mediated by different mechanisms to the

infiltration of MDSCs. For that reason, combination of anti-angiogenic therapy with other treatments such as macrophage depletion can potentiate the anti-tumorigenic role of both therapies.

DISCUSSION

Apart from the tumour cells, it is well known how other cell types within the tumour and the stroma orchestrate the behaviour of the tumour, as well as modulate several processes including angiogenesis, migration or inflammation (Hanahan & Weinberg, 2011). Among the complexity of the tumour microenvironment (TME), non-cellular components in general, and extracellular proteases specifically, have been defined as essential players for the evolution of tumours. In this thesis, we have focused on the extracellular protease A Disintegrin And Metalloprotease with Thrombospondin motifs 1 (ADAMTS1), involved in angiogenesis and tumour growth (Rodríguez-Manzaneque et al., 2015)(Cal & López-Otín, 2015).

ADAMTS1 is a well-known protease with proteolytic activity over several substrates including extracellular constituents such as Nidogens (Canals et al., 2006), Versican (Sandy et al., 2001) or Syndecan 4 (Rodríguez-Manzaneque et al., 2009), among others. Moreover, the extended use of knockout mice for the protease (Ats1-KO) allowed understanding its contribution during physiological and pathological processes, mediated by its proteolytic activity in most of the cases. In fact, this Ats1-KO mouse displays deficiencies including kidneys and ureter malformations, null female fertility and increased lethality at neonatal stage (Shindo et al., 2000)(Mittaz et al., 2004). Likewise, it participates in pathologies such as vascular disorders and atherosclerosis (Jo et al., 2005)(Ren et al., 2013).

Relative to cancer and tumour angiogenesis, ADAMTS1 has been defined by its controversial actions. In one side, it has been reported its capacity to enhance endothelial-like phenotypes of tumour cells, promoting tumour aggressiveness and growth in sarcoma (Casal et al., 2010), uveal melanoma (Peris-Torres et al., 2020) or glioblastoma (Serrano-Garrido et al., 2021). In addition, it has been described as a tumour promoter in several tumour types (Fernández-Rodríguez et al., 2016)(Martino-Echarri et al., 2014)(Tan et al., 2019)(Ricciardelli et al., 2011) and, in contrast, as a tumour suppressor molecule (Kuno et al., 2004)(Reynolds et al., 2010)(Martino-Echarri et al., 2013b), mainly based on its action on tumour vasculature.

Important for this thesis, ADAMTS1 has been related with inflammation since its discovery (Kuno et al., 1997). Indeed, ADAMTS1 can modulate or be modulated by different inflammatory-related cytokines such as TGFβ, IL1β, LPS, IL17 or IL33 (Bourd-Boittin et al., 2011)(Ng et al., 2006)(Oveland et al., 2012)(Ashli et al., 2013)(Ashlin et al., 2014). Although it has been deeply studied for other members of the same family, little is still known about ADAMTS1 connection with immune

regulation and its possible contribution to the activity of specific immune populations (Redondo-García et al., 2021).

Some literature and previous works of our group already highlighted the regulation of immune genes and molecules influenced by ADAMTS1 (Fernández-Rodríguez et al., 2016)(Redondo-García et al., 2021). In fact, changes triggered by ADAMTS1 in the immune landscape are suggestive to explain the halt of B16F1 tumour growth in Ats1-KO mice (Rodríguez-Baena, Redondo-García, Peris-Torres, et al., 2018). Considering such background, in this work we continued this research topic, emphasizing the study of the contribution of ADAMTS1 in the immune landscape both in healthy and in tumour scenarios, including two immunogenically different models: B16F1 and the immune-challenging LLC.

1. Characterization of LLC and B16F1 tumour models: revealing their secretome and their effects on macrophage polarisation.

One of the particularities of this thesis is the comparative work between two murine tumour cell models: Lewis Lung Carcinoma (LLC) and B16F1 melanoma. They have been compared at different levels, starting with the different response to the deficiency of ADAMTS1 using syngeneic tumour model. Significantly, while B16F1 tumours were reduced in absence of stromal ADAMTS1, in contrast LLC ones were not altered. This starting point leads us to deeply characterise both tumours.

According to the literature, LLC and B16F1 tumours have been classified as immunologically cold and hot, respectively. In fact, cold or poorly immunogenic tumour such as LLC are characterized by the high infiltration of myeloid cells (Binnewies et al., 2018). For that reason, we wondered in what way those tumour cells modulate the phenotype of immune cells. In particular, we evaluated how the different cell lines educate macrophages *in vitro*. For this purpose, we polarised bone marrow-derived macrophages (BMDM) with the conditioned medium (CM) of each cell line. This approach revealed a more powerful activity of LLC secretome to polarise macrophages both to anti-tumorigenic or M1 (increase of Nos2) and pro-tumorigenic or M2 (increase of Cd206). Moreover, principal component analysis and the study of other macrophage polarisation genes by RNA sequencing indicated that, although LLC induced M2 polarisation, it was not the canonical one induced by IL4, as it was observed by other molecules such as IL33 (Faas et al., 2021). In contrast, B16F1 secretome did not alter the macrophages polarisation, according to their similarities with the negative control.

Attending to the changes in polarisation and considering the differences between LLC group and the M2 positive control, it was necessary to study the secretome of each cell line in order to elucidate the possible molecules behind that effect. For that, we used a proteome profiler array. As far as we know, in the literature there is no comparison of these characteristics for these two secretome. Using this technique, we observed 15 of them more secreted by LLC cells than B16F1. From all of them, CX3CL1, CXCL1, CCL20, LIX/CXCL5, CCL2/MCP-1 and M-CSF/CSF-1 were involved in the recruitment of monocytes, neutrophils and immunosuppression (Shiao et al., 2011)(Poh & Ernst, 2018)(Kohli et al, 2021). In addition to the well-known chemokines, we found also osteopontin, which has been associated with M2 macrophage and MDSCs recruitment and T cell inhibition (Moorman et al., 2020), LDLR that has been found upregulated in M2 macrophages in atherosclerosis (Baidžajevas et al., 2020), and VEGF, which is expressed in all the M2 macrophages

(Stockmann et al., 2014)(Goswami et al., 2017). These molecules support the ability of LLC cells to generate pro-tumorigenic environments and M2 macrophage polarisation. Interestingly, when we looked to the genes that encoded these molecules in our RNAseq, we found that *Cx3cl1*, *Ccl2*, *Csf1*, *Ldlr* and *Vegfa* were more expressed in LLC-WT tumours than in B16F1-WT, reinforcing the idea of its immunosuppressive environment.

Additionally, among the five proteins that were more secreted by B16F1 cells, two of the molecules are clearly connected with inflammation and regulation of immune populations. First, CCL5 has a controversial role, since it is known to increase the recruitment of T cells, DCs and monocytes (Hinohara & Polyak, 2019)(Daftarian et al., 2020)(Bejarano et al., 2021), but also pro-tumorigenic macrophages, MDSCs and Treg (Goswami et al., 2017)(Madden et al., 2020)(Erin et al., 2020)(J. Wu et al., 2021). The second inflammatory molecule, CXCL10, is a pro-inflammatory chemokine (Wu et al., 2017) necessary for $CD8^+$ T cell recruitment (Larsen et al., 2020)(Zhou et al., 2021) and related to M1 polarisation (Keklikoglou et al., 2018). Furthermore, both molecules are considered as Th1 cytokines and promote de deviation from M2 features of TAMs, indicating a less immunosuppressive environment (Sica et al., 2008)(Pitt et al., 2016). In addition, *Cxcl10* was more expressed in B16F1-WT tumours compare to LLC-WT ones, corroborating again the pro-tumorigenic environment in LLC tumours.

These differences in the ability of each secretome to modulate macrophage polarisation encouraged us to analyse the tumour models in more detailed. By RNAseq we analysed specific gene signatures, including a 200-gene inflammatory response signature. In this case, we obtained an activation of GO terms related to cytokine signalling and cellular response to LPS in B16F1-WT tumours compared to LLC-WT, evoking to a lower activation of these inflammatory pathways in LLC tumours.

The experiments comparing LLC *versus* B16F1 cell lines and tumours revealed the different immune landscape that can be produced by each of them, both *in vitro* and *in vivo*. In addition, LLC cells and tumours exhibited a high expression of Versican, a substrate of ADAMTS1 that is known by its immunomodulatory properties (Wight et al., 2020)(Hatano & Watanabe, 2020). This higher expression of Versican in LLC-WT tumours compared to B16F1-WT ones was found by RNAseq and by immunofluorescence in the tumours. Interestingly, our results corroborate the described correlation between CCL2 levels and Versican *in vitro* and *in vivo* (Keire et al., 2017), in which CCL2 likely interact with the chondroitin sulphate chains of

Versican in a positive feedback loop such as in systemic sclerosis patients monocytes (Masuda et al., 2013). It is important to highlight that immunodetection of Versican was focused on intact Versican, which has been linked to a more immunosuppressive environment. For that reason, big efforts must be put to unveil if the proteolysis of Versican by ADAMTS1 or other proteases in models such as the LLC one can reverse this scenario.

2. Stromal *versus* tumour-derived ADAMTS1: impairing tumour vascularisation with different final consequences in LLC and B16F1 tumours

As already mentioned, the fact that B16F1 and LLC tumours responded in a different way to the absence of ADAMTS1 was struggling. However, they are two different models with several particularities, as it was shown before, that can provoke these differences.

According to the well-known connection of ADAMTS1 with vasculature, we wanted to know if it was differently regulated in each tumour model, which could explain their different behaviour. We observed that stromal absence of ADAMTS1 provoked an increased vascularisation in both tumour models, confirming -at least partially- the inhibitory role of the protease in angiogenesis as it was described in other tumour models (Vázquez et al., 1999)(Iruela-Arispe et al., 2003)(Luque et al., 2003)(Sun et al., 2015)(Rodríguez-Manzaneque et al., 2015). However, the final impact in the tumour growth of each model was quite different. Focusing in the vasculature, while in the LLC model this increase was only found when endothelial structures were quantified, in the B16F1 the changes were more relevant, observed also by gene expression (Fernández-Rodríguez et al., 2016). Additionally, we also evaluated whether tumour-derived ADAMTS1 regulate vasculature in tumours. Although it did not alter it in B16F1 tumours (Fernández-Rodríguez et al., 2016), in LLC model ADAMTS1 has the same angio-inhibitory effect. In fact, reduction of ADAMTS1 in stromal and LLC cells showed an accumulative effect.

Those differences in vascularisation do not explain the evolution of the tumour in the LLC model. In the case of B16F1-Ats1-KO tumours, although they were more vascularised, tumour vessels were less functional, indicating the poor contribution of this phenomenon to tumour growth (Fernández-Rodríguez et al., 2016). One limitation of this work is that vessel functionality was not assessed in LLC model. However, even if the vasculature helped shrink the tumour, probably the immunosuppression produced by LLC cells would mask that effect. In spite of it, it is also important to evaluate if the use of anti-angiogenic therapies, which have a greater impact on vasculature, could block tumour growth in LLC model, but this issue will be discussed later. In addition, this increase in angiogenesis in LLC-Ats1-KO tumours can be provoked by other factors such as the presence of pro-angiogenic M2 macrophages (C. Li et al., 2021), so their contribution must be also addressed.

Parallel, due to the relevance of Nidogen 1 in vascular basement membrane (vBM) (Martino-Echarri et al., 2013b) it was evaluated in tumours. In both tumour models, the reduction of ADAMTS1 in the stroma or the tumour cells increased the deposition of this molecule. However, the observed pattern was different. While it was found all around LLC tumours, in B16F1 ones it was accumulated in the vasculature. Our group has previously described that high accumulation of Nidogen 1 in the vBM in a human breast carcinoma model correlates with bigger tumours (Martino-Echarri et al., 2013b), opposite to what was found in B16F1 tumours. Moreover, less functional vessels in B16F1-Ats1-KO tumours were accompanied by an increase of Nidogen 1. Interestingly, preliminary results in our lab suggest that Nidogen 1 overexpression in tumour cells enhances M1 polarisation in macrophages, similar to the inhibition of ADAMTS1. However, our results suggest that this substrate is not as relevant in LLC tumour, at least in the vasculature. According to its accumulation pattern in these tumours, Nidogen 1 can be produced by other stromal cells such as immune cells, what should be evaluated in future approaches in order to elucidate its possible role in LLC progression.

3. ADAMTS1 as an immunomodulatory molecule

At the moment of its discovery, ADAMTS1 was described as an inflammation associated gene (Kuno et al., 1997), and it was later known to be modulated by several inflammatory cytokines (Bourd-Boittin et al., 2011)(Ng et al., 2006)(Oveland et al., 2012)(Ashli et al., 2013)(Ashlin et al., 2014). Importantly, our work describing the role of ADAMTS1 in the B16F1 model showed a downregulation of *Cd11b* and *F4/80* in B16F1-Ats1-KO tumours compare to B16F1-WT, suggesting the role of ADAMTS1 in immunomodulation (Fernández-Rodríguez et al., 2016). These clues encouraged us to study in detail the contribution of stromal and tumour-derived ADAMTS1 in the immune system and its specific populations, both in physiological and pathological conditions, similar to other works demonstrating a connection between extracellular milieu and immune system, as we have recently reviewed (Redondo-García et al., 2021).

3.1. Contribution of stromal ADAMTS1 in immune regulation: promoting macrophage migration and phagocytosis *in vitro*

Our *in vivo* characterisation of Ats1-KO mouse demonstrated that the absence of stromal protease produced a pro-inflammatory and cytotoxic phenotype provoke by T cells in the two immune organs spleen and bone marrow, which can defend itself from external agents such as tumour cells. However, the regulation of myeloid populations and macrophages markers also suggest a prone anti-inflammatory response, revealing that the regulation of immune populations by ADAMTS1 can orchestrate different immune responses according to their infiltration in tumours.

Considering the differences that stromal ADAMTS1 provokes in the proportion of T and myeloid cells *in vivo*, our purpose was to evaluate the contribution of the protease in the behaviour of such immune populations. Preliminary results of our group have suggested a reduced proliferation of Ats1-KO T cells (data not shown). However, deeper analyses are still needed. In contrast, due to the differences that are well described regarding the immune infiltration in both tumour models and the results obtained using our Ats1-KO mouse, we performed an exhaustive characterisation of the myeloid population regarding relevant processes for tumour growth. These approaches revealed that the absence of stromal ADAMTS1 in bone marrow-derived macrophages (BMDM) impeded their migration (as it was previously

described for ADAMTS4 (Ren et al., 2013)) and phagocytosis, defining the immunomodulatory role of the protease.

Interestingly, our *in vitro* characterisation of macrophages also demonstrates that ADAMTS1 deficiency produces a reduction in their phagocytic activity. This alteration can have a strong impact in several pathologies such as cancer, since it would impede tumour cell clearance. This result was corroborated *in vivo*, since the treatment of Ats1-KO mice with clodronate liposomes did not show macrophage depletion due to their reduced phagocytosis. Moreover, LLC-WT treated tumours had a delayed in tumour evolution that was not observed in LLC-Ats1-KO group, suggesting that WT macrophages were being depleted since the beginning of the experiment, which was reflected in less engrafted mice and tumours with a slowed down growth. In models such as LLC one, which are well-recognised by their high infiltration of pro-tumorigenic myeloid cells, this type of deficiencies can have a big impact in tumour progression. However, other myeloid cells with more anti-tumorigenic roles are also found. For that reason, the reduction of an important processes such as tumour cell phagocytosis and clearance can be considered as a bad prognosis factor. Some strategies focus their attention in improvement of tumour cell recognition by macrophages, for instance with anti-CD47 antibodies (Mantovani, Marchesi, Malesci, Laghi, & Allavena, 2017). However, in this case it is more important to enhance this capacity, which is modulated by ADAMTS1 according to our results, by directly affecting the macrophages.

Although the absence of the protease in macrophages did not alter their ability to polarise *in vitro*, we observed an interesting upregulation of *Adamts1* in M2 macrophages. A previous work revealed that *ADAMTS1* is induced in THP-1 monocytes when differentiated into macrophages (Ashlin et al., 2013). Moreover, it has been described the overexpression of ADAMTS1 in macrophages in muscle tissue after the injury (Du et al., n.d.), where tissue-remodelling M2 macrophages are presumably more necessary. It suggests the relevance of the protease in this specific population, for example for ECM remodelling can cell invasion (Mantovani, et al., 2002). In the case of Versican, it was clearly induced in M1 population, independently to stromal ADAMTS1, correlation that was already described in infectious lung disease (Chang et al., 2014). Nevertheless, it was also overexpressed in Ats1-KO M2, according to its definition as a promoter of pro-tumorigenic landscape (Tzanakakis, et al., 2019). Although more studies are needed, these results can be indicating that there can be a compensation mechanism during macrophage polarisation that

induces the expression of the ECM markers *Adamts1* and *Versican* in M2 macrophages to regulate their remodelling function.

Analysis of the contribution of stromal ADAMTS1 to immune landscape confirmed a higher cytotoxicity of T cells in absence of stromal ADAMTS1 but a more immunosuppressive environment modulated by myeloid cells. Nevertheless, macrophages had a reduced ability to migrate *in vitro* and also to phagocyte, which reduced their anti-tumoricidal role. All these results demonstrate that Ats1-KO mice had a mainly pro-inflammatory and anti-tumorigenic phenotype. In spite of it, immune response can be governed by each tumour model, depending on if it recruits more T cells, myeloid cells or other type of cells. For that reason, immune infiltration must be evaluated in tumour conditions, as it will be discussed in the following section.

3.2. Contribution of tumour-derived ADAMTS1 in immune regulation: impairing M1 macrophage polarisation *in vitro*

Although stromal ADAMTS1 did not modify macrophage polarisation, tumour-derived protease might alter it. For that reason, we culture WT BMDM in presence of the CM of WT and –shAts1 LLC and B16F1 cell lines and we evaluated BMDM polarisation. Surprisingly, we found that the inhibition of ADAMTS1 in both tumour cell lines produced a downregulation of gene and protein levels of Cd206 and an upregulation of Nos2. This result indicates that the secretion of ADAMTS1 by the tumour cells blocks the polarisation of macrophages to M1, probing the role of tumoral ADAMTS1 in this phenomenon and indicating its contribution in pro-tumorigenic polarisation of macrophages, in contrast to stromal contribution. In fact, this connection between low levels of ADAMTS1 and high levels of NOS2 was already described in a mouse model of Marfan Syndrome (Oller et al., 2017). Interestingly, in a previous work of our group it was described that the reduction of ADAMTS1 in uveal melanoma cells affected their capacity to engraft in different immunocompromised mouse strains (Peris-Torres et al., 2020), suggesting the immunomodulatory role of tumour-derived ADAMTS1 and its interaction with immune populations. Briefly, Peris-Torres and colleagues showed that, while WT cells engrafted similarly in NSG and Swiss nude mice, Ats1-KO cells only engrafted in Swiss nude strain, which is less immunocompromised. Moreover, although NSG mice have several immune populations altered, it is known that their macrophages are

defective, so according to our results, this population was leading the engraftment depending on tumour-derived ADAMTS1.

Considering that the effect was similar independently to the tumour cell line, we wanted to know which common molecules were altered in the secretome of inhibited cell lines compare to WT mates. From this analysis, osteopontin, IL33 and LDLR appeared as mediator candidates for the changes in polarisation. As it was described in the first section, osteopontin and LDLR are associated to M2 macrophages (Moorman et al., 2020)(Baidžajevas et al., 2020), reinforcing the idea that reduced levels of those molecules can promote M1 polarisation. In the case of IL33, it is considered as an alarmin, that is implicated in Th2 responses and which correlates with macrophage recruitment and M2 polarisation in different pathologies (Besnard et al., 2015)(Fang et al., 2017)(Pinto et al., 2018)(Mai et al., 2021). In fact, IL33 induces a non-canonical M2 macrophage polarisation (Faas et al., 2021), as it has been observed for LLC secretome. Interestingly, it has been described that IL33 also promote the expression of *ADAMTS1* in human macrophages (Ashlin et al., 2014), corroborating the connection between both of them. According to the literature, there are clues that indicate that the three molecules can be behind the changes in macrophage polarisation after tumour-derived ADAMTS1 inhibition. For that reason, current efforts are also put on that direction.

Apart from the described secreted molecules, reduced secretion of Versican in –shAts1 LLC cells can also explain the shift in macrophage polarisation *in vitro* due to its pro-tumorigenic role (Islam & Watanabe, 2020)(Papadas et al., 2020). However, deeper analyses involving other versicanases and Versican proteolysis are still needed.

4. Immunomodulatory properties of stromal and tumoral ADAMTS1 depend on tumour heterogeneity

When looking at B16F1 model, its impaired tumour growth in Ats1-KO mice was supported by an increase of T cells and less pro-tumorigenic myeloid cells in tumours, spleen and BM, similar to the healthy mice. However, the high infiltration of myeloid cells, MDSCs and macrophages in LLC tumours can block the action of other anti-tumorigenic immune cells. In fact, all the differences derived from the Ats1-KO mouse were attenuated or even shift to immunosuppressive states. These results lead us to think that the reduction of myeloid cells in LLC-Ats1-KO tumours could enhance the anti-tumorigenic environment generated by the absence of the protease. For that reason, myeloid-targeted therapies must be considered. One of them is the depletion of this population. However, as it was shown in the results, their reduction in phagocytosis impeded their depletion. For that reason, other approaches focused on the inhibition of their recruitment, immunosuppressive functions or polarisation would be likely more efficient.

Those contradictions between both tumour models were demonstrated by different techniques. Indeed, RNAseq analysis of B16F1-Ats1-KO *versus* LLC-Ats1-KO tumours revealed that stromal ADAMTS1 deficiency in B16F1 tumours reduced cell motility and promoted T cell migration and chemotaxis and IFNɣ production, which is mainly produced by NKs and T cells and has anti-tumorigenic roles (Jorgovanovic et al., 2020), and which is known to downregulate ADAMTS1 levels in human macrophages (Ashlin et al., 2013). Again, this results support the immunomodulatory function of stromal ADAMTS1, whose deficiency in B16F1-bearing mice generate an anti-tumorigenic immune environment.

The compilation of the results of this part remarks how different tumour models can regulate and educate the immune system. Similarities between healthy and B16F1 model in absence of stromal ADAMTS1 suggested that this model is less efficient educating the immune system than LLC one, hindering the regulation of the tumour growth. In spite of the different interpretations that can be obtained from these results, we decided to focus this discussion in three main points: versican due to its immunomodulatory properties, and type I IFN and collagen structures according to the differences in RNAseq analysis and to the literature.

One of the biggest differences between both models is the levels of Versican. This substrate of ADAMTS1 is more expressed in LLC model compare to B16F1, corroborated by RNAseq and immunodetection, coinciding with a higher

immunosuppressive and immunotolerant environment (Islam & Watanabe, 2020) (Papadas et al., 2020). In addition, the opposite regulation of Versican in both models in Ats1-KO conditions (Rodríguez-Baena, Redondo-García, Peris-Torres, et al., 2018) propose it as a key factor for LLC progression. In addition, intact Versican accumulation correlated with an increase of Treg and M2 macrophage markers in LLC-shAts1 tumours, especially in Ats1-KO conditions, reflecting the connection of reduced ADAMTS1, increased intact Versican and immunosuppression, explaining why LLC growth was not reduced. Moreover, it can also participate in myeloid cell maturation, since it correlated with an increase of $CD11b^{+}/Gr1^{-}$ cells and a reduction of $F4/80^{+}$ macrophages. Controversially, the connection between –shAts1 tumour cells and M2 polarisation markers *in vivo* is the opposite of what was observed *in vitro*. This suggests that that crosstalk of tumour cells with immune cells in the TME alters their ability to educate macrophages highlight the relevance of the stroma. Interestingly, LLC-shAts1-Ats1-KO tumours also showed an overexpression of *Il33* and *Ldlr* (data not shown), coinciding with the overexpression of M2 macrophages and intact Versican levels, highlight again the mediation of those molecules in M2 macrophage polarisation.

Interestingly, we also found that type I IFN pathway was upregulated in LLC-Ats1-KO tumours compared to WT ones, while it was downregulated in B16F1 model. Type I IFN regulates processes such as cellular proliferation, apoptosis, antigen presentation or immunosuppression (Vidal, 2020)(Boukhaled et al., 2021). During elimination phase of tumour cells, type I IFNs are crucial to potentiate anti-tumour immunity (Vidal, 2020). However, in acute scenarios such as chronic inflammation and cancer, negative effects of type I IFN become dominant, for instance inducing PD-L1 and PD-L2 expression (Saleiro & Platanias, 2019). Moreover, tumour cells use type I IFN responses to transform immune cells in dysfunctional or immunosuppressive (Vidal, 2020)(Boukhaled et al., 2021), suggesting that it is the scenario of our LLC model. Interestingly, we analysed gene expression of all the genes related to pro-tumorigenic function of type I IFN in our LLC model, and all of them were upregulated in LLC-Ats1-KO tumours compare to WT mates (data not shown), proposing type I IFN as a key regulator of LLC tumour growth in Ats1-KO mice. In addition, it has been described that IFN regulatory factor 9 (IRF9) expression correlates with *VCAN* expression in lung adenocarcinoma as it is observed in LLC-Ats1-KO tumours and B16F1-WT ones. In fact, *VCAN* is a target of IRF9, and its high expression correlates with decreased survival (Brunn et al., 2021). In addition, the same correlation between type I IFN and Versican was found in macrophages and it was described that Versican produced by macrophages is considered as an induce IFN-stimulated genes

(ISGs) that is essential for IL10 expression by macrophages (Chang et al., 2017). Despite these connections must be corroborated in our tumour models, and although we still do not know how the reduction of ADAMTS1 promotes a decrease in the type I IFN signalling in LLC tumours, these results highlight type I IFN and Versican as a likely explanation to the behaviour of LLC tumours to the absence of ADAMTS1.

Similarly to type I IFN, matrisome signature GO enrichment analysis showed that supramolecular and collagen fiber organisations were differently regulated in both models. While these pathways were activated in LLC-WT compared to Ats1-KO mates, they were repressed in B16F1-WT ones compare to Ats1-KO. In fact, all the analysed collagens were more expressed in LLC-WT tumours than B16F1-WT ones. As it happens with Versican, collagen is described to have immunomodulatory properties. In fact, stiff collagen structures have been associated with tumour progression, invasion and metastasis (Jürgensen et al., 2020). Moreover, collagen density decrease cytotoxicity of T cells, enhance immunosuppressive roles of macrophages and difficult their crosstalk (Kuczek et al., 2019)(Larsen et al., 2020). In addition, it is known that collagen is engulfed by macrophages expressing CD206 or by phagocytosis (Madsen et al., 2017)(Jürgensen et al., 2020). Probably, in the case of LLC model, it is engulfed by M2 macrophages. However, in B16F1-Ats1-KO tumours, the low levels of those M2 macrophages and the deficient phagocytosis of those cells enhances the accumulation of collagen in the tumour. Nevertheless, its accumulation does not correlate with tumour growth, suggesting that this protein is not relevant in B16F1 model, although it must be studied in more detail in LLC model.

In summary, all these data indicate that differences between both models and how they do respond to the absence of ADAMTS1 is due mainly to the composition of their ECM, its immune infiltration and the regulation between them. Moreover, in the LLC model there are clues suggesting that stromal and tumoral ADAMTS1 regulate tumour behaviour in a different way. Interestingly, we have demonstrated that LLC-shAts1-Ats1-KO tumours were the most vascularized tumours, coinciding with a gene regulation of macrophage polarisation markers that reflect a polarisation to M2 pro-tumorigenic and pro-angiogenic macrophages. Moreover, stromal absence of ADAMTS1 revealed a regulation of type I IFN signalling, which seem to be the responsible of Versican accumulation and tumour growth. Nevertheless, our results indicate that tumoral inhibition of ADAMTS1 promotes LLC progression by the modulation of macrophage polarisation. To corroborate that hypothesis, RNA sequencing of tumours generated with the inhibited cell line can provide more

information about it. Moreover, although it did not work by the deficiency in phagocytosis of Ats1-KO macrophages, macrophage depletion by clodronate liposomes or other known therapies in LLC-shAts1 tumours can demonstrate the relevance of this population in those conditions.

5. Stromal and tumoral ADAMTS1 actions on vasculature and immune system: unfolding the resistance to anti-angiogenic therapy.

Due to the relation of ADAMTS1 and its inhibitory role in vasculature both in LLC and B16F1 tumours, we wanted to evaluate its contribution during anti-angiogenic therapies using the VEGF-Trap drug Aflibercept. The two tumour models of this work, B16F1 and LLC, are considered as sensitive and refractory to this kind of therapies respectively (Shojaei et al., 2007). Nevertheless, as far as we know there is one work in which is described that LLC model responds to VEGF-Trap (Zhou et al., 2013).

LLC model is a challenging situation, since it does not respond to the reduction of ADAMTS1 neither to anti-angiogenic therapy, mainly due to its environment. For that reason, we treated with Aflibercept all the experimental groups, including tumours generated with the inhibited cell line and in Ats1-KO mice in order to unveil the contribution of the protease in this environment. Although LLC tumour growth was not reduced (neither in Ats1-KO mice nor when ADAMTS1 was inhibited in the tumour cells), both B16F1 and LLC model tumours had a decrease in vessel density after the treatment. Nevertheless, gene expression of endothelial markers was differently regulated depending on ADAMTS1 origin. While LLC-WT and LLC-Ats1-KO tumours had a downregulation of *Endoglin* and the same tendency for *Cdh5* and *Cd31*, Aflibercept did not altered those genes in tumours generated with LLC-shAts1 cells. This result suggests that stromal and tumoral ADAMTS1 have a different effect on endothelium according to its origin. Moreover, although vasculature is reduced in all the groups, alternative mechanisms of vascularisation or other pro-angiogenic cells can be involved in this resistance.

As it has been described in the literature, we confirmed that LLC resistance was mediated by an increase of MDSCs after the therapy, which was not observed in the responder B16F1 model (Shojaei et al., 2007)(Shojaei et al., 2009)(H. Zhang et al., 2013). Those MDSCs were more infiltrated after the treatment in LLC-WT, LLC-Ats1-KO and LLC-shAts1-Ats1-OK tumours, which was compensated by a reduction of $F4/80^{+}$ macrophages. Nevertheless, those alterations were not observed in LLC-shAts1-WT. In addition, *Cd206* was only upregulated in LLC-Ats1-KO group and LLC-shAts1-WT group showed the same tendency.

According to the displayed results, LLC model is resistant to Aflibercept, independently to ADAMTS1. However, the resistance to the therapy is mediated by different pathways depending on the origin of ADAMTS1. Tumours generated in Ats1-KO mice revealed similar characteristics to LLC-WT group, with the exception of

the overexpression of *Cd206*. These results suggest that resistance to Aflibercept in absence of stromal ADAMTS1 is mainly mediated by MDSCs as in WT conditions, although M2 macrophages can be also involved. In contrast, the inhibition of *Adamts1* in the tumour cells revealed a completely different scenario. Interestingly, although LLC-shAts1-WT tumours neither respond to the therapy, there was not an increase of MDSCs recruitment, and although macrophages markers did not show statistically significant differences, there was an increased tendency of both *Nos2* and *Cd206* markers. These results open a door to a discussion regarding other mechanisms of resistance to the therapy, and force to the evaluation of combined therapy. It is clear that stromal ADAMTS1 has a poor effect on the response to the therapy due to its similarities to WT mates, while LLC-shAts1 cells produce a different environment. In both cases, it was observed an overexpression of *Cd206* that suggest that those pro-angiogenic macrophages can be playing an essential role in the resistance. This, together with the high infiltration of MDSCs in most of the groups reinforces the idea of using anti-angiogenic therapy in combination with treatments that block the myeloid lineage. This combination can be performed using clodronate liposomes. However it presumably will not work in Ats1-KO mice due to the deficiency of their macrophages. In contrast, it can be used in LLC-shAts1-WT tumours to unveil the mechanism behind its resistance. Moreover, other treatments can involve the use of CSF1R inhibitors, which have been already used (Priceman et al., 2010). In fact, this combination not only reduced angiogenesis and myeloid infiltration but also reduced the expression of M2 macrophages markers without altering M1 ones. In addition, we previously described how LLC-shAts1 and LLC-shAts1-Ats1-KO tumours produced an environment in which M2 macrophage marker genes are upregulated, so these group can be especially benefited from the combined therapy. However, its translation to human can be controversial due to the adverse effect that it would generate. As it was described in the Introduction Section, the most promising approach is the reprogramming of macrophages, due to the necessity of macrophages in other processes, which can be limited by the previously mentioned therapies.

Apart from the regulation of immune populations, it is well known that during cancer development, alternative mechanisms of neo-vascularisation take place. In fact, those mechanisms can be enhanced during anti-angiogenic therapy as a compensatory phenomenon. LLC-shAts1 tumours were resistant to the therapy, but it was not mediated by MDSCs. The results indicate the relevance of M2 macrophage in this resistance, but the differences in gene expression of endothelial markers with other groups suggest that there might be an upregulation of those markers in the

whole tumour, probably due to cancer cells that are acquiring them, as in vasculogenic mimicry phenomenon.

CONCLUSIONS

1. Our RNAseq studies uncover significant differences between Lewis Lung Carcinoma (LLC) and B16F1 syngeneic tumour models in terms of their extracellular compartment and their immune environment.

2. LLC cells mediate the *in vitro* polarisation of macrophages to a non-canonical M2 pro-tumorigenic and immunosuppressive state, likely mediated by secreted molecules such as CX3CL1, CCL2, CSF1, LDLR, VEGF and/or Versican.

3. Our tumour studies using Ats1-KO mice confirm the angio-inhibitory properties of stromal ADAMTS1 using both LLC and B16F1 tumour models, although only B16F1 tumours were reduced in absence of the protease.

4. The levels and deposition patterns of the ADAMTS1 substrates Nidogen 1 and Versican in tumours highlight their contribution to vascularisation and immunomodulation, respectively.

5. Our studies unveil an immunomodulatory role of ADAMTS1, mostly based in two sets of approaches. First, ADAMTS1 deficiency in macrophages limits their *in vitro* migration and phagocytosis. Second, Ats1-KO mice show a significant modulation of immune populations in spleen, bone marrow, and tumours.

6. Our RNAseq analyses comparing these tumour models in wild type and Ats1-KO mice disclose the significant implication of biological processes to explain their different behaviours, highlighting the role of versican, collagen structures and type I interferon.

7. Inhibition of ADAMTS1 in tumour cell lines enhances M1 macrophage polarisation *in vitro*, probably mediated by osteopontin, IL33, LDLR and/or Versican. In contrast, ADAMTS1-inhibited LLC tumours have an immunosuppressive environment *in vivo* defined by M2 macrophages and high levels of intact Versican.

8. ADAMTS1 levels do not alter the resistance of LLC tumours to anti-angiogenic therapy. However, depending on whether stromal or tumour ADAMTS1 is inhibited, the resistance is mediated by myeloid-derived suppressor cells or M2 macrophages, respectively. This remarks the necessity to better understand these phenomena to improve current therapies.

CONCLUSIONES

1. Nuestros estudios de RNAseq muestran diferencias significativas en el compartimento extracelular y el ambiente inmune entre los modelos tumorales singénicos Lewis Lung Carcinoma (LLC) y melanoma B16F1.

2. Las células LLC promueven la polarización de macrófagos *in vitro* a un estado pro-tumorigénico e inmunosupresor M2 no canónico, posiblemente mediado por la secreción de CX3CL1, CCL2, CSF1, LDLR, VEGF y/o Versicano.

3. Nuestros estudios en el ratón deficiente para ADAMTS1 (Ats1-KO) confirman las propiedades angio-inhibidoras de la proteasa de origen estromal en ambos modelos, aunque sólo los tumores B16F1 se redujeron en su ausencia.

4. Los niveles y la deposición en tumores de los sustratos de ADAMTS1 Nidógeno 1 y Versicano destacan su contribución en vascularización y modulación inmune, respectivamente.

5. Nuestros estudios demuestran el papel inmunomodulador de ADAMTS1 basado en dos aproximaciones. Por un lado, su deficiencia en macrófagos limita sus capacidades de migración y fagocitosis *in vitro*. Por otro lado, el ratón Ats1-KO muestra una modulación significativa de las poblaciones inmunes en bazo, médula ósea y tumor.

6. Los análisis de RNAseq comparando los dos modelos tumorales en ratones salvajes y Ats1-KO revelan la implicación de procesos biológicos que explican su comportamiento diferencial, destacando el papel del Versicano, la organización de estructuras de colágeno y el interferón tipo I.

7. La inhibición de ADAMTS1 en las líneas celulares promueven la polarización de macrófagos a M1 *in vitro*, probablemente mediada por osteopontina, IL33, LDLR y/o Versicano. Por lo contrario, los tumores generados a partir de células LLC inhibidas para ADAMTS1 muestran un ambiente inmunosupresor *in vivo* debido a un aumento de macrófagos M2 y altos niveles de Versicano.

8. ADAMTS1 no modifica la resistencia de los tumores LLC a terapias anti-angiogénicas. Sin embargo, dicha resistencia es mediada por células supresoras mieloides o macrófagos M2 según si la inhibición de ADAMTS1 es estromal o tumoral. Esto destaca la importancia de comprender a fondo este fenómeno para mejorar las terapias actuales.

MATERIALS AND METHODOLOGY

1. Cell Culture.

1.1. Cell lines and reagents.

Mouse Lewis Lung Carcinoma (LLC) and melanoma B16F1 cells, and human fibrosarcoma HT1080 and Embryonic Kidney 293T (HEK293T) cells were cultured in DMEM (Dulbecco's Modified Eagle's Medium) High Glucose (Biowest, USA) supplemented with 10 % of FBS (fetal bovine serum) (Gibco, USA) and 1 % of penicillin/streptomycin (P/S) (Sigma-Aldrich, USA). All cells were cultured at 37 °C with 5 % of CO_2 and 95 % of relative humidity.

1.2. Adamts1 genetic modification in tumour cells.

1.2.1. Plasmid DNA production.

In order to inhibit ADAMTS1 in the tumour cell lines, short hairpin RNA MISSION system was used (Sigma-Aldrich, USA) (TCRN0000032034, NM_009621.1-2330slcl for *Adamts1* inhibition). For plasmids expansion, supercompetent DH5α cells were transformed by heat-shock with 5 ng of MISSION plasmids and also with the necessary plasmid to construct the lentiviral particles (envelope vector vSVG and packaging vector psPAX2, kindly donated by Dr. P. Menéndez (*Instituto de Investigación Josep Carreras*, Barcelona)). Bacteria were cultured in LB-agar plates with ampicillin 1 mg/mL at 37 °C and colonies were isolated and incubated for 16-18 hours in agitation (220 rpm). Plasmid DNA was obtained using the NucleoSplin plasmid kit (Macherey Nagel, Germany).

1.2.2. Lentiviral transduction to obtain *Adamts1*-inhibited LLC and B16F1 cell lines.

HEK293T cells were used for lentiviral particles production, transfected by calcium chloride ($CaCl_2$) method. For that, $5 \cdot 10^4$ cells were cultured in a 100 mm plate up to optimal confluence (50-80%). 20 µg of the expression vector, 6µg of envelope vector (vSVG) and 15 µg of packaging vector (psPAX2) were mixed in 2M $CaCl_2$ and 2X HBS buffers. After 30 min incubation at RT, the mix was added to HEK293T culture drop by drop while swirling the plate. After 9-14 h of cell incubation, culture media was replaced with 5 mL of fresh media. After 48 h, virus-containing supernatant was collected and centrifuged 5 min at 3000 rpm. After it, supernatant was cleared using a 0.45 µm filter and it was directly used to infect tumour cells or stored at -80 °C.

$2 \cdot 10^6$ cells (LLC or B16F1) were resuspended and incubated with the virus-containing media for 10 min at room temperature (RT). Then, cell suspension was plated in a

100 mm plate adding 9 mL more of fresh media. After overnight incubation, media was renewed. After expansion and passage of the cells (after 4 days, approximately), puromycin-containing media (1 µg/mL) was used for 2 weeks to select the transfected cells (obtaining LLC-shAts1 and B16F1-shAts1 cell lines, respectively). Finally, *Adamts1* inhibition in selected cells was evaluated by quantitative PCR (qPCR) and western blot (WB).

1.2.3. *Adamts1* overexpression in HT1080 cell line.

For *Adamts1* overexpression, HT1080 cells were co-transfected by calcium chloride ($CaCl_2$) method with ADAMTS1 plasmid (kindly provided by Dr. Luisa Iruela-Arispe) in presence of Hygromycin, obtaining HT1080-Ats1 cell line (Casal et al., 2010).

1.3. Adhesion and proliferation assays.

Cell adhesion was studied using pre-coated 96-well plates. Coating included: bovine type I collagen solution (1:30 dilution, 5005-B, Advanced Biomatrix, USA) and fibronectin (FN, FC010-10MG, Merck, USA) 1:30) for 2h at 37°C, performing a final wash with PBS/BSA 1 mg/mL prior to assay. $6 \cdot 10^4$ cells/well were added and incubated for 1 h at 37 °C. Then, media was discarded and wells were washed twice with warm PBS. Attached cells were fixed with 4 % PFA for 5 minutes and stained with Toluidine blue (0.5 % in 4% PFA) for 5 minutes. Toluidine excess was discarded and rinsed three times with tap water. When wells were dried, 100 µl/well of 1 % SDS in H_2O was added and plate was shaken for 10 minutes. Finally, absorbance was measured at the Infinite 200 Pro NanoQuant (Tecan, Switzerland) at 595 nm.

Alternatively, cell adhesion was evaluated together with cell proliferation using E-plates in the xCelligence system (ACEA Biosciences, USA) that offers real-time cell behaviour analyses. These plates are formed by 16 wells with a sheet of microelectrodes that detect cell attachment. When the interaction between cells and the underlying electrode surface takes place, electrodes ability to sense conductive media is blocked. It is reported as cell impedance, modulated by cell number and interaction strength (Figure 75).

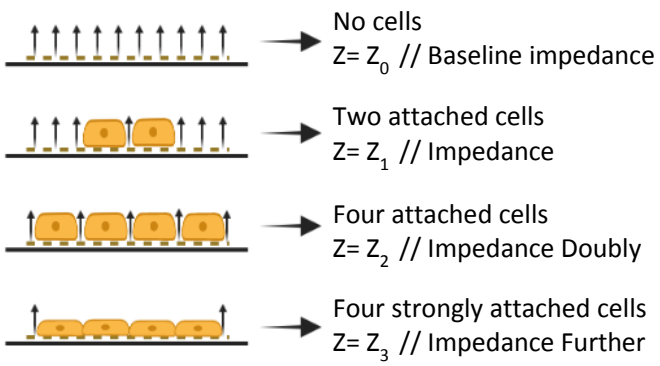

Figure 75. xCELLigence impedance mechanism for measuring cell adhesion and proliferation. Representation of cells adhering to microelectrodes of xCELLigence platform. Impedance is regualted by the number of cells and their attachment and proliferation. [Created in BioRender].

Following manufacturer's instructions, these assays were performed on previously coated wells with a 1:30 Matrigel (BD Bioscience, USA) dilution. Adhesion was considered up to the first 9 hours (including measures every 15 minutes) while proliferation followed from 9 to 70 hours (with measures every hour) since the experiment started. For these experiments the number of tumour cells was $3{\cdot}10^4$ and $4{\cdot}10^4$ cells/well of LLC (and LLC-shAts1) and B16F1 respectively, $1{\cdot}10^4$ and $2{\cdot}10^4$ cell/well of HUVEC and MPAEC respectively, and $4{\cdot}10^4$ cells/well of BMDM.

2. Mouse colony maintenance, genotyping and ethical approval.

C57Bl/6 Wild Type (WT) and Ats1-KO (Shindo et al., 2000) mice were maintained at *Centro de Investigación Biomédica, University of Granada* animal facility. Mice were properly housed on a 12h day/night cycle in sterilised cages, under pathogen-free conditions, and were provided with food and water *ad libitum*. Four weeks after birth, mice were weaned, labelled by ear notch punch, and genotyped with genomic DNA isolated from ears tissue.

For genotyping, Nucleospin tissue kit (Macherey Nagel, Germany) was used to isolate the DNA and qPCR was performed using iQ SYBR Green Supermix (Bio-Rad, USA) during 37 cycles at 60 °C of annealing temperature. WT gene was amplified with primers recognising exons 5 and 6 of murine *Adamts1* gene, generating a DNA product of 333bp. *Adamts1* KO allele was amplified using primers that recognise the PGK-Neo cassette (Figure 76) found in transgenic mice, generating a DNA product of 177bp (Lee et al., 2005). Primer sequences are found in Table 2.

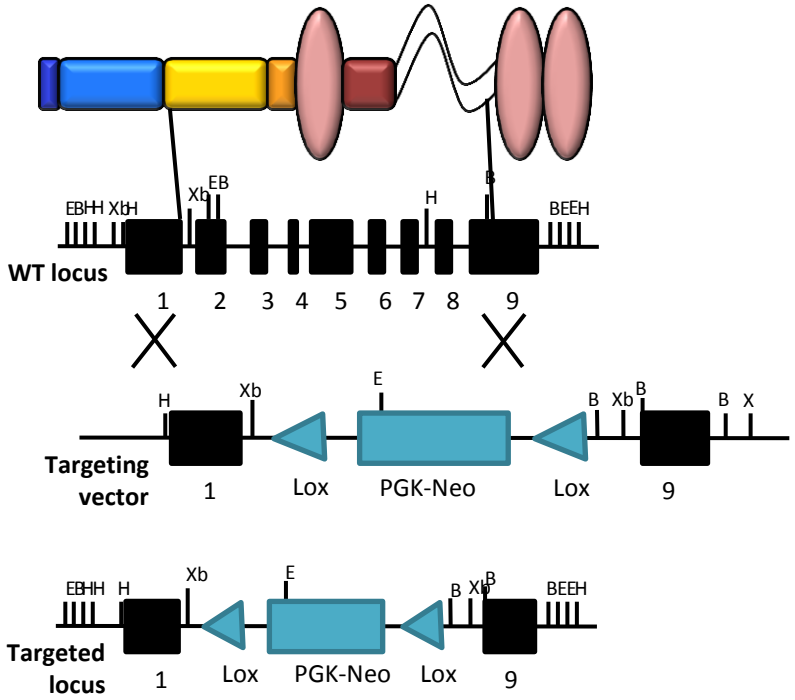

Figure 76. *Adamts1* inactivation by homologous recombination. Schematic diagram of gene targeting strategy to generate Ats1-KO mouse. PGK-Neo cassete was introduced inside *Adamts1* gene and it is used to detected the genetically modified genotype. E, B, H, Xb are sequences that recognise the different digestion enzimes.

All animals were handled and sacrificed according to ethical guidelines internationally accepted and established by the Approved Ethical Committee 152-CEEA-OH-2016.

3. Isolation, culture and in vitro assays with bone marrow (BM) and bone marrow-derived macrophages (BMDM).

These cells were isolated from WT and Ats1-KO mice, properly sacrificed according to healthcare guidelines. Tibia and femur of both legs were taken and, to obtain bone marrow (BM) cell suspension, they were flushed with 5mL of PBS using a 23G syringe. Suspension was filtered through a 100 µm cell strainer and centrifuged for 5 min at 300 g. Cell pellet was resuspended in 5 mL of Red Blood Cell Lysis Buffer (RBC) (150 mM NH_4Cl, 10 mM $KHCO_3$, 0.1 mM Na_2 EDTA, pH 7.2-7.4) and incubated 4 min at RT. Cell suspension was centrifuged for 10 min at 200 g, and cells were resuspended in PBS. BM cells were cultured at a concentration of $4{\cdot}10^5$ cells/mL in 100 mm non-treated plates with 10 mL of Selection medium (DMEM low glucose with 20 % of

heat-inactivated FBS, 2 % of P/S and 20 ng/mL of M-CSF (Peprotech, USA)). Macrophages (BMDM) were selected by their adherence properties after 7 days. At day 4 post-seeding, culture media was refreshed adding 4 mL of fresh selection media. At day 7, culture media and non-attached cells were discarded and selected macrophages were detached with 5 mL of 4mM EDTA for 10 min. BMDM enrichment and purity were evaluated by flow cytometry with CD11b antibody (see Table 3).

3.1. *In vitro* BMDM polarisation.

$3 \cdot 10^5$ BMDM cells/well were seeded in 24-well tissue plates in 500 µL of media according to experimental requirements. As controls during polarisation assays, the following media containing different cytokines were used: i) BMDM-MØ media as negative control of polarisation (DMEM low glucose, 10 % of heat-inactivated FBS, 1 % of P/S, 20 ng/mL of M-CSF); ii) BMDM-M1 media (BMDM-MØ media supplemented with 20n g/mL IFNɣ (Peprotech, USA) and 100 ng/ml LPS) for classically activated macrophages (M1); iii) BMDM-M2 media (BMDM-MØ media supplemented with 20 ng/ml IL-4 (Peprotech, USA)) for alternatively activated macrophages (M2) (Figure 77).

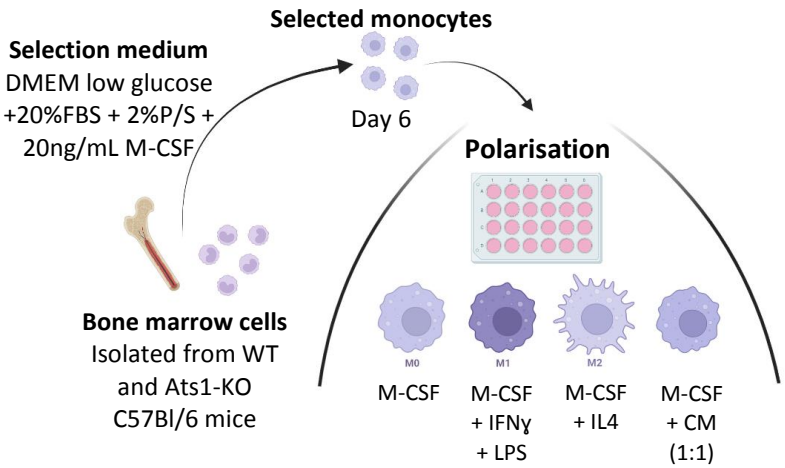

Figure 77. BMDM polarisation protocol. Schematic representation of BMDM selection and polarisation *in vitro*. Bone marrow cells are obtanied by flushing mouse femur and tibia and monocytes are selected during 6 day by M-CSF. After selection, cells are cultured with different cytokines to polarise macrophages to M0, M1 and M2 or with CM of tumour cells. [Created in BioRender].

To evaluate how the secretome of tumours cells affects polarisation of BMDM, fresh 24-hour conditioned medium (CM) from tumour cell lines was collected and used the

same day that BMDM were detached. These media were filtered using a 0.2 µm filter to remove floating cells and cell debris. For these polarisation experiments, BMDM were cultured in a ratio of 1:1 of double-BMDM-MØ media (DMEM low glucose with 20 % of heat-inactivated FBS, 2 % of P/S and 40 ng/mL of M-CSF) and CM (Figure 77). After 24 h, BMDM were detached and analysed by FC and RNA expression, as described later.

3.2. *In vitro* migration of BMDM in transwell.

To achieve the migration activity of WT and Ats1-KO macrophages, BMDM isolated from these mice were detached and cultured on 24-well 6.5 mm Transwell® with 8.0 µm Pore Polycarbonate Membrane Inserts (Corning, USA). $5{\cdot}10^4$ macrophages were added to the upper side of the membrane in 100 µL of media. Then, 600 µL of media with or without chemoattractant were added to the well. Negative control media (without chemoattractant) contained DMEM low glucose with 20 ng/mL M-CSF, while positive control (with chemoattractant) was prepared with DMEM low glucose, 20 ng/mL M-CSF and 10 % FBS. Cells were let to migrate for 24 hours (Figure 78). Later, migrated macrophages on the lower side of the insert were properly stained.

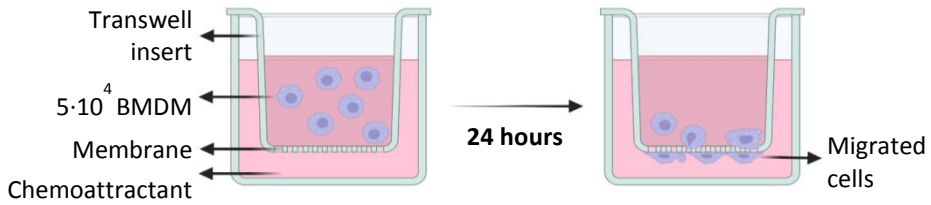

Figure 78. Transwell migration experiment. Schematic representation of migration experiment. WT and Ats1-KO BMDM were cultured on the transwell in order to migrate to the chemoattractant (FBS). After 24 hours, migrated cells were stained and counted. [Created in BioRender].

For the staining, inserts were washed once with PBS and cells were fixed with cold absolute methanol for 10 minutes at RT. Inserts were air dried for 10 minutes and stained with 0.2 % crystal violet in a 20 % methanol solution for 10 minutes at RT. Non-migrated cells were removed from the upper side of the membrane with a cotton swab, and inserts were washed twice with PBS for 5 minutes in gentle agitation, removing such non-migrated cells. Next, inserts were air dried for 10 minutes. To visualise the cells, inserts were plated on µ-Slide 8 well chambered coverslips (ibidi, Germany) and pictures were taken on a PALM Microbeam Laser Microdissection system (Zeiss, Germany). 4-6 pictures were taken of each membrane and migrated macrophages were counted using ImageJ software (NIH, USA). For each

WT and Ats1-KO group, average of migrated cells was calculated and relative migration was computed comparing positive control (with chemoattractant) *versus* negative control (without chemoattractant).

3.3. *In vitro* phagocytosis of cancer cells by BMDM.

Phagocytosis experiments (adapted from (Nam et al., 2019)) were performed using WT and Ats1-KO BMDM. Using 24-well tissue plates, $3{\cdot}10^5$ BMDM-MØ cells/well in 500 µL were seeded the day prior to starting the phagocytosis assay. The next day, tumour cells (LLC, B16F1, HT1080 and HT1080-Ats1) were labelled with the fluorescent dye carboxyfluorescein diacetate succinimidyl ester (CFSE) in PBS following manufacturer's instruction and concentration. In order to avoid CFSE toxicity, staining was performed in presence of 2 % FBS. Then, these tumour cells were added to the BMDM culture in a ratio of 1:2 (BMDM : tumour cells) in 500 µL of BMDM-MØ medium. After 2.5 hours of incubation, cells were collected and analysed by flow cytometry (Figure 79). CD11b label was used to detect BMDM among the whole cell suspension.

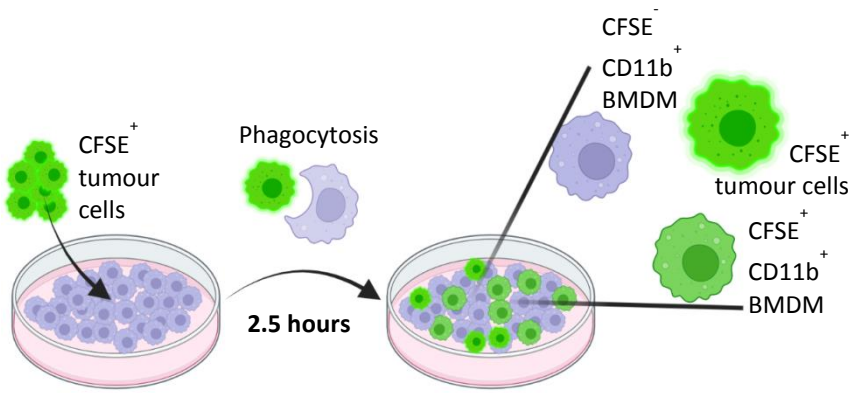

Figure 79. Phagocytosis of tumour cells by macrophages. Representation of engulfment of tumour cells mediated by macrophages. CFSE-labelled tumour cells were added to BMDM culture and phagocytosis was measured after 2.5 hours by FC thanks to the fluorescent dye. [Created in BioRender].

Phagocytosis was calculated as the percentage of $CFSE^+/CD11b^+$ cells (BMDM which have engulfed tumour cells) according to the formula (Nam et al., 2019):

$$Phagocytosis\ \% = \frac{CFSEpositive\ CD11bpositive\ cells}{Total\ CD11bpositive\ cells} \times 100$$

3.4. *In vitro* BMDM apoptosis assay induced by clodronate liposomes.

Clodronate liposomes have been extensively used *in vivo* to deplete macrophages since clodronate is toxic and those cells (mostly macrophages). After internalisation of the liposomes due to their phagocytic activity, they will die (Rooijen & Sanders, 1994). Indeed, they can be used *in vitro* to measure the phagocytosis ability of the macrophages in culture. Accordingly, $3 \cdot 10^5$ WT and Ats1-KO BMDM cells/well were seeded in 24-well tissue plates in 500 µL of BMDM-MØ the day before starting the treatment. The next day, media was replaced by new one containing liposomes (PBS and clodronate liposomes, purchased from Liposoma BV (Netherlands). The experimental groups are: i) no liposomes, ii) PBS liposomes (1:2000 dilution), and iii) - iv) clodronate liposomes (1:20000 and 1:2000 dilutions). After 24 hours of treatment, cells were collected and analysed by FC for Annexin V (apoptosis marker) and 7-amino-actinomycin D (7AAD) solution (death marker). Each sample was incubated 5 minutes at RT with 100 µL of 1X binding buffer with 2 µL of Annexin V and 2 µL of 7AAD (PE Annexin V Apoptosis Detection Kit I, 559763, BD Bioscience, USA).

4. Syngeneic tumour assays.

Subcutaneous (s.c.) tumours were generated injecting the tumour cell lines (LLC, LLC-shAts1 and B16F1) in the right flank of both WT and Ats1-KO mice. $2.5 \cdot 10^5$ cells were injected in the case of LLC and LLC-shAts1 cell lines, while $5 \cdot 10^5$ cells were injected to obtain B16F1 tumours, always in 100µL of PBS. Mouse weight and tumour size were monitored twice per week since cell inoculation. All animals were sacrificed following healthcare guidelines. At ending-point, mouse weight was measured and tumours were dissected for further analyses. Tumour weight was noted, and tumour dimensions were measured with a digital calliper (length (L), width (W) and height (H)). To calculate tumour volume while the tumour progressed in the tumour-bearing mouse, H dimension was considered as the smallest dimension between L and W, following the formula (Tomayko & Reynolds, 1989):

$$\text{Tumour volume} = \frac{\pi}{6} \text{ x L x W x H}$$

When possible, whole tumour was divided into pieces for different analyses, such as flow cytometry (FC), RNA isolation, immunohistochemistry (IHC) and protein extraction.

In various experiments, spleen and bone marrow were also taken. In the case of spleens, they were weighted, photographed and divided for FC, RNA isolation and IHC. Spleen ratio was calculated using the following formula (Turcotte et al., 2004):

$$Spleen\ index = \frac{\sqrt{(spleen\ weigth)} \times 100}{body\ weight}$$

In the case of bone marrow, femur and tibia from each mouse were obtained and processed as described above (part 3).

For assays including Aflibercept therapy, intraperitoneal (i.p.) administration of the drug started when tumours reached 50mm^3 of volume (between 2 and 3 weeks after cell inoculation). Aflibercept treatment consisted on 2 doses (25 mg/kg) per week during 2 weeks (4 doses in total). Two weeks after the start of the treatment, mice were euthanized (Figure 80)

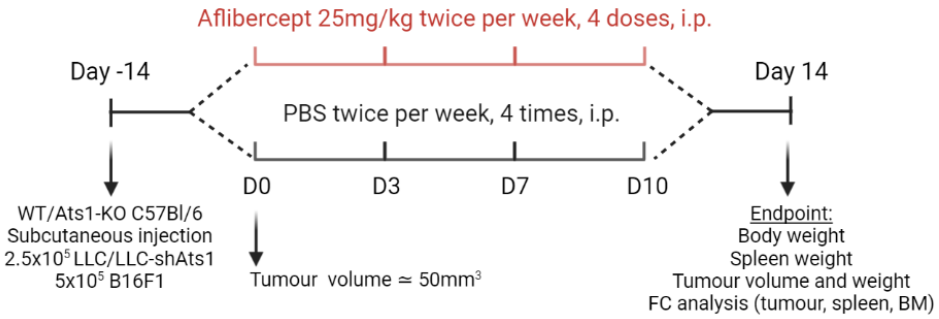

Figure 80. Aflibercept treatment scheme *in vivo*. Experimental design of Aflibercept treatment of LLC/LLC-shAts1/B16F1 tumour-bearing mice. [Created in BioRender].

In mice, macrophage depletion was approached by treatment with clodronate liposomes (Rooijen & Sanders, 1994). WT and Ats1-KO C57Bl/6 mice were subcutaneously injected in the right flank with LLC tumour cells as described above. At the same time, an initial dose of 200 µL of PBS or clodronate liposomes was intraperitoneally injected. Then, in order to avoid macrophage repopulation, 5 injections of 100 µL each were delivered every three days (Ding et al., 2015). At day 17 from cell inoculation (2 days after last liposome injection), mice were sacrificed and macrophage depletion was assessed by flow cytometry of spleen and tumours using both CD11b and F4/80 markers (Figure 81).

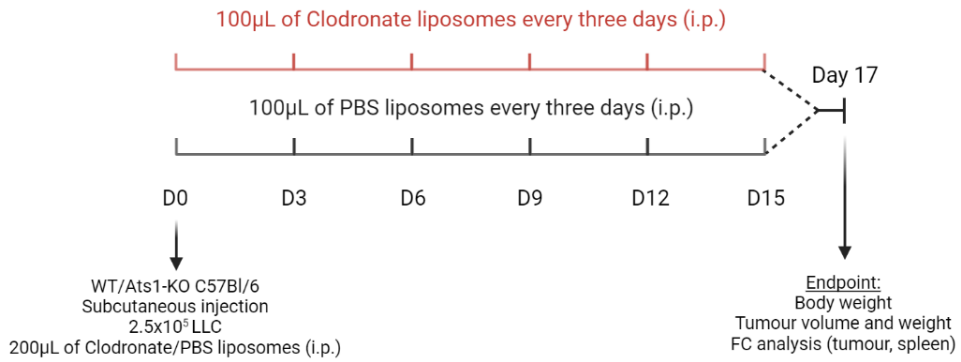

Figure 81. Clodronate liposomes treatment scheme *in vivo*. Experimental design of macrophage depletion by clodronate liposomes of LLC tumour-bearing mice. [Created in BioRender].

5. Flow cytometry (FC) analyses

Depending on the type of sample, different procedures were performed. For cell culture, cells were trypsinized for 5 min at 37 °C and washed once with media before starting the staining protocol. For spleens, half of the organ was kept in 1 mL of fresh 0.1 % type I collagenase in PBS (Gibco, USA) at sacrifice time. Then, tissue was mechanically disrupted with a plastic plunger of a 5 mL syringe on a petri-dish plate. Then, solution was passed through a 70 µm cell strainer. In the case of tumour samples, they were kept in fresh RPMI-1640 medium with 10 % FBS on ice. For its mechanical disruption, tissue was cut with curve scissors on a petri-dish plate until pâté-like consistency was obtained. Once both spleen and tumours tissues were mechanically disrupted, enzymatic digestion took place. Samples were incubated in 2-10 mL of collagenase depending on sample size for 1h at 37 °C in the water bath, shaking every 10 minutes. After incubation, cell suspension was passed through a 5 mL syringe with a 19.5 G needle 3-4 times and cleared through a 70 µm filter. Cell suspension was centrifuged for 5 min at 300 g and cells were resuspended with 5 ml of RBC buffer. After 4 min incubation at RT, cell suspension was centrifuged 10 min at 200 g and cells were resuspended in PBS for counting them. Finally, BM samples were obtained as it was explained in part 3 of this material and methods section.

For FC staining of tumour cell culture, spleen, tumour and BM, $1 \cdot 10^6$ cells were used for each staining. In the case of BMDM polarisation, all the cells from one well were used for each staining. First, CD16/32 blocking solution (2.4G2, 1:100, 553142, BD Bioscience, USA) and eBioscience™ 7-amino-actinomycin D (7AAD) solution (1:100, eBioscience, 00-6993-50, USA) were added to the cell suspension to reduce background and identify dead cells (step not required in the case of tumour cells).

After 5 min incubation on ice, conjugated antibodies were added and incubated for 25 min on ice. Wash steps and antibody media preparation were performed with FC buffer (PBS, 1 % FBS and 2 mM EDTA). After incubation, cells were centrifuged for 5min at 300 g, resuspended in FC buffer and analysed using a FacsCanto II (BD Bioscience, USA). In the case of intracellular NOS2 staining, fixation and permeabilization were performed after surface antigens staining following manufacturer protocol (Fix&Perm® Cell fixation and permeabilization kit, GAS-002, Nordic MUbio, Netherlands). The used antibodies are found in Table 3.

6. Immunofluorescence (IF).

6.1. BMDM coverslips and Phalloidin staining.

In order to characterize the structure and morphology of cultured polarised macrophages, polarisation protocol was performed on glass coverslips coated with 5 $\mu g/cm^2$ fibronectin for 1 hour at 37 °C. After 24 h of polarisation, coverslips were washed once with PBS for 5 min while shaking and then fixed in 4 % of paraformaldehyde (PFA) in PBS for 20 min at RT and agitation. After it, cells were permeabilized with 0.1 % Triton X-100 for 10 min and washed twice with PBS-Tween. Then, samples were blocked using a 3 % BSA with 1 % secondary antibody host serum solution in PBS-Tween for 1 h at RT. Next, coverslips were washed three times with PBS-Tween and incubated overnight at 4 °C with primary antibodies against α-tubulin in 1 % BSA with 1 % secondary antibody host serum in PBS-Tween. After washing three times with PBS-Tween, incubation with secondary antibody together with Phalloidin-TRITC (1:400, Sigma-Aldrich, USA) was done for 1 h at RT (in 1%BSA with 1 % secondary antibody host serum in PBS-Tween). Finally, coverslips were washed and stained with final mounting using DAPI with Mowiol mounting medium including 1,4-Diazabicyclo(2,2,2)octane (DABCO, Sigma-Aldrich, USA). Confocal images were taken in a LSM710 confocal microscopy (Zeiss, Germany) at 63X magnification.

6.2. Fixed tissues.

Tumour and spleen samples were fixed in 4 % of formaldehyde for 12 h at RT, dehydrated and embedded in paraffin. For staining, 5 µm sections were deparaffinizated and properly rehydrated. Then, heat-based antigen retrieval was carried out in Tris-HCl Buffer (0.5 M, pH 10) for 10 min in a microwave at 650 W. Sections were allowed to reach RT during 30 min. After a 5-minute-wash with PBS-Tween-20 0.05 % (PBS-Tween), sections were blocked with 3 % bovine serum albumin (BSA) and 1 % secondary antibody host serum in PBS-Tween for 1 h at RT. These sections were washed three times in PBS-Tween for 5 min and incubated

overnight at 4 °C with the primary antibodies in 1 % BSA with 1 % secondary antibody host serum in PBS-Tween. Then, sections were washed again three times as previously detailed and were incubated with the secondary antibodies for 1 h at RT (in 1 % BSA with 1 % secondary antibody host serum in PBS-Tween). After it, sections were washed three times for 10 min in DBPS-Tween and cell nuclei were stained with DAPI (4', 6-diamidine-2-fenilindol, 0.5 µg/mL in PBS) for 5 min at RT. Then, a final wash was done with PBS for 5 min at RT, and slides were mounted with Mowiol with DABCO. The antibodies used in these analyses are found in Table 3. Confocal images were taken using a LSM710 confocal microscopy (Zeiss, Germany) at 63X magnification.

7. Vasculature quantification.

Endomucin-stained tumour sections (immunofluorescence section) images were taken at 10X magnification in the AxioImager A.1 microscope (Zeiss, Germany). Morphometric analyses were performed using 8 bits grey images and ImageJ software following the methodology described (Rodríguez-Baena, *et al.*, 2018). For every set of pictures, threshold and particle size were established in order to identify real staining and background pixels. Further processing of the data gave information regarding vessel density (number of vessels per area), vessel perimeter and vessel area (percentage of area occupied by vessels respect to the total area of the tissue).

8. RNA isolation, complementary DNA (cDNA) synthesis and quantitative PCR (qPCR).

Tumour or spleen frozen tissue fragments were submitted to physical disruption on 2 mL tubes with a metallic bead on TissueLyser LT (Qiagen, Netherlands) for 1 min at 50 oscillation/sec. RNA from cell lines and tissue was isolated using the RNAII Nucleospin kit (Macherey-Nagel, Germany) and quantified with a NanoDrop 2000 (ThermoScientific, USA). To evaluate quality, 400 ng of isolated RNA were loaded in a 0.7 % agarose gel in TAE buffer (tris base, acetic acid and EDTA). After running the electrophoresis, the proper presence and ratio of both 28S and 18S ribosomal RNA isoforms indicated good quality.

cDNA was obtained from 200 to 1000 ng of RNA using the iScript cDNA kit (Bio-Rad, USA), and qPCR was performed with 5 ng of cDNA per reaction using Fast SybrGreen. To run the reactions, 7900HT and QuantStudio 6 Flex Real-Time PCR systems (Applied Biosystems, USA) were used. qPCR data are represented as $2^{-\Delta\Delta Ct}$ using different endogenous controls (actin, 18S or GAPDH) to normalize, and showing mean and

standard error of the mean (SEM). Primers used for this purpose are included in Table 2.

9. RNAseq and data processing.

RNA sequencing was performed in several samples throughout the project. In all the cases, RNA quantity and purity was measured using Agilent 2100 BioAnalyzer (Agilent, USA). Then, 500-2000ng of total RNA with RIN values > 8.6 were used for RNA sequencing using different platforms.

In the case of mouse tumours, B16F1-WT and B16F1-Ats1-KO samples (3 samples of each group) were sequenced at Genomics Unit at GENyO (Granada). Libraries were prepared using the TruSeq Stranded mRNA Library Prep Kit (Illumina, USA) according to the manufacturer's protocol, which captures poly-adenylated RNA by transcription by oligo-dT primer. Then RNA is fragmented and cDNA was synthesized. Next, 3'ends were adenylated, adapters and barcodes were ligated, and finally it is enriched by PCR. Adapters and samples codes (index-barcodes) are added to the libraries to sequence them simultaneously. Then, mRNA libraries quality was assessed using High Sensitivity DNA Bioanalyzer Chip (Agilent, USA) and sequenced on the NextSeq500 platform (Illumina, USA) using the 150bp paired reading kit and a depth of 17-25 million reads for each sample.

For LLC-WT and LLC-Ats1-KO tumours (3 samples of each group), RNA sequencing was performed at Genomics Unit at Centre de Regulació Genòmica (CRG, Barcelona). Libraries were prepared using the TrueSeq Stranded mRNA Library Prep Kit (Illumina, USA) according to the manufacturer's protocol. Next, RNA was fragmented and cDNA was synthesized using reverse transcriptase (SuperScript II, Invitrogen, USA) and random primers. Next, 3'ends were adenylated, adapters and barcodes were ligated, and finally it is enriched by PCR. Then, library quality was assessed using a Bioanalyzer DNA 1000 (Agilent, USA) or a Frament Analyzer Standard Sensitivity (Agilent, USA) and quantified (KAPPA library quantification kit, Roche, USA). Sequencing was performed on a NextSeq2000 platform (Illumina, USA) with a paired end read length of 50bp and a depth of 35-45 million reads for each sample.

For the transcriptome and gene signature comparison between tumour models (B16F1-WT, B16F1-Ats1-KO, LLC-WT and LLC-Ats1-KO), we used RSEM software (B. Li & Dewey, 2011) to quantify transcript expression with the mouse reference from the UCSC Genome Browser. Raw counts obtained were analysed using R software (version 4.1.3). First the counts were filtered using filtered.data function from

NOISeq package and normalised with TMM method (Robinson & Oshlack, 2010). Due to the difference sequencing methodology and in order to avoid "batch effect" in the comparison between different groups, normalised values from both datasets (B16F1-WT/ B16F1-KO and LLC-WT/LLC-Ats1-KO) were merged and we corrected batch effects with removeBatchEffect function from the limma package.

Using differentially expressed genes with p-value<0.05, gene signature heatmaps of each comparison were done using scaled gene values after normalisation of the homolog genes between human and mouse. The information about the homology was obtained from BioMart using the biomaRt R package, filtering out those genes with more than one homolog gene. Genes included in each signature (angiogenesis, inflammatory response and matrisome) are found in Table 4. Those genes were selected according to Gene Set Enrichment Analysis (GSEA) specific signatures. For Gene Ontology (GO) enrichment, differentially expressed genes from the whole transcriptome and specific signatures were used. Genes included in each GO enrichment of each comparison are found in Tables 5-8. Top five GO terms of each comparison were selected according to p-value<0.05 (in B16F1 *versus* LLC comparison) or adj. p-value<0.05 (in WT *versus* Ats1-KO comparison). –Log(p-value/adj. p-value) was represented. As supplementary information, top 5 GO terms of each comparison are found in Tables 9-12.

For BMDM-derived samples, RNAs from M0, M2, LLC-CM and B16F1-CM BMDM conditions (3 samples of each group) were sequenced after polydT-mediated cDNA synthesis using Illumina's random priming NEBNext RNA Library Preparation Kit. Library quality was assessed using a Frament Analyzer (Agilent, USA) and quantified (KAPPA library quantification kit, Roche, USA). Sequencing was performed on a HiSeq1500 platform (Illumina, USA) with a read length of 50bp and sequenced reads were aligned to *mus musculus* mm9 using STAR (Dobin et al., 2013). Uniquely aligned reads were quantified at exons of annotated genes and normalised with TMM method. Then, prcompt function was applied to count data in order to perform a principal component analysis (PCA) and visualise the first two principal components. In the case of MA-plot, it was done after applying differential expression analysis with DESeq2 package, comparing LLC and B16F1 group.

10. Western Blot (WB).

CM from the different cell lines was analysed. To obtain it, cells were grown up to reaching 80 % of confluence and medium was changed to serum-free medium. After 24 h on incubation, CM was collected, clarified and concentrated with StrataClean

resin (400714, Agilent, USA). After it, resin was resuspended in Laemmli buffer with β-mercaptoethanol for protein denaturalization. Prior to SDS-PAGE, the desired amount of protein was denaturalized with Laemmli buffer containing β-mercaptoethanol.

All samples were heat-shocked during 5 min at 100 °C and resolved by sodium dodecyl sulphate polyacrylamide gel electrophoresis (SDS-PAGE) using a 10 % of polyacrylamide gel. Then, proteins were transferred to methanol-activated polyvinylidene difluoride (PVDF) membranes (Bio-Rad, USA). In order to check whether the transfer worked properly, and to detect the amount of protein in the CM, PVDF membranes were stained with 0.1 % Red Ponceau (Sigma Aldrich, USA) in 5% acetic acid. Membranes were blocked with 5 % low-fat milk for 1 h at RT and incubated overnight at 4 °C with the primary antibodies (found in Table 3). Following, membranes were incubated 1 h at RT with horseradish peroxidase (HRP)-conjugated secondary antibodies and signal was detected using the ECL Prime Western Blotting Detection Reagent (GE Healthcare LifeScience, USA). Images were captured in the ImageQuant LAS 4000 mini (GE Healthcare LifeScience, USA).

10.1. Versican WB.

Due to the singular nature of versican, its size and post-translational modifications, protein isolation from CM and detection protocol differs from the one previously exposed. In this case, CM (resin-concentrated as previously showed), were treated for 1 h at 37 °C in the shaker with gentle agitation with 5 U/mL Chondroitinase ABC (Sigma-Aldrich, USA), chondroitinase buffer (180 mM Tris, 216 mM sodium acetate) and 200 µg/mL ovomucoid (Sigma-Aldrich, USA). After the treatment, Laemmli buffer with β-mercaptoethanol was added and samples were heated for 10 min at 100 °C. Finally, proteins were resolved in 4-20 % Mini-PROTEAN® TGX™ Precast protein gels (Bio-Rad, USA). The primary antibody is the polyclonal rabbit anti-Versican GAGβ domain (AB1033, Millipore, USA) to recognise full-length VCAN.

11. Proteome profiler cytokine array.

Secretome of various cell lines was evaluated using the Proteome Profiler Mouse XL Cytokine Array (ARY028, R&D, USA), which allows to measure the levels of 111 cytokines, chemokines and grow factors at the same time. Following manufacturer indications, 24-hour fresh CM from cells was collected and particles were removed by centrifugation. 400 µL of each CM were used for the array. Nitrocellulose membranes containing control and capture antibodies spotted in duplicate (as provided in the kit)

were first blocked for one hour and incubated with the CM overnight at 4 °C in a rocking platform. After washing, Detection Antibody Cocktail was incubated for 1 hour at RT in a rocking platform, followed by 30 min incubation with Streptavidin-HRP. Finally, membranes were incubated for 1 min with Chemi Reagent Mix and signal was detected in the ImageQuant LAS 4000 mini (GE Healthcare LifeScience, USA).

For quantification of the signal, pictures of membranes were analysed using the Protein Array Tool for Math Works (Danny Allen 2021. Protein Array Tool, MATALAB Central File Exchange. Retrieved June 18, 2021). Signal intensity was calculated according to the reference spots, and mean intensity of duplicate spots for each molecule was compared between the different membranes. For further analyses, only molecules with greater differences than 15 % were considered.

12. Statistical analysis

Statistical analyses were performed with GraphPad Prism 6.0 software (GraphPad software Inc., USA) with studies of median and outliers in all sample cohorts by Tukey's test prior to two-tailed *t* Student tests. *P value*>0.05 was considered as statistically significant. All data was expressed as mean ± SEM.

Table 2. List of primers used for different purposes.

Gene	Specie	Forward	Reverse	Group
Adamts1	Mouse	CAAGTGCGTGAACAAGACAGACA	GTATTGAACTCCACCACCACAG	**Genotyping**
PGK-Neo	-	TGAATGAACTGCAGGACGAG	TGAATGAACTGCAGGACGAG	
Cdh5	Mouse	TTACTCAATCCACATACACATTTTCG	GCATGATGCTGTACTTGGTCATC	**Endothelial-related genes**
Cd31	Mouse	TCCAGGTGTGCGAAATGCT	TGGCAGCTGATGCCTATGG	
Endoglin	Mouse	TCGATAGCAGCACTGGATGAC	AGCTTCTGGCAAGCACAAGAA	
Adamts1	Mouse	CTGGCAGAAACAACACAACAG	TGAATTGGGCCATGTGTTTAAC	**ECM-related genes**
Adamts4	Mouse	CAGACGAAGCACTCACCTT	CCAGCCTGAGGAACATTGA	
Adamts9	Mouse	GCCTGTGCTACCTTACCTAAAC	CCACAAGTCACGGAACAAGAG	
Nidogen 1	Mouse	CGGTCTATGTCACCACAAATGGTA	AGGTTCCGGGATGGTATTCTGT	
Versican	Mouse	CTTTGCTCATCGACGCACAT	TGTCATTGAGGCCGATCCA	
Arg1	Mouse	CCGATTCACCTGAGCTTTGA	AAAGGAGCCCTGTCTTGTAAAT	**Immune system genes**
Cd3	Mouse	CAGTCAAGAGCTTCAGACAAG	GATGGCTGTACTGGTCATATTC	
Cd4	Mouse	GAGTTCCCAGAAGAAGATCAC	AAGGCGAACCTCCTCTAA	
Cd8	Mouse	CCATGAGGGACACGAATAATAA	GAGTTCACTTTCTGAAGGACTG	
Cd11b	Mouse	GCAGCACTGAGATCCTGTTTA	CTCCACTTTGGTCTCTGTCTTAG	
Cd163	Mouse	GAGGAAACTGTAAGTCGCTGAA	ACGGCACTCTTGGTTTGT	
Cd206	Mouse	TATGGCAACAGACAAGAGAAG	GGAGTACATGGCTTCATATCC	
FoxP3	Mouse	CAATAGTTCCTTCCCAGAGTTC	TCGGATAAGGGTGGCATAG	
Gr1	Mouse	TATTGTGGACTCTCACAGAAGC	GTCTTCACGTTGACAGCATTAC	
Il6	Mouse	AGGAGACTTCACAGAGGATACC	GAATTGCCATTGCACAACTCTT	
Nos2	Mouse	CTTGGTGAAAGTGGTGTTCTTTG	TCAGACTTCCCTGTCTCAGTAG	
Tnfα	Mouse	GCCTCCCTCTCATCAGTTCTAT	CACTTGGTGGTGGTTTGCTACGA	

Table 3. **List of antibodies used for WB, IF and/or FC.**

Protein	Antibody	Application
ADAMTS1	Monoclonal mouse anti-human ADAMTS1 (AF5867, R&D, USA)	WB
CD11b	Monoclonal APC rat anti-mouse CD11b (553312 BD Bioscience, USA)	FC
CD206	Monoclonal PE rat anti-mouse CD206 (141706, Biolegend, USA)	FC
CD3e	Monoclonal PE Arm. hamster anti-mouse CD3e (12-0031, eBioscience, USA)	FC
CD45R-B220	Monoclonal FITC rat anti-mouse/human CD45R/B220 (11-0452, eBioscience, USA)	FC
Endomucin	Monoclonal rat anti-mouse Endomucin (SC65495, SCBT, USA)	IF
F4/80	Monoclonal PE rat anti-mouse F4/80 (123110, Biolegend, USA)	FC
Gr1	Monoclonal FITC rat anti-mouse Gr1 (130-102-338, Miltenyi Biotech, Germany)	FC
NID1	Polyclonal goat anti-human NID1 (AF2570, R&D, USA)	IF/WB
NOS2	Monoclonal PE-eFluor 610 rat anti-mouse iNOS (61-5920-80, eBioscience, USA)	FC
Tubulin	Polyclonal rabbit anti-mouse α-Tubulin (sc-5546, SCBT, USA)	IF
SMA	Monoclonal Cy3 mouse anti-mouse SMA (C6198, Sigma-Aldrich, USA)	IF
VERSICAN V1	Polyclonal rabbit anti-mouse Versican GAGβ domain (AB1033, Millipore, USA)	IF/WB

APPENDICES

Table 4. Genes included in specific signatures. List of human genes included in each gene signature, extracted from Gene Set Enrichment Analysis database.

Matrisome (1026 genes)					
A2M	A2ML1	ABI3BP	ACAN	ADAM10	ADAM11
ADAM12	ADAM15	ADAM17	ADAM18	ADAM19	ADAM2
ADAM20	ADAM21	ADAM22	ADAM23	ADAM28	ADAM29
ADAM30	ADAM32	ADAM33	ADAM7	ADAM8	ADAM9
ADAMDEC1	ADAMTS1	ADAMTS10	ADAMTS12	ADAMTS13	ADAMTS14
ADAMTS15	ADAMTS16	ADAMTS17	ADAMTS18	ADAMTS19	ADAMTS2
ADAMTS20	ADAMTS3	ADAMTS4	ADAMTS5	ADAMTS6	ADAMTS7
ADAMTS8	ADAMTS9	ADAMTSL1	ADAMTSL2	ADAMTSL3	ADAMTSL4
ADAMTSL5	ADIPOQ	AEBP1	AGRN	AGT	AMBN
AMBP	AMELX	AMELY	AMH	ANGPT1	ANGPT2
ANGPT4	ANGPTL1	ANGPTL2	ANGPTL3	ANGPTL4	ANGPTL5
ANGPTL6	ANGPTL7	ANOS1	ANXA1	ANXA10	ANXA11
ANXA13	ANXA2	ANXA3	ANXA4	ANXA5	ANXA6
ANXA7	ANXA8	ANXA8L1	ANXA9	AREG	ARTN
ASPN	ASTL	BCAN	BDNF	BGLAP	BGN
BMP1	BMP10	BMP15	BMP2	BMP3	BMP4
BMP5	BMP6	BMP7	BMP8A	BMP8B	BMPER
BRINP2	BRINP3	BSPH1	BTC	C17orf58	C1QA
C1QB	C1QC	C1QL1	C1QL2	C1QL3	C1QL4
C1QTNF1	C1QTNF2	C1QTNF3	C1QTNF4	C1QTNF5	C1QTNF6
C1QTNF7	C1QTNF8	C1QTNF9	C1QTNF9B	CBLN1	CBLN2
CBLN3	CBLN4	CCBE1	CCL1	CCL11	CCL13
CCL14	CCL15	CCL16	CCL17	CCL18	CCL19
CCL2	CCL20	CCL21	CCL22	CCL23	CCL24
CCL25	CCL26	CCL27	CCL28	CCL3	CCL3L3
CCL4	CCL4L2	CCL5	CCL7	CCL8	CCN1
CCN2	CCN3	CCN4	CCN5	CCN6	CD109
CD209	CDCP2	CELA1	CELA2A	CELA2B	CELA3A
CELA3B	CFC1	CFC1B	CHAD	CHADL	CHRD
CHRDL1	CHRDL2	CILP	CILP2	CLC	CLCF1
CLEC10A	CLEC11A	CLEC12A	CLEC12B	CLEC14A	CLEC17A
CLEC18A	CLEC18B	CLEC18C	CLEC19A	CLEC1A	CLEC1B
CLEC2A	CLEC2B	CLEC2D	CLEC2L	CLEC3A	CLEC3B

Matrisome (1026 genes)					
CLEC4A	CLEC4C	CLEC4D	CLEC4E	CLEC4F	CLEC4G
CLEC4M	CLEC5A	CLEC6A	CLEC7A	CLEC9A	CNTF
COCH	COL10A1	COL11A1	COL11A2	COL12A1	COL13A1
COL14A1	COL15A1	COL16A1	COL17A1	COL18A1	COL19A1
COL1A1	COL1A2	COL20A1	COL21A1	COL22A1	COL23A1
COL24A1	COL25A1	COL26A1	COL27A1	COL28A1	COL2A1
COL3A1	COL4A1	COL4A2	COL4A3	COL4A4	COL4A5
COL4A6	COL5A1	COL5A2	COL5A3	COL6A1	COL6A2
COL6A3	COL6A5	COL6A6	COL7A1	COL8A1	COL8A2
COL9A1	COL9A2	COL9A3	COLEC10	COLEC11	COLEC12
COLQ	COMP	CPAMD8	CPN2	CRELD1	CRELD2
CRHBP	CRIM1	CRISPLD1	CRISPLD2	CRLF1	CRLF3
CRNN	CSF1	CSF2	CSF3	CSH1	CSH2
CSHL1	CSPG4	CSPG5	CST1	CST11	CST2
CST3	CST4	CST5	CST6	CST7	CST8
CST9	CST9L	CSTA	CSTB	CSTL1	CTF1
CTHRC1	CTSA	CTSB	CTSC	CTSD	CTSE
CTSF	CTSG	CTSH	CTSK	CTSL	CTSO
CTSS	CTSV	CTSW	CTSZ	CX3CL1	CXCL1
CXCL10	CXCL11	CXCL12	CXCL13	CXCL14	CXCL2
CXCL3	CXCL5	CXCL6	CXCL8	CXCL9	DCN
DHH	DMBT1	DMP1	DPT	DSPP	EBI3
ECM1	ECM2	EDA	EDIL3	EFEMP1	EFEMP2
EGF	EGFL6	EGFL7	EGFL8	EGFLAM	EGLN1
EGLN2	EGLN3	ELANE	ELFN1	ELFN2	ELN
ELSPBP1	EMCN	EMID1	EMILIN1	EMILIN2	EMILIN3
EPGN	EPO	EPYC	EREG	ESM1	EYS
F10	F12	F13A1	F13B	F2	F7
F9	FAM20A	FAM20B	FAM20C	FASLG	FBLN1
FBLN2	FBLN5	FBLN7	FBN1	FBN2	FBN3
FCN1	FCN2	FCN3	FGA	FGB	FGF1
FGF10	FGF11	FGF12	FGF13	FGF14	FGF16
FGF17	FGF18	FGF19	FGF2	FGF20	FGF21
FGF22	FGF23	FGF3	FGF4	FGF5	FGF6
FGF7	FGF8	FGF9	FGFBP1	FGFBP2	FGFBP3
FGG	FGL1	FGL2	FLG	FLG2	FLT3LG

Matrisome (1026 genes)					
FMOD	FN1	FNDC1	FNDC7	FNDC8	FRAS1
FREM1	FREM2	FREM3	FRZB	FST	FSTL1
FSTL3	GAS6	GDF1	GDF10	GDF11	GDF15
GDF2	GDF3	GDF5	GDF6	GDF7	GDF9
GDNF	GH1	GH2	GLDN	GPC1	GPC2
GPC3	GPC4	GPC5	GPC6	GREM1	GRIFIN
HABP2	HAPLN1	HAPLN2	HAPLN3	HAPLN4	HBEGF
HCFC1	HCFC2	HGF	HGFAC	HHIP	HMCN1
HMCN2	HMSD	HPSE	HPSE2	HPX	HRG
HRNR	HSPG2	HTRA1	HTRA3	HTRA4	HYAL1
HYAL2	HYAL3	HYAL4	IBSP	IFNA1	IFNA10
IFNA13	IFNA14	IFNA16	IFNA17	IFNA2	IFNA21
IFNA4	IFNA5	IFNA6	IFNA7	IFNA8	IFNB1
IFNE	IFNG	IFNK	IFNW1	IGF1	IGF2
IGFALS	IGFBP1	IGFBP2	IGFBP3	IGFBP4	IGFBP5
IGFBP6	IGFBP7	IGFBPL1	IGSF10	IHH	IL10
IL11	IL12A	IL12B	IL13	IL15	IL16
IL17A	IL17B	IL17C	IL17D	IL17F	IL18
IL19	IL1A	IL1B	IL1F10	IL1RN	IL2
IL20	IL22	IL23A	IL24	IL25	IL26
IL3	IL34	IL36A	IL36B	IL36G	IL36RN
IL37	IL4	IL5	IL6	IL7	IL9
IMPG1	IMPG2	INHA	INHBA	INHBB	INHBC
INHBE	INS	INS-IGF2	INSL3	INSL5	INSL6
INTS14	INTS6L	ISM1	ISM2	ITIH1	ITIH2
ITIH3	ITIH4	ITIH5	ITIH6	ITLN1	ITLN2
KAZALD1	KCP	KERA	KITLG	KNG1	KY
LAMA1	LAMA2	LAMA3	LAMA4	LAMA5	LAMB1
LAMB2	LAMB3	LAMB4	LAMC1	LAMC2	LAMC3
LEFTY1	LEFTY2	LEP	LGALS1	LGALS12	LGALS13
LGALS14	LGALS16	LGALS2	LGALS3	LGALS4	LGALS7
LGALS8	LGALS9	LGALS9B	LGALS9C	LGALSL	LGI1
LGI2	LGI3	LGI4	LIF	LMAN1	LMAN1L
LOX	LOXL1	LOXL2	LOXL3	LOXL4	LPA
LRG1	LTA	LTB	LTBP1	LTBP2	LTBP3
LTBP4	LUM	MASP1	MASP2	MATN1	MATN2

Matrisome (1026 genes)					
MATN3	MATN4	MBL2	MDK	MEGF10	MEGF11
MEGF6	MEGF8	MEGF9	MEP1A	MEP1B	MEPE
MFAP1	MFAP2	MFAP3	MFAP4	MFAP5	MFGE8
MGP	MMP1	MMP10	MMP11	MMP12	MMP13
MMP14	MMP15	MMP16	MMP17	MMP19	MMP2
MMP20	MMP21	MMP23B	MMP24	MMP25	MMP26
MMP27	MMP28	MMP3	MMP7	MMP8	MMP9
MMRN1	MMRN2	MST1	MST1L	MSTN	MUC1
MUC12	MUC13	MUC15	MUC16	MUC17	MUC19
MUC2	MUC20	MUC21	MUC22	MUC3A	MUC4
MUC5AC	MUC5B	MUC6	MUC7	MUCL1	MXRA5
NCAN	NDNF	NELL1	NELL2	NGF	NGLY1
NID1	NID2	NODAL	NPNT	NRG1	NRG2
NRG3	NRG4	NRTN	NTF3	NTF4	NTN1
NTN3	NTN4	NTN5	NTNG1	NTNG2	NYX
OGFOD1	OGFOD2	OGN	OIT3	OMD	OPRPN
OPTC	OSM	OTOG	OTOL1	OVGP1	P3H1
P3H2	P3H3	P4HA1	P4HA2	P4HA3	P4HTM
PAMR1	PAPLN	PAPPA	PAPPA2	PARM1	PCOLCE
PCOLCE2	PCSK5	PCSK6	PDGFA	PDGFB	PDGFC
PDGFD	PF4	PF4V1	PGF	PI3	PIK3IP1
PLAT	PLAU	PLG	PLOD1	PLOD2	PLOD3
PLXDC1	PLXDC2	PLXNA1	PLXNA2	PLXNA3	PLXNA4
PLXNB1	PLXNB2	PLXNB3	PLXNC1	PLXND1	PODN
PODNL1	POMZP3	POSTN	PPBP	PRELP	PRG2
PRG3	PRG4	PRL	PRSS1	PRSS12	PRSS2
PRSS3	PSPN	PTN	PXDN	PXDNL	PZP
REG1A	REG1B	REG3A	REG3G	REG4	RELN
RPTN	RSPO1	RSPO2	RSPO3	RSPO4	S100A1
S100A10	S100A11	S100A12	S100A13	S100A14	S100A16
S100A2	S100A3	S100A4	S100A5	S100A6	S100A7
S100A7A	S100A7L2	S100A8	S100A9	S100B	S100G
S100P	S100Z	SBSPON	SCUBE1	SCUBE2	SCUBE3
SDC1	SDC2	SDC3	SDC4	SEMA3A	SEMA3B
SEMA3C	SEMA3D	SEMA3E	SEMA3F	SEMA3G	SEMA4A
SEMA4B	SEMA4C	SEMA4D	SEMA4F	SEMA4G	SEMA5A

Matrisome (1026 genes)					
SEMA5B	SEMA6A	SEMA6B	SEMA6C	SEMA6D	SEMA7A
SERPINA1	SERPINA10	SERPINA11	SERPINA12	SERPINA2	SERPINA3
SERPINA4	SERPINA5	SERPINA6	SERPINA7	SERPINA9	SERPINB1
SERPINB10	SERPINB11	SERPINB12	SERPINB13	SERPINB2	SERPINB3
SERPINB4	SERPINB5	SERPINB6	SERPINB7	SERPINB8	SERPINB9
SERPINC1	SERPIND1	SERPINE1	SERPINE2	SERPINE3	SERPINF1
SERPINF2	SERPING1	SERPINH1	SERPINI1	SERPINI2	SFRP1
SFRP2	SFRP4	SFRP5	SFTA2	SFTA3	SFTPA1
SFTPA2	SFTPB	SFTPC	SFTPD	SHH	SLIT1
SLIT2	SLIT3	SLPI	SMOC1	SMOC2	SNED1
SPAM1	SPARC	SPARCL1	SPOCK1	SPOCK2	SPOCK3
SPON1	SPON2	SPP1	SRGN	SRPX	SRPX2
SSPOP	ST14	SULF1	SULF2	SVEP1	TCHH
TCHHL1	TDGF1	TECTA	TECTB	TGFA	TGFB1
TGFB2	TGFB3	TGFBI	TGM1	TGM2	TGM3
TGM4	TGM5	TGM6	TGM7	THBS1	THBS2
THBS3	THBS4	THPO	THSD4	TIMP1	TIMP2
TIMP3	TIMP4	TINAG	TINAGL1	TLL1	TLL2
TMPRSS15	TNC	TNF	TNFAIP6	TNFSF10	TNFSF11
TNFSF12	TNFSF13	TNFSF13B	TNFSF14	TNFSF15	TNFSF18
TNFSF4	TNFSF8	TNFSF9	TNN	TNR	TNXB
TPO	TSKU	TSPEAR	USH2A	VCAN	VEGFA
VEGFB	VEGFC	VEGFD	VIT	VTN	VWA1
VWA2	VWA3A	VWA3B	VWA5A	VWA5B1	VWA5B2
VWA7	VWC2	VWC2L	VWCE	VWDE	VWF
WFIKKN1	WFIKKN2	WIF1	WNT1	WNT10A	WNT10B
WNT11	WNT16	WNT2	WNT2B	WNT3	WNT3A
WNT4	WNT5A	WNT5B	WNT6	WNT7A	WNT7B
WNT8A	WNT8B	WNT9A	WNT9B	XCL1	XCL2
ZFP91	ZP1	ZP2	ZP3	ZP4	ZPLD1

Inflammatory response (200 genes)					
ABCA1	ABI1	ACVR1B	ACVR2A	ADM	ADORA2B
ADRM1	AHR	APLNR	AQP9	ATP2A2	ATP2B1
ATP2C1	AXL	BDKRB1	BEST1	BST2	BTG2
C3AR1	C5AR1	CALCRL	CCL17	CCL2	CCL20
CCL22	CCL24	CCL5	CCL7	CCR7	CCRL2
CD14	CD40	CD48	CD55	CD69	CD70
CD82	CDKN1A	CHST2	CLEC5A	CMKLR1	CSF1
CSF3	CSF3R	CX3CL1	CXCL10	CXCL11	CXCL6
CXCL9	CXCR6	CYBB	DCBLD2	EBI3	EDN1
EIF2AK2	EMP3	ADGRE1	EREG	F3	FFAR2
FPR1	FZD5	GABBR1	GCH1	GNA15	GNAI3
GP1BA	GPC3	GPR132	GPR183	HAS2	HBEGF
HIF1A	HPN	HRH1	ICAM1	ICAM4	ICOSLG
IFITM1	IFNAR1	IFNGR2	IL10	IL10RA	IL12B
IL15	IL15RA	IL18	IL18R1	IL18RAP	IL1A
IL1B	IL1R1	IL2RB	IL4R	IL6	IL7R
CXCL8	INHBA	IRAK2	IRF1	IRF7	ITGA5
ITGB3	ITGB8	KCNA3	KCNJ2	KCNMB2	KIF1B
KLF6	LAMP3	LCK	LCP2	LDLR	LIF
LPAR1	LTA	LY6E	LYN	MARCO	MEFV
MEP1A	MET	MMP14	MSR1	MXD1	MYC
NAMPT	NDP	NFKB1	NFKBIA	NLRP3	NMI
NMUR1	NOD2	NPFFR2	OLR1	OPRK1	OSM
OSMR	P2RX4	P2RX7	P2RY2	PCDH7	PDE4B
PDPN	PIK3R5	PLAUR	PROK2	PSEN1	PTAFR
PTGER2	PTGER4	PTGIR	PTPRE	PVR	RAF1
RASGRP1	RELA	RGS1	RGS16	RHOG	RIPK2
RNF144B	ROS1	RTP4	SCARF1	SCN1B	SELE
SELL	SELENOS	SEMA4D	SERPINE1	SGMS2	SLAMF1
SLC11A2	SLC1A2	SLC28A2	SLC31A1	SLC31A2	SLC4A4
SLC7A1	SLC7A2	SPHK1	SRI	STAB1	TACR1
TACR3	TAPBP	TIMP1	TLR1	TLR2	TLR3
TNFAIP6	TNFRSF1B	TNFRSF9	TNFSF10	TNFSF15	TNFSF9
TPBG	VIP				

Angiogenesis (103 genes)					
ACVRL1	AGGF1	AKT1	AMOT	ANG	ANGPT1
ANGPTL3	ANGPTL4	APOH	APP	ARNT	ATP5IF1
BTG1	C1GALT1	CANX	CCND2	CDH13	CHRNA7
COL3A1	COL4A2	COL4A3	COL5A2	CREBBP	CXCL6
CXCL8	EGF	EMCN	EPGN	ERAP1	FGF2
FGFR1	FGFR2	FLT1	FOXO4	FSTL1	HIF1A
HTATIP2	IL17F	IL18	ITGAV	JAG1	JAG2
KCNJ8	KDR	LPL	LRPAP1	LUM	MAPK1
MAPK14	MMP9	MSX1	MYH9	NCL	NF1
NOS3	NOTCH4	NPPB	NPR1	OLR1	PDGFA
PDGFB	PDGFRA	PF4	PGLYRP1	PIK3CA	PLCG1
PLG	PML	POSTN	PRG2	PROK2	PTK2
RHOB	RNH1	ROBO4	RUNX1	S100A4	SCG2
SERPINA5	SERPINF1	SHH	SLCO2A1	SMAD1	SPHK1
SPINK5	SPP1	SRC	STAB1	STC1	TEK
TGFB2	THBD	THY1	TIMP1	TIMP2	TIMP3
TNFRSF21	TNFSF12	TNNI3	VAV2	VCAN	VEGFA
VTN					

Table 5. Differentially expressed genes between B16F1-WT and LLC-WT tumours. Differential expression of genes included in each signature in the comparison B16F1-WT and LLC-WT. Corresponding fold change (LogFC) is included in brackets. Some of these lists of genes were used to perform GO enrichment.

25 upregulated genes in B16F1-WT *vs* LLC-WT (matrisome)			
Adam12 (2.44)	Adam22 (0.85)	Adamts12 (0.49)	Adamts5 (2.34)
Clec7a (1.07)	Cxcl10 (2.63)	Cxcl11 (1.57)	Cxcl9 (0.67)
Ecm2 (0.91)	Fbln5 (3.92)	Fgf1 (1.22)	Fgl2 (1.77)
Hpse (2.01)	Ifng (2.28)	Il10 (0.74)	Il18 (0.62)
Il7 (2.68)	Lox (1.35)	Megf9 (2.66)	Npnt (1.65)
Plxnc1 (2.97)	Sema6a (1.09)	Slit2 (1.18)	Sparcl1 (2.1)
Tnfsf10 (1.2)			

248 downregulated genes in B16F1-WT *vs* LLC-WT (matrisome)			
Adam15 (-5.65)	Adam17 (-0.72)	Adam8 (-4.54)	Adamts10 (-3.62)
Adamts2 (-2.2)	Adamts4 (-0.61)	Adamts6 (-1.98)	Adamts9 (-0.46)
Adamtsl4 (-2.82)	Adamtsl5 (-4.59)	Aebp1 (-4.2)	Agrn (-3.13)
Angpt2 (-1.34)	Angptl2 (-3.72)	Angptl7 (-5.89)	Anxa1 (-2.09)
Anxa11 (-4.09)	Anxa2 (-4.44)	Anxa3 (-3.06)	Anxa5 (-1.54)
Anxa6 (-3.14)	Anxa7 (-1.77)	Anxa9 (-2.31)	Areg (-5.62)
Bgn (-1.42)	Bmp1 (-7.17)	Bmp2 (-1.45)	Btc (-2.6)
C1qb (-5.75)	C1qc (-2.55)	C1qtnf6 (-3.23)	Ccbe1 (-5.34)
Ccl2 (-1.82)	Ccl22 (-1.5)	Ccn1 (-2.77)	Ccn2 (-1.24)
Ccn4 (-2.62)	Cd109 (-0.56)	Cela1 (-3.08)	Cilp (-2.51)
Clcf1 (-5.94)	Clec14a (-1.2)	Clec1a (-4.73)	Clec1b (-3.57)
Clec4d (-1.49)	Clec4n (-3.24)	Clec5a (-1.16)	Clec9a (-2.14)
Cntf (-1.16)	Col14a1 (-1.87)	Col15a1 (-1.05)	Col16a1 (-5.16)
Col18a1 (-8.01)	Col1a1 (-1.49)	Col23a1 (-2.73)	Col3a1 (-3.95)
Col4a1 (-4.6)	Col4a2 (-6.35)	Col5a1 (-4.69)	Col5a3 (-5.73)
Col6a1 (-7.08)	Col6a2 (-7.33)	Col6a3 (-3.84)	Col8a1 (-2.48)
Colec12 (-3.57)	Creld1 (-2.44)	Creld2 (-3.02)	Crim1 (-0.69)
Crispld2 (-3.39)	Crlf3 (-1.02)	Csf1 (-3.67)	Cst6 (-2.3)
Cst7 (-1.54)	Cstb (-3.08)	Cthrc1 (-1.68)	Ctsa (-3.76)
Ctsb (-1.55)	Ctsh (-1.37)	Ctsk (-6.32)	Ctsz (-3.62)
Cx3cl1 (-5.06)	Cxcl12 (-0.86)	Dcn (-4.23)	Dpt (-5.17)
Ebi3 (-2.49)	Ecm1 (-6.13)	Efemp2 (-4.7)	Egf (-1.31)

248 downregulated genes in B16F1-WT *vs* LLC-WT (matrisome)			
Egln3 (-4.55)	Eln (-2.37)	Emcn (-1.61)	Emilin2 (-4.89)
Ereg (-4.66)	Esm1 (-0.98)	F10 (-3.13)	F13a1 (-1.31)
Fam20b (-0.44)	Fam20c (-3.64)	Fbln2 (-1.64)	Fbn1 (-2.77)
Fgf7 (-3.53)	Fgfbp3 (-0.88)	Flt3l (-2.51)	Fn1 (-4.21)
Fstl1 (-3.35)	Gdf15 (-2.24)	Gdf3 (-1.19)	Gpc1 (-4.85)
Gpc4 (-1.77)	Grem1 (-3.25)	Hapln4 (-2.88)	Hbegf (-2.98)
Hcfc1 (-1.58)	Hcfc2 (-0.75)	Hgf (-1.03)	Hspg2 (-8.74)
Htra1 (-7.46)	Hyal2 (-5.99)	Igfbp3 (-2.22)	Igfbp4 (-4.84)
Igfbp7 (-1.86)	Igsf10 (-2.37)	Il16 (-3.51)	Il1b (-2.97)
Il1rn (-0.48)	Impg2 (-0.82)	Inhbb (-2.09)	Insl6 (-1.29)
Ints14 (-1.4)	Kitl (-2.1)	Lama5 (-4.87)	Lamb1 (-4.03)
Lamb2 (-5.49)	Lamc1 (-2.64)	Lgals1 (-7.21)	Lgals3 (-3.05)
Lgi2 (-1.22)	Lif (-4.2)	Lman1 (-1.13)	Loxl2 (-2.44)
Loxl3 (-3.53)	Ltbp1 (-4.81)	Ltbp2 (-2.98)	Ltbp3 (-4.3)
Lum (-4.12)	Masp1 (-4.36)	Matn2 (-2.6)	Megf8 (-4.8)
Mfap3 (-0.92)	Mfge8 (-6.14)	Mgp (-2.66)	Mmp12 (-0.72)
Mmp14 (-4.08)	Mmp19 (-1.87)	Mmp2 (-4.94)	Mmp25 (-1.48)
Mmp3 (-5.38)	Mmp8 (-0.83)	Mmrn2 (-2.09)	Nid1 (-3.95)
Nid2 (-2.53)	Nrg1 (-1.76)	Ntn1 (-7.41)	Ntn4 (-2.53)
Ogfod1 (-1.32)	Ogfod2 (-3.93)	Ogn (-1.21)	Oit3 (-1.89)
Ovgp1 (-0.86)	P3h1 (-2.71)	P3h3 (-3.02)	P4ha1 (-0.87)
P4ha2 (-1.01)	P4ha3 (-4.69)	Pcolce (-4.78)	Pdgfa (-2.35)
Pdgfb (-4.7)	Pdgfc (-2.04)	Pgf (-2)	Plat (-3.11)
Plau (-3.18)	Plod1 (-3.88)	Plod3 (-4.5)	Plxdc2 (-0.84)
Plxna1 (-1.89)	Plxna2 (-2.44)	Plxna3 (-5)	Plxnb2 (-4.24)
Plxnd1 (-3.16)	Ptn (-3.59)	Pxdn (-5.98)	S100a1 (-1.86)
S100a10 (-3.67)	S100a11 (-4.18)	S100a13 (-4.83)	S100a16 (-5.74)
S100a4 (-8.08)	S100a6 (-7.23)	S100a8 (-3.14)	Sdc1 (-3.91)
Sdc2 (-1.58)	Sdc3 (-2.98)	Sdc4 (-2.17)	Sema3a (-3.33)
Sema3e (-2.91)	Sema3g (-1.71)	Sema4a (-3.09)	Sema4b (-3.99)
Sema4c (-4.44)	Sema4d (-0.82)	Sema7a (-3.62)	Serpinb8 (-0.56)
Serpinc1 (-2.94)	Serpine1 (-2.58)	Serpine2 (-1.24)	Serpinf1 (-6.96)
Serping1 (-2.02)	Serpinh1 (-1.66)	Slit3 (-1.67)	Slpi (-4.8)
Sned1 (-2.6)	Sparc (-1.93)	Spp1 (-2.62)	Sulf2 (-0.81)
Svep1 (-1.11)	Tgfa (-2.47)	Tgfb1 (-5.87)	Tgfb3 (-3.61)
Tgfbi (-3.67)	Tgm2 (-4.66)	Thbs1 (-1.63)	Thbs2 (-4.35)

248 downregulated genes in B16F1-WT *vs* LLC-WT (matrisome)			
Timp1 (-4.38)	Timp2 (-3.7)	Tll1 (-1.31)	Tnf (-2.46)
Tnfsf11 (-1.77)	Tnfsf12 (-4.85)	Tnfsf13 (-2.5)	Tnfsf13b (-0.85)
Tnfsf9 (-0.97)	Tnn (-2.54)	Vcan (-4.43)	Vegfb (-2.44)
Vegfc (-0.83)	Vwa1 (-4.52)	Vwf (-4.83)	Wnt5a (-3.52)

18 upregulated genes in B16F1-WT *vs* LLC-WT (inflam. response)			
Acvr2a (0.82)	Cd69 (1.4)	Cxcl10 (2.63)	Cxcl11 (1.57)
Cxcl9 (0.67)	Cxcr6 (1.92)	Hif1a (0.48)	Il10 (0.74)
Il18 (0.62)	Il18r1 (1.08)	Il7r (1.38)	Met (1.44)
Nampt (1.49)	Rgs1 (1.57)	Rtp4 (1.52)	Slc31a1 (0.46)
Tlr3 (2.18)	Tnfsf10 (1.2)		

107 downregulated genes in B16F1-WT *vs* LLC-WT (inflam. Response)			
Acvr1b (-2.2)	Adgre1 (-0.59)	Adm (-5.22)	Adora2b (-2.21)
Aplnr (-2.82)	Aqp9 (-1.42)	Atp2b1 (-1.57)	Atp2c1 (-0.53)
Axl (-0.99)	Bst2 (-2.89)	Btg2 (-1.65)	C3ar1 (-0.78)
C5ar1 (-2.52)	Calcrl (-1.35)	Ccl2 (-1.82)	Ccl22 (-1.5)
Ccr7 (-2.99)	Cd14 (-4.81)	Cd40 (-2.07)	Cd48 (-0.93)
Cd82 (-4.45)	Cdkn1a (-0.96)	Chst2 (-3.79)	Clec5a (-1.16)
Cmklr1 (-3.82)	Csf1 (-3.67)	Csf3r (-2.78)	Cx3cl1 (-5.06)
Dcbld2 (-1.09)	Ebi3 (-2.49)	Edn1 (-1.74)	Emp3 (-6.03)
Ereg (-4.66)	Fpr1 (-1.9)	Fzd5 (-1.53)	Gabbr1 (-1.41)
Gch1 (-2.22)	Gnai3 (-0.77)	Gpr183 (-2.81)	Has2 (-2.48)
Hbegf (-2.98)	Icam1 (-1.62)	Ifnar1 (-1.52)	Ifngr2 (-1.45)
Il10ra (-3.78)	Il15ra (-2.29)	Il18rap (-3.57)	Il1b (-2.97)
Il1r1 (-4.82)	Il2rb (-1.51)	Il4ra (-5.35)	Irak2 (-1.07)
Irf1 (-2.58)	Irf7 (-2.06)	Itga5 (-6.06)	Kcnj2 (-1.32)
Kif1b (-1.29)	Klf6 (-0.94)	Lck (-1.66)	Ldlr (-2.32)
Lif (-4.2)	Lpar1 (-3.29)	Ly6e (-5.1)	Lyn (-1.55)
Mefv (-3.38)	Mmp14 (-4.08)	Mxd1 (-1.38)	Nfkb1 (-2.64)
Nfkbia (-3.96)	Nlrp3 (-2.78)	Nod2 (-1.95)	Olr1 (-2.69)
Osmr (-1.25)	P2rx4 (-2.53)	P2rx7 (-1.96)	P2ry2 (-3.11)
Pdpn (-3.86)	Pik3r5 (-4.02)	Plaur (-4.24)	Psen1 (-1.88)
Ptafr (-2.11)	Ptgir (-1.87)	Ptpre (-1.92)	Pvr (-0.64)
Raf1 (-1.82)	Rela (-5.82)	Rgs16 (-2.52)	Rhog (-4.16)
Rnf144b (-1.33)	Selenos (-0.7)	Sema4d (-0.82)	Serpine1 (-2.58)
Sgms2 (-4.97)	Slc11a2 (-1.06)	Slc31a2 (-2.57)	Slc7a1 (-0.78)
Sphk1 (-3.68)	Sri (-0.79)	Stab1 (-6.33)	Tapbp (-2.24)
Timp1 (-4.38)	Tlr1 (-0.64)	Tlr2 (-1.7)	Tnfrsf1b (-3.7)
Tnfrsf9 (-2.56)	Tnfsf9 (-0.97)	Tpbg (-4.26)	

Table 6. Differentially expressed genes between LLC-WT and LLC-Ats1-KO tumours. Differential expression of genes included in each signature in the comparison LLC-WT and LLC-Ats1-KO. Corresponding fold change (LogFC) is included in brackets. Some of these lists of genes were used to perform GO enrichment.

28 upregulated genes in LLC-WT *vs* LLC-Ats1-KO (matrisome)			
Adam12 (0.39)	Adamts12 (0.5)	Btc (0.83)	Ccn2 (0.61)
Clec14a (0.77)	Col15a1 (0.46)	Col4a1 (0.34)	Col4a2 (0.32)
Col6a1 (0.56)	Col6a2 (0.7)	Col6a3 (0.73)	Creld1 (0.49)
Cst6 (0.79)	Ctsk (1.33)	Cxcl13 (1.2)	Fam20c (0.67)
Gpc4 (0.75)	Hgf (0.75)	Igfbp7 (0.49)	Itih5 (0.89)
Lama4 (0.63)	Nid2 (0.65)	Pdgfb (0.62)	Plxna2 (0.3)
Ptn (1.68)	Sema6a (0.64)	Sparcl1 (0.69)	Tgfb3 (0.51)

44 downregulated genes in LLC-WT *vs* LLC-Ats1-KO (matrisome)			
Agrn (-0.37)	Ccl2 (-0.95)	Ccl7 (-0.93)	Clcf1 (-0.28)
Clec7a (-1.08)	Csf1 (-0.33)	Cst7 (-0.72)	Cthrc1 (-1.14)
Ctsc (-0.44)	Cxcl10 (-1.59)	Cxcl11 (-1.21)	Cxcl9 (-1)
F10 (-1.39)	Fbln2 (-0.62)	Fgl2 (-1.29)	Fst (-1.37)
Gdf15 (-0.65)	Grem1 (-0.96)	Ifng (-1.45)	Il15 (-0.91)
Il18 (-0.6)	Il1a (-0.86)	Il1b (-1.26)	Il1rn (-0.79)
Il7 (-0.9)	Impg2 (-0.59)	Lgals8 (-0.38)	Ltbp2 (-0.74)
Mmp13 (-1.5)	Mmp19 (-0.71)	Mmp25 (-1)	Mmp27 (-1.31)
Mmp3 (-1.22)	Mmp8 (-1.1)	Nrg1 (-1.61)	Pcsk5 (-0.9)
Sdc3 (-0.34)	Sdc4 (-0.26)	Serping1 (-0.49)	Spon1 (-1.43)
Sulf1 (-0.59)	Thbs1 (-0.98)	Tnfsf10 (-1.2)	Tnfsf15 (-0.91)

1 upregulated genes in LLC-WT *vs* LLC-Ats1-KO (inflam. response)			
Itgb8 (0.84)			

52 downregulated genes in LLC-WT *vs* LLC-Ats1-KO (inflam. response)			
Adora2b (-0.32)	Aqp9 (-0.83)	Bst2 (-0.78)	Ccl2 (-0.95)
Ccl7 (-0.93)	Ccrl2 (-1.06)	Cd40 (-0.63)	Cd69 (-1.57)
Cmklr1 (-0.43)	Csf1 (-0.33)	Csf3r (-0.93)	Cxcl10 (-1.59)
Cxcl11 (-1.21)	Cxcl9 (-1)	Cxcr6 (-0.65)	Eif2ak2 (-0.59)
Icam1 (-0.55)	Il10ra (-0.56)	Il15 (-0.91)	Il15ra (-0.72)
Il18 (-0.6)	Il1a (-0.86)	Il1b (-1.26)	Il2rb (-0.88)
Irak2 (-0.44)	Irf1 (-0.73)	Irf7 (-1.43)	Klf6 (-0.28)
Lck (-0.86)	Lpar1 (-0.58)	Ly6e (-0.49)	Lyn (-0.25)
Mefv (-0.6)	Mxd1 (-0.86)	Nampt (-0.32)	Nlrp3 (-0.68)
Nmi (-0.55)	Nod2 (-0.94)	Olr1 (-1.02)	Plaur (-0.35)
Ptafr (-0.66)	Rgs16 (-0.81)	Ripk2 (-0.33)	Rtp4 (-1.54)
Sell (-1.59)	Slc4a4 (-0.81)	Sphk1 (-1.05)	Tapbp (-0.5)
Tlr1 (-0.52)	Tlr3 (-0.61)	Tnfsf10 (-1.2)	Tnfsf15 (-0.91)

3 upregulated genes in LLC-WT *vs* LLC-Ats1-KO (angiogenesis)			
Col4a2 (0.32)	Pdgfb (0.62)	Tek (0.49)	

5 downregulated genes in LLC-WT *vs* LLC-Ats1-KO (angiogenesis)			
Erap1 (-0.53)	Il18 (-0.6)	Olr1 (-1.02)	Pml (-0.34)
Sphk1 (-1.05)			

Table 7. Differentially expressed genes between B16F1-WT and B16F1-Ats1-KO tumours. Differential expression of genes included in each signature in the comparison B16F1-WT and B16F1-Ats1-KO. Corresponding fold change (LogFC) is included in brackets. Some of these lists of genes were used to perform GO enrichment.

4 upregulated genes in B16F1-WT *vs* B16F1-Ats1-KO (matrisome)			
Adam22 (0.67)	Angpt1 (0.87)	Anxa4 (0.62)	Edil3 (0.68)

65 downregulated genes in B16F1-WT *vs* B16F1-Ats1-KO (matrisome)			
Adam8 (-1.18)	Adamts2 (-0.91)	Areg (-1.36)	C1qc (-0.98)
Ccbe1 (-2.35)	Ccl22 (-0.5)	Clcf1 (-1.77)	Clec1b (-1)
Clec4d (-1.65)	Clec4e (-1.48)	Clec4n (-1.5)	Clec5a (-1.31)
Clec7a (-0.83)	Col16a1 (-0.71)	Col18a1 (-0.88)	Col23a1 (-1.42)
Col5a1 (-1.33)	Col5a2 (-1.12)	Col6a2 (-0.93)	Col6a3 (-1.39)
Colec12 (-1.18)	Crispld2 (-1.77)	Ctsb (-0.71)	Ctsk (-1.57)
Ctss (-0.97)	Cxcl11 (-0.74)	Cxcl9 (-0.67)	Emcn (-0.86)
Ereg (-1.88)	F10 (-0.99)	Fasl (-0.73)	Fbln2 (-1.49)
Fgf7 (-1.31)	Grem1 (-2.64)	Il15 (-0.63)	Il1a (-2.04)
Impg2 (-0.5)	Inhba (-1.84)	Inhbb (-1.09)	Masp1 (-1.49)
Mmp19 (-1.22)	Mmp3 (-2.1)	Mmrn2 (-0.98)	Nid2 (-1.08)
Nrg1 (-2.12)	P4ha3 (-1.69)	Plau (-0.71)	Pxdn (-1.15)
S100a10 (-1.02)	S100a6 (-1.48)	S100a8 (-3.04)	Serpinb2 (-1.36)
Serpinc1 (-2.6)	Serpine1 (-1.2)	Serpine2 (-0.95)	Slpi (-3.16)
Spon1 (-1.13)	Sulf2 (-0.44)	Tnc (-1.73)	Tnf (-1.5)
Tnfsf13b (-0.81)	Tnfsf8 (-0.97)	Tnn (-3.03)	Vcan (-1.1)
Wnt5a (-2.3)			

4 upregulated genes in B16F1-WT *vs* B16F1-Ats1-KO (inflam. response)			
Atp2a2 (0.77)	Hif1a (0.64)	Nampt (0.59)	Tlr3 (0.63)

38 downregulated genes in B16F1-WT *vs* B16F1-Ats1-KO (inflam. response)			
Aqp9 (-1.27)	Btg2 (-1.09)	C5ar1 (-0.71)	Ccl22 (-0.5)
Cd40 (-0.88)	Chst2 (-0.72)	Clec5a (-1.31)	Csf3r (-1.18)
Cxcl11 (-0.74)	Cxcl9 (-0.67)	Cxcr6 (-0.59)	Edn1 (-1.01)
Ereg (-1.88)	Has2 (-1.29)	Icam1 (-0.64)	Il15 (-0.63)
Il15ra (-0.68)	Il18r1 (-0.74)	Il18rap (-1.02)	Il1a (-2.04)
Il1r1 (-1.23)	Il7r (-0.77)	Inhba (-1.84)	Nfkbia (-0.91)
Nlrp3 (-1.38)	Nod2 (-1.04)	Osmr (-0.73)	Plaur (-1.33)
Ptafr (-1.01)	Ptger2 (-0.84)	Ptgir (-1.08)	Rgs1 (-0.47)
Serpine1 (-1.2)	Slc31a2 (-0.87)	Slc7a2 (-0.68)	Tlr2 (-1.01)
Tnfrsf1b (-1.19)	Tpbg (-1.62)		

8 upregulated genes in B16F1-WT *vs* B16F1-Ats1-KO (angiogenesis)			
Amot (0.63)	Angpt1 (0.87)	C1galt1 (0.58)	Canx (0.6)
Erap1 (0.41)	Hif1a (0.64)	Itgav (0.5)	Stc1 (0.7)

8 downregulated genes in B16F1-WT *vs* B16F1-Ats1-KO (angiogenesis)			
Btg1 (-0.71)	Cdh13 (-1.16)	Col5a2 (-1.12)	Emcn (-0.86)
Fgfr1 (-1.58)	Flt1 (-0.62)	Tnfrsf21 (-0.73)	Vcan (-1.1)

Table 8. Differentially expressed genes between B16F1-Ats1-KO and LLC-Ats1-KO tumours. Differential expression of genes included in each signature in the comparison B16F1-Ats1-KO and LLC-Ats1-KO. Corresponding fold change (LogFC) is included in brackets. Some of these lists of genes were used to perform GO enrichment.

24 upregulated genes in B16F1-Ats1-KO *vs* LLC-Ats1-KO (matrisome)			
Adam12 (2.16)	Adamts5 (2.2)	Clec12a (1.04)	Clec7a (0.82)
Ctss (0.95)	Cxcl10 (0.9)	Cxcl11 (1.1)	Cxcl13 (4.42)
Fasl (0.69)	Fbln1 (1.08)	Fbln5 (3.33)	Hpse (1.02)
Ifng (1.28)	Igf1 (1.19)	Il7 (1.41)	Inhba (1.73)
Ints6l (0.66)	Lox (1.1)	Megf9 (2.77)	Pdgfd (1.04)
Plxnc1 (2.16)	Sema6a (1.76)	Slit2 (1.42)	Sparcl1 (2.44)

210 downregulated genes in B16F1-Ats1-KO *vs* LLC-Ats1-KO (matrisome)			
Adam15 (-5.26)	Adam17 (-0.69)	Adam8 (-3.68)	Adamts10 (-3.24)
Adamts2 (-1.18)	Adamts4 (-0.72)	Adamts6 (-1.78)	Adamtsl4 (-2.75)
Adamtsl5 (-4.4)	Aebp1 (-4.44)	Agrn (-3.15)	Angpt2 (-0.88)
Angptl2 (-3.68)	Angptl7 (-5.08)	Anxa1 (-1.96)	Anxa11 (-3.88)
Anxa2 (-4.12)	Anxa3 (-2.91)	Anxa5 (-1.67)	Anxa6 (-3.05)
Anxa7 (-1.73)	Anxa9 (-1.55)	Areg (-3.83)	Bgn (-1.05)
Bmp1 (-6.26)	Btc (-1.57)	C1qb (-5.02)	C1qc (-1.45)
C1qtnf6 (-3.66)	Ccbe1 (-3.2)	Ccl2 (-2.72)	Ccl22 (-0.8)
Ccn1 (-2.2)	Ccn4 (-1.92)	Cela1 (-2.97)	Cilp (-2.85)
Clcf1 (-4.45)	Clec1a (-4.53)	Clec1b (-2.12)	Clec4n (-1.97)
Clec9a (-2.25)	Col11a2 (-1.08)	Col16a1 (-4.41)	Col18a1 (-6.82)
Col23a1 (-1.7)	Col3a1 (-3.08)	Col4a1 (-3.79)	Col4a2 (-5.43)
Col5a1 (-3.04)	Col5a3 (-4.93)	Col6a1 (-5.25)	Col6a2 (-5.7)
Col6a3 (-1.72)	Col8a1 (-2.2)	Colec12 (-2.07)	Creld1 (-2.43)
Creld2 (-3.12)	Crim1 (-1.06)	Crispld2 (-2.3)	Crlf3 (-1.18)
Csf1 (-3.85)	Cst6 (-1.03)	Cst7 (-2.33)	Cstb (-2.38)
Cthrc1 (-3.06)	Ctsa (-3.6)	Ctsb (-0.93)	Ctsh (-1.2)
Ctsk (-3.42)	Ctsz (-3.58)	Cx3cl1 (-4.56)	Dcn (-3.33)
Dpt (-4.2)	Ebi3 (-2.48)	Ecm1 (-4.98)	Efemp2 (-5.41)
Egf (-1.19)	Egln3 (-3.85)	Emilin2 (-4.56)	Ereg (-3.29)
F10 (-3.53)	F13a1 (-1.54)	Fam20b (-0.85)	Fam20c (-2.8)
Fbn1 (-2.54)	Fgf7 (-2.78)	Flt3l (-2.29)	Fn1 (-3.19)

210 downregulated genes in B16F1-Ats1-KO *vs* LLC-Ats1-KO (matrisome)			
Fstl1 (-2.56)	Gdf11 (-1.15)	Gdf15 (-1.87)	Gdf3 (-0.99)
Gpc1 (-5.01)	Grem1 (-1.57)	Hapln4 (-3.17)	Hbegf (-2.44)
Hcfc1 (-1.5)	Hcfc2 (-0.81)	Hspg2 (-7.6)	Htra1 (-6.6)
Hyal2 (-5.26)	Igfbp3 (-1.27)	Igfbp4 (-5.29)	Il16 (-3.01)
Il1b (-2.35)	Impg2 (-0.91)	Inhbb (-0.73)	Insl6 (-1.73)
Ints14 (-1.41)	Kitl (-2.16)	Lama5 (-4.69)	Lamb1 (-3.28)
Lamb2 (-5.21)	Lamc1 (-2.96)	Lgals1 (-6.89)	Lgals3 (-2.58)
Lgals8 (-0.54)	Lif (-4.1)	Lman1 (-1.8)	Loxl2 (-1.69)
Loxl3 (-3.21)	Ltbp1 (-4.29)	Ltbp2 (-2.84)	Ltbp3 (-4.17)
Lum (-3.61)	Masp1 (-2.64)	Matn2 (-2.08)	Megf8 (-4.99)
Mfap3 (-1.61)	Mfge8 (-6.13)	Mgp (-2.24)	Mmp14 (-3.56)
Mmp19 (-1.37)	Mmp2 (-4.05)	Mmp25 (-2.3)	Mmp27 (-0.92)
Mmp3 (-4.5)	Mmrn2 (-0.9)	Nid1 (-3.57)	Nid2 (-0.8)
Nrg1 (-1.25)	Ntn1 (-6.36)	Ntn4 (-1.66)	Ogfod1 (-1.82)
Ogfod2 (-3.56)	P3h1 (-2.65)	P3h3 (-2.49)	P4ha1 (-1.23)
P4ha3 (-3.07)	Pcolce (-4.82)	Pdgfa (-2.51)	Pdgfb (-3.85)
Pdgfc (-1.81)	Plat (-2.04)	Plau (-2.38)	Plod1 (-3.59)
Plod3 (-4.69)	Plxna1 (-2.14)	Plxna3 (-4.45)	Plxnb1 (-0.73)
Plxnb2 (-4.79)	Plxnd1 (-3.03)	Pxdn (-4.61)	S100a1 (-1.65)
S100a10 (-2.62)	S100a11 (-3.52)	S100a13 (-3.77)	S100a16 (-4.17)
S100a4 (-6.78)	S100a6 (-5.64)	Sdc1 (-3.6)	Sdc2 (-1.74)
Sdc3 (-2.55)	Sdc4 (-2.86)	Sema3a (-2.57)	Sema3e (-3.89)
Sema3g (-1.49)	Sema4a (-2.58)	Sema4b (-4.03)	Sema4c (-3.68)
Sema4d (-1.05)	Sema6d (-1.29)	Sema7a (-3.82)	Serpine1 (-1.43)
Serpinf1 (-6.29)	Serping1 (-2)	Serpinh1 (-1.9)	Slpi (-2.6)
Sned1 (-2.4)	Sparc (-1.38)	Spp1 (-2.1)	Tgfa (-1.53)
Tgfb1 (-5.49)	Tgfb3 (-3.64)	Tgfbi (-3.04)	Tgm2 (-4.32)
Thbs1 (-1.74)	Thbs2 (-3.5)	Timp1 (-4.05)	Timp2 (-3.71)
Tnf (-1.46)	Tnfsf12 (-4.03)	Tnfsf13 (-1.91)	Tnfsf9 (-1.16)
Vcan (-3.2)	Vegfa (-0.7)	Vegfb (-2.45)	Vegfc (-0.92)
Vwa1 (-3.05)	Vwf (-4.11)		

10 upregulated genes in B16F1-Ats1-KO *vs LLC*-Ats1-KO (inflam. response)			
Cxcl10 (0.9)	Cxcl11 (1.1)	Cxcr6 (1.86)	Il18r1 (1.11)
Il7r (1.32)	Inhba (1.73)	Met (0.87)	Nampt (0.58)
Rgs1 (1.56)	Tlr3 (0.93)		

106 downregulated genes in B16F1-Ats1-KO *vs* LLC-Ats1-KO (inflam. response)			
Acvr1b (-2.04)	Adm (-4.62)	Adora2b (-2.3)	Aplnr (-1.96)
Aqp9 (-0.99)	Atp2a2 (-1.17)	Atp2b1 (-1.72)	Atp2c1 (-1.02)
Axl (-1.29)	Bst2 (-3.74)	Btg2 (-1.1)	C5ar1 (-1.9)
Calcrl (-1.19)	Ccl2 (-2.72)	Ccl22 (-0.8)	Ccr7 (-3.19)
Ccrl2 (-1.39)	Cd14 (-3.44)	Cd40 (-1.81)	Cd48 (-0.58)
Cd82 (-3.91)	Cdkn1a (-1.66)	Chst2 (-3.11)	Cmklr1 (-3.42)
Csf1 (-3.85)	Csf3r (-2.53)	Cx3cl1 (-4.56)	Dcbld2 (-1.67)
Ebi3 (-2.48)	Eif2ak2 (-0.93)	Emp3 (-5.79)	Ereg (-3.29)
Fpr1 (-1.02)	Fzd5 (-1.27)	Gabbr1 (-1.14)	Gch1 (-2.04)
Gnai3 (-1.13)	Gpr183 (-2.62)	Has2 (-1.47)	Hbegf (-2.44)
Icam1 (-1.53)	Ifnar1 (-2.14)	Ifngr2 (-1.93)	Il10ra (-4.18)
Il15ra (-2.32)	Il18rap (-3.01)	Il1b (-2.35)	Il1r1 (-3.86)
Il2rb (-1.83)	Il4ra (-5.68)	Irak2 (-1.41)	Irf1 (-3.18)
Irf7 (-3.72)	Itga5 (-5.77)	Kif1b (-1.52)	Klf6 (-1.19)
Lck (-1.54)	Ldlr (-2.54)	Lif (-4.1)	Lpar1 (-2.97)
Ly6e (-5.44)	Lyn (-1.59)	Mefv (-2.8)	Mmp14 (-3.56)
Mxd1 (-2.03)	Nfkb1 (-2.67)	Nfkbia (-3.34)	Nlrp3 (-2.08)
Nod2 (-1.85)	Olr1 (-2.6)	Osmr (-1)	P2rx4 (-2.42)
P2rx7 (-2.06)	P2ry2 (-3)	Pdpn (-2.7)	Pik3r5 (-3.93)
Plaur (-3.26)	Psen1 (-2.26)	Ptafr (-1.76)	Ptgir (-1.03)
Ptpre (-2.04)	Pvr (-1.37)	Raf1 (-1.69)	Rela (-5.35)
Rgs16 (-2.92)	Rhog (-4.13)	Rnf144b (-0.66)	Selenos (-0.61)
Sell (-1.11)	Sema4d (-1.05)	Serpine1 (-1.43)	Sgms2 (-3.83)
Slc11a2 (-1.53)	Slc31a2 (-2.1)	Slc4a4 (-0.89)	Slc7a1 (-1.06)
Sphk1 (-3.36)	Sri (-0.88)	Stab1 (-4.49)	Tapbp (-2.7)
Timp1 (-4.05)	Tlr2 (-0.75)	Tnfrsf1b (-2.76)	Tnfrsf9 (-2.59)
Tnfsf9 (-1.16)	Tpbg (-2.98)		

Table 9. GO enrichment analysis of differentially expressed genes in B16F1-WT *versus* LLC-WT tumours. Table including GO ID, description and genes from the data set (previous tables) that were included in each GO Biological Process term.

GO ID	Description	Upregulated genes from the inflammatory response			
GO:0019221	cytokine-mediated signaling pathway	IL10	CXCL10	CXCL9	CXCL11
		IL18	IL7R	HIF1A	IL18R1
GO:0071222	cellular response to lipopolysaccharide	IL10	CXCL10	CXCL9	CXCL11
		IL18			
GO:0045944	positive regulation of transcription by RNA polymerase II	IL10	CXCL10	NAMPT	IL18
		HIF1A	MET	ACVR2A	TLR3
GO:1904427	positive regulation of calcium ion transmembrane transport	CXCL10	CXCL9	CXCL11	
GO:0071219	cellular response to molecule of bacterial origin	IL10	CXCL10	CXCL9	CXCL11

GO ID	Description	Upregulated genes from the matrisome			
GO:0043062	extracellular structure organisation	ADAMTS5	ECM2	LOX	ADAM12
		ADAMTS12	NPNT	FBLN5	
GO:0045229	external encapsulating structure organisation	ADAMTS5	ECM2	LOX	ADAM12
		ADAMTS12	NPNT	FBLN5	
GO:1901509	regulation of endothelial tube morphogenesis	CXCL10	ADAMTS12	FGF1	
GO:1905330	regulation of morphogenesis of an epithelium	CXCL10	ADAMTS12	FGF1	
GO:0030198	extracellular matrix organisation	ADAMTS5	ECM2	LOX	ADAM12
		ADAMTS12	NPNT	FBLN5	

Table 10. GO enrichment analysis of differentially expressed genes in LLC-WT *versus* LLC-Ats1-KO tumours. Table including GO ID, description and genes from the data set (previous tables) that were included in each GO Biological Process term.

GO term ID	Description	Upregulated genes from the matrisome			
GO:0030198	extracellular matrix organisation	COL15A1	COL4A2	COL4A1	LAMA4
		CTSK	COL6A2	COL6A1	ADAM12
		PDGFB	COL6A3	ADAMTS12	NID2
GO:0043062	extracellular structure organisation	COL15A1	COL4A2	COL4A1	LAMA4
		COL6A2	COL6A1	ADAM12	PDGFB
		COL6A3	ADAMTS12	NID2	
GO:0045229	external encapsulating structure organisation	COL15A1	COL4A2	COL4A1	LAMA4
		COL6A2	COL6A1	ADAM12	PDGFB
		COL6A3	ADAMTS12	NID2	
GO:0030199	collagen fibril organisation	COL15A1	COL4A2	COL4A1	COL6A2
		COL6A1	COL6A3		
GO:0097435	supramolecular fiber organisation	COL15A1	COL4A2	COL4A1	COL6A2
		COL6A1	COL6A3		

GO term ID	Description	Downregulated genes from the matrisome			
GO:0006954	inflammatory response	IL1A	CXCL10	IL1RN	CXCL9
		MMP25	CXCL11	CCL7	IFNG
		IL1B	IL18	CCL2	THBS1
GO:0019221	cytokine-mediated signaling pathway	IL1RN	CXCL9	CSF1	TNFSF15
		IL15	MMP3	IL18	IL1A
		CXCL10	CXCL11	CCL7	IFNG
		IL7	CLCF1	IL1B	CCL2
GO:0042127	regulation of cell population proliferation	CXCL9	CSF1	IL15	NRG1
		THBS1	GREM1	IL1A	CXCL10
		CXCL11	IFNG	CLEC7A	IL7
		CLCF1	IL1B		
GO:0008284	positive regulation of cell population proliferation	GREM1	CSF1	IFNG	CLEC7A
		IL15	IL7	CLCF1	IL1B
		IL18	NRG1	THBS1	

GO term ID	Description	Downregulated genes from the matrisome			
GO:0071345	cellular response to cytokine stimulus	IL1A	CXCL10	IL1RN	CSF1
		CCL7	IL7	CLCF1	IL1B
		MMP3	IL18	CCL2	

Table 11. GO enrichment analysis of differentially expressed genes in B16F1-WT *versus* B16F1-Ats1-KO tumours. Table including GO ID, description and genes from the data set (previous tables) that were included in each GO Biological Process term.

GO term ID	Description	Upregulated genes from the matrisome			
GO:0051897	positive regulation of protein kinase B signalling	ANGPT1	HPSE	FGF1	
GO:0051896	regulation of protein kinase B signalling	ANGPT1	HPSE	FGF1	
GO:0042060	wound healing	HPSE	FGF1		
GO:0007162	negative regulation of cell adhesion	ANGPT1	ADAM22		
GO:0010595	positive regulation of endothelial cell migration	ANGPT1	FGF1		

GO term ID	Description	Downregulated genes from the matrisome			
GO:0030198	extracellular matrix organization	COL18A1	COL16A1	SERPINE1	COL23A1
		MMP3	TNC	NID2	CTSS
		GREM1	ADAMTS2	VCAN	COL5A1
		CTSK	COL6A2	P4HA3	PXDN
		COL5A2	MMP19	COL6A3	ADAM8
GO:0043062	extracellular structure organization	COL18A1	COL16A1	SERPINE1	COL23A1
		MMP3	TNC	NID2	ADAMTS2
		VCAN	COL5A1	COL6A2	PXDN
		COL5A2	MMP19	COL6A3	
GO:0045229	external encapsulating structure organization	COL18A1	COL16A1	SERPINE1	COL23A1
		MMP3	TNC	NID2	ADAMTS2
		VCAN	COL5A1	COL6A2	PXDN
		COL5A2	MMP19	COL6A3	
GO:0030199	collagen fibril organization	GREM1	COL18A1	ADAMTS2	COL16A1
		COL5A1	COL6A2	P4HA3	
		COL23A1	PXDN	COL5A2	COL6A3
GO:0097435	supramolecular fiber organization	GREM1	COL18A1	ADAMTS2	COL16A1
		COL5A1	COL6A2	P4HA3	COL23A1
		PXDN	COL5A2	COL6A3	

Table 12. GO enrichment analysis of differentially expressed genes in B16F1-Ats1-KO *versus* LLC-Ats1-KO tumours. Table including GO ID, description and genes from the data set (previous tables) that were included in each GO Biological Process term.

GO term ID	Description	Upregulated genes from the inflammatory response			
GO:0032649	regulation of interferon-gamma production	INHBA	IL18R1	TLR3	
GO:0010818	T cell chemotaxis	CXCL10	CXCL11		
GO:0042127	regulation of cell population proliferation	CXCL10	CXCL11	NAMPT	INHBA
		IL7R			
GO:0072678	T cell migration	CXCL10	CXCL11		
GO:0045944	positive regulation of transcription by RNA polymerase II	CXCL10	NAMPT	INHBA	MET
		TLR3			

GO term ID	Description	Upwnregulated genes from the matrisome			
GO:0042127	regulation of cell population proliferation	CXCL10	CXCL11	IFNG	IL7
		CLEC7A	PDGFD	INHBA	IGF1
GO:0014902	myotube differentiation	ADAMTS5	ADAM12	IGF1	
GO:0030334	regulation of cell migration	SEMA6A	CLEC7A	PDGFD	IGF1
		PLXNC1	SLIT2		
GO:0030335	positive regulation of cell migration	SEMA6A	IFNG	CLEC7A	PDGFD
		IGF1			
GO:0008284	positive regulation of cell population proliferation	IFNG	IL7	CLEC7A	PDGFD
		IGF1	HPSE		

BIBLIOGRAPHY

Apte, S. S. (2004). A disintegrin-like and metalloprotease (reprolysin type) with thrombospondin type 1 motifs: The ADAMTS family. *International Journal of Biochemistry and Cell Biology*, *36*(6), 981–985. https://doi.org/10.1016/j.biocel.2004.01.014

Apte, S. S., & Parks, W. C. (2015). Metalloproteinases: A parade of functions in matrix biology and an outlook for the future. *Matrix Biology*, *44*, 1–6. https://doi.org/10.1016/j.matbio.2015.04.005

Asano, K., Nelson, C. M., Nandadasa, S., Hattori, N. A.-, Lindner, J., Alban, T., … Hirohata, S. (2017). Stromal Versican Regulates Tumor Growth by Promoting Angiogenesis. *Scientific Reports*, (September), 1–11. https://doi.org/10.1038/s41598-017-17613-6

Ashlin, T. G., Buckley, M. L., Salter, R. C., Johnson, J. L., Kwan, A. P. L., & Ramji, D. P. (2014). The anti-atherogenic cytokine interleukin-33 inhibits the expression of a disintegrin and metalloproteinase with thrombospondin motifs-1, -4 and -5 in human macrophages: Requirement of extracellular signal-regulated kinase, c-Jun N-terminal kinase and pho. *International Journal of Biochemistry and Cell Biology*, *46*(1), 113–123. https://doi.org/10.1016/j.biocel.2013.11.008

Ashlin, T. G., Kwan, A. P. L., & Ramji, D. P. (2013). Regulation of ADAMTS-1, -4 and -5 expression in human macrophages: Differential regulation by key cytokines implicated in atherosclerosis and novel synergism between TL1A and IL-17. *Cytokine*, *64*(1), 234–242. https://doi.org/10.1016/j.cyto.2013.06.315

Baidžajevas, K., Hadadi, É., Lee, B., Lum, J., Shihui, F., Sudbery, I., … Wilson, H. L. (2020). Macrophage polarisation associated with atherosclerosis differentially affects their capacity to handle lipids. *Atherosclerosis*, *305*, 10–18. https://doi.org/10.1016/j.atherosclerosis.2020.05.003

Balkwill, F. R., Capasso, M., & Hagemann, T. (2012). The tumor microenvironment at a glance. *Journal of Cell Science*, *125*(23), 5591–5596. https://doi.org/10.1242/jcs.116392

Balzano, M., De Grandis, M., Vu Manh, T. P., Chasson, L., Bardin, F., Farina, A., … Mancini, S. J. C. (2019). Nidogen-1 Contributes to the Interaction Network Involved in Pro-B Cell Retention in the Peri-sinusoidal Hematopoietic Stem Cell Niche. *Cell Reports*, *26*(12), 3257-3271.e8. https://doi.org/10.1016/j.celrep.2019.02.065

Bejarano, L., Jordão, M. J. C., & Joyce, J. A. (2021). Therapeutic targeting of the tumor microenvironment. *Cancer Discovery*, *11*(4), 933–959. https://doi.org/10.1158/2159-8290.CD-20-1808

Benavente, S., Sánchez-García, A., Naches, S., LLeonart, M. E., & Lorente, J. (2020). Therapy-Induced Modulation of the Tumor Microenvironment: New Opportunities for Cancer Therapies. *Frontiers in Oncology*, *10*(October), 1–18. https://doi.org/10.3389/fonc.2020.582884

Besnard, A. G., Guabiraba, R., Niedbala, W., Palomo, J., Reverchon, F., Shaw, T. N., … Liew, F. Y. (2015). IL-33-Mediated Protection against Experimental Cerebral Malaria Is Linked to Induction of Type 2 Innate Lymphoid Cells, M2 Macrophages and Regulatory T Cells. *PLoS Pathogens*, *11*(2), 1–21. https://doi.org/10.1371/journal.ppat.1004607

Biffi, G., & Tuveson, D. A. (2020). Diversity and Biology of Cancer-Associated Fibroblasts. *Physiological Reviews*, *53*(9), 1689–1699.

Binnewies, M., Roberts, E. W., Kersten, K., Chan, V., Fearon, D. F., Merad, M., … Krummel, M. F. (2018). Understanding the tumor immune microenvironment (TIME) for effective therapy. *Nat Med*, *24*(5), 541–550. https://doi.org/10.4324/9781315102269-3

Bonnans, C., Chou, J., & Werb, Z. (2014). Remodelling the extracellular matrix in development and disease. *Nature Reviews. Molecular Cell Biology*, *15*(12), 786–801. https://doi.org/10.1038/nrm3904.Remodelling

Boukhaled, G. M., Harding, S., & Brooks, D. G. (2021). Opposing Roles of Type i Interferons in Cancer Immunity. *Annual Review of Pathology: Mechanisms of Disease*, *16*, 167–198. https://doi.org/10.1146/annurev-pathol-031920-093932

Bourd-Boittin, K., Bonnier, D., Leyme, A., Mari, B., Tuffery, P., Samson, M., … Theret, N. (2011). Protease profiling of liver fibrosis reveals the ADAM metallopeptidase with thrombospondin type 1 motif, 1 as a central activator of transforming growth factor beta. *Hepatology*, *54*(6), 2173–2184. https://doi.org/10.1002/hep.24598

Boyle, S. T., Zahied Johan, M., & Samuel, M. S. (2021). Tumour-directed microenvironment remodelling at a glance. *Journal of Cell Science*, *133*(24), 1–9. https://doi.org/10.1242/jcs.247783

Brunn, D., Turkowski, K., Günther, S., Weigert, A., Muley, T., Kriegsmann, M., … Savai, R. (2021). Interferon regulatory factor 9 promotes lung cancer progression via regulation of versican. *Cancers*, *13*(2), 1–19. https://doi.org/10.3390/cancers13020208

Bruno, A., Mortara, L., Baci, D., Noonan, D. M., & Albini, A. (2019). Myeloid Derived Suppressor Cells Interactions With Natural Killer Cells and Pro-angiogenic Activities: Roles in Tumor Progression. *Frontiers in Immunology*, *10*(April), 771.

https://doi.org/10.3389/fimmu.2019.00771

Caiado, F., Silva-Santos, B., & Norell, H. (2016). Intra-tumour heterogeneity – going beyond genetics. *FEBS Journal*, *283*, 2245–2258. https://doi.org/10.1111/febs.13705

Cal, S., & López-Otín, C. (2015). ADAMTS proteases and cancer. *Matrix Biology*, *44–46*, 77–85. https://doi.org/10.1016/j.matbio.2015.01.013

Campbell, N. E., Kellenberger, L., Greenaway, J., Moorehead, R. a, Linnerth-Petrik, N. M., & Petrik, J. (2010). Extracellular matrix proteins and tumor angiogenesis. *Journal of Oncology*, *2010*, 586905. https://doi.org/10.1155/2010/586905

Canals, F., Colome, N., Ferrer, C., Plaza-Calonge Mdel, C., & Rodriguez-Manzaneque, J. C. (2006). Identification of substrates of the extracellular protease ADAMTS1 by DIGE proteomic analysis. *Proteomics*, *6 Suppl 1*, S28-35. https://doi.org/10.1002/pmic.200500446

Carmeliet, P., & Jain, R. K. (2011a). Molecular mechanisms and clinical applications of angiogenesis. *Nature*, *473*(7347), 298–307. https://doi.org/doi:10.1038/nature10144

Carmeliet, P., & Jain, R. K. (2011b). Principles and mechanisms of vessel normalization for cancer and other angiogenic diseases. *Nature Reviews Drug Discovery*, *10*(6), 417–427. https://doi.org/10.1038/nrd3455

Casal, C., Torres-Collado, A. X., Plaza-Calonge, M. D. C., Martino-Echarri, E., Y Cajal, S. R., Rojo, F., … Rodríguez-Manzaneque, J. C. (2010). ADAMTS1 contributes to the acquisition of an endothelial-like phenotype in plastic tumor cells. *Cancer Research*, *70*(11), 4676–4686. https://doi.org/10.1158/0008-5472.CAN-09-4197

Chang, M. Y., Kang, I., Gale Jr, M., Manicone, A. M., Kinsella, M. G., Braun, K. R., … Frevert, C. W. (2017). Versican is produced by Trif- and type I interferon-dependent signaling in macrophages and contributes to fine control of innate immunity in lungs. *Am J Physiol Lung Cell Mol Physiol*, *313*(6), L1069–L1086. https://doi.org/10.1152/ajplung.00353.2017

Chang, M. Y., Tanino, Y., Vidova, V., Kinsella, M. G., Chan, C. K., Johnson, P. Y., … Frevert, C. W. (2014). A rapid increase in macrophage-derived versican and hyaluronan in infectious lung disease. *Matrix Biology*, *34*, 1–12. https://doi.org/10.1016/j.matbio.2014.01.011

Chen, D. S., & Mellman, I. (2017). Elements of cancer immunity and the cancer-immune set point. *Nature*, *541*(7637), 321–330. https://doi.org/10.1038/nature21349

Ciombor, K. K., Berlin, J., & Chan, E. (2013). Aflibercept. *Clinical Cancer Research*, *19*(8), 1920–1925. https://doi.org/10.1158/1078-0432.CCR-12-2911

Cox, T. R. (2021). The matrix in cancer. *Nature Reviews Cancer 2021*, *0123456789*, 1–22. https://doi.org/10.1038/s41568-020-00329-7

Crawford, Y., & Ferrara, N. (2009). VEGF inhibition: Insights from preclinical and clinical studies. *Cell and Tissue Research*, *335*(1), 261–269. https://doi.org/10.1007/s00441-008-0675-8

Daftarian, N., Zandi, S., Piryaie, G., Nikougoftar Zarif, M., Ranaei Pirmardan, E., Yamaguchi, M., … Hafezi-Moghadam, A. (2020). Peripheral blood CD163(+) monocytes and soluble CD163 in dry and neovascular age-related macular degeneration. *FASEB Journal*, *34*(6), 8001–8011. https://doi.org/10.1096/fj.201901902RR

Dagogo-Jack, I., & Shaw, A. T. (2018). Tumour heterogeneity and resistance to cancer therapies. *Nature Reviews Clinical Oncology*, *15*(2), 81–94. https://doi.org/10.1038/nrclinonc.2017.166

De Arao Tan, I., Ricciardelli, C., & Russell, D. L. (2013). The metalloproteinase ADAMTS1: A comprehensive review of its role in tumorigenic and metastatic pathways. *International Journal of Cancer*, *133*(10), 2263–2276. https://doi.org/10.1002/ijc.28127

De Bock, K., Cauwenberghs, S., & Carmeliet, P. (2011). Vessel abnormalization: another hallmark of cancer? Molecular mechanisms and therapeutic implications. *Current Opinion in Genetics & Development*, *21*(1), 73–79. https://doi.org/10.1016/j.gde.2010.10.008

De Cicco, P., Ercolano, G., & Ianaro, A. (2020). The New Era of Cancer Immunotherapy: Targeting Myeloid-Derived Suppressor Cells to Overcome Immune Evasion. *Frontiers in Immunology*, *11*(July), 1–21. https://doi.org/10.3389/fimmu.2020.01680

De Palma, M., Biziato, D., & Petrova, T. V. (2017). Microenvironmental regulation of tumour angiogenesis. *Nature Reviews Cancer*, *17*(8), 457–474. https://doi.org/10.1038/nrc.2017.51

Dhakal, B., Pagenkopf, A., Mushtaq, M. U., Cunningham, A. M., Flietner, E., Morrow, Z., … Asimakopoulos, F. (2019). Versican proteolysis predicts immune effector infiltration and post-transplant survival in myeloma. *Leukemia and Lymphoma*, *60*(10), 2558–2562. https://doi.org/10.1080/10428194.2019.1585836

Ding, L., Liang, G., Yao, Z., Zhang, J., Liu, R., Chen, H., … He, Q. (2015). Metformin prevents cancer metastasis by inhibiting M2-like polarization of tumor

associated macrophages. *Oncotarget*, *6*(34), 36441–36455. https://doi.org/10.18632/oncotarget.5541

Dobin, A., Davis, C. A., Schlesinger, F., Drenkow, J., Zaleski, C., Jha, S., … Gingeras, T. R. (2013). STAR: Ultrafast universal RNA-seq aligner. *Bioinformatics*, *29*(1), 15–21. https://doi.org/10.1093/bioinformatics/bts635

Du, H., Shih, C., Wosczyna, M. N., Mueller, A. A., Cho, J., Aggarwal, A., … Feldman, B. J. (n.d.). Macrophage-released ADAMTS1 promotes muscle stem cell activation. *Nature Communications*. https://doi.org/10.1038/s41467-017-00522-7

Dubail, J., & Apte, S. S. (2015). Insights on ADAMTS proteases and ADAMTS-like proteins from mammalian genetics. *Matrix Biology*, *44–46*, 24–37. https://doi.org/10.1016/j.matbio.2015.03.001

Eble, J. A., & Niland, S. (2019). The extracellular matrix in tumor progression and metastasis. *Clinical and Experimental Metastasis*, *36*(3), 171–198. https://doi.org/10.1007/s10585-019-09966-1

Erin, N., Grahovac, J., Brozovic, A., & Efferth, T. (2020). Tumor microenvironment and epithelial mesenchymal transition as targets to overcome tumor multidrug resistance. *Drug Resistance Updates*, *53*(May), 100715. https://doi.org/10.1016/j.drup.2020.100715

Esselens, C., Malapeira, J., Colomé, N., Casal, C., Rodríguez-Manzaneque, J. C., Canals, F., & Arribas, J. (2010). The cleavage of semaphorin 3C induced by ADAMTS1 promotes cell migration. *Journal of Biological Chemistry*, *285*(4), 2463–2473. https://doi.org/10.1074/jbc.M109.055129

Faas, M., Ipseiz, N., Ackermann, J., Culemann, S., Grüneboom, A., Schröder, F., … Krönke, G. (2021). IL-33-induced metabolic reprogramming controls the differentiation of alternatively activated macrophages and the resolution of inflammation. *Immunity*, *54*, 1–16. https://doi.org/10.1016/j.immuni.2021.09.010

Fang, M., Li, Y., Huang, K., Qi, S., Zhang, J., Zgodzinski, W., … Wang, L. (2017). IL33 promotes colon cancer cell stemness via JNK activation and macrophage recruitment. *Cancer Research*, *77*(10), 2735–2745. https://doi.org/10.1158/0008-5472.CAN-16-1602

Fanhchaksai, K., Okada, F., Nagai, N., Pothacharoen, P., Kongtawelert, P., Hatano, S., … Watanabe, H. (2016). Host stromal versican is essential for cancer-associated fibroblast function to inhibit cancer growth. *International Journal of Cancer*, *138*(3), 630–641. https://doi.org/10.1002/ijc.29804

Fernández-Rodríguez, R., Rodríguez-Baena, F. J., Martino-Echarri, E., Peris-Torres, C.,

Plaza-Calonge, M. del C., & Rodríguez-Manzaneque, J. C. (2016). Stroma-derived but not tumor ADAMTS1 is a main driver of tumor growth and metastasis. *Oncotarget*, *7*(23), 34507–34519. https://doi.org/10.18632/oncotarget.8922

Folkman, J. (1971). Tumor angiogenesis: therapeutic implications. *New England Journal of Medicine*, *285*(21), 1182–1186.

Gaggero, S., Bruschi, M., Petretto, A., Parodi, M., Zotto, G. Del, Lavarello, C., … Cantoni, C. (2018). Nidogen-1 is a novel extracellular ligand for the NKp44 activating receptor. *OncoImmunology*, *7*(9). https://doi.org/10.1080/2162402X.2018.1470730

Gajewski, T. F., Schreiber, H., & Fu, Y.-X. (2013). Innate and adaptive immune cells in the tumor microenvironment. *Nature Immunology*, *14*(10), 1014–1022. https://doi.org/10.1038/ni.2703

Gao, H., Cheng, Y., Chen, Y., Luo, F., Shao, Y., Sun, Z., & Bai, C. (2020). The expression of versican and its role in pancreatic neuroendocrine tumors. *Pancreatology*, *20*(1), 142–147. https://doi.org/10.1016/j.pan.2019.11.009

Garner, H., & de Visser, K. E. (2020). Immune crosstalk in cancer progression and metastatic spread: a complex conversation. *Nature Reviews Immunology*, *20*(8), 483–497. https://doi.org/10.1038/s41577-019-0271-z

Gonzalez, H., Hagerling, C., & Werb, Z. (2018). Roles of the immune system in cancer: From tumor initiation to metastatic progression. *Genes and Development*, *32*(19–20), 1267–1284. https://doi.org/10.1101/GAD.314617.118

Gorter, A., Zijlmans, H. J., van Gent, H., Trimbos, J. B., Fleuren, G. J., & Jordanova, E. S. (2010). Versican expression is associated with tumor-infiltrating CD8-positive T cells and infiltration depth in cervical cancer. *Modern Pathology*, *23*(12), 1605–1615. https://doi.org/10.1038/modpathol.2010.154

Goswami, K. K., Ghosh, T., Ghosh, S., Sarkar, M., Bose, A., & Baral, R. (2017). Tumor promoting role of anti-tumor macrophages in tumor microenvironment. *Cellular Immunology*, (April), 1–10. https://doi.org/10.1016/j.cellimm.2017.04.005

Greten, F. R., & Grivennikov, S. I. (2019). Inflammation and cancer: Triggers, mechanisms and consequences. *Immunity*, *51*(1), 27–41. https://doi.org/10.1016/j.immuni.2019.06.025.Inflammation

Gupta, N., Kumar, R., & Sharma, A. (2016). Versikine, a proteolysis product of Versican: novel therapeutics for multiple myeloma. *Translational Cancer Research*, *5*(S7), S1437–S1439. https://doi.org/10.21037/tcr.2016.12.67

Gustavsson, H., Wang, W., Jennbacken, K., Welén, K., & Damber, J. E. (2009).

ADAMTS1, a putative anti-angiogenic factor, is decreased in human prostate cancer. *BJU International*, *104*(11), 1786–1790. https://doi.org/10.1111/j.1464-410X.2009.08676.x

Haibe, Y., Kreidieh, M., El Hajj, H., Khalifeh, I., Mukherji, D., Temraz, S., & Shamseddine, A. (2020). Resistance Mechanisms to Anti-angiogenic Therapies in Cancer. *Frontiers in Oncology*, *10*(February). https://doi.org/10.3389/fonc.2020.00221

Hanahan, D. (2022). Hallmarks of Cancer: New Dimensions. *Cancer Discovery*, *12*(1), 31–46. https://doi.org/10.1158/2159-8290.CD-21-1059

Hanahan, D., & Coussens, L. M. (2012). Accessories to the Crime: Functions of Cells Recruited to the Tumor Microenvironment. *Cancer Cell*, *21*(3), 309–322. https://doi.org/10.1016/j.ccr.2012.02.022

Hanahan, D., & Weinberg, R. A. (2000). The Hallmarks of Cancer. *Cell*, *100*, 57–70.

Hanahan, D., & Weinberg, R. A. (2011). Hallmarks of cancer: The next generation. *Cell*, *144*(5), 646–674. https://doi.org/10.1016/j.cell.2011.02.013

Hatano, S., & Watanabe, H. (2020). Regulation of Macrophage and Dendritic Cell Function by Chondroitin Sulfate in Innate to Antigen-Specific Adaptive Immunity. *Frontiers in Immunology*, *11*(March), 1–10. https://doi.org/10.3389/fimmu.2020.00232

Hausser, J., & Alon, U. (2020). Tumour heterogeneity and the evolutionary trade-offs of cancer. *Nature Reviews Cancer*, *20*(4), 247–257. https://doi.org/10.1038/s41568-020-0241-6

He, X., & Xu, C. (2020). Immune checkpoint signaling and cancer immunotherapy. *Cell Research*, *30*(8), 660–669. https://doi.org/10.1038/s41422-020-0343-4

Hinohara, K., & Polyak, K. (2019). Intratumoral Heterogeneity: More Than Just Mutations. *Trends in Cell Biology*, *29*(7), 569–579. https://doi.org/10.1016/j.tcb.2019.03.003

Hope, C., Emmerich, P. B., Papadas, A., Pagenkopf, A., Matkowskyj, K. A., De, D. R. Van, … Johnson, M. G. (2017). Versican-Derived Matrikines Regulate Batf3 − Dendritic Cell Differentiation and Promote T Cell Infiltration in Colorectal Cancer. https://doi.org/10.4049/jimmunol.1700529

Hope, C., Foulcer, S., Jagodinsky, J., Chen, S. X., Jensen, J. L., Patel, S., … Asimakopoulos, F. (2016). Immunoregulatory roles of versican proteolysis in the myeloma microenvironment. *Blood*, *128*(5), 680–685. https://doi.org/10.1182/blood-2016-03-705780

Hu, F., Dzaye, O. D. A., Hahn, A., Yu, Y., Scavetta, R. J., Dittmar, G., … Kettenmann, H. (2015). Glioma-derived versican promotes tumor expansion via glioma-associated microglial/macrophages Toll-like receptor 2 signaling. *Neuro-Oncology*, *17*(2), 200–210. https://doi.org/10.1093/neuonc/nou324

Iruela-Arispe, ML. Carpizo, D. Luque, A. (2003). ADAMTS1: A matrix metalloprotease with angioinhibitory properties. *Ann. N.Y Acad. Sci.*, *995*, 183–190.

Ishikawa, E., Miyazaki, T., Takano, S., & Akutsu, H. (2021). Anti-angiogenic and macrophage-based therapeutic strategies for glioma immunotherapy. *Brain Tumor Pathology*, *38*(3), 149–155. https://doi.org/10.1007/s10014-021-00402-5

Islam, S., & Watanabe, H. (2020). Versican: A Dynamic Regulator of the Extracellular Matrix. *Journal of Histochemistry and Cytochemistry*. https://doi.org/10.1369/0022155420953922

Itatani, Y., Kawada, K., Yamamoto, T., & Sakai, Y. (2018). Resistance to anti-angiogenic therapy in cancer-alterations to anti-VEGF pathway. *International Journal of Molecular Sciences*, *19*(4), 1–18. https://doi.org/10.3390/ijms19041232

Jakab, M., Rostalski, T., Lee, K. H., Mogler, C., & Augustin, H. G. (2022). Tie2 Receptor in Tumor-In fi ltrating Macrophages Is Dispensable for Tumor Angiogenesis and Tumor Relapse after Chemotherapy. *Cancer Research*, *82*, 1353–1364. https://doi.org/10.1158/0008-5472.CAN-21-3181

Jászai, J., & Schmidt, M. H. H. (2019). Trends and challenges in tumor anit-angiogenic therapies. *Cells*, *8*(1102), 1–35.

Jo, A., Nilsson, T., Fritsche-danielson, R., Hammarstro, A., Behrendt, M., Andersson, J., … Hurt-camejo, E. (2005). Role of ADAMTS-1 in Atherosclerosis Remodeling of Carotid Artery , Immunohistochemistry , and Proteolysis of Versican. https://doi.org/10.1161/01.ATV.0000150045.27127.37

Jorgovanovic, D., Song, M., Wang, L., & Zhang, Y. (2020). Roles of IFN-γin tumor progression and regression: A review. *Biomarker Research*, *8*(1), 1–16. https://doi.org/10.1186/s40364-020-00228-x

Junttila, M. R., & Sauvage, F. J. De. (2013). Influence of tumour micro-environment. https://doi.org/10.1038/nature12626

Jürgensen, H. J., van Putten, S., Nørregaard, K. S., Bugge, T. H., Engelholm, L. H., Behrendt, N., & Madsen, D. H. (2020). Cellular uptake of collagens and implications for immune cell regulation in disease. *Cellular and Molecular Life Sciences : CMLS*. https://doi.org/10.1007/s00018-020-03481-3

Karamanos, N. K., Piperigkou, Z., Passi, A., Götte, M., Rousselle, P., & Vlodavsky, I. (2021). Extracellular matrix-based cancer targeting. *Trends in Molecular Medicine*, *27*(10), 1000–1013. https://doi.org/10.1016/j.molmed.2021.07.009

Keire, P. A., Kang, I., & Wight, T. N. (2017). Versican : Role in Cancer Tumorigenesis. https://doi.org/10.1007/978-3-319-60907-2_4

Keklikoglou, I., Kadioglu, E., Bissinger, S., Orend, G., Ries, C. H., Palma, M. De, … Bissinger, S. (2018). Periostin Limits Tumor Response to VEGFA Inhibition Report Periostin Limits Tumor Response to VEGFA Inhibition, 2530–2540. https://doi.org/10.1016/j.celrep.2018.02.035

Kelwick, R., Desanlis, I., Wheeler, G. N., & Edwards, D. R. (2015). The ADAMTS (A Disintegrin and Metalloproteinase with Thrombospondin motifs) family. *Genome Biology*, *16*, 113. https://doi.org/10.1186/s13059-015-0676-3

Khandia, R., & Munjal, A. (2020). Interplay between inflammation and cancer. *Advances in Protein Chemistry and Structural Biology*, *119*, 199–245. https://doi.org/10.1016/bs.apcsb.2019.09.004

Kim, S. I., Cassella, C. R., & Byrne, K. T. (2021). Tumor Burden and Immunotherapy: Impact on Immune Infiltration and Therapeutic Outcomes. *Frontiers in Immunology*, *11*(February), 1–15. https://doi.org/10.3389/fimmu.2020.629722

Kim, S., Takahashi, H., Lin, W. W., Descargues, P., Grivennikov, S., Kim, Y., … Karin, M. (2009). Carcinoma-produced factors activate myeloid cells through TLR2 to stimulate metastasis. *Nature*, *457*(7225), 102–106. https://doi.org/10.1038/nature07623

Kohli, K., Pillarisetty, V. G., & Kim, T. S. (2021). Key chemokines direct migration of immune cells in solid tumors. *Cancer Gene Therapy*. https://doi.org/10.1038/s41417-021-00303-x

Kruegel, J., & Miosge, N. (2010). Basement membrane components are key players in specialized extracellular matrices. *Cellular and Molecular Life Sciences*, *67*(17), 2879–2895. https://doi.org/10.1007/s00018-010-0367-x

Kuczek, D. E., Larsen, A. M. H., Thorseth, M. L., Carretta, M., Kalvisa, A., Siersbæk, M. S., … Madsen, D. H. (2019). Collagen density regulates the activity of tumor-infiltrating T cells. *Journal for ImmunoTherapy of Cancer*, *7*(1), 1–15. https://doi.org/10.1186/s40425-019-0556-6

Kuno, K, Kanada, N., Nakashima, E., Fujiki, F., Ichimura, F., & Matsushima, K. (1997). Molecular cloning of a gene encoding a new type of metalloproteinase-disintegrin family protein with thrombospondin motifs as an inflammation associated gene. *The Journal of Biological Chemistry*, *272*(1), 556–562.

https://doi.org/10.1074/jbc.272.1.556

Kuno, Kouji, Bannai, K., Hakozaki, M., Matsushima, K., & Hirose, K. (2004). The carboxyl-terminal half region of ADAMTS-1 suppresses both tumorigenicity and experimental tumor metastatic potential. *Biochemical and Biophysical Research Communications*, *319*(4), 1327–1333. https://doi.org/10.1016/j.bbrc.2004.05.105

Laplane, L., Duluc, D., Bikfalvi, A., Larmonier, N., & Pradeu, T. (2019). Beyond the tumour microenvironment. *International Journal of Cancer*, *145*(10), 2611–2618. https://doi.org/10.1002/ijc.32343

Larsen, A. M., Kuczek, D., Kalvisa, A., Siersbæk, M., Thorseth, M.-L., Johansen, A. Z., … Madsen, D. (2020). Collagen Density Modulates the Immunosuppressive Functions of Macrophages. *The Journal of Immunology*, *205*(5), 1461–1472. https://doi.org/doi:10.4049/jimmunol.1900789

Lee, N. V., Rodriguez-Manzaneque, J. C., Thai, S. N. M., Twal, W. O., Luque, A., Lyons, K. M., … Iruela-Arispe, M. L. (2005). Fibulin-1 acts as a cofactor for the matrix metalloprotease ADAMTS-1. *Journal of Biological Chemistry*, *280*(41), 34796–34804. https://doi.org/10.1074/jbc.M506980200

Lee, N. V, Sato, M., Annis, D. S., Loo, J. a, Wu, L., Mosher, D. F., & Iruela-Arispe, M. L. (2006). ADAMTS1 mediates the release of antiangiogenic polypeptides from TSP1 and 2. *The EMBO Journal*, *25*(22), 5270–5283. https://doi.org/10.1038/sj.emboj.7601400

Li, B., & Dewey, C. N. (2011). RSEM: Accurate transcript quantification from RNA-Seq data with or without a reference genome. *BMC Bioinformatics*, *12*(323), 1–16. https://doi.org/10.1186/1471-2105-12-323

Li, C., Xu, X., Wei, S., Jiang, P., Xue, L., & Wang, J. (2021). Tumor-associated macrophages: potential therapeutic strategies and future prospects in cancer. *Journal for ImmunoTherapy of Cancer*, *9*(1). https://doi.org/10.1136/jitc-2020-001341

Li, L., Yu, R., Cai, T., Chen, Z., Lan, M., Zou, T., … Cai, Y. (2020). Effects of immune cells and cytokines on inflammation and immunosuppression in the tumor microenvironment. *International Immunopharmacology*, *88*(August), 106939. https://doi.org/10.1016/j.intimp.2020.106939

Li, T., Kang, G., Wang, T., & Huang, H. (2018). Tumor angiogenesis and anti-angiogenic gene therapy for cancer (Review). *Oncology Letters*, *16*(1), 687–702. https://doi.org/10.3892/ol.2018.8733

Lind, T., Birch, M. A., & McKie, N. (2006). Purification of an insect derived

recombinant human ADAMTS-1 reveals novel gelatin (type I collagen) degrading activities. *Molecular and Cellular Biochemistry*, *281*(1–2), 95–102. https://doi.org/10.1007/s11010-006-0637-y

Liu, Y.-J., Xu, Y., & Yu, Q. (2006). Full-length ADAMTS-1 and the ADAMTS-1 fragments display pro- and antimetastatic activity, respectively. *Oncogene*, *25*(17), 2452–2467. https://doi.org/10.1038/sj.onc.1209287

Lopes-Coelho, F., Martins, F., Pereira, S. A., & Serpa, J. (2021). Anti-angiogenic therapy: Current challenges and future perspectives. *International Journal of Molecular Sciences*, *22*(7). https://doi.org/10.3390/ijms22073765

Lu, Peirong, Li, L., Kuno, K., Wu, Y., Li, Y., Zhang, X., … Alerts, E. (2017). Protective Roles of the Fractalkine/CX3CL1-CX3CR1 Interactions in Alkali-Induced Corneal Neovascularization through Enhanced Antiangiogenic Factor Expression. https://doi.org/10.4049/jimmunol.180.6.4283

Lu, Pengfei, Weaver, V. M., & Werb, Z. (2012). The extracellular matrix: A dynamic niche in cancer progression. *Journal of Cell Biology*, *196*(4), 395–406. https://doi.org/10.1083/jcb.201102147

Lugano, R., Ramachandran, M., & Dimberg, A. (2020). Tumor angiogenesis: causes, consequences, challenges and opportunities. *Cellular and Molecular Life Sciences*, *77*(9), 1745–1770. https://doi.org/10.1007/s00018-019-03351-7

Luque, A., Carpizo, D. R., & Iruela-Arispe, M. L. (2003). ADAMTS1/METH1 inhibits endothelial cell proliferation by direct binding and sequestration of VEGF165. *Journal of Biological Chemistry*, *278*(26), 23656–23665. https://doi.org/10.1074/jbc.M212964200

Mabuchi, S., Sasano, T., & Komura, N. (2021). Targeting myeloid-derived suppressor cells in ovarian cancer. *Cells*, *10*(2), 1–12. https://doi.org/10.3390/cells10020329

Madden, E. C., Gorman, A. M., Logue, S. E., & Samali, A. (2020). Tumour Cell Secretome in Chemoresistance and Tumour Recurrence. *Trends in Cancer*, *6*(6), 489–505. https://doi.org/10.1016/j.trecan.2020.02.020

Madsen, D. H., Siersbæk, M. S., Grøntved, L., Weigert, R., Siersbæk, M. S., & Kuczek, D. E. (2017). Tumor-Associated Macrophages Derived from Circulating Inflammatory Monocytes Degrade Collagen through Cellular Uptake Report Tumor-Associated Macrophages Derived from Circulating Inflammatory Monocytes Degrade Collagen through Cellular Uptake, 3662–3671. https://doi.org/10.1016/j.celrep.2017.12.011

Mai, S., Liu, L., Jiang, J., Ren, P., Diao, D., Wang, H., & Cai, K. (2021). Oesophageal

squamous cell carcinoma–associated IL-33 rewires macrophage polarization towards M2 via activating ornithine decarboxylase. *Cell Proliferation*, *54*(2), 1–12. https://doi.org/10.1111/cpr.12960

Mantovani, A., Marchesi, F., Malesci, A., Laghi, L., & Allavena, P. (2017). Tumor-Associated Macrophages as Treatment Targets in Oncology. *Nat Rev Clin Oncol.*, *14*(7), 399–416. https://doi.org/10.1038/nrclinonc.2016.217.Tumor-Associated

Mantovani, A., Sozzani, S., Locati, M., Allavena, P., & Sica, A. (2002). Macrophage polarization: Tumor-associated macrophages as a paradigm for polarized M2 mononuclear phagocytes. *Trends in Immunology*, *23*(11), 549–555. https://doi.org/10.1016/S1471-4906(02)02302-5

Martino-Echarri, E., Fernandez-Rodriguez, R., Bech-Serra, J. J., Plaza-Calonge, M. del C., Vidal, N., Casal, C., … Rodriguez-Manzaneque, J. C. (2014). Relevance of IGFBP2 proteolysis in glioma and contribution of the extracellular protease ADAMTS1. *Oncotarget*, *5*(12), 4295–4304. https://doi.org/10.18632/oncotarget.2009

Martino-Echarri, E., Fernández-Rodríguez, R., Rodríguez-Baena, F. J., Barrientos-Durán, A., Torres-Collado, A. X., Del Carmen Plaza-Calonge, M., … Rodríguez-Manzaneque, J. C. (2013a). Contribution of ADAMTS1 as a tumor suppressor gene in human breast carcinoma. Linking its tumor inhibitory properties to its proteolytic activity on nidogen-1 and nidogen-2. *International Journal of Cancer*, *133*(10), 2315–2324. https://doi.org/10.1002/ijc.28271

Martino-Echarri, E., Fernández-Rodríguez, R., Rodríguez-Baena, F. J., Barrientos-Durán, A., Torres-Collado, A. X., Del Carmen Plaza-Calonge, M., … Rodríguez-Manzaneque, J. C. (2013b). Contribution of ADAMTS1 as a tumor suppressor gene in human breast carcinoma. Linking its tumor inhibitory properties to its proteolytic activity on nidogen-1 and nidogen-2. *International Journal of Cancer*, *133*(10), 2315–2324. https://doi.org/10.1002/ijc.28271

Marusyk, A., Janiszewska, M., & Polyak, K. (2020). Intratumor Heterogeneity: The Rosetta Stone of Therapy Resistance. *Cancer Cell*, *37*(4), 471–484. https://doi.org/10.1016/j.ccell.2020.03.007

Marusyk, A., & Polyak, K. (2010). Tumor heterogeneity: causes and consequences. *Biochim Biophys Acta*, *1805*(1), 105–117. https://doi.org/10.1016/j.earlhumdev.2006.05.022

Masuda, A., Yasuoka, H., Satoh, T., Okazaki, Y., Yamaguchi, Y., & Kuwana, M. (2013). Versican is upregulated in circulating monocytes in patients with systemic sclerosis and amplifies a CCL2-mediated pathogenic loop. *Arthritis Research & Therapy*, *15*(4), R74. https://doi.org/10.1186/ar4251

Mead, T. J., & Apte, S. S. (2018). ADAMTS proteins in human disorders. *Matrix Biology*, *71–72*, 225–239. https://doi.org/10.1016/j.matbio.2018.06.002

Mittaz, L., Russell, D. L., Wilson, T., Brasted, M., Tkalcevic, J., Salamonsen, L. A., … Pritchard, M. A. (2004). Adamts-1 Is Essential for the Development and Function of the Urogenital System. *Biology of Reproduction*, *70*(4), 1096–1105. https://doi.org/10.1095/biolreprod.103.023911

Mohamedi, Y., Fontanil, T., Cobo, T., Cal, S., & Obaya, A. J. (2020). New Insights into ADAMTS Metalloproteases in the Central Nervous System. *Biomolecules*, *10*(3), 1–17. https://doi.org/10.3390/biom10030403

Moorman, H. R., Poschel, D., Klement, J. D., Lu, C., Redd, P. S., & Liu, K. (2020). Osteopontin: A key regulator of tumor progression and immunomodulation. *Cancers*, *12*(11), 1–31. https://doi.org/10.3390/cancers12113379

Mushtaq, M. U., Papadas, A., Pagenkopf, A., Flietner, E., Morrow, Z., Chaudhary, S. G., & Asimakopoulos, F. (2018). Tumor matrix remodeling and novel immunotherapies: The promise of matrix-derived immune biomarkers. *Journal for ImmunoTherapy of Cancer*, *6*(1), 1–14. https://doi.org/10.1186/s40425-018-0376-0

Najafi, M., Farhood, B., & Mortezaee, K. (2019). Extracellular matrix (ECM) stiffness and degradation as cancer drivers. *Journal of Cellular Biochemistry*, *120*(3), 2782–2790. https://doi.org/10.1002/jcb.27681

Nam, G. H., Hong, Y., Choi, Y., Kim, G. B., Kim, Y. K., Yang, Y., & Kim, I. S. (2019). An optimized protocol to determine the engulfment of cancer cells by phagocytes using flow cytometry and fluorescence microscopy. *Journal of Immunological Methods*, *470*(March), 27–32. https://doi.org/10.1016/j.jim.2019.04.007

Ng, Y. H., Zhu, H., Pallen, C. J., Leung, P. C. K., & MacCalman, C. D. (2006). Differential effects of interleukin-1β and transforming growth factor-β1 on the expression of the inflammation-associated protein, ADAMTS-1, in human decidual stromal cells in vitro. *Human Reproduction*, *21*(8), 1990–1999. https://doi.org/10.1093/humrep/del108

Oller, J., Méndez-Barbero, N., Ruiz, E. J., Villahoz, S., Renard, M., Canelas, L. I., … Redondo, J. M. (2017). Nitric oxide mediates aortic disease in mice deficient in the metalloprotease Adamts1 and in a mouse model of Marfan syndrome. *Nature Medicine*, (December 2016). https://doi.org/10.1038/nm.4266

Oveland, E., Karlsen, T. V., Haslene-Hox, H., Semaeva, E., Janaczyk, B., Tenstad, O., & Wiig, H. (2012). Proteomic evaluation of inflammatory proteins in rat spleen interstitial fluid and lymph during LPS-induced systemic inflammation reveals

increased levels of ADAMST1. *Journal of Proteome Research*, *11*(11), 5338–5349. https://doi.org/10.1021/pr3005666

Papadas, A., Arauz, G., Cicala, A., Wiesner, J., & Asimakopoulos, F. (2020). Versican and Versican-matrikines in Cancer Progression, Inflammation, and Immunity. *Journal of Histochemistry and Cytochemistry*. https://doi.org/10.1369/0022155420937098

Pappas, A. G., Magkouta, S., Pateras, I. S., Skianis, I., Moschos, C., Vazakidou, M. E., … Kalomenidis, I. (2019). Versican modulates tumor-associated macrophage properties to stimulate mesothelioma growth. *OncoImmunology*, *8*(2), 1–9. https://doi.org/10.1080/2162402X.2018.1537427

Peris-Torres, C., Plaza-calonge, M. C., López-domínguez, R., Barrientos-durán, A., Carmona-sáez, P., & Carlos, J. (2020). Extracellular Protease ADAMTS1 Is Required at Early Stages of Human Uveal Melanoma Development by Inducing Stemness and Endothelial-Like Features on Tumor Cells. *Cancers*, *12*(801), 1–20. https://doi.org/10.3390/cancers12040801

Pickup, M. W., Mouw, J. K., & Weaver, V. M. (2014). The extracellular matrix modulates the hallmarks of cancer. *EMBO Reports*, *15*, 1243–1253.

Pinto, S. M., Subbannayya, Y., Rex, D. A. B., Raju, R., Chatterjee, O., Advani, J., … Pandey, A. (2018). A network map of IL-33 signaling pathway. *Journal of Cell Communication and Signaling*, *12*(3), 615–624. https://doi.org/10.1007/s12079-018-0464-4

Pitt, J. M., Marabelle, A., Eggermont, A., & Soria, J. (2016). Targeting the tumor microenvironment : removing obstruction to anticancer immune responses and immunotherapy. *Annals of Oncology Advance Access*, 1–43. https://doi.org/10.1093/annonc/mdw168

Poh, A. R., & Ernst, M. (2018). Targeting macrophages in cancer: From bench to bedside. *Frontiers in Oncology*, *8*(MAR), 1–16. https://doi.org/10.3389/fonc.2018.00049

Porter, S., Clark, I. M., Kevorkian, L., & Edwards, D. R. (2005). The ADAMTS metalloproteinases. *The Biochemical Journal*, *386*(Pt 1), 15–27. https://doi.org/10.1042/BJ20040424

Potente, M., Gerhardt, H., & Carmeliet, P. (2011). Basic and therapeutic aspects of angiogenesis. *Cell*, *146*(6), 873–887. https://doi.org/10.1016/j.cell.2011.08.039

Priceman, S. J., Sung, J. L., Shaposhnik, Z., Burton, J. B., Torres-Collado, A. X., Moughon, D. L., … Wu, L. (2010). Targeting distinct tumor-infiltrating myeloid cells by inhibiting CSF-1 receptor: Combating tumor evasion of antiangiogenic

therapy. *Blood*, *115*(7), 1461–1471. https://doi.org/10.1182/blood-2009-08-237412

Ramadan, W. S., Zaher, D. M., Altaie, A. M., Talaat, I. M., & Elmoselhi, A. (2020). Potential therapeutic strategies for lung and breast cancers through understanding the anti-angiogenesis resistance mechanisms. *International Journal of Molecular Sciences*, *21*(2). https://doi.org/10.3390/ijms21020565

Redondo-García, S., Peris-Torres, C., Caracuel-Peramos, R., & Rodríguez-Manzaneque, J. C. (2021). ADAMTS proteases and the tumor immune microenvironment : Lessons from substrates and pathologies. *Matrix Biology Plus*, *9*(2021), 100054. https://doi.org/10.1016/j.mbplus.2020.100054

Ren, P., Zhang, L., Xu, G., Palmero, L. C., Albini, P. T., Coselli, J. S., … LeMaire, S. A. (2013). ADAMTS-1 and ADAMTS-4 levels are elevated in thoracic aortic aneurysms and dissections. *Ann. Thorac. Surg.*, *95*(2), 570–577. https://doi.org/10.1016/j.athoracsur.2012.10.084.ADAMTS-1

Reynolds, L. E., Watson, A. R., Baker, M., Jones, T. a, Amico, D., Robinson, S. D., … Aurrand-lions, M. (2010). Tumour angiogenesis is reduced in the Tc1 mouse model of Down Syndrome, *465*(7299), 813–817. https://doi.org/10.1038/nature09106.Tumour

Ribatti, D., Annese, T., Ruggieri, S., Tamma, R., & Crivellato, E. (2019). Limitations of Anti-Angiogenic Treatment of Tumors. *Translational Oncology*, *12*(7), 981–986. https://doi.org/10.1016/j.tranon.2019.04.022

Ricciardelli, C., Frewin, K. M., Tan, I. D. A., Williams, E. D., Opeskin, K., Pritchard, M. a., … Russell, D. L. (2011). The ADAMTS1 Protease Gene Is Required for Mammary Tumor Growth and Metastasis. *The American Journal of Pathology*, *179*(6), 3075–3085. https://doi.org/10.1016/j.ajpath.2011.08.021

Robinson, M. D., & Oshlack, A. (2010). A scaling normalization method for differential expression analysis of RNA-seq data. *Genome Biology*, *11*(R25), 1–9.

Rocks, N., Paulissen, G., Quesada-Calvo, F., Munaut, C., Gonzalez, M. L. A., Gueders, M., … Cataldo, D. D. (2008). ADAMTS-1 metalloproteinase promotes tumor development through the induction of a stromal reaction in vivo. *Cancer Research*, *68*(22), 9541–9550. https://doi.org/10.1158/0008-5472.CAN-08-0548

Rodríguez-Baena, F. J., Redondo-García, S., Peris-Torres, C., Martino-Echarri, E., Fernández-Rodríguez, R., Plaza-Calonge, M. del C., … Rodríguez-Manzaneque, J. C. (2018). ADAMTS1 protease is required for a balanced immune cell repertoire and tumour inflammatory response. *Scientific Reports*, *8*(1), 1–11. https://doi.org/10.1038/s41598-018-31288-7

Rodríguez-Baena, F. J., Redondo-García, S., Plaza-Calonge, M. C., Fernández-Rodríguez, R., & Rodríguez-Manzaneque, J. C. (2018). Evaluation of tumor vasculature using a syngeneic tumor model in wild-type and genetically modified mice. In *Methods in Molecular Biology* (Vol. 1731, pp. 179–192).

Rodríguez-Manzaneque, J. C., Carpizo, D., Plaza-Calonge, M. del C., Torres-Collado, A. X., Thai, S. N. M., Simons, M., … Iruela-Arispe, M. L. (2009). Cleavage of syndecan-4 by ADAMTS1 provokes defects in adhesion. *International Journal of Biochemistry and Cell Biology*, *41*(4), 800–810. https://doi.org/10.1016/j.biocel.2008.08.014

Rodríguez-Manzaneque, J. C., Fernández-Rodríguez, R., Rodríguez-Baena, F. J., & Iruela-Arispe, M. L. (2015). ADAMTS proteases in vascular biology. *Matrix Biology*, *44*, 38–45. https://doi.org/10.1016/j.matbio.2015.02.004

Rodríguez-Manzaneque, J. C., Milchanowski, A. B., Dufour, E. K., Leduc, R., & Iruela-Arispe, M. L. (2000). Characterization of METH-1/ADAMTS1 processing reveals two distinct active forms. *Journal of Biological Chemistry*, *275*(43), 33471–33479. https://doi.org/10.1074/jbc.M002599200

Rodríguez-Manzaneque, J. C., Westling, J., Thai, S. N. M., Luque, A., Knauper, V., Murphy, G., … Iruela-Arispea, M. L. (2002). ADAMTS1 cleaves aggrecan at multiple sites and is differentially inhibited by metalloproteinase inhibitorsq. *Biochemical and Biophysical Research Communications*, *293*(1), 501–508. https://doi.org/10.1016/S0006-291X(02)00254-1

Rooijen, N. Van, & Sanders, A. (1994). Liposome mediated depletion of macrophages: mechanism of action, preparation of liposomes and applications. *Journal of Immunological Methods*, *174*(1–2), 83–93. https://doi.org/10.1016/0022-1759(94)90012-4

Rose, K. W. J., Taye, N., Karoulias, S. Z., & Hubmacher, D. (2021). Regulation of ADAMTS Proteases. *Frontiers in Molecular Biosciences*, *8*(June), 1–16. https://doi.org/10.3389/fmolb.2021.701959

Rowley, A. T., Nagalla, R. R., Wang, S., & Liu, W. F. (2019). Extracellular Matrix-Based Strategies for Immunomodulatory Biomaterials Engineering, *1801578*, 1–18. https://doi.org/10.1002/adhm.201801578

Rudge, J. S., Holash, J., Hylton, D., Russell, M., Jiang, S., Leidich, R., … Yancopoulos, G. D. (2007). VEGF Trap complex formation measures production rates of VEGF, providing a biomarker for predicting efficacious angiogenic blockade. *Proceedings of the National Academy of Sciences of the United States of America*, *104*(47), 18363–18370. https://doi.org/10.1073/pnas.0708865104

Saleiro, D., & Platanias, L. C. (2019). Interferon signaling in cancer. Non-canonical pathways and control of intracellular immune checkpoints. *Seminars in Immunology*, *43*(August), 101299. https://doi.org/10.1016/j.smim.2019.101299

Sandy, J. D., Westling, J., Kenagy, R. D., Iruela-Arispe, M. L., Verscharen, C., Rodriguez-Mazaneque, J. C., … Clowes, A. W. (2001). Versican V1 Proteolysis in Human Aorta in Vivo Occurs at the Glu 441-Ala442 Bond, a Site That Is Cleaved by Recombinant ADAMTS-1 and ADAMTS-4. *Journal of Biological Chemistry*, *276*(16), 13372–13378. https://doi.org/10.1074/jbc.M009737200

Schmitt, M. (2016). Versican vs versikine : tolerance vs attack. *Blood*, *128*(5), 612–613. https://doi.org/10.1182/blood-2016-06-717496

Senior, R. M., Gresham, H. D., Griffin, G. L., Brown, E. J., & Chung, A. E. (1992). Entactin stimulates neutrophil adhesion and chemotaxis through interactions between its Arg-Gly-Asp (RGD) domain and the leukocyte response integrin. *Journal of Clinical Investigation*, *90*(6), 2251–2257. https://doi.org/10.1172/JCI116111

Serrano-Garrido, O., Peris-Torres, C., Redondo-García, S., Asenjo, H. G., Plaza-Calonge, M. D. C., Fernandez-Luna, J. L., & Rodríguez-Manzaneque, J. C. (2021). ADAMTS1 supports endothelial plasticity of glioblastoma cells with relevance for glioma progression. *Biomolecules*, *11*(1), 1–17. https://doi.org/10.3390/biom11010044

Shiao, S. L., Ganesan, a P., Rugo, H. S., & Coussens, L. M. (2011). Immune microenvironments in solid tumors : new targets for therapy Immune microenvironments in solid tumors : new targets for therapy. *Genes & Development*, 2559–2572. https://doi.org/10.1101/gad.169029.111

Shindo, T., Kurihara, H., Kuno, K., Yokoyama, H., Wada, T., Kurihara, Y., … Matsushima, K. (2000). ADAMTS-1: A metalloproteinase-disintegrin essential for normal growth, fertility, and organ morphology and function. *Journal of Clinical Investigation*, *105*(10), 1345–1352. https://doi.org/10.1172/JCI8635

Shojaei, F., Wu, X., Malik, A. K., Zhong, C., Baldwin, M. E., Schanz, S., … Ferrara, N. (2007). Tumor refractoriness to anti-VEGF treatment is mediated by CD11b+Gr1+ myeloid cells. *Nature Biotechnology*, *25*(8), 911–920. https://doi.org/10.1038/nbt1323

Shojaei, F., Wu, X., Qu, X., Kowanetz, M., Yu, L., Tan, M., … Ferrara, N. (2009). G-CSF-initiated myeloid cell mobilization and angiogenesis mediate tumor refractoriness to anti-VEGF therapy in mouse models. *PNAS*, *106*(16), 6742–6747. https://doi.org/10.1073/pnas.0902280106

Sica, A., Larghi, P., Mancino, A., Rubino, L., Porta, C., Totaro, M. G., … Mantovani, A. (2008). Macrophage polarization in tumour progression. *Seminars in Cancer Biology*, *18*(5), 349–355. https://doi.org/10.1016/j.semcancer.2008.03.004

Sica, A., Schioppa, T., Mantovani, A., & Allavena, P. (2006). Tumour-associated macrophages are a distinct M2 polarised population promoting tumour progression: Potential targets of anti-cancer therapy. *European Journal of Cancer*, *42*(6), 717–727. https://doi.org/10.1016/j.ejca.2006.01.003

Siemann, D. W. (2010). Tumor Microenvironment. *Tumor Microenvironment*. https://doi.org/10.1002/9780470669891

Silva, S. V., Lima, M. A., Cella, N., Jaeger, R. G., & Freitas, V. M. (2016). ADAMTS-1 Is Found in the Nuclei of Normal and Tumoral Breast Cells. *Plos One*, *11*(10), 1–17. https://doi.org/10.1371/journal.pone.0165061

Sionov, R. V., Lamagna, C., & Granot, Z. (2022). Recognition of Tumor Nidogen-1 by Neutrophil C-Type Lectin Receptors. *Biomedicines*, *10*(908), 1–18.

Sorokin, L. (2010). The impact of the extracellular matrix on inflammation. *Nature Reviews Immunology*, *10*(10), 712–723. https://doi.org/10.1038/nri2852

Stockmann, C., Schadendorf, D., Klose, R., & Helfrich, I. (2014). The impact of the immune system on tumor: angiogenesis and vascular remodeling. *Frontiers in Oncology*, *4*(April), 69. https://doi.org/10.3389/fonc.2014.00069

Su, S.-C., Mendoza, E. A., Kwak, H.-I., & Bayless, K. J. (2008). Molecular profile of endothelial invasion of three-dimensional collagen matrices: insights into angiogenic sprout induction in wound healing. *American Journal of Physiology. Cell Physiology*, *295*(5), C1215–C1229. https://doi.org/10.1152/ajpcell.00336.2008

Sun, Y., Huang, J., & Yang, Z. (2015). The roles of ADAMTS in angiogenesis and cancer. *Tumor Biology*, *36*(6), 4039–4051. https://doi.org/10.1007/s13277-015-3461-8

Tan, I. A., Frewin, K., Ricciardelli, C., & Russell, D. L. (2019). ADAMTS1 promotes adhesion to extracellular matrix proteins and predicts prognosis in early stage breast cancer patients. *Cellular Physiology and Biochemistry*, *52*(6), 1553–1568. https://doi.org/10.33594/000000108

Teleanu, R. I., Chircov, C., Grumezescu, A. M., & Teleanu, D. M. (2020). Tumor angiogenesis and anti-angiogenic strategies for cancer treatment. *Journal of Clinical Medicine*, *9*(1). https://doi.org/10.3390/jcm9010084

Tian, W., Cao, C., Shu, L., & Wu, F. (2020). Anti-Angiogenic Therapy in the Treatment of Non-Small Cell Lung Cancer. *OncoTargets and Therapy*, *13*, 12113–12129.

Tomayko, M. M., & Reynolds, C. P. (1989). Determination of subcutaneous tumor size in athymic (nude) mice. *Cancer Chemotherapy and Pharmacology*, *24*(3), 148–154. https://doi.org/10.1007/BF00300234

Torres-Collado, A. X., Kisiel, W., Iruela-Arispe, M. L., & Rodríguez-Manzaneque, J. C. (2006). ADAMTS1 interacts with, cleaves, and modifies the extracellular location of the matrix inhibitor tissue factor pathway inhibitor-2. *Journal of Biological Chemistry*, *281*(26), 17827–17837. https://doi.org/10.1074/jbc.M513465200

Turcotte, K., Gauthier, S., Mitsos, L. M., Shustik, C., Copeland, N. G., Jenkins, N. A., … Gros, P. (2004). Genetic control of myeloproliferation in BXH-2 mice. *Blood*, *103*(6), 2343–2350. https://doi.org/10.1182/blood-2003-06-1852

Tzanakakis, G., Neagu, M., Tsatsakis, A., & Nikitovic, D. (2019). Proteoglycans and immunobiology of cancer-therapeutic implications. *Frontiers in Immunology*, *10*(APR), 1–8. https://doi.org/10.3389/fimmu.2019.00875

Vaday, G. G., & Lider, O. (2000). Extracellular matrix moieties, cytokines, and enzymes: Dynamic effects on immune cell behavior and inflammation. *Journal of Leukocyte Biology*, *67*(2), 149–159. https://doi.org/10.1002/jlb.67.2.149

Vázquez, F., Hastings, G., Ortega, M. A., Lane, T. F., Oikemus, S., Lombardo, M., & Iruela-Arispe, M. L. (1999). METH-1, a human ortholog of ADAMTS-1, and METH-2 are members of a new family of proteins with angio-inhibitory activity. *Journal of Biological Chemistry*, *274*(33), 23349–23357. https://doi.org/10.1074/jbc.274.33.23349

Viallard, C., & Larrivée, B. (2017). Tumor angiogenesis and vascular normalization: alternative therapeutic targets. *Angiogenesis*, *20*(4), 409–426. https://doi.org/10.1007/s10456-017-9562-9

Vidal, P. (2020). Interferon α in cancer immunoediting: From elimination to escape. *Scandinavian Journal of Immunology*, *91*(5), 1–8. https://doi.org/10.1111/sji.12863

Vitale, I., Shema, E., Loi, S., & Galluzzi, L. (2021). Intratumoral heterogeneity in cancer progression and response to immunotherapy. *Nature Medicine*, *27*(2), 212–224. https://doi.org/10.1038/s41591-021-01233-9

Wang, S., Liu, Y., Zhao, G., He, L., Fu, Y., Yu, C., … Zheng, J. (2018). Postnatal deficiency of ADAMTS1 ameliorates thoracic aortic aneurysm and dissection in mice. *Experimental Physiology*, *103*(12), 1717–1731. https://doi.org/10.1113/EP087018

Wang, Z., Li, Z., Wang, Y., Cao, D., Wang, X., Jiang, M., … Luo, F. (2015). Versican silencing improves the antitumor efficacy of endostatin by alleviating its

induced inflammatory and immunosuppressive changes in the tumor microenvironment. *Oncology Reports*, *33*(6), 2981–2991. https://doi.org/10.3892/or.2015.3903

Wight, T. N., Frevert, C. W., Debley, J. S., Reeves, S. R., Parks, W. C., & Ziegler, S. F. (2017). Interplay of extracellular matrix and leukocytes in lung inflammation. *Cellular Immunology*. https://doi.org/10.1016/j.cellimm.2016.12.003

Wight, T. N., Kang, I., Evanko, S. P., Harten, I. A., Chang, M. Y., Pearce, O. M. T., … Frevert, C. W. (2020). Versican — A Critical Extracellular Matrix Regulator of Immunity and Inflammation, *11*(March). https://doi.org/10.3389/fimmu.2020.00512

Winkler, J., Abisoye-Ogunniyan, A., Metcalf, K. J., & Werb, Z. (2020). Concepts of extracellular matrix remodelling in tumour progression and metastasis. *Nature Communications*, *11*(1), 1–19. https://doi.org/10.1038/s41467-020-18794-x

Wu, J., Chen, Z., Wickström, S. L., Gao, J., He, X., Jing, X., … Cao, Y. (2021). Interleukin-33 is a Novel Immunosuppressor that Protects Cancer Cells from TIL Killing by a Macrophage-Mediated Shedding Mechanism. *Advanced Science*, *8*(21), 1–14. https://doi.org/10.1002/advs.202101029

Wu, K., Lin, K., Li, X., Yuan, X., Xu, P., Ni, P., & Xu, D. (2020). Redefining Tumor-Associated Macrophage Subpopulations and Functions in the Tumor Microenvironment. *Frontiers in Immunology*, *11*(August), 1731. https://doi.org/10.3389/fimmu.2020.01731

Wu, Q., Allouch, A., Martins, I., Modjtahedi, N., Deutsch, E., & Perfettini, J. L. (2017). Macrophage biology plays a central role during ionizing radiation-elicited tumor response. *Biomedical Journal*, *40*(4), 200–211. https://doi.org/10.1016/j.bj.2017.06.003

Yoo, S. Y., & Kwon, S. M. (2013). Angiogenesis and its therapeutic opportunities. *Mediators of Inflammation*, *2013*(1). https://doi.org/10.1155/2013/127170

Yoshimura, T., Liu, M., Chen, X., Li, L., & Wang, J. M. (2015). Crosstalk between tumor cells and macrophages in stroma renders tumor cells as the primary source of MCP-1/CCL2 in Lewis lung carcinoma. *Frontiers in Immunology*, *6*(JUN), 1–10. https://doi.org/10.3389/fimmu.2015.00332

Zhang, H., Wang, Z., Peng, Q., Liu, Y.-Y., Zhang, W., Wu, L., … Luo, F. (2013). Tumor refractoriness to endostatin anti-angiogenesis is associated with the recruitment of CD11b+Gr1+ myeloid cells and inflammatory cytokines. *Tumori Journal*, *99*(6), 723–733. https://doi.org/10.1177/030089161309900613

Zhang, Y., & Brekken, R. A. (2022). Are TEMs Canceled ? Questioning the Functional

Relevance of Tie2-Expressing Macrophages. *Cancer Research*, *82*, 1172–1173. https://doi.org/10.1158/0008-5472.CAN-22-0330

Zhangyuan, G., Wang, F., Zhang, H., Jiang, R., Tao, X., Yu, D., … Sun, B. (2020). VersicanV1 promotes proliferation and metastasis of hepatocellular carcinoma through the activation of EGFR–PI3K–AKT pathway. *Oncogene*, *39*(6), 1213–1230. https://doi.org/10.1038/s41388-019-1052-7

Zhao, X., & Subramanian, S. (2017). Intrinsic Resistance of Solid Tumors to Immune Checkpoint Blockade Therapy. *Cancer Research*, *77*(4), 817–822. https://doi.org/10.1158/0008-5472.CAN-16-2379

Zhong, S., & Khalil, R. A. (2019). A Disintegrin and Metalloproteinase (ADAM) and ADAM with thrombospondin motifs (ADAMTS) family in vascular biology and disease. *Biochemical Pharmacology*, *164*(617), 188–204. https://doi.org/10.1016/j.bcp.2019.03.033

Zhou, J., Wang, W., & Li, Q. (2021). Potential therapeutic targets in the tumor microenvironment of hepatocellular carcinoma: reversing the protumor effect of tumor-associated macrophages. *Journal of Experimental and Clinical Cancer Research*, *40*(1), 1–12. https://doi.org/10.1186/s13046-021-01873-2

Zhou, S., Yang, Y., Yang, Y., Tao, H., Li, D., Zhang, J., … Fang, J. (2013). Combination Therapy of VEGF-Trap and Gemcitabine Results in Improved Anti-Tumor Efficacy in a Mouse Lung Cancer Model. *PLoS ONE*. https://doi.org/10.1371/journal.pone.0068589

Zhou, Y., Zhu, Y., Fan, X., Zhang, C., & Wang, Y. (2017). NID1 , a new regulator of EMT required for metastasis and chemoresistance of ovarian cancer cells, *8*(20), 33110–33121.